# SEISMIC STRATIGRAPHY, SEDIMENTATION HISTORY AND TECTONICS OF THE SOUTHWEST CONTINENTAL MARGIN OF INDIA

Thesis submitted to

**GOA UNIVERSITY**
Taleigao Plateau, Goa, India

For the award of the degree of
**DOCTOR OF PHILOSOPHY**
**in**
**Marine Sciences**

**by**



**K.K. AJAY**

National Institute of Oceanography
(Council of Scientific and Industrial Research)
Dona Paula-403 004, Goa, India

**January 2011**

*To my*

*"Amma & Achchan"*

# DECLARATION

*As required under the university ordinance OB-9.9 (vi), I hereby state that the present thesis entitled "**Seismic stratigraphy, sedimentation history and tectonics of the southwest continental margin of India"** is my original contribution and the same has not been submitted elsewhere for award of any degree to any other University on any previous occasion. To the best of my knowledge, the present study is the first comprehensive work of its kind from the area mentioned.*

*Literature related to the problem investigated has been cited. Due acknowledgement has been made wherever facilities and suggestions have been availed of.*

***(K.K. Ajay)***

राष्ट्रीय समुद्र विज्ञान संस्थान
( वैज्ञानिक एवं औद्योगिक अनुसंधान परिषद )
national institute of oceanography
(Council of Scientific & Industrial Research)

***Dr. A.K. Chaubey***
***Scientist 'F'***

*Date: 14th January 2011*

# CERTIFICATE

*As required under the university ordinance OB-9.9 (viii), I hereby certify that the thesis entitled "**Seismic stratigraphy, sedimentation history and tectonics of the southwest continental margin of India**", submitted by **Mr. K.K. Ajay** for the award of the degree of **Doctor of Philosophy** in Marine Sciences, is based on his own studies carried out under my supervision. The thesis or any part thereof has not been previously submitted for any other degree or diploma in any university or institution.*

AKChaubey

***(A.K. Chaubey)***
*Research Supervisor*

All the corrections suggested by the referees have been incorporated.

AKChaubey
18/6/2011

M. S BR. Khe
18/6/11

दोना पावला, गोवा-403 004, भारत
**DONA PAULA, GOA-403 004, India**

☎ : 91-(0)832-2450 450
fax : 91-(0)832-2450 602/03

e-mail : ocean@nio.org
URL : **http://www.nio.org**

**Reginal Centres**
Mumbai, Kochi, Visakhapatnam

# Acknowledgement

*It gives me immense pleasure to acknowledge the assistances and the advices received during the course of my Ph.D. thesis work. I am indebted to my research supervisor* ***Dr. A.K. Chaubey,*** *Scientist, National Institute of Oceanography (NIO), Goa, for his valuable advices, constant guidance, encouragement and patience. The prolific criticisms made by him during the discussion have provided great potency and strength to the thesis.*

*I express my deep sense of gratitude to* ***Dr. Satish Shetye****, Director, NIO, for providing permission, facilities, encouragement and leaning environment to grow me personally as well as professionally during the course of Ph.D. work at NIO, Goa.*

*I express my sincere gratitude to* ***Council of Scientific & Industrial Research*** *(CSIR) for awarding me the Junior Research Fellowship (JRF) and subsequently Senior Research Fellowship (SRF), which have provided great support to me during the entire course of the research work.*

*I am grateful to* ***Prof. G.N. Nayak****, Dean, Faculty of Life Sciences and Environment, Goa University, and* ***Prof. H.B. Menon****, Head, Department of Marine Sciences, Goa University, for their encouragement, advice and assistance on various occasions. I am indeed grateful to* ***Dr. Rajiv Nigam****-Vice Chancellor's nominee- for his constructive comments, suggestions and support.*

*The patience and support provided by the staff of Human Resource Development Group of NIO is highly appreciated. The assistance received from* ***Dr. M.P. Tapaswi****-Documentation Officer and his colleagues of NIO library during the course of this work is greatly appreciated.*

*I am very much thankful to* ***Dr. K.S. Krishna,*** *Scientist, NIO, for generously providing me part of the data used for the study. I owe many thanks to Dr. D. Gopala Rao, Shri. G.C. Bhattacharya, Shri. T. Ramprasad, Dr. V. Yatheesh and Dr. K. Srinivas for their advices, suggestions and helps extended to me at various stages of the work.*

*I would like to express my sense of gratitude to **Dr. Pratima Jauhari,** Scientist, NIO, for generously devoting her valuable time for critically editing the manuscript.*

*I express deep sense of gratitude to my colleagues in NIO, Ritej Banaulikar, Sudheesh T.S., Sergio Raposo, Pradnya Parab, Tripti Naik, Ratan Raj Sharma, Anoop K.V., Pradeep Kumar, Faizal K.V., Unnikrishnan C., Hari Krishna, Shyju C.P., Niyati G. Kalangutkar, Ratnesh Kumar Pandey and Tina Gadekar for their kind helps, without which this work would have not been realized.*

*I am thankful to my loving friends in NIO, Vineesh, Aboobacker, Grinson, Sindhumol, Sini, Nisha, Pallavi, Laju, Vijay, Manoj, Syam, Ricky, Ramya, Rajini, Jensen, Sijin Kumar, Ganesha Prasad, Manu, Suprit Kumar, Chandran, Ratheesh, Ramesh and Sitara for their kind support, caring and encouragement. Their lovely friendship made me relaxed, and helped me to enjoy the days in NIO to be treasured for the rest of my life.*

*I am so thankful to Prof. G. Srinivas, Principal, Government College-Kottayam, Kerala, Prof. Benno Joseph, Head, Department of Geology, Government College-Kottayam, and Prof. A. Chandrasekharan, Head, Department of PG studies and research in Geology, Government College-Kasargod, Kerala, for their kind support and encouragement shown towards the completion of my Ph.D. thesis. The valuable suggestions, advices and encouragement given by my colleagues in the Government College-Kottayam and Government College-Kasargod are also highly acknowledged.*

*I am indebted to my loving father and mother who devoted their life to make me to reach higher destinies, and rewarded me with their unconditional love, care, continuous encouragement and support. I am grateful also to my brother and sisters for their love, care, support and encouragement. I am blessed to be gifted with such loving and understanding parents and siblings, because I would have been nothing without them.*

*I thank the almighty for the strength, patience and all the goodness blessed on me.*

# Contents

## Chapter-3 Geological and geophysical data



## Chapter-4 Analysis and interpretation of multi channel seismic reflection profiles



## Chapter-5 Structural features and basement depth anomaly

## Chapter-6 Seaward dipping reflectors and crustal structure



## Chapter-7 Sedimentation history and tectonics of the southwest continental margin of India



## Chapter-8 Summary and Conclusions

# List of figures

# List of tables

# Preface

The Western Continental Margin of India (WCMI) mainly evolved during two major rift-drift episodes in the geological past. The first phase of rifting commenced during the Late Cretaceous between southwest India and eastern Madagascar was associated with the Marion hotspot volcanism. The second phase of rifting commenced during the Early Tertiary between India-Laxmi Ridge and Seychelles preceded by a short span of rifting between Seychelles-Laxmi Ridge and India. The latter phase of rifting was associated with the emplacement of Massive Deccan flood basalt erupted by the Rèunion hotspot during 68.5–62 Ma. The Rèunion hotspot related volcanism occurred on continental to oceanic lithosphere as the Indian plate moved over the hotspot, emplacing numerous magmatic intrusive/extrusive bodies along the western continental margin of India. Considerable stretching during the rifting episodes, and volcanism associated with the hotspots had obliterated the pre-existing geology and initial configuration of the margin. The margin, which is considered as a passive margin, is characterized by i) a northward widening NW-SE trending continental shelf, ii) a shelf edge limited by ~200 m isobath, iii) a continental slope deepening from 200 to 2000 m isobaths, and iv) deep sedimentary basins. The WCMI is characterized by ~300 km wide continental shelf in Kutch-Saurashtra region which gradually narrows down southward to ~50 km in Kerala offshore region.

The present study is focused on the southwestern part of the western continental margin of India, which is comprised of narrow continental shelf, wide slope, Laccadive Basin, Laccadive Ridge and eastern part of the Arabian Basin. Despite the fact that the India-Madagascar breakup produced an extensive volcanic province along eastern Madagascar and numerous volcanic flows and intrusives in the southwest Indian shield, the Southwest Continental Margin of India (SWCMI) is generally considered as a non volcanic passive margin. Whereas the northwest continental margin of India developed during the breakup between Laxmi Ridge-India and Seychelles, is considered as a volcanic passive margin due to contemporaneous outbursts of the Deccan volcanics. SWCMI is characterized by a number of structural and tectonic features which were formed due to extensional tectonics during India – Madagascar breakup under the

influence of Marion hotspot, and later modified by magmatic episodes of the Rèunion hotspot as well as collision between Indian and Eurasian continental plates. Considerable parts of these features are concealed under thick sediment cover and volcanic flows.

The present study aims to decipher stratigraphy, sedimentation history, crustal structure and Continent Ocean Transition (COT) along SWCMI, in order to provide constraints to improve the understanding of tectonic evolution of the margin. The primary dataset used for the study is 2D Multi-Channel Seismic (MCS) reflection data acquired along twelve seismic lines across the SWCMI. Other major data set used for the study include shipborne as well as satellite altimetry derived free air gravity anomalies across the margin. Published results on seismic refraction, drill wells and magnetic isochrones have also been utilized for the study.

The study reveals five major seismic stratigraphic units in the sedimentary basins as well as several structural and tectonic features of the SWCMI. The study brings out, for the first time, Seaward Dipping Reflectors (SDRs) along the western flank of the Laccadive Ridge, and the anomalous basement depth of the Arabian Basin. 2D crustal modeling using gravity data reveals Lower Crustal Body (LCB) of high P-wave velocity beneath the SWCMI. The results of the study explain the volcanic nature of the continental margin, continent-ocean transition and impact of the Reunion hotspot on the margin.

The study forms the thesis that has been organized in eight chapters as follows:

**Chapter 1** gives a brief description of southwest continental margin of India. The chapter presents study area, and the scope and objectives of the present study. Further the chapter discusses briefly the continental margins with a special reference to passive continental margin.

**Chapter 2** presents a review of previous pertinent studies to synthesize present knowledge about the geologic and tectonic settings of the study area and adjoining region. The chapter deals with the present knowledge of subsidence,

sedimentation and general stratigraphy of the study area and briefly describes the evolutionary history of the western continental margin of India.

**Chapter 3** deals with various types of geological and geophysical data used for the present study. Major geophysical data include multi channel seismic reflection and ship borne as well as satellite altimetry derived free air gravity anomaly data. Results of seismic refraction studies in the Arabian Sea, and Deep Seismic Sounding (DSS) studies of the Western Dharwar Craton (WDC) and Deccan Traps adjacent to the study area are used for crustal structure modeling across the southwest continental margin of India. Published drill well data of the southwest continental margin of India constitute major geological dataset to study litho- and chrono-stratigraphy of the study area. Data compiled from published magnetic isochron map of the Arabian Basin, tectonic chart of SW India and General Bathymetry Chart for the Oceans (GEBCO) are used as supporting database for the study.

**Chapter 4** deals with the analysis of multi channel seismic reflection profiles across the southwest continental margin of India. Numerous structural and tectonic features are identified during the analysis. The interpreted seismic profiles are presented in the form of line drawing sections. Further, the identified seismic sequences are correlated with published drill well information to describe them in terms of various sedimentary depositional units and to understand the sedimentation history of the study area.

**Chapter 5** presents discussion on various structural and tectonic features delineated during analysis of the MCS reflection profiles. Further the chapter presents computation of basement depth anomalies in the Arabian Basin. The basement depth anomalies in the basin are calculated as the difference between the depths to the oceanic basement corrected for sediment load, and predicted by lithospheric thermal model. The results indicate anomalous depth to basement of oceanic crust in the Arabian Basin of age range 63–42 Ma, suggesting that subsidence in this basin does not follow the age–depth relationship of normal oceanic crust.

**Chapter 6** discusses in detail the occurrence of Seaward Dipping Reflectors (SDRs) along the western flank of the Laccadive Ridge and its relationship with the Indo-Madagascar separation associated with Marion hotspot volcanism during the Late Cretaceous. The chapter further presents 2D crustal models across the SWCMI and discusses the crustal structure of the margin.

**Chapter 7** discusses sedimentation history of the study area. The chapter further deals with tectonic implications of seaward dipping reflectors along the western flank of the Laccadive Ridge, and basement depth anomalies in the Arabian Basin. Finally, the chapter addresses continent-ocean transition, rift related magmatism and neotectonic activities along the SWCMI.

**Chapter 8** presents summary and conclusions of the study. The chapter is followed by references, in alphabetical order, of the literatures cited in the text.

# Chapter-1

# GENERAL BACKGROUND

# Chapter-1

# GENERAL BACKGROUND

## 1.1 Introduction

The Indian Ocean, the third largest of the world's oceans, is a storehouse of diverse and complex tectonic and sedimentary features. The Arabian Sea and the Bay of Bengal, which border Indian peninsula west and east respectively, form the northwestern and northeastern parts of the Indian Ocean. Geological and geophysical studies in the Indian Ocean revealed several major tectonic and structural features of the ocean, as well as basement ages of part of the ocean basins. However there are unexplored regions in the Indian Ocean which require systematic study on their tectonic and sedimentological evolution. Evidences of the early opening history of the Indian Ocean lie in the continental margins and adjacent deep sea basins surrounding the continents.

The passive continental margins, to which the western continental margin of India belongs, are considered as the places where the breakup and rifting of continents took place. The passive margins are subsequently covered by a thick pile of synrift and postrift sediments which may provide the source of significant natural resources. Detailed geological and geophysical investigations of western continental margin of India have been mostly confined to the continental shelf for the purpose of commercial exploration of natural resources. The likelihood of further prospects in the adjacent deeper parts necessitated better understanding of ongoing geological and tectonic processes, and evolutionary history of the western continental margins of India. The present study aims to enhance knowledge of stratigraphy, sedimentation history, and tectonics of the southwest continental margin of India. Knowledge of crustal structure, tectonics and sedimentation will not only improve scientific understanding but also be crucial to the future wealth and well-being of the nation.

In this introductory chapter the Western Continental Margin of India (WCMI) is briefly described along with the geographical entity of the study area. Further the chapter presents objectives and scope of the present study. Finally, a brief

description of various types of continental margins with special emphasis on passive margins is presented.

## 1.2 Western continental margin of India

The Western Continental Margin of India (WCMI) extends NW-SE from Kutch in the north to Cape Comorin in the south (Figure 1.1). It has evolved after the break-up of Madagascar in the Late-Cretaceous and Seychelles micro-continent in the Early Tertiary from India (McKenzie and Sclater, 1971; Norton and Sclater, 1979; Schlich, 1982; Besse and Courtillot, 1988; Patriat and Segoufin, 1988; Scotese et al., 1988; Royer et al., 1989; White and McKenzie., 1989; Storey et al., 1995; Reeves and de Wit, 2000; Reeves and Leven, 2001; Royer et al., 2002). The break-ups were associated with massive extrusive and intrusive magmatism due to interaction of hotspots (Richards et al., 1989; White and McKenzie, 1989; Duncan, 1990; Storey, 1995; Storey et al., 1995; Courtillot et al., 1999). The tectonic and structural features classify the WCMI under the category of passive continental margins (Biswas, 1982; Chandrasekharam, 1985). The WCMI is characterized by i) a NW-SE trending continental shelf limited by the shelf edge at about 200 m isobath, ii) a continental slope bounded between 200 and 2000 m isobath, iii) deep offshore sedimentary basins, and iv) basement ridges more or less parallel to the continental shelf edge. The continental shelf widens more than 300 km off Kutch-Saurashtra and gradually narrows down southward to about 50 km off Cochin. In contrast, the continental slope is narrow in the north but widens towards south (Biswas, 1982, 1987, 1988).

The continental shelf separated by southwesterly plunging basement highs is comprised mainly of four shelfal basins, namely Kutch, Saurashtra, Ratnagiri and Kerala-Konkan basins (Biswas, 1988). The margin hosts a number of deep-seated faults, rift systems, basement highs, numerous NW-SE trending structural features such as Laccadive Ridge, Laxmi Ridge, Prathap Ridge Complex, Panikkar Ridge (seamount chain comprising Raman Seamount, Panikkar Seamount and Wadia Guyot), which are mostly buried under the Indus Fan sediments. Three major deep offshore sedimentary basins - Indus Basin, Laxmi Basin and Laccadive Basin - are located between the continental slope and the Laxmi-Laccadive

ridges. The Arabian Basin is located west of the Laxmi and Laccadive ridges and continues up to the Carlsberg Ridge. Several onshore structural lineaments of the Indian subcontinent extend to a considerable distance into the offshore region (Kolla and Coumes, 1990). The host-graben structures, basement arches and fault patterns of the shelf areas, mainly parallel to the Dharwar (NW-SE to NNW-SSE) and Eastern Ghat (NE-SW) trends, are formed due to rifting and movements along the ancient Precambrian structural trends (Biswas, 1987). The WCMI consists of modified and attenuated continental crust, with Archaean granitic basement juxtaposed with oceanic crust, which underlies the abyssal plain of the adjacent Arabian Basin. Major structural and tectonic features of the WCMI are concealed under thick sedimentary cover and volcanic flows impeding the initial configuration of the margin. A large continental flood basalt province - Deccan Trap - emplaced by the Rèunion hotspot (68.5-62 Ma) is found on central western Indian shield along WCMI as well as on the Praslin Island in the Seychelles micro-continent (Devey and Stephens, 1991). The Deccan Trap is the largest known continental flood basalt province formed by series of eruptions (Courtillot et al., 1986; Vandamme et al., 1991; Venkatesan et al., 1993; Bhattacharji et al., 1996). As a result of continued interaction of the Rèunion hotspot with the northward moving Indian Plate, the adjacent offshore areas came under the influence of the Rèunion hotspot that resulted in magmatic intrusions within the western continental margin of India (Shipboard scientific party, 1988; Richards et al., 1989; Duncan, 1990, Pandey et al., 1996; Singh, 2002) and built the northern part of the Chagos-Laccadive Ridge on the rifted lithospheric crust of India.

## 1.3 Study area

Study area is located between the latitudes 6°-16°N and longitudes 66°-78°E on the southern part of the western continental margin of India, approximately south of Goa (Figure 1.1). The major geological domains of the study area are (i) narrow shelf comprised of Kerala-Konkan Basin formed by horst-graben structures, (ii) wide continental slope bounded between 200 and 2000 m isobath (iii) shelf margin sedimentary basin known as the Laccadive Basin, (iv) the Prathap Ridge, (v) the Laccadive Ridge, and (vi) the deep Arabian Basin west of the Laccadive

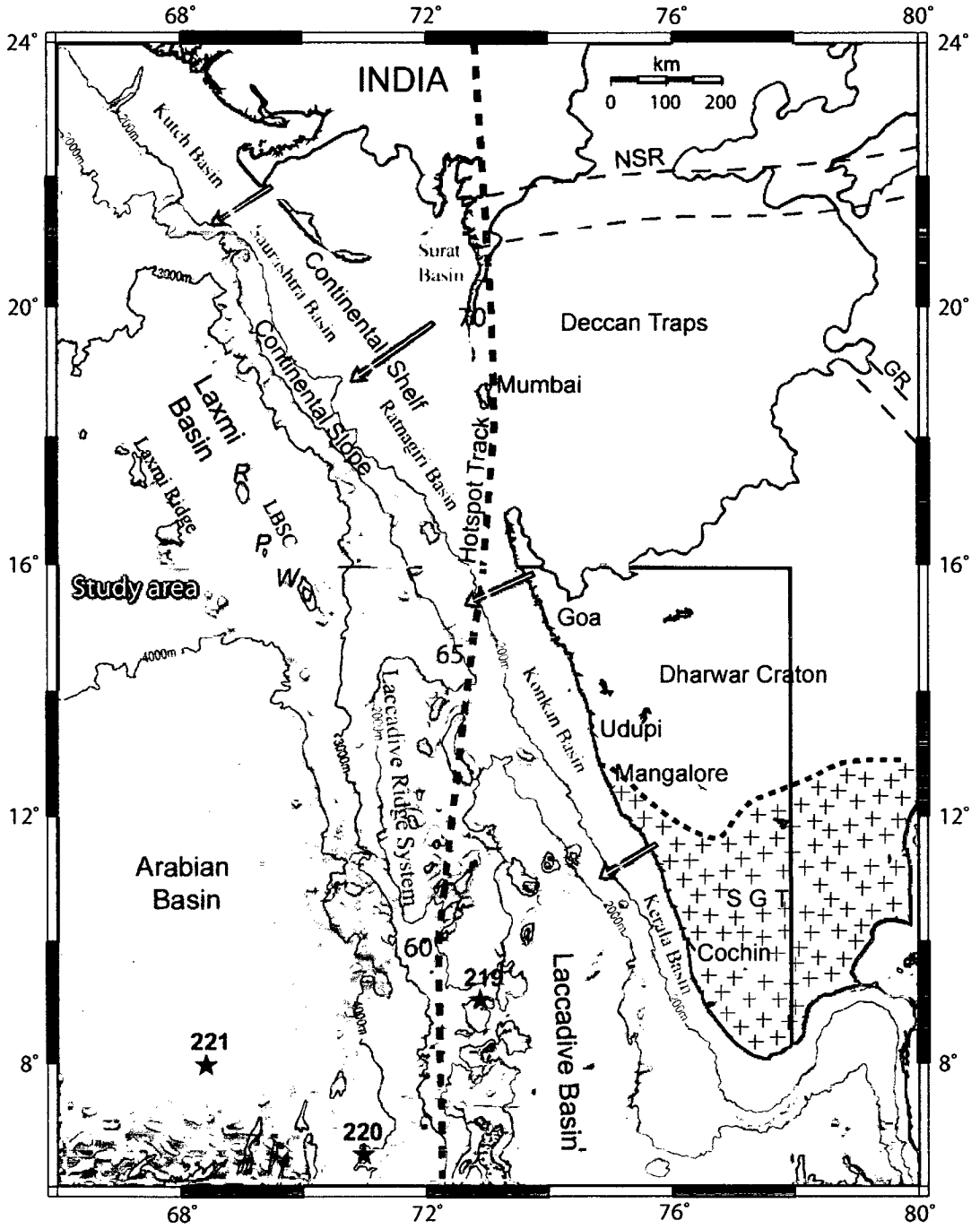


**Figure 1.1** Generalized map of Western Continental Margin of India (WCMI) and adjacent regions. Study area is shown within rectangle. DSDP drill sites (Whitmarsh et al., 1974) are represented by solid annotated stars; GEBCO bathymetry contours are shown by annotated thin lines; solid thick dashed lines represents computer-modeled Rèunion hotspot track; numbers along the hotspot track are predicted ages in My (Shipboard Scientific Party, 1988); SW trending arrows in the continental shelf represent strike of basement archs (Biswas, 1987). SGT: Southern Granulite Terrain; GR: Godavari Rift; NSR: Narmada Sone Rift; LBSC: Laxmi Basin Seamount Chain; W: Wadia Guyot; R, P: Raman, Panikkar seamounts respectively.

Ridge. The study area assumes significance in the context of evolution of southwest continental margin of India as it contains numerous prominent and varied geologic features whose genesis and evolution are not yet well understood. Detailed description of these features and present understanding of their genesis are presented in chapter-2.

## 1.4 Scope and objectives of the study

The western continental margin of India is considered as a typical passive rifted margin (Biswas, 1982; Chandrasekaram, 1985). Despite the fact that the India-Madagascar breakup produced an extensive volcanic province along eastern Madagascar and numerous volcanic flows and intrusives in the southwest Indian shield, southwest continental margin of India is generally considered as a non volcanic passive margin. Whereas the northwest continental margin of India, developed during the breakup between Laxmi Ridge-India and Seychelles, is considered as a volcanic passive margin due to contemporaneous outbursts of the Deccan volcanics. In view of the above facts, nature of southwest continental margin of India remains poorly understood and therefore warrants detailed investigation.

Southwest Continental Margin of India (SWCMI) is characterized by a number of structural and tectonic features which were formed due to extensional tectonics during India–Madagascar breakup under influence of the Marion hotspot, magmatic episodes of the Rèunion hotspot and subsequent evolution of the margin. The major structural features include present- and paleo-shelf breaks, Kerala-Konkan Basin, Shelf Margin High, Laccadive Basin, Prathap Ridge and Laccadive Ridge. The lateral extent of some of the structural features was demarcated earlier based on physiographic expressions and seismic reflection data (Naini and Talwani, 1983; Biswas and Singh, 1988). Since considerable parts of the features are concealed under thick sediment cover and volcanic flows, their extent yet to be demarcated based on crustal structure obtained from integrated interpretation of geophysical data. It is believed that the Marion and Rèunion hotspots related magmatism had a profound influence on crustal evolution of the

SWCMI concealing pre-existing geology and crustal structure. Therefore, reported crustal structure of this complex margin is equivocal. Radhakrishna et al. (2002) inferred a thick under-plated oceanic crust below the Laccadive Ridge and Continent-Ocean Boundary (COB) to the east of the ridge based on the analysis of seismic and free-air gravity data. Whereas Chaubey et al. (2002b), in their 2-D crustal model based on integrated interpretation of gravity and magnetic data, depicted a heavily intruded continental crust for the Laccadive Ridge with an inferred continent-ocean boundary to the west of the ridge. The results of these studies are equivocal in resolving the crustal nature of the Laccadive Ridge and COB along SWCMI. In order to address the impact of hotspot on the SWCMI, crustal structure, continent-ocean boundary/transition and anomalous basement depths needs to be investigated.

Most of the earlier investigations on the stratigraphy and sedimentation pattern of the margin, were focussed on the continental shelf and slope region in connection with hydrocarbon exploration (Nair and Rao, 1980; Raju et al., 1981,Rao and Srivastava, 1981, 1984; Raha et al., 1983; Singh and Lal, 1993, 2001; Pandey and Dave, 1998; Thakur et al., 1999; Gunnel, 2001; Chaubey et al., 2002b; Rao et al., 2002; Campanile et al., 2008). Studies are very sparse in the deep offshore region of SWCMI. Therefore, understanding of the sedimentation history of various geological domains of the SWCMI is still limited.

The present study is primarily aimed at deciphering sedimentation, crustal architecture and Continent-Ocean Transition (COT) along the SWCMI, and to provide constraints to improve the understanding of tectonics of the margin. Specific objectives of the study are formulated as:

- Identification and mapping of detailed structural and tectonic features to understand nature of the margin.
- Identification of seismic sequences and their correlation with litho- and chrono-stratigraphy to understand the sedimentation history.
- Computation of basement depth anomalies to understand Rèunion Hotspot interaction with the SWCMI.

- Elucidation of crustal structure across the margin to delineate the continent-ocean transition and the nature of crust of the margin.
- Implications of identified structural and tectonic features in the tectonics of the margin.

In order to achieve these objectives, multi-channel seismic reflection data supplemented by shipborne as well as satellite altimetry derived free-air gravity anomaly data are analyzed. Bathymetric, drill-well and seismic refraction information are also utilized to constrain the results of the present study.

Since the present study is focused on the southwest continental margin of India which is classified as a passive continental margin, a brief account on the concept of continental margin (Symonds et al., 2000 and references therein) is presented in the following sections.

## 1.5 Continental margins

Two major types of morphological features dominating the Earth's surface are continents and oceans. The oceans cover about 71% of the total Earth's surface. The continents and oceans are separated by the coastline, which is a transitory boundary. A much more fundamental subdivision of the Earth's surface is in terms of geological provinces composed of either continental or oceanic crust. Continental margins are a zone between the thin, dense, oceanic crust and the thicker, lighter, chemically different continental crust. Continental margins occupy about 28% of the total area of the oceans and about 20% of the continental crust lies beneath the oceans (Kennett, 1982). The geomorphological and geologic characteristics of a continental margin are a function of its tectonic, magmatic, and sedimentation history. The transition from continental to oceanic crust commonly occurs beneath the outer part of continental margins. Important province boundaries are continent-ocean boundary/continent-ocean transition. They are difficult to define because of their complexity and transitional nature.

There are three main types of continental margins which are differentiated based on their relationship to plates, plate boundaries, and presence or absence of

seismic and volcanic activities. They are referred to in a variety of ways in scientific literature. They are:

(i) Divergent / rifted / passive / aseismic or Atlantic type
(ii) Convergent / active / seismic or Pacific type
(iii) Transform / translational or sheared type

Transform margins can occur in both divergent and convergent tectonic settings.

### 1.5.1 Divergent continental margins

The divergent continental margins are formed by rifting and drifting of continental lithosphere. An intracontinental rift system evolves into a continental margin when the two diverging pieces of lithosphere are separated by seafloor spreading centers. The continental rifting process marks the zone where active divergent plate tectonic processes commence. Although divergent margins initially form at divergent plate boundaries, they move away from these boundaries, progressively cool, subside and accumulate sediments in the fault grabens. Thus, divergent margins, located within a plate on the transition from continental to oceanic crust characterized by extensional tectonics, are commonly called 'Passive margins'. Divergent margins are tectonically active for a few million years during their formation, but they become inactive soon after the continent breaks into two parts and the oceanic spreading center retreats from the margins. There are two important classes of passive margins:

i) Non-volcanic passive margins
ii) Volcanic passive margins

#### 1.5.1.1 *Non-volcanic passive margins*

In the non-volcanic passive margins (Figure 1.2a) magmatism is either absent or incidental (e.g., west Iberia margin). They are characterized by a zone of synrift sediments deposited in the rift system overlain by a broad zone of post rift or post breakup sediments deposited following the initiation of seafloor spreading.

Lithospheric deformation on a nonvolcanic margin is dominated by block faulting related to brittle deformation in the upper crust and ductile deformation in the lower crust and upper mantle, producing a broad extensional crust. Magmatism does occur but is probably confined to the deeper parts of the lithosphere, with only minor volcanism in the upper crust. Rifting is commonly viewed as progressing from an intercontinental rift to an active rifted margin. Along the non-volcanic passive margins COB can be distinguished in the narrow zones of initial dyke injection and by abrupt change from continental to oceanic basement. The final morphology of the margin is heavily controlled by the amount of post breakup sediment deposition. On sediment-poor margins, the original rift architecture will have a significant influence on margin morphology, but it will be overwhelmed by sediment depositional processes on sediment-rich margins.

#### 1.5.1.2 *Volcanic passive margins*

Volcanic passive margins (Figure 1.2b) are characterized by extensive extrusive constructions emplaced during continental breakup and the initial phase of seafloor spreading. These constructions commonly include formations which appear as Seaward Dipping Reflector (SDR) sequences in the seismic record (Hinz, 1981; Coffin and Eldholm, 1992). The volcanic passive margins, together with continental flood basalts, oceanic plateaus and ocean basin flood basalts have been defined as sites of voluminous emplacements of predominantly mafic rocks which do not originate at normal seafloor spreading centers (Coffin and Eldholm, 1992). The episodic, massive melting associated with large igneous provinces is commonly related to hotspot activity or thermal plume rising from deep within the earth. The magmatic activity is manifested by extensive volcanism, producing lavas from numerous feeders, volcanoes, and fissures, both above sea level and in shallow waters. The volcanism is centered along the line of continental breakup. However, the basaltic lavas may flow for long distances and cover large areas of the neighboring continents. The magmatic activity which takes place during both the final phase of continental thinning and the initial period of seafloor spreading are short-lived (few million years) on a geological time scale. As the excess volcanism abates, the main feeder system subsides to become a mid-oceanic ridge that produces new oceanic crust. As the ocean matures, the

volcanic complexes on the conjugate continental margins subside and are gradually buried below the sediments. Many of the volcanic passive margins are also characterized by thicker than normal oceanic crust beneath the extrusive complex, including a high velocity (7.1 - 7.7 km/sec.) Lower Crustal Body (LCB). On volcanic passive margins, the definition of COB is complex, and the use of the term COT is probably more appropriate. Because, the early stage subaerial or submarine basaltic lava flows may spread over the broad preexisting rift zone basement disguising the location of the COB forming a wide COT. However, a complex COT may result if the start of spreading is slow, episodic with low magma supply and jumps around within the rift system.

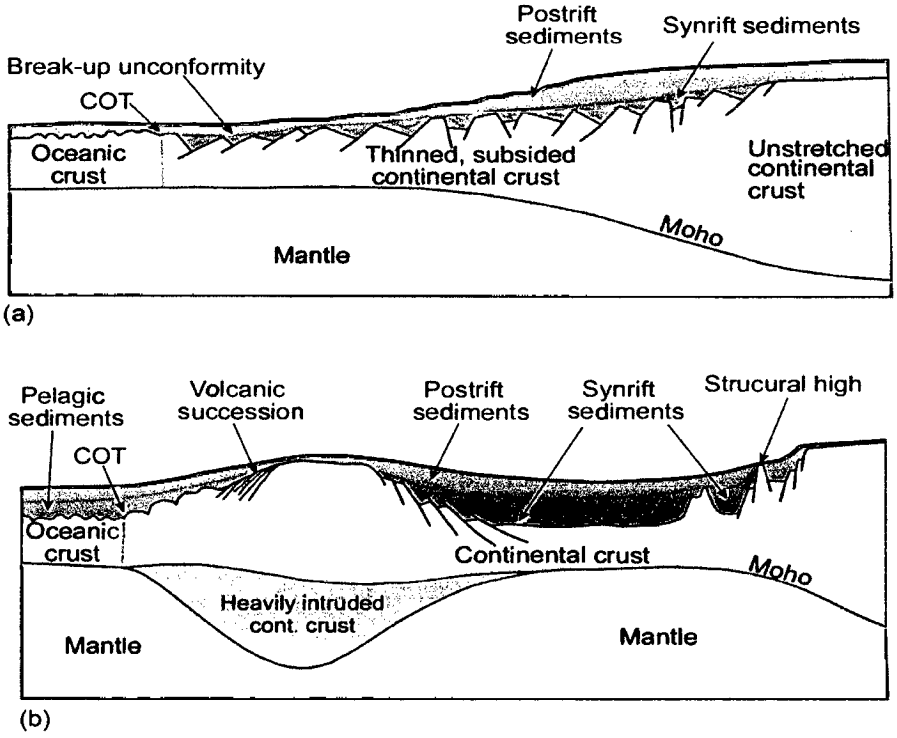


**Figure 1. 2** Schematic diagrams of (a) non-volcanic and (b) volcanic passive margins.

Volcanic or non-volcanic nature of the margin, is not directly evident from bathymetric and geomorphic features. Volcanic passive margins exist both in regular shelf-slope-rise settings, as well as in settings where the slope is interrupted by a marginal high bounded by an upper and a lower slope. Whereas on non-volcanic passive margins marginal highs may be poorly developed or even absent. The main factors governing volcanic passive margin architecture, including the construction of buried marginal highs and marginal plateaus are

(i) style and distribution of structural deformation since onset of rifting, (ii) volume and rate of magma production and geological environment during breakup; and (iii) subsidence and sedimentation history since breakup. Differences in these factors can result in a range of morphological and structural configurations and great variation in volcanic margin architecture.

### 1.5.2 Convergent continental margins

Convergent continental margins are generally defined as the broad area between the active subduction zone and the continental land mass (National Research council, 1979). This definition includes the trench, accretionary prism, forearc and backarc basins, volcanic arc, remnant arcs, island arcs and collision complex within the convergent margin terrain. Convergent continental margins mark the boundaries between continental and oceanic plates or two converging, continental or oceanic plates. The convergent continental margins are associated with deformation and subduction of continental and oceanic crusts. The interaction of continental and oceanic plates creates deep-sea trenches, volcanic arcs, remnant arcs and forearc basins (Figure 1.3a; e.g., westcoast of Indonesia and Sumatra). Collision between two oceanic plates (Figure 1.3b; e.g., South Sandwich Islands, South Georgia) forms island arcs, trenches, forearc and backarc basins. Whereas the collision between two continental plates is characterized by orogenic mountain ranges at their margins (Figure 1.3c; e.g., Himalayan ranges). The convergent continental margins are sometimes referred to as active or seismic margins because they are often marked by shallow to deep-seated earth quakes, volcanism, crustal deformation and metamorphism. They form much of the margin around the Pacific Ocean, as well as parts of the southern Atlantic Ocean and the northeast Indian Ocean. The transition from continent to oceanic crust on convergent continental margin is generally much more complex than the divergent continental margins. The morphology of a typical Pacific active convergent margin consists of a continental shelf and slope bounded on the seaward side by a trough or trench. Sediment accumulations on the slope appear to be less, compared to divergent margins, and continental rises are generally absent since the continental slope bottoms in a deep trench.

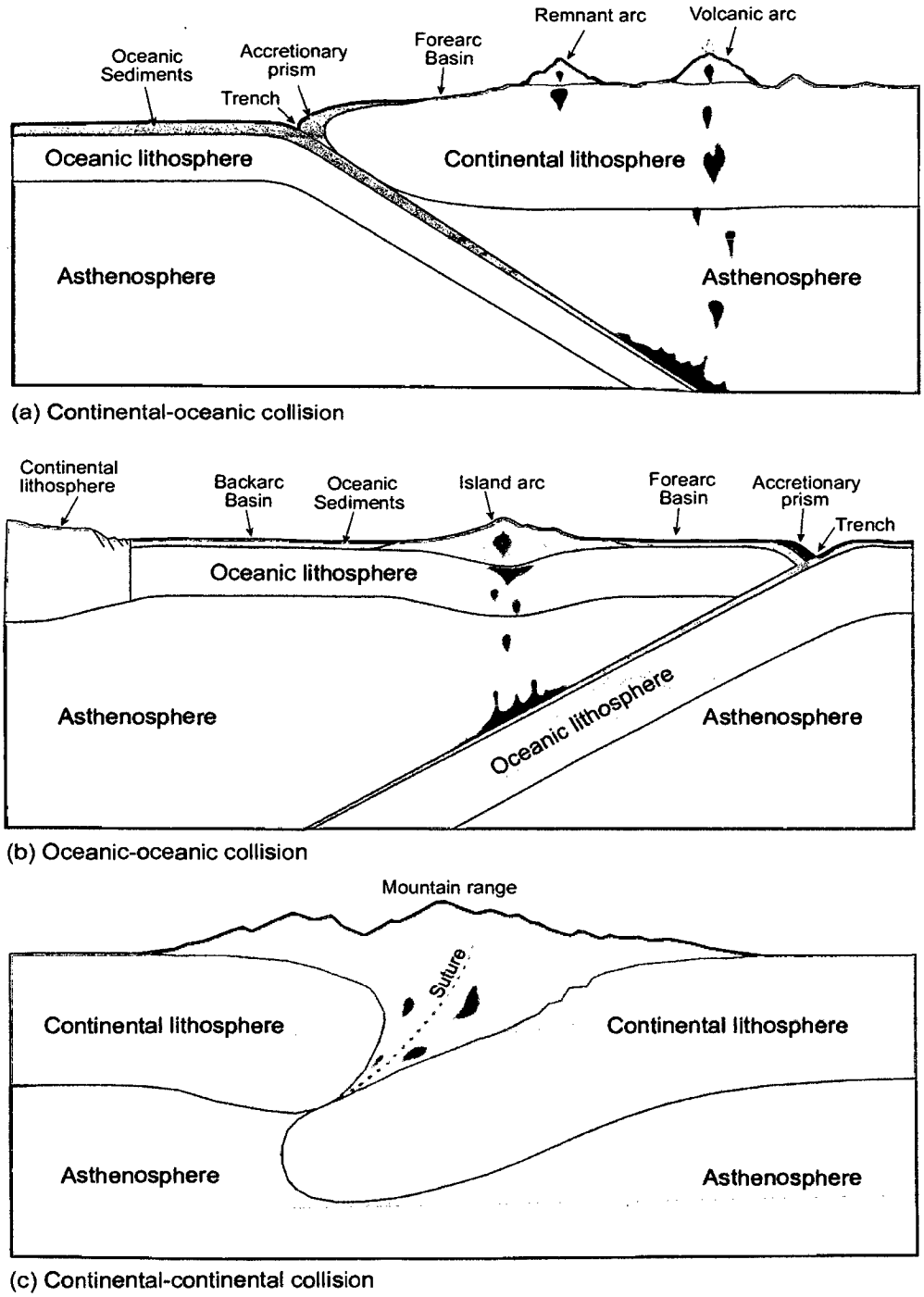


**Figure 1.3** Schematic diagrams of (a) continent-ocean collision, (b) oceanic-oceanic collision and (c) continent-continent collision.

### 1.5.3 Transform margins

Plate tectonic motion that is more or less perpendicular to the rift system and the locus of breakup creates divergent rifted margins. In some places, these rifted margin segments are linked by margins where the locus of breakup is more or less parallel to the initial plate motions between parting continents. Such margins

are called transform (rift-transform, translational, sheared) margins (Figure 1.4; Mascle and Blarez, 1987). They evolve within a thermomechanical regime that includes significant components of strike-slip shear as well as extensional strain deformation owing to sharp contrast for their morphological, crustal and sedimentary characteristics between the continental domain and the nearby younger oceanic crust. Most of the structural characteristics of transform margins develop during their early intracontinental stage, when the two continents progressively slide past each other. During this stage syn-sedimentary and syn-diagenetic deformation characterizes a wide, linear zone located between the two parting continents in association with severe tectonism, structural inversion and erosion (Mascle et al., 1998). These processes lead to the development of incipient marginal ridge features. Transform margins exhibit distinctive morphological characteristics such as strong linearity, declivity and large scale margin parallel ridges called marginal ridges. The transform margin slopes representing geologic scars resulting from the transcurrent movement between the separating continents. The distribution of sediments across transform margin is strongly dependent on their tectonic evolution and related morphostructural features. The steep continental slopes preclude substantial deposition. At transform margins the transition from continent to oceanic crust appears quite abrupt. The COT is quite narrow (<10 km) and correlates with an abrupt seaward shallowing of the Moho. Even though some of the transform margins appear to be a sharp and simple juxtaposition of continental and oceanic crust, with no evidences of magmatic activity, there are transform margins with complexities related to continental crust contamination, magmatic intrusions and underplating.

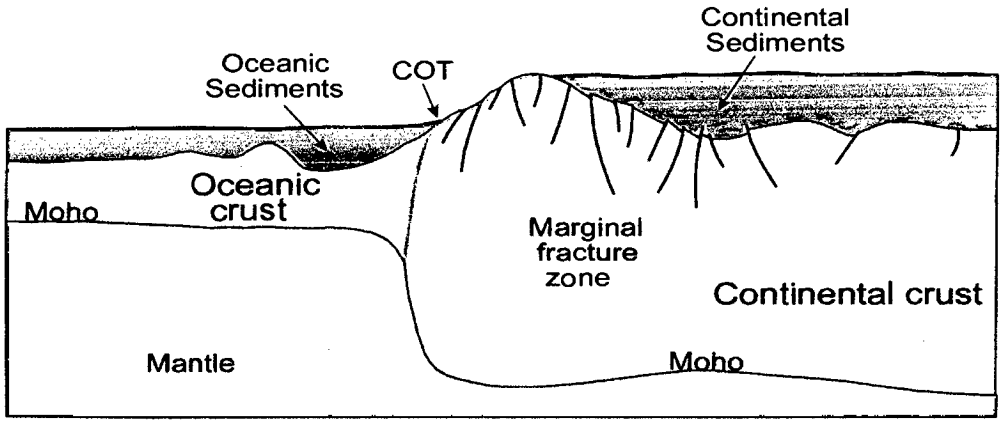


**Figure 1.4** Schematic diagram of a transform margin.

# Chapter-2

# GEOLOGY AND TECTONIC SCENARIO

# Chapter-2

# GEOLOGY AND TECTONIC SCENARIO

## 2.1 Introduction

The present day geology and tectonic scenario of the western continental margin of India is mainly the result of rifting of India from Madagascar and later from Seychelles under the influence of hotspots. The subsequent northward drifting of the Indian plate, collision with the Eurasian Plate and sediment depositional episodes modified the initial margin configuration. Earlier studies carried out in this region identified various structural and tectonic features and suggested nature and evolution of the margin. The available information on geology, crustal structure, and tectonic and sedimentation history of the study area with adjacent regions are compiled to facilitate meaningful interpretation of the geophysical data. In turn, it will provide better understanding of the structural and tectonic features, and the sedimentary evolution of the region. In this chapter, geologic and tectonic settings of the study area are presented in the following sections.

## 2.2 Regional geology and tectonic settings

The study area, located on the southern part of the western continental margin of India, is evolved by various geodynamic processes, such as rifting and drifting of Madagascar from southern India associated with Marion hotspot activity in the Late Cretaceous and interaction of Rèunion hotspot with northward moving Indian Plate in the Early Tertiary (Norton and Sclater, 1979; Patriat and Achache, 1984; Besse and Courtillot, 1988; Richards et al., 1989; White and McKenzie, 1989; Duncan, 1990; Storey, 1995; Storey et al., 1995, 1997; Torsvik et al., 1998, 2000; Courtillot et al., 1999; Yatheesh et al., 2006). The Shelf margin high, Prathap Ridge, Laccadive Ridge, Kerala-Konkan Basin, Laccadive Basin and Arabian Basin are major structural and tectonic features of the study area (Figure 2.1). The study area is also characterized by numerous magmatic intrusive bodies and structural trends, which are mostly covered by variable thickness of sediments. Offshore extension of onshore tectonic and structural trends, over a considerable distance, is suggested by several geological and geophysical investigations

(Eremenko and Datta, 1968; Bhattacharya and Subrahmanyam, 1986; Ramana, 1986; Kolla and Coumes, 1990; Subrahmanyam, 1992). These features along with major structural features of the study area are briefly described in the following sections.

### 2.2.1 Laccadive Ridge

The Laccadive Ridge (Figure 2.1) is the northern segment of the Chagos-Laccadive Ridge system lying roughly parallel to the southwest coast of India between 8°N and 16°N (Chaubey et al., 2008). It is the most distinct aseismic ridge on the SWCMI with an average width of 270 km. The ridge, popularly known as Lakshadweep, is comprised of about twenty islands and banks grouped as Laccadive Islands (Whitmarsh et al., 1974). Deep Sea Drilling Project (DSDP) Site 219, located on the crest of the Laccadive Ridge, indicated presence of Late Paleocene sediment composed of shallow water limestone, sandstone and siltstones at the bottom of the drill-well. The Paleocene sediment is succeeded by Early to Middle Eocene chert, chalk and ooze (Whitmarsh et al., 1974).

Interpretation of multichannel seismic reflection profiles across the Laccadive Ridge revealed raised acoustic basement overlain by sediment of thickness varying up to 1.0 km, prominent Middle Eocene chert reflectors, magmatic intrusive bodies and continent-ocean transition to the west of the ridge (Talwani and Kahle, 1975; Avraham and Bunce, 1977; Naini, 1980; Naini and Talwani, 1983; Biswas and Singh, 1988; Chaubey et al., 2002b, 2008). The basement of the ridge is comprised of sharp peaks which are devoid of sediment cover and deep local sediment grabens. Some of the peaks reach very close to the sea surface and form beautiful coral atolls.

The eastern and western limits of the ridge are bounded by fault scarps, which apparently separate the ridge from Laccadive and Arabian basins respectively (Avraham and Bunce, 1977; Balakrishnan, 1997; Chaubey et al., 2002b). In the area north of 12°N, the basement consist of crustal blocks dropped in a step like fashion to the west (Naini and Talwani, 1983; Reddy et al., 1988). A graben like tectonic feature of about 20 km width was reported by Gopala Rao et al. (1987)

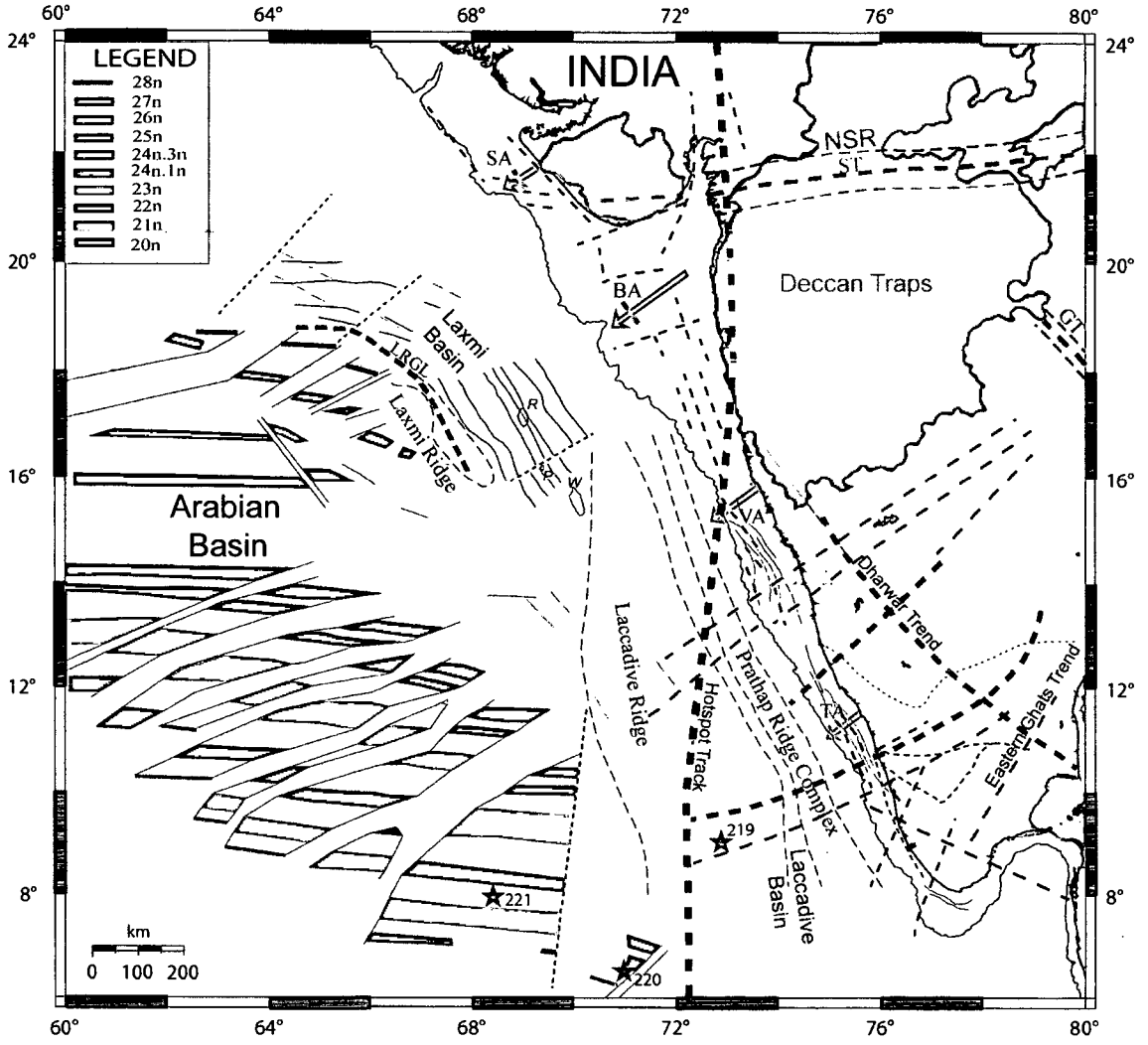


**Figure 2.1** Generalized tectonic map of the WCMI and adjacent regions, showing magnetic isochrons (coloured blocks) and pseudo faults (thin blue lines) in the Arabian Basin (Chaubey et al., 2002a); magnetic lineations in the Laxmi Basin (thin red lines; Bhattacharya et al., 1994a and Malod et al., 1997) and fracture zones (blue dashed lines). DSDP drill sites (Whitmarsh et al., 1974) are shown by solid annotated stars; solid thick dashed lines represent computer-modeled Rèunion hotspot track; numbers along the hotspot track are predicted ages in My (Shipboard Scientific Party, 1988); major tectonic trends and principle fault patterns of inland and offshore regions of western India are compiled from Biswas (1987; 1988); Kolla and Coumes (1990); Singh and Lal (1993); Ghosh et al. (2004) and Mishra et al. (2004). Magnetic lineations compiled from Naini and Talwani (1983) are shown by thin grey dashed lines more or less parallel to the coast and boundaries of Laxmi and Laccadive ridges. Laxmi Ridge boundary is considered after Chaubey et al. (1998). LRGL: Laxmi Ridge Gravity Low; NSR: Narmada-Sone Rift; ST: Satpura Trend; GT: Godavary Trend; W: Wadia Guyot; R, P: Raman and Panikkar seamounts respectively; SA, BA, VA, TA: Saurashtra, Bombay, Vengurla and Tellicherry archs respectively.

based on seismic reflection data interpretation. The graben, located at the crest of the ridge, is bounded by steep scarps.

The ridge is associated with relatively positive but subdued free-air gravity anomalies compared to the surrounding region (Kahle and Talwani, 1973; Naini and Talwani, 1983). The overall positive subdued free-air gravity anomaly of the ridge was considered to indicate a compensation of its mass at deeper depths (Avraham and Bunce, 1977). Based on the 2D crustal model, Radhakrishna et al. (2002) suggested a thick oceanic crust of density 3.0 g/cm$^3$ below the ridge which juxtaposes the continental crust along its eastern margin. Magnetic anomalies over the ridge do not show any definite pattern. The ridge is associated with subdued magnetic anomalies to its eastern part and several prominent high magnetic anomalies to the western part (Naini and Talwani, 1983; Gopala Rao et al., 1987). The latter were interpreted due to densely spaced igneous intrusives (Chaubey et al., 2002b). The seismic refraction studies by Francis and Shor (1966), south of the Laccadive Ridge, suggested 5 km of volcanic rocks of seismic velocity 3.85 - 5 km/s overlying more than 10 km of crustal material of an average seismic velocity of 6.84 km/s. Seismic refraction measurements by Babenko et al. (1981) indicated the Moho at a depth of about 18-19 km below the Laccadive Ridge. Admittance analysis of gravity and bathymetry data across the ridge suggested stretched and heavily intruded continental crust of the Laccadive Ridge with an average crustal thickness of 17±2 km and density of 2.7 x 10$^3$ kg/m$^3$ (Chaubey et al., 2008).

The Laccadive Ridge is considered a transition between oceanic crust to the west and continental crust to the east based on seaward thinning of the crust from about 37 km on the western Indian shield to about 15 km beneath the Laccadive Ridge (Narain et al., 1968). Naini and Talwani (1983) suggested a continental fragment origin for the Laccadive Ridge from interpretation of seismic refraction velocity and crustal structure. DSDP and Ocean Drilling Project (ODP) results suggest that the Deccan Traps volcanic province of the Indian peninsula and the Chagos Laccadive Ridge (CLR) were formed during the northward motion of Indian plate over the Reunion hotspot (Shipboard Scientific Party, 1988; Richards et al., 1989; Duncan, 1990). Analysis of the geothermal regime and the

progressively reducing age of basalts along CLR led Verzhbitsky (2003) to suggest that the ridge was formed due to the Reunion hotspot.

K-Ar dating of different continental basalt flows of an industry drill well located at the Padua Bank (northern Laccadive Ridge), revealed 60.2–102 Ma age (Murty et al., 1999; Kothari et al., 2001). Identification of several rotated fault blocks from multi-channel seismic reflection data led Murty et al. (1999) to infer continental ribbon structures of the Laccadive Ridge. Based on the analysis of seismic reflection, free-air gravity and magnetic anomaly data, Chaubey et al. (2002b) inferred that the Laccadive Ridge is a continental fragment intermingled with volcanic intrusives.

### 2.2.2 Prathap Ridge

Harbison and Bassinger (1973) first reported the presence of small and isolated basement highs off western continental shelf of India. Subsequently, Ramaswamy and Rao (1980) have identified basement highs with steep flanks near the shelf edge between Goa and Mangalore coast. They postulated that some of the basement highs are part of a continuous basement ridge parallel to the coast. Naini (1980) mapped these basement highs along the continental rise off southwest coast of India between 8° and 17°N in a NNW-SSE direction. These basement highs vary in width from 50 to 100 km and are distributed parallel to the western continental shelf-edge of India for about 1100 km (Figure 2.1). Naini (1980) named this basement structural feature as the Prathap Ridge (PR). The ridge, apparently dividing the basin into two parts, is mostly buried under the thick Tertiary sediments of the Laccadive Basin. The ridge appears at places as single and multiple peaks above the sediment and therefore it is termed as Prathap Ridge Complex. The ridge is characterized by well-developed free-air gravity and magnetic anomalies over its exposed parts (Gopala Rao et al., 1987; Subrahmanyam et al., 1989; Krishna et al., 1992 and 1994). Naini (1980) and Subrahmanyam (1992) have suggested that the ridge might have originated during the initial phase of rifting along the western margin of India and represent a continental sliver intermingled with dykes and volcanics. Whereas, Krishna et al. (1992) suggested that the ridge is a volcanic construct that might have formed due

to Rèunion hotspot during northward movement of the Indian plate over the hotpot. Radhakrishna et al. (2002) proposed that the ridge is a shallow uncompensated basement high over thinned rifted continental crust.

### 2.2.3 Shelf margin high

The western continental margin of India is characterized by several structural highs which evolved during initial stage of margin formation and subsequent geodynamic events. A set of isolated structural highs are identified adjacent to the eastern boundary of the Prathap ridge complex at different locations of the SWCMI. Even though these isolated structural highs have distinct geological identity, several researchers have interpreted them as part of the NNW-SSE trending Prathap Ridge Complex or Kori–Comorin Ridge (Naini, 1980; Biswas, 1988; Subrahmanyam et al., 1991, 1993a, 1995; Chakraborty et al., 2006). Although the Prathap Ridge and Shelf-Margin High are seen as continuous structure on a regional scale parallel to the continental shelf in the study area, they are offset along the pre-existing ENE–WSW trending Precambrian faults reactivated with the commencement of seafloor spreading at the Carlsberg Ridge (Subrahmanyam et al., 1993a and 1995). Chaubey et al. (2002b) interpreted the isolated structural high as a flat topped bathymetric high, known as shelf margin high which divides the eastern part of the Laccadive Basin into two parts. Based on multibeam swath bathymetry survey on part of the western continental slope of India, Mukhopadhyay et al. (2008) reported prominent structural highs with flat summits to the east of the conical structural highs of the Prathap ridge. The structural highs with flat summit are considered by them as upper slope ridge.

### 2.2.4 Kerala-Konkan Basin

The various phases of rifting along WCMI and the reactivation of existing major faults and week zones along Precambrian structural trends produced a series of regional and local horst-graben structures, basement arches, fault patterns and sedimentary basins of the shelf areas. They are mainly parallel to the Dharwar (NW-SE to NNW-SSE) and Eastern Ghat (NE-SW) trends (Biswas, 1987). The Kerala-Konkan Basin (KKB) (Figure 1.4) is a sedimentary basin located on the continental shelf of SWCMI between Vengurla Arch basement high in the north

(~17°N) and Cape Comorin in the south (Biswas, 1987; Biswas and Singh, 1988). The western and southwestern limits of the basin appeared to be opened up into the deeper Laccadive Basin. The Vengurla Arch basement high is the natural barrier for the Kerala-Konkan Basin in the north. The basin represents stretched pre-Deccan continental basement developed during the rifting of India from Madagascar (Singh and Lal, 1993; Storey, 1995). The fringe of the basin extends onto the land in the coastal area where isolated outcrops of the Miocene and younger sediments are preserved. The basin is again divided into two sub-basins, Konkan and Kerala basins, by Tellicherry Arch located at about 11°N (Ramaswamy and Rao, 1980; Biswas, 1987). However, because of their similar morphological, sedimentological and depositional characters they are considered as a single basin, known as Kerala-Konkan Basin. Kerala-Konkan Basin is considered as a part of the high-elevation passive continental margin, which is characteristic of Gondwanian continents (Ollier, 1985; Gilchrist and Summerfield, 1990; Campanile et al., 2008). In the northern part of the basin the continental shelf is about 100 km wide and progressively narrows down to about 50 km in the south. Alleppey platform, bounded by deep faults, is a prominent tectonic feature in the south where the continental shelf becomes abruptly wide (>100 km) from an average width of 50 km. Nair and Qasim (1978) reported a coral bank at 80 m water depth, named as Gaveshani Bank, from the central western continental shelf of India, off Malpi. The bank is about 42 m high and 2 km long and appears to be an isolated physiographic feature in the continental shelf between Kasargod and Karwar (Rao et al., 1993).

The Kerala-Konkan Basin constitutes a major depocentre for the gneissic source of sediment derived by the denudation of Western Ghats. The drill well information and results of seismic reflection studies along the SWCMI suggest that the Kerala-Konkan Basin provides a sedimentary record since 80-90 Ma (Singh and Lal, 1993). However, the bulk of sediment in the Kerala-Konkan Basin appears to have been deposited during the Cenozoic. Sediment isopach map of the Kerala-Konkan Basin indicates Cenozoic sediment thickness of up to 4 km (Rao and Srivastava, 1984). The basin accommodates considerable thickness of Mesozoic sediments of early rift phase, overlain by a seismic reflector approximately corresponding to the Deccan Trap lava flows below the Cenozoic sediment

deposits of post-rift phase (Biswas, 1982; 1988). Late Cretaceous sediments in the deepest wells of Kerala-Konkan Basin overlie altered volcanic rocks. The outcrops of similar volcanic rocks at the St. Mary's Island, near the coast, are dated as 85.6 Ma (Pande et al., 2001), and hence are contemporaneous with the Marion hotspot magmatism (Joseph and Nambiar, 1996). The Kerala-Konkan Basin is different from northern continental shelf basins (Ratnagiri, Saurashtra and Kutch basins) in their depositional history and hydro-carbon potential.

### 2.2.5 Laccadive Basin

The Laccadive Basin, a narrow triangular shaped basin, is located between the Laccadive Ridge in the west and the southwest continental shelf edge of India in the east (Figure 2.1). Towards north the basin narrows down and tapers near 16°N where the northern extremity of the Laccadive Ridge apparently meets the adjacent continental slope of central western India. In the south it opens into the Central Indian Basin (Bhattacharya and Chaubey, 2001). The water depth in this basin varies from about 2000 m in the north to about 2800 m in the south. The geophysical studies in the basin suggest that the underlying basement is block faulted (Rao and Bhattacharya, 1975). Maximum sediment thickness in the basin is about 3.5 sec (TWT) in the north, which gradually decreases to about 2.5 sec (TWT) in the southern part of the basin (Ramaswamy and Rao, 1980; Naini and Talwani, 1983; Gopala Rao et al., 1987; Singh and Lal, 1993; Chaubey, 1998). The aggraded and prograded sediment of the basin is Paleocene to Holocene age (Chaubey et al., 2002b). The drill well information and results of seismic reflection studies across the SWCMI suggest that the Laccadive Basin accommodates considerable thickness of Mesozoic sediments of early rift phase (Biswas, 1982, 1988). The Mesozoic sediments are overlain by a seismic reflector approximately corresponding to the Deccan Traps lava flows which is overlain by Cenozoic sediment of post-rift phase. The Laccadive Basin is associated with broad low to subdued magnetic anomaly and generally low free air gravity anomaly (Gopala Rao and Bhattacharya, 1977; Naini and Talwani, 1983; Gopala Rao et al., 1987; Subrahmanyam et al., 1995). However, these geophysical signatures are occasionally altered due to the presence of isolated peaks of Prathap ridge complex associated with relatively high free-air gravity anomalies. The nature of

crystalline basement of the basin is debated as transitional (Naini and Talwani, 1983) and oceanic (Biswas, 1988; Biswas and Singh, 1988; Biswas, 1989). Chaueby et al. (2002b), based on interpretation of multi-channel seismic reflection data, suggested that the basin is bounded on both sides (east and west) by well-developed half-graben structures with tilted and rotated fault blocks and underlain by stretched continental crust emplaced with numerous magmatic intrusives. The well developed half-graben structure of the stretched continental crust indicates possibility of a failed rift in the basin.

### 2.2.6 Arabian Basin

The Arabian Basin is located west of the Laccadive Ridge in the study area. The Basin is bounded to the northwest by the Owen fracture zone which demarcates the transform boundary between the Indian and Arabian plates and to the southwest by uneven topography of the NW-SE trending active Carlsberg Ridge that separates the Indian and African plates. The aseismic Laxmi and the Laccadive ridges bound most of the northern and eastern limit of the basin. The Indus Fan sediments cover most part of the basin and determine submarine topography. Water depth in this basin varies from 3400 m in the north to about 4400 m in the south with relatively smooth seafloor which generally dips southward.

The Arabian Basin is characterized by well developed Early Tertiary magnetic lineations established through various studies (McKenzie and Sclater, 1971; Whitmarsh, 1974; Norton and Sclater, 1979; Naini and Talwani, 1983; Bhattacharya et al., 1992; Chaubey et al., 1993, 1995). Different interpretations exist regarding identification of the oldest magnetic anomaly in the basin. Recent studies (Chaubey et al., 2002a; Royer et al., 2002) precisely located the oldest magnetic isochrones as 28ny (62.449 Ma) in the basin. Detailed study of magnetic anomalies of this basin indicated that the accretionary process of the early Tertiary oceanic crust in the Arabian Basin has been greatly influenced by paleo-spreading ridges (Miles and Roest, 1993; Mercuriev et al., 1996; Chaubey et al., 1998, 2002a; Dyment, 1998; Miles et al., 1998; Royer et al., 2002). The oblique

offsets of magnetic lineations are considered to represent the pseudofaults associated with paleo-propagating ridges.

Seismic refraction study (Naini, 1980; Naini and Talwani, 1983) suggests that the basin consists of a sediment layer with variable thickness, ranging from 1.3 to 4.2 km, and two distinct oceanic crustal layers with a Moho at a depth of 11.5 km below sea level. The upper crustal layer has an average velocity and thickness of about 5.51 km/sec and 1.69 km respectively. An average velocity of 6.67 km/sec and a thickness of 3.0 km are estimated for the lower crust. These results suggest that the crustal structure of the Arabian Basin is similar to that of a normal oceanic crust. Two DSDP drill Sites (220 and 221) are located in the southeastern part of the Arabian Basin (Figure 2.1). The micropaleontological age of the oldest sediment overlying the basaltic basement at Sites 220 and 221 were inferred to be Early Eocene and middle Eocene respectively (Whitmarsh et al., 1974). Therefore, a period of continuous sedimentation in the Arabian Basin is believed to have begun during Early to Middle Eocene (Weser, 1974).

The analysis of seismic reflection profiles in the Arabian Basin indicates the presence of strong reflector 'R' dividing the sediment column into two parts. This reflector marks a major unconformity surface between the lower pelagic and upper terrigenous sedimentary sequences. Results of DSDP drill well 221 suggested that the illite rich terrigenous sedimentary sequence is deposited by the turbidity currents initiated by the Indus Fan sedimentation in the Arabian Basin during middle – Late Oligocene (Weser, 1974). The magnetic anomaly studies (Chaubey et al., 1995) suggest that both the DSDP Sites 220 and 221 are underlain by oceanic crust. The site 221 is located on the reversely magnetized oceanic crust between the magnetic anomalies 22 and 21, which provided a reliable age constraint (~48 My) for the oceanic crust at this site, whereas the Site 220 is located on the reversely magnetized oceanic crust between the magnetic anomalies 24 and 23. Bhattacharya and Subrahmanyam (1991) reported the presence of a 2,464 m high seamount with 1 km wide flat summit, located in the Arabian Basin about 200 km west of the Laccadive Ridge off Cochin and named it as Sagarkanya Seamount.

### 2.2.7 Western Dharwar Craton

The Western Dharwar Craton (WDC) is the western geotectonic block of the Dharwar Craton (Ramakrishnan et al., 1976; Swami Nath et al., 1976) which comprises peninsular Indian shield of the oldest rock formations of Archaean age (Figure 1.7 and Figure 2.1). The WDC, covered by the Deccan Traps towards north, is bordered by Southern Granulite Terrain (SGT) composed of Archaean gneissic basement rocks towards south, Eastern Dharwar Craton towards east and the Arabian Sea to the west (Verma, 1991). Nearly E-W trending lineaments defined as shear zones divide the Peninsular Indian Shield into different crustal blocks. Deep Seismic Sounding (DSS) studies along the Kavali-Udupi profile across the WDC suggest a crustal thickness of about 40 km and a simple velocity structure consisting of an upper and lower crust. The granitic upper crust of velocity 6.0 – 6.2 km/sec and an average thickness of 23 km is underlain by a lower crust of velocity 6.8 to 7.0 km/sec. The velocities in Dharwar schists range between 5.5 – 5.8 km/sec (Kaila et al., 1981). Moho is identified with a $P_n$ velocity of 8.4 km/sec at an average depth of 40 km (Kaila et al., 1979; Sarkar et al., 2001, Reddy, 2005). Relatively low velocities associated with the lower crust suggest the absence of seismically distinct high velocity layer of underplated maffic cumulates overlying the Moho (Sarkar et al., 2001; Rai et al., 2003).

### 2.2.8 Precambrian structural trends

The Precambrian structural trends of Indian subcontinent are considered as the zones of deformed and weakened basement crust resulting from the Orogenisis of more than 2000 Ma and have availed all the Phanerozoic movements and rifting responsible for the present day configuration of the subcontinent (Biswas, 1982; 1987; Biswas and Singh, 1988). The NW-SE to NNW-SSE trending Dharwar structural trends (Figure 2.1) are the most prominent Precambrian structural trends of western peninsular India (Krishnan, 1968; Biswas, 1987). The Dharwar trends, which are more or less parallel to the west coast of India, are considered to extend below the Deccan Traps, from the southern India to the north until the Kutch region (Krishnan, 1968; Das and Ray, 1976; Biswas, 1982, 1987; Gombos et al., 1995). In addition to the structural trends which are parallel to the NW-SE

Dharwar trends, NE-SW trending faults and basement highs are parallel to the Eastern Ghats trend. They also extend from western peninsular India to the western offshore region. The Dharwar structural trends are intersected at many places by NE-SW trending structural lineaments (Ramana, 1986). A series of regional and local horst-graben structures have resulted in response to rifting along the dominant Precambrian basement structural and tectonic trends. The NNW-SSE trending Western Ghats escarpment, which forms the western edge of the mountainous Sahyadri Range, more or less parallel to the west coast, is a major geomorphic as well as structural feature of the western peninsular Indian shield. The time of formation of Western Ghats is still debated between the tectonic formation of new continental edge at the time of Gondwanaland break up (Ollier and Powar, 1985; Subrahmanya, 1998) and the rifting of Seychelles from India (Widdowson, 1997; Widdowson and Gunnel, 1999).

The NE-SW Aravalli trend, E-W Delhi trend, ENE-WSW Satpura trend along the Narmada – Son lineament and NE-SW Eastern Ghats trend are the other prominent Precambrian trends in the northern part of western India. The presence of major NW-SE, NNW-SSE, ENE-WSW, NE-SW and N-S trending Precambrian structural trends on the western continental margin of India are established from geophysical studies (Balakrishna and Sharma, 1981; Biswas, 1982, 1987; Gopala Rao, 1984; Bhattacharya and Subrahmanyam, 1986; Ramana, 1986; Subrahmanyam, 1987; Biswas and Singh, 1988; Subrahmanyam et al., 1989, 1991). Kolla and Coumes (1990) have summarized various structural and tectonic trends which extend from the Indian subcontinent into the eastern Arabian Sea.

### 2.2.9 Deccan Traps

The Deccan continental flood basalt province, which is known as Deccan Traps, is one of the largest known continental flood basalt provinces formed by a series of volcanic eruptions at Chron 29r about 65.5 Ma (Vandamme et al., 1991; Courtillot and Renne, 2003). The emplacement of Deccan Traps, lasted for less than 1 My, was more or less coincident with the India-Seychelles breakup (Norton and Sclater, 1979; Courtillot et al., 1986; Hooper, 1990; Devey and Stephens, 1991). It has uniform tholeiitic basalt composition (Wellman and McElhinny, 1970) and an

than 10 km and a minimum thickness of less than 2 km are identified at the proximal and distal areas of the fan (Naini and Kolla, 1982). The results from the DSDP sites 220 to 223 reveal that the Indus Fan sedimentation in the Arabian Sea began in the Late Oligocene by turbidity currents.

## 2.3 Subsidence and sedimentation history

The drifting of the Indian subcontinent from southern hemisphere to northern hemisphere after separation from Madagascar, the upliftment of the western part of the Indian peninsula by the impact of Rèunion hotspot, and the collision of Indian subcontinent with the Eurasian had profound impacts on the subsidence and sedimentation history of the WCMI. Various results on drill well and marine geomorphic studies suggest that the WCMI have undergone considerable amount of subsidence at various stages of its evolution. The subsidence of the WCMI can be divided into two components, i) an initial episode of rapid subsidence accompanying active extension, ii) a long period of thermal subsidence that tends to be regionally distributed and decreases as a function of time (Whiting et al., 2001) since the cessation of rifting. This post rift subsidence is a consequence of the cooling and isostatic adjustment of the lithosphere following the extension. Subsidence studies of the WCMI have recognized not only the slow post rift subsidence component but also a relatively rapid phase of subsidence which occurred late in the history of the basin (Mohan, 1985) during the Late Oligocene to Early Miocene. Gombos et al. (1995) interpreted that the Kerala–Konkan Basin, begun with rapid initial subsidence, followed a normal subsidence throughout the Cenozoic similar to a rifted passive margin.

Various studies on subsidence of the margin indicated that the different geological domains of the margin have subsided at different rates. Sedimentation record at DSDP site 219, located at the crest of the Laccadive Ridge, suggested 2075 m of subsidence since early to late Paleocene time (Shipboard scientific party, 1988). A subsidence of about 1980 m is inferred for the basement of Bombay High region, off Mumbai since the Oligocene (Raju et al., 1999). The observations made by Bhattacharya et al. (1994b) on the relict dendritic drainage patterns of Laxmi Basin seamount chain suggested a subsidence of at least 3700 m.

The sedimentation history of the study area suggests that the sedimentation in the Kerala-Konkan Basin occurred in shallow depths of < 100 m during the Late Cretaceous (~85 Ma) (Raju et al., 1999). The basin became major depocentre at 85 – 75 Ma as its depth increased to > 200 m. However the onset of rifting between India and Seychelles, and Rèunion hotspot activity led to a decrease in basin depth by the uplift to near sea level during 65 to 60 Ma. Later, re-submergence of the basin occurred in the Paleocene/Eocene following a period of non deposition (Campanile et al., 2008). Even though the sedimentation in the southwest offshore basins is evident since the Cretaceous period, most of the studies document the sedimentation history only since the Paleocene (Ramaswamy and Rao, 1980; Raju et al., 1981; Mohan, 1985; Pandey, 1986; Nair et al., 1992; Rao, 1994; Pandey and Dave, 1998; Chaubey et al., 2002b; Campanile et al., 2008). The results of analyses of drill well information from the continental shelf region suggests that the western margin of India experienced heavy influx of terrigenous clastic sediments after the Middle Miocene. This post Middle Miocene terrigenous influx coincides with the emergence of Himalaya and onset of Indian Monsoon (Valdiya, 1999). As a result of these two developments, accelerated weathering and erosion of the Indian landmass brought heavy terrigenous influx into the continental shelf and offshore basins, and generated large Indus Fan sedimentation in the Arabian Basin. Prior to the Middle Miocene the depositional conditions over the SWCMI were conducive for pelagic carbonate sedimentation since Indo-Madagascar break up. The development of the thick pelagic carbonate sequence throughout the basins of the SWCMI has been linked to increased sea level, and warmer climate in the Middle Miocene (Clift et al., 2001; Molnar, 2004) when the Indian subcontinent was in the warm latitude belt of the equator with very low terrigenous influx.

The depositional history of the southern basins is different from that of the northern basins. Sediments deposited in the northern basins (north of the Vengurla Arch) are not derived solely from the denudation of the Western Ghats. Instead, they contain sediments from Deccan Continental Flood Basalt terrain, Cambay and Kutch grabens, as well as from the Indus Fan (Rao and Rao, 1995). The northern basins contain larger volumes of Mesozoic sediments and rifted remnants of the extensive sub-aerial volcanism generated during the Deccan

eruptive episodes. Thus the northern basins generally have a basaltic source. Whereas the sediments deposited in the southern basins have a gneissic source (Rao and Rao, 1995; Rao and Wagle, 1997; Kessarker et al., 2003). This indicates that the southern basins are closed sediment sinks for the erosional products of the Western Ghats. Based on the percentage of the mineral smectite in the present day sediments of the shelf and offshore regions of SW India, Kolla et al. (1981) suggested that the Narmada and Tapti rivers of the western Peninsular India are the major sediment contributors to the western continental shelf region of India. Sediments are also being brought by the surface water currents from the Bay of Bengal to the southwest region of WCMI. Based on the observations of high percentage of illite in most parts of the deep offshore regions, Kolla et al. (1981) concluded that the Indus Fan is the main source for sedimentation in the deep offshore basins at present. Even though the rate of present day terrigenous sedimentation is very high in the deep sea basins, the physiographic highs in the basins experience pelagic sedimentation regime on their crest.

## 2.4 General Stratigraphy

Sedimentation along the SWCMI is mainly found within the coast parallel basins separated by major structural features. The southern sediment basins of gneissic source are compartmentalized from the sediments of basaltic origin from the north due to presence of the Laccadive Ridge and basement highs. The Kerala-Konkan and Laccadive basins are the major depocentre for the onshore denudation of sediment especially from Western Ghats. The huge terrigenous sediments deposited on the continental shelf basins are transferred to the offshore basins by means of river canyons and slumping. The Upper Cretaceous, early rift phase sedimentation in the Kerala-Konkan Basin is localized in narrow grabens southwest of Cochin. This sedimentation took place in shallow continental settings (Singh and Lal, 1993).

Seismic reflection profiles across the Southwest Continental Margin of India indicate a total sediment thickness ranging from 0.5 to 3.5 sec (TWT) over the Laccadive Ridge, and the presence of differential movements of stratigraphic

columns with respect to the prevailing fault system (Rao and Srivastava, 1984). They have interpreted four major seismic sequences from the Kerala-Konkan and Laccadive Basins based on the analysis of seismic reflection profiles across the SWCMI. The interpreted seismic sequences are named as i) Sequence I, a lower sequence identified with basement and mostly characterized by the absence of correlatable reflectors, ii) Sequence II, comprised of Paleogene sediments, iii) Sequence III of Miocene sediments and iv) Sequence IV, an upper sequence of post Miocene sediments. Whereas, Chaubey et al. (2002b) interpreted six seismic sequences, H1 – H6 (Paleocene to Recent) from the outer shelf and Laccadive Basin, and L1 – L6 (Eocene to Recent) over the Laccadive Ridge by analyzing a MCS reflection profile across the central-western continental margin of India. The stratigraphic range for these interpreted seismic sequences are assigned by correlating them with the drill well results of KR-1 (Singh and Lal, 1993; Pandey and Dave, 1998) and DSDP site 219 (Whitmarsh et al., 1974), global seal-level curve (Haq et al., 1987) and published results (Ramaswamy and Rao, 1980; Biswas and Singh, 1988). They have also identified a well marked Middle Miocene unconformity separating carbonate and clastic sedimentation. The bottom layer identified over the Laccadive Ridge is interpreted as the Chert layer of Early - Middle Eocene age. In a recent study, Campanile et al. (2008) combined the seismic sequences of Rao and Srivastava (1984) and Chaubey et al. (2002b) and revised chronostratigraphy as i) Late Cretaceous to Late Oligocene, ii) Late Oligocene to Late Pleistocene, and iii) Late Pleistocene to Recent.

The published drill well results from SWCMI (Singh and Lal, 1993; Gunnell, 2001; Rao et al., 2002; Pandey and Dave, 1998) suggests a thick carbonate sediment accumulation of Eocene to Middle Miocene sandwiched between clastic dominated sequences. The widespread carbonate sedimentation under stable platform conditions (Aubert and Droxler, 1996) during the Eocene to Middle Miocene are reported on the shelf (Rao and Srivastava, 1984; Nair et al., 1992). The identified depositional breaks in the Middle Paleocene, Early Eocene, Late Eocene – Early Oligocene and Lower to Middle Miocene are marked as major unconformity surfaces in the Kerala-Konkan Basin (Singh and Lal, 1993). Major sedimentary litho-stratigraphic units identified in the Kerala-Konkan Basin include, 1) Cochin, 2) Kasargod, 3) Karwar, 4) Calicut, 5) Quilon, 6) Mangalore, 7) Warkali

and 8) Vembanad formations (Nair and Rao, 1980; Singh and Lal, 1993; Rao et al., 2002). The Warkali and Vembanad formations are conspicuous only in the southern part of the WCMI along shallow continental shelf and coastal regions. From the northern part of the WCMI, considerably thick Panaji sedimentary formation is also identified.

Arabian basin is characterized by markedly thicker Indus Fan sediments. The results of DSDP site 221 suggest that the illite rich sediments characteristic of Indus Fan sediments started deposition in the distal Arabian Basin prior to the Late Oligocene (Whitmarsh, 1974). Naini (1980) suggested that the Indus Fan sedimentation reaches over 3 km in the Arabian Basin at places. The pelagic and turbidite sedimentation in the Arabian Basin is divided by a major unconformity surface of Early to Late Oligocene age (Chaubey et al., 2002b).

## 2.5 Evolution of the WCMI

The WCMI is mainly evolved due to reactivation of existing major faults and weak zones along the Precambrian structural trends by (i) rifting between India and Madagascar during the Late Cretaceous, (ii) short span of rifting between Seychelles-Laxmi Ridge and India, and (iii) rifting between Laxmi Ridge-India and Seychelles during the early-Tertiary. Several studies (McKenzie and Sclater 1971, Norton and Sclater, 1979; Schlich, 1982; Besse and Courtillot, 1988; Courtillot et al., 1988; Scotese et al., 1988; White and McKenzie, 1989; Royer et al., 1989; Bhattacharya et al., 1994a; Storey, 1995; Storey et al., 1995; Reeves and de Wit, 2000; Reeves and Leven., 2001; Royer et al., 2002) on paleogeographic reconstruction have revealed major tectonic events of the evolution of the WCMI. Since the study area is a part of the WCMI, major tectonic episodes in the development of WCMI, based on the results of the above studies and two review articles (Bhattacharya and Chaubey, 2001; Krishna et al., 2010), is briefly presented below.

### 2.5.1 Breakup of Madagascar from Seychelles-India

The first major tectonic event in the development of the western continental margin of India was the breakup of Madagascar from Seychelles-India block

during the Late Cretaceous (Norton and Sclater, 1979; Patriat and Segoufin, 1988; Scotese et al., 1988; White and McKenzie 1989; Storey, 1995; Storey et al., 1995; Torsvik et al., 1998, 2000; Raval and Veeraswamy, 2003; Sreejith et al., 2008). The rifting of Madagascar-Seychelles-India block took place along ancient Dharwar structural trends (NNW-SSE), under the influence of Marion hotspot. The associated hotspot volcanism is reported along the east coast of Madagascar (Vallier, 1974). Norton and Sclater (1979) have opined that if similar volcanism existed in southwest India, its record might have been obliterated by the later volcanic event of the Rèunion hotspot. However, basaltic flows and magmatic intrusives related to Marion hotspot volcanism are found in the southwest India (Radhakrishna et al., 1994; Anilkumar et al., 2001; Pande et al., 2001). Magmatism related to the Marion hotspot is recorded in the Cretaceous Dolerite (91.6 ± 0.3 Ma) of Madagascar (Torsvik et al., 1998) and columnar acid volcanics of St. Mary Islands (85.6 ± 0.9 Ma) off sothwest India (Pande et al., 2001).

Seafloor spreading between India-Seychelles and Madagascar started opening the Mascarene Basin shortly before magnetic chron 34 ny (~83 Ma; Norton and Sclater, 1979; Morgon, 1981; Besse and Courtillot, 1988; Muller et al., 1993) and established a three plate system with a triple junction at 55°S, known as Rodrigues Triple Junction, in the western Indian Ocean (Besse and Courtillot, 1988). Based on dated onshore volcanics, this separation is considered to have been initiated around 88–93 Ma (Valsangkar et al., 1981; Storey et al., 1995; Torsvik et al., 2000; Pande et al., 2001; Anil Kumar et al., 2001). In a recent study, Yatheesh et al. (2006) suggested about 86.5 Ma for the separation of Madagascar from Seychelles-India based on modified finite rotation parameters of Norton and Sclater (1979).

The separation of Madagascar from Seychelles-India block shaped the southwest continental margin of India. The NNW-SSE trending Precambrian structural trends on both the continental blocks are nearly parallel to the general trend of the southwest continental margin of India and the eastern continental margin of Madagascar (Curray, 1980). After the Madagascar separation, the Seychelles-India block continued its rapid northward drift with gradual counter clockwise rotation (Patriat and Achache, 1984) due to extremely high spreading rate (12-13

cm/yr) in the Mascarene Basin between the chrons 34 and 28 (Norton and Sclater, 1979).

### 2.5.2 Rifting between Seychelles-Laxmi Ridge and India

A short span of rifting between Seychelles-Laxmi Ridge and India, which is considered as the second major tectonic event in the evolution of WCMI, took place during the Late Cretaceous. The Laxmi Basin evolved during this phase of rifting. This rifting event was contemporaneous with the Rèunion hotspot volcanic activity (69-65 Ma; White and McKenzie, 1989). It has not yet been conclusively established whether seafloor spreading followed this rift event or not. The studies carried out so far (Naini and Talwani 1983; Bhattacharya et al., 1994a; Talwani and Reif, 1998; Todal and Eldholm, 1998; Radhakrishana et al., 2002; Krishna et al., 2006) are equivocal in establishing the nature of crust below the Laxmi Basin.

### 2.5.3 Breakup between Seychelles and Laxmi Ridge-India

The separation of Seychelles from Indian subcontinent during Early Paleocene is considered as the third major tectonic event in the evolution of the western continental margin of India. During the course of northward drift of Indian Plate, the Seychelles-India continental block came over the Réunion hotspot at the end of Late Cretaceous (Courtillot et al., 1986; Vandamme et al., 1991; Bhattacharji et al., 1996). The Réunion hotspot activity caused widespread volcanism over the Indian landmass and created the Deccan Continental Flood Basalt (DCFB) province on western and central India (Duncan, 1990) as well as continental flood basalt on the Praslin Island of the Seychelles (Devey and Stephens, 1991). The DCFB mainly erupted in less than 1 My during chron 29r (~65.6 - 64.8; Coutillot et al., 1988). The extrusion of DCFB is inferred as late syn-rift to breakup volcanism, contemporaneous with separation between Seychelles and Laxmi Ridge-India (Todal and Eldholm, 1998). Seafloor spreading between Seychelles and Laxmi Ridge-India started at chron 28ny by spreading ridge propagation and initiated evolving conjugate Arabian and eastern Somali basins (Chaubey et al., 2002a and Royer et al., 2002 and references there in). Réunion hotspot related volcanism occurred from continental to oceanic lithosphere as the Indian Plate

moved northward at a velocity of about 13.5 cm/yr between 83 and 48 Ma. As a result the adjacent offshore area came under the influence of the Réunion hotspot and received large amount of volcanics within the stretched continental crust obliterating the pre-existing geology and initial configuration of SWCMI.

### 2.5.4 India-Eurasia collision

The India-Eurasia continental collision is another major tectonic event which played important role in the evolution of the WCMI. As a result of rapid northward drift, the Indian subcontinent came in contact with the Eurasian plate along the Kohistan-Ladakh Island arc system, closing the Neo-Tethys Sea along Indus-Zangbo suture by subduction under the Eurasian margin in Early Eocene (~50 Ma; Sengör, 1979; Windley, 1996; Storey, 1995; Aacharya, 2000). This event which is termed as 'soft collision' or the first contact between India and Eurasia coincides with drastically reduced seafloor spreading rates in the Indian Ocean (Patriat and Achache, 1984; Patriat and Segoufin, 1988; Chaubey et al., 1993). Major reorganization of the spreading geometry in the Indian Ocean took place during this waning phase of seafloor spreading (McKenzie and Sclater, 1971; Norton and Sclater, 1979; Schich, 1982; Chaubey et al., 1993, 1998 and 2002a; Royer et al., 2002). Consequent to the continued collision between India and Eurasia the spreading along the Carlsberg Ridge almost stopped or became imperceptible during anomaly 18N (~47 Ma; Chaubey et al., 1993, 1998). Due to this relative tectonic quiescence the spreading ridge cooled and rapidly subsided causing increase in volume of the ocean basin and emerging the continents by consequent marine regression (Windley, 1996). As a result of this, many parts of the western Indian Ocean would have emerged resulting into its observed Eocene to Oligocene widespread depositional hiatus (Bhattacharya and Chaubey, 2001). The seafloor spreading along the Carlsberg Ridge rejuvenated shortly before the formation of anomaly 11 of Early Oligocene (~31 Ma) with a slow rate of 0.7 cm/year till anomaly 6. This rate of spreading increased between chrons 5c and 6A to about 1.2 cm/yr and continues till today (Chaubey et al., 1993).

# Chapter-3

# GEOLOGICAL AND GEOPHYSICAL DATA

# Chapter-3

# GEOLOGICAL AND GEOPHYSICAL DATA

## 3.1 Introduction

Major dataset used for this study comprise of 2D Multi Channel Seismic (MCS) reflection, ship borne gravity and satellite altimetry derived free-air gravity anomaly data. Published results of i) seismic refraction studies from the Arabian Sea, ii) Deep Seismic Sounding studies on adjacent onshore region, iii) drill well studies along the SWCMI, and iv) magnetic isochron of the Arabian Basin are used as supporting database for the present study. Besides, bathymetry data of the Arabian Sea from General Bathymetric Chart of the Oceans (GEBCO) is used to plot the bathymetry contours of the study area. This chapter describes the types and sources of the data used for the study.

## 3.2 Seismic reflection data

2D multi channel seismic data includes twelve reflection profiles of ~6455 line km (Table 3.1) acquired across the southwest continental margin of India spanning continental shelf, slope, Laccadive Basin, Laccadive Ridge and eastern part of the Arabian Basin (Figure 3.1). Out of these seismic profiles, six reflection profiles (RE23, RE21, RE19, RE17, RE15 and RE13) of about 3043 line km, acquired by the Oil and Natural Gas Corporation (ONGC) during 1979-80, are used for seismic sequence stratigraphic analysis and demarcation of structural features along the SWCMI. These reflection profiles were collected in 100 to 4000 m water depth onboard *M/V Anweshak* using Digital Field System-IV (DFS-IV) instrument with 48-channel seismic streamer and bolt type air gun array of 10 liters total capacity as a controlled seismic source. A recording duration of 8 s, a sampling interval of 4 ms and a shot interval of 50 m were chosen with a ship speed of 3-4 knots to achieve a 12-fold coverage during the data acquisition (Table 3.2). The data were processed by the ONGC at the Computer Services Division, Institute of Petroleum Exploration, Dehradun and stacked seismic sections were generated.

**Table 3. 1** MCS reflection datasets used for the present study

| Sl. No. | Seismic line | Length (km) | Water depth (TWT) | Type |
|---|---|---|---|---|
| 1 | RE23 | 472 | 0.1 – 4.6 | Multi channel |
| 2 | RE21 | 410 | 0.15 – 3.9 | Multi channel |
| 3 | RE19 | 400 | 0.65 – 5.25 | Multi channel |
| 4 | RE17 | 460 | 0.17 – 5 | Multi channel |
| 5 | RE15 | 852 | 0.25 – 5.7 | Multi channel |
| 6 | RE13 | 449 | 0.2 – 5.45 | Multi channel |
| 7 | SK1203 | 881 | 0.4 – 6.17 | Multi channel |
| 8 | SK1206 | 772 | 0.2 – 5.8 | Multi channel |
| 9 | SK0518 | 243 | 0.2 – 2.56 | Multi channel |
| 10 | SK1201 | 250 | 0.2 – 3.38 | Multi channel |
| 11 | SK1207 | 754 | 0.2 – 5.77 | Multi channel |
| 12 | SK1208 | 512 | 0.21 – 5.51 | Multi channel |

Other six seismic reflection profiles (SK0518, SK1201, SK1203, SK1206, SK1207 and SK1208) of 3412 line km, used in this study to demarcate structural features, were collected during 1983-1985 onboard *ORV Sagar Kanya* by the National Institute of Oceanography, Goa. The data were acquired using DFS-V seismic system with 24-channel seismic streamer at a ship speed of 4-5 knots. A recording length of 8 s and a sampling interval of 4 ms were chosen to achieve a 12-fold coverage. The seismic source consisted a D-type air gun array - combination of 7 air guns spaced at varied intervals - of 7.98 liters total capacity. The data were processed at NIO, Goa using standard processing packages "NORSEIS" and "ProMAX-2D" to obtain stacked seismic sections. The seismic data SK0518, SK1201, SK1203 and SK1206 are processed for two near channels data, whereas, SK1207 is processed for all 24 channel data. The parameters of acquisition of marine seismic data are given in Table 3.2.

The hard copy seismic sections of ONGC data were generated with a horizontal scale of 1 inch = 2.54 km and vertical scale of 2.5 inch = 1 sec of TWT. Whereas, the MCS sections of SK1207 were generated with a horizontal scale of 1 inch = 833 m and vertical scale of 4 inches = 1 sec of TWT. Further, seismic data

stacked for two near channels were used to generate hard copy seismic sections with a horizontal scale of 1 inch = 6.25 km and vertical scale of 4 inches = 1 sec of TWT.

**Table 3.2** Acquisition parameters of marine seismic reflection data

| Sl. No. | | ONGC data | NIO data |
|---|---|---|---|
| 1 | Vessel | M/V Anweshak | ORV Sagar Kanya |
| 2. | Recording year | 1979-80 | 1983-85 |
| **Recording system** | | | |
| 3 | Instrument type | DFS-IV | DFS-V |
| 4. | Recording format | SEG-B | SEG-B |
| 5. | Recording filter | 0-62 Hz | 4-64 Hz |
| 6. | Sample interval | 4 ms | 4 ms |
| 7. | Record length | 8 s | 8 s |
| **Streamer** | | | |
| 8. | Length | 2350 m | 575 |
| 9. | Number of channels | 48 | 24 |
| 10 | Receivers per channel | 46 | 32 |
| 11 | Receiver interval | 50 m | 25 m |
| 12 | Towing depth below Sealevel | 10 m | 10 m |
| 13 | Distance from navigation antenna to source | 55 m | 95 m |
| 14 | Location of channel 1 | Farthest from vessel | Near to source |
| 15 | Location of channel 48 | Near to source | Farthest from vessel |
| **Positioning system** | | | |
| 16 | Navigation system | SATNAV | Integrated Navigational System using dual channel satellite receiver |
| **Energy source** | | | |
| 17 | Source type | B-type Air gun array | D-type Air gun array |
| 18 | Air gun array volume | 10 Liters | 7.98 Liters |
| 20 | Towing depth of air gun below sea surface | 6 m | 6 m |
| 21 | Near offset | 265 m | 175 m |
| 22 | Far offset | 2615 m | 750 m |
| 23 | Shot interval | 50 m | 25 m |
| 24 | Recording configuration | End On | End On |

## 3.3 Free-air gravity anomaly data

Free-air gravity anomaly data along five seismic lines (RE15, RE17, RE19, RE21 and RE23) are used in this study to generate 2D crustal models across the SWCMI. The gravity anomaly profiles have been reconstructed using satellite altimetry derived free-air gravity anomalies whereever shipborne free-air gravity anomaly data were either partly available or absent. The satellite altimetry derived free-air gravity anomaly data of the study area is also used to demarcate the major structural and tectonic features of the study area.

The shipborne gravity data have been acquired simultaneously with MCS reflection data along the seismic lines using Lacoste-Rhomberg gravimeter onboard *M/V Anweshak*. Free-air gravity anomalies were then computed after applying Eötvos correction and normal gravity at each observation point.

Satellite free-air gravity anomaly data are obtained from gridded database of Sandwell and Smith (1997). The data were derived from closely spaced satellite altimeter profiles collected during the Geosat Geodetic Mission (~6 km) and the ERS 1 Geodetic phase (8 km). Accuracy of the satellite altimetry derived free-air gravity anomaly data is reported as 4-7 mGal by a comparison with shipboard gravity data for random ship tracks (Sandwell and Smith, 1997).

## 3.4 Seismic refraction data

In the present study, seismic refraction results are used to define crustal layers, compute density of various crustal layers and derive information on basement depth anomalies. The details of refraction stations and P-wave seismic velocities (Francis and Shor, 1966; Rao, 1970; Naini and Talwani, 1983) in the study area are compiled and presented in Table 3.3 and Table 3.4. The seismic velocity structures are derived from the refraction data based on short-range as well as long-range sonobuoy refraction surveys (Naini and Talwani, 1983). The data were collected onboard the Lamont-Doherty Geological Observatory research vessels Robert D. Conrad and Vema, equipped with 3.5 kHz and 12 kHz precision depth recording devices, during 1974 and 1977. An air gun sound source was used for

shorter source-receiver distance less than 25 km. The air gun was replaced by explosives at longer source-receiver distances beyond 25 km where the returning refracted waves are attenuated.

Moho was not detected on the Laccadive Ridge, Laccadive Basin and adjoining continental shelf region of the study area, even in long range sonobuoy refraction survey (Naini and Talwani, 1983). It may be mentioned here that Moho was not observed at any of the refraction stations located on entire WCMI. However, minimum depth to Moho was reported assuming P-wave velocity of 8.2 km/s for the upper mantle. In the Arabian Basin, Moho was observed at an average depth of about 11.5 km at nine stations with velocities ranging between 7.9 and 8.3 km/s. In order to derive crustal structure of the continental shelf, Deep Seismic Sounding (DSS) studies carried out by National Geophysical Research Institute, Hyderabad on adjoining onshore region are compiled (Kaila et al., 1979; Sarkar et al., 2001; Reddy, 2005) and presented in Table 3.5.

## 3.5 Drill well data

Drill well information (Table 3.6) along the SWCMI, available in public domain (Whitmarsh et al., 1974; Singh and Lal, 1993; Pandey and Dave, 1998; Rao et al., 2002) are compiled to study litho-stratigraphy and sedimentation history of the study area. Eight drill wells spatially distributed in the continental shelf, slope and Laccadive Ridge (Figure 3.1) are utilized in the present study. A stratigraphic chart (Figure 3.2) prepared for the Kerala-Konkan Basin by Mathur et al. (1993) and modified by Rao et al. (2002) is also used to derive litho- and chrono-stratigraphic information of the study area.

**Table 3.3** Details of refraction stations and P-wave velocity structure in the Arabian Basin

| Sl. No. | Refraction stations | Location | | Water depth (km) | Sediment layer | | Oceanic layer II | | Oceanic layer III | | Depth to Moho (km) |
|---|---|---|---|---|---|---|---|---|---|---|---|
| | | Lat. (Deg.) | Long. (Deg.) | | Av. Vel. (km/s) | Thickness (km) | Av. Vel. (km/s) | Thickness (km) | Av. Vel. (km/s) | Thickness (km) | |
| 1 | ST2-3 | 07.367 | 70.666 | 3.940 | 2.150 | 0.880 | 5.400 | 1.300 | 6.630 | 3.100 | 09.220 |
| 2 | 133V | 09.130 | 63.840 | 4.361 | 1.750 | 0.925 | 5.311 | 2.168 | 6.667 | 0.368 | 11.800 |
| 3 | 74V | 09.850 | 68.336 | 4.340 | 2.480 | - | - | - | - | - | - |
| 4 | 53V | 11.200 | 65.470 | 4.198 | 2.210 | 0.980 | 5.200 | 1.690 | 6.700 | - | - |
| 5 | 65C | 11.333 | 66.033 | 4.220 | 2.213 | 1.300 | 5.400 | 1.410 | 6.650 | - | - |
| 6 | 73V | 11.886 | 66.956 | 4.128 | 2.865 | 1.380 | 5.700 | 2.430 | 6.600 | - | - |
| 7 | 84C | 12.580 | 68.326 | 4.120 | 2.780 | 1.430 | 5.500 | 1.700 | 6.600 | - | - |
| 8 | 52V | 12.786 | 65.036 | 3.996 | 2.420 | 2.050 | 5.600 | 1.120 | 6.600 | 4.660 | 11.826 |
| 9 | 66C | 12.905 | 66.022 | 4.030 | 2.440 | 1.950 | 5.750 | 1.510 | 6.600 | - | - |
| 10 | 54V | 13.168 | 67.118 | 3.983 | 2.585 | 1.850 | 5.400 | 1.280 | 6.600 | - | - |
| 11 | 72V | 13.268 | 69.450 | 4.017 | 2.750 | 1.440 | 5.500 | 1.180 | 6.400 | - | - |
| 12 | 70V | 13.686 | 67.236 | 3.814 | 2.695 | 2.660 | 5.700 | 1.300 | 6.600 | 2.410 | 10.184 |
| 13 | 66V | 13.800 | 63.550 | 3.992 | 2.623 | 2.750 | 5.100 | 1.520 | 6.500 | 2.840 | 11.102 |
| 14 | 67C | 14.543 | 66.072 | 3.780 | 2.353 | 3.490 | 5.600 | - | - | - | - |
| 15 | 68C | 14.698 | 66.078 | 3.840 | 2.730 | 3.550 | 5.500 | 2.080 | 6.800 | - | - |
| 16 | 55V | 14.906 | 67.350 | 3.769 | 2.395 | 2.290 | 5.300 | 1.840 | 6.600 | 2.420 | 10.319 |
| 17 | 64V | 15.236 | 66.206 | 3.703 | 2.732 | 3.380 | 5.100 | 1.780 | 6.700 | 2.650 | 11.513 |
| 18 | 80C | 15.988 | 67.348 | 3.720 | 2.105 | 0.970 | 5.600 | - | - | - | - |
| 19 | 69C | 15.993 | 66.106 | 3.730 | 2.740 | 3.070 | 5.500 | 1.400 | 6.700 | - | - |
| 20 | 70C | 16.896 | 66.148 | 3.580 | 2.770 | 3.770 | 5.600 | - | - | - | - |
| 21 | 61V | 17.586 | 63.900 | 3.505 | 2.747 | 3.640 | 5.400 | 2.310 | 6.800 | 3.630 | 13.085 |

All refraction derived P-wave velocity data are compiled from Naini and Talwani (1983), except for the refraction station ST2-3 which is from Francis and Shor (1966).

**Table 3.4** Details of refraction stations and P-wave velocity structure of the southwest continental margin of India

| Sl. No. | Refraction stations | Location | | Water depth (km) | Sediment layer | | Chert/Basalt flow ? | | Meta sediment ? | | Upper cont. crust | | Lower cont. crust | |
|---|---|---|---|---|---|---|---|---|---|---|---|---|---|---|
| | | Lat. (Deg.) | Long (Deg.) | | Av. Vel. (km/s) | Thick-ness (km) | Av. Vel. (km/s) | Thick-ness (km) | Av. Vel. (km/s) | Thick-ness (km) | Av. Vel. (km/s) | Thick-ness (km) | Av. Vel. (km/s) | Thick-ness (km) |
| 1 | 88C | 07.905 | 77.192 | 0.060 | 1.68 | 0.169 | 4.10 | - | - | - | - | - | - | - |
| 2 | 87C | 10.807 | 75.438 | 0.056 | 1.65 | 0.478 | 4.50 | - | - | - | - | - | - | - |
| 3 | L08 | 11.906 | 71.175 | 2.135 | 1.88 | 0.830 | 4.40 | 0.66 | 5.60 | 1.49 | 6.30 | 4.69 | 7.2 | 8.4 |
| 4 | 85C | 15.015 | 73.602 | 0.016 | 2.41 | 2.410 | - | - | - | - | 6.40 | - | - | - |
| 5 | S4 | 15.472 | 73.558 | 0.090 | 2.15 | 2.530 | 4.40 | 3.14 | - | - | 6.40 | - | - | - |
| 6 | L12V | 14.275 | 70.000 | 3.628 | 2.00 | 0.43 | 4.20 | 1.70 | 5.70 | 1.93 | 6.30 | 1.84 | 7.30 | 7.99 |
| 7 | L13V | 10.556 | 70.386 | 3.779 | 1.74 | 0.52 | - | - | 5.40 | 1.80 | 6.10 | 2.88 | 7.20 | 8.40 |

All refraction derived P-wave velocity data are compiled from Naini and Talwani (1983), except for the refraction station S4 which is from Rao (1970).

**Table 3.5** P-wave velocity structure derived from DSS studies on western Dharwar Craton

| Crustal layers | Velocity range (km/s) | Depth range (km) | Thickness (km) |
|---|---|---|---|
| Dharwar schist | 5.5 – 5.8 | 2 – 15 | 13 |
| Upper crust | 6.0 – 6.65 | 15 – 23 | 8 |
| Lower crust | 6.8 – 7.1 | 23 – 40 | 17 |
| Moho | 8.1 – 8.4 | > 40 | - |

Compiled from Kaila et al. (1979); Sarkar et al. (2001) and Reddy (2005)

**Table 3.6** Compiled drill wells in the study area

| Sl. No. | Name of Wells | Water depth (km) | Basement depth (km) | Geographic location |
|---|---|---|---|---|
| 1 | CH-1-1 | 0.13 | 3.93 | Continental shelf |
| 2 | K-1-1 | 0.05 | -- | Continental shelf |
| 3 | KK-OS-VI-1 | 0.08 | 2.24 | Continental shelf |
| 4 | KG-1-1 | 0.21 | -- | Continental slope |
| 5 | KR-1-1 | 0.11 | -- | Continental shelf |
| 6 | KK-OS-II/B-1 | 0.34 | 2.71 | Continental slope |
| 7 | Well-D | 0.08 | 1.89 | Continental shelf |
| 8 | DSDP-219 | 1.76 | 2.18 | Laccadive Ridge |
| 9 | DSDP-220 | 4.04 | 4.39 | Arabian Basin |
| 10 | DSDP-221 | 4.65 | 4.92 | Arabian Basin |

## 3.6 Other data sets

Magnetic isochron map of the Arabian Basin, tectonic chart of the SW India and data from General Bathymetric Chart of the Oceans are used to derive supporting database for the present study. The seafloor spreading type magnetic lineations of the Arabian Basin were digitized from the magnetic isochron map of Chaubey et al. (2002a) and database was prepared to derive age of oceanic basement of the Arabian Basin following polarity chron nomenclature proposed by Cande and Kent (1995). The digital bathymetry data of the study area was retrieved from the GEBCO database of National Geophysical Data Centre (NGDC), Colorado, USA. Published structural trends of the study area and adjoining region are digitized from the tectonic chart of SW India, and a digital database of major structural trends are prepared. This database is used to plot the major structural and tectonic features of the study area to facilitate the present study.

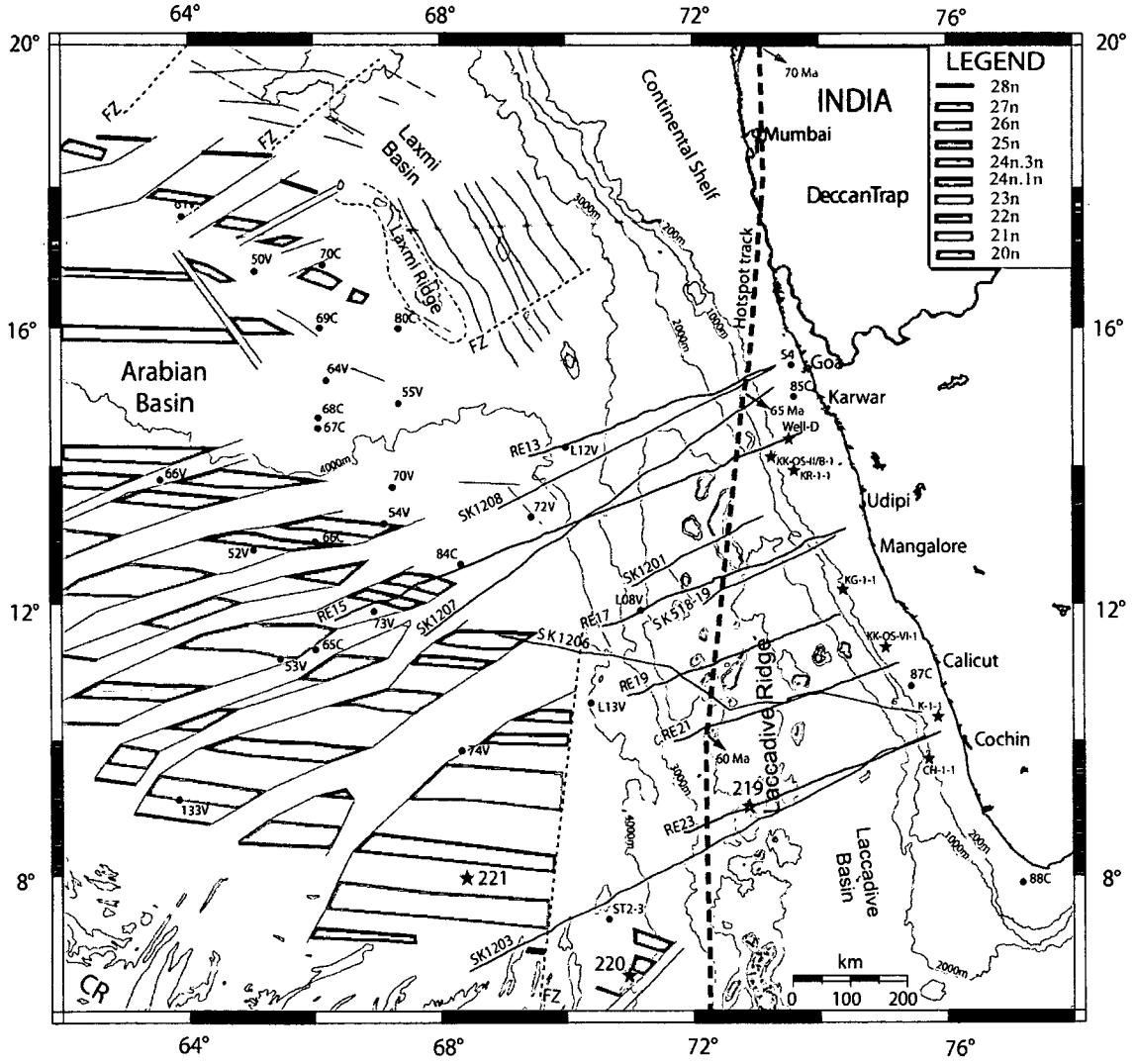


**Figure 3.1** Map showing seismic lines along which seismic reflection data are acquired (black annotated lines), locations of seismic refraction stations (solid annotated dots; Naini and Talwani, 1983), magnetic lineations (coloured blocks), pseudofaults (thin blue lines), fracture zones (dashed blue lines annotated as FZ) (Chaubey et al., 2002a). DSDP and ONGC drill sites are shown by solid stars (Whitmarsh et al., 1974; Singh and Lal, 1993; Pandey and Dave, 1998 and Rao et al., 2002); solid thick dashed line represents the computer-modeled Rèunion hotspot track with predicted ages in Ma (blue annotated arrows) (Shipboard Scientific Party, 1988); magnetic lineations in the Laxmi Basin (thin brown lines; Bhattacharya et al., 1994a; Malod et al., 1997).

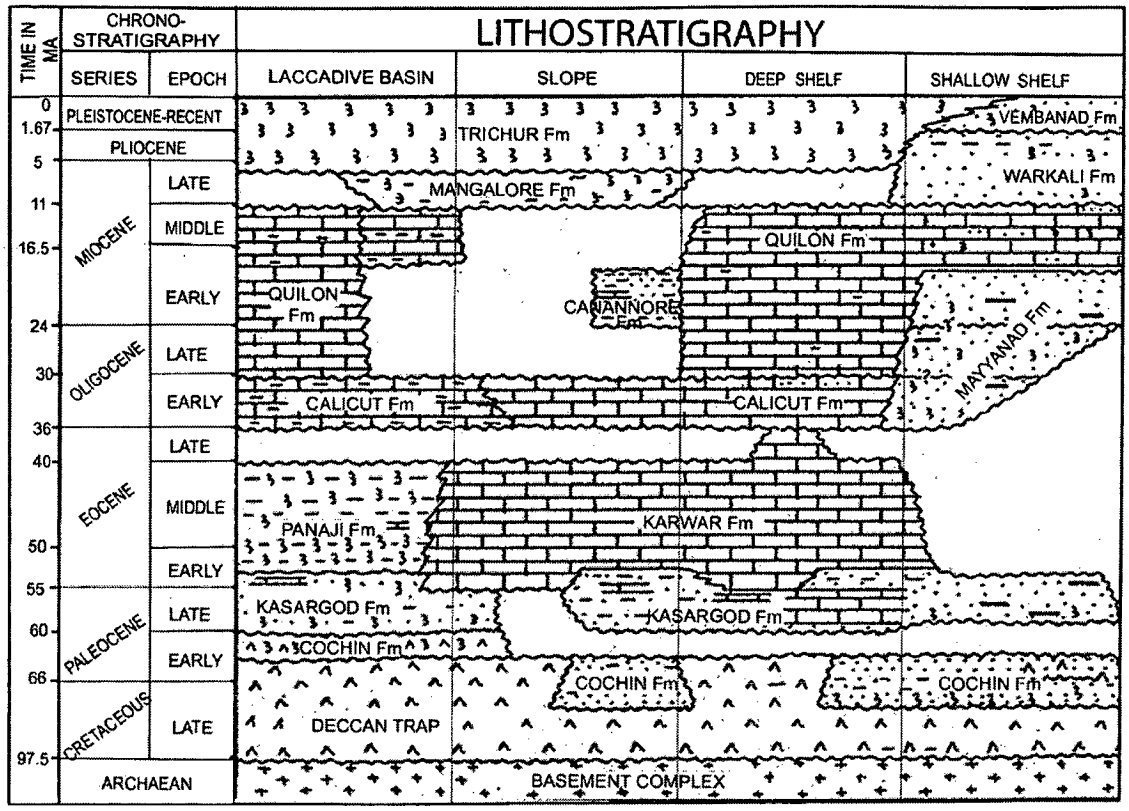


**Figure 3.2** Stratigraphic chart of the Kerala-Konkan Basin (Mathur et al., 1993 and modified by Rao et al., 2002).

# Chapter-4

# ANALYSIS AND INTERPRETATION OF MULTI CHANNEL SEISMIC REFLECTION PROFILES

# Chapter-4

# ANALYSIS AND INTERPRETATION OF MULTI CHANNEL SEISMIC REFLECTION PROFILES

## 4.1 Introduction

2D Multi Channel Seismic (MCS) reflection profiles (RE23, RE21, RE19, RE17, RE15 and RE13) constitute the primary database to study seismic stratigraphy, intra sedimentary features and acoustic basement structures in the present study. The seismic profiles extend from the continental shelf, across the Laccadive Basin and Laccadive Ridge, to the eastern part of the Arabian Basin nearly perpendicular to the strike of major structural features of the SWCMI. Inorder to study the seismic stratigraphy and depositional history of the study area, MCS profiles are analyzed and interpreted to identify various seismic sequences and are correlated with major litho-stratigraphic units identified in the drill wells located in the study area. The litho-stratigraphic correlation of seismic sequences also provides chronologic order of deposition of various litho units.

## 4.2 Method of seismic stratigraphic analysis

Method of seismic stratigraphic analysis (Mitchum et al., 1977; Mitchum and Vail, 1977; Sheriff, 1980; Bertram and Milton, 1996) include three major steps i) seismic sequence analysis, ii) seismic facies analysis and iii) stratigraphic correlation.

The technique of seismic sequence analysis involves dividing the processed seismic sections into seismic sequences according to their internal reflection pattern, boundary geometry and structure produced by the reflected P-waves. The reflected energy depends upon difference in acoustic impedance (i.e. impedance contrast), which is the product of velocity and density of rock strata. On a seismic section, beds which have contrasting acoustic impedances stand out as strong reflectors. The strong reflectors generally indicate the interface involving appreciable lithologic contrast and/or a surface of erosion or non deposition for a considerable period of time. This makes it possible to map characteristic seismic

sequences. Seismic sequences are the unit of seismic reflections representing a depositional sequence (package of sediment) formed at a definite period of time and bounded by unconformity surfaces or time surface above and below. Since the seismic sequence boundaries are isochronal or unconformity surfaces, the seismic sequences represent a sedimentary unit deposited in a specific duration of geological time scale. Therefore, the identification of seismic sequences facilitates the seismic stratigraphic analysis. In seismic stratigraphic analysis, depth to seismic sequences is commonly referred to in terms of Two Way Travel Time (TWT) in seconds (s). TWT is the time required for acoustic energy to travel to a particular depth and return at normal incidence with the reflective surfaces.

The seismic sequences can be subdivided into different seismic units known as seismic facies. The seismic facies are distinguished by different reflection characteristics and represent change in their environment of deposition. Seismic facies analysis is the description and geological interpretation of seismic reflection parameters such as reflection continuity, amplitude, frequency and interval velocity (Figure 4.1). The reflection continuity is closely associated with continuity of strata itself. Reflection amplitude contains information on fluid content, the velocity-density contrast of individual interfaces/reflectors and their spacing. Reflection frequency is a characteristic of seismic pulse and is related to spacing of reflectors (i.e. bed thickness) or lateral changes in interval velocity and fluid content. Interval velocity helps to estimate the lithology, porosity and fluid content in the sediment unit. The seismic reflection parameters differ for various facies. The inter-relationship of the seismic reflection parameters with the seismic sequences gives various reflection patterns. The reflection pattern reveals a gross stratification pattern from which depositional process, erosion, paleo-topography and fluid content can be inferred. The reflection patterns can be divided into four subgroups, (i) simple reflection patterns, (ii) reflection patterns at sequence boundaries, (iii) prograding clinoforms and (iv) complex reflection patterns. The types of seismic reflection patterns are given in Table 4.1.

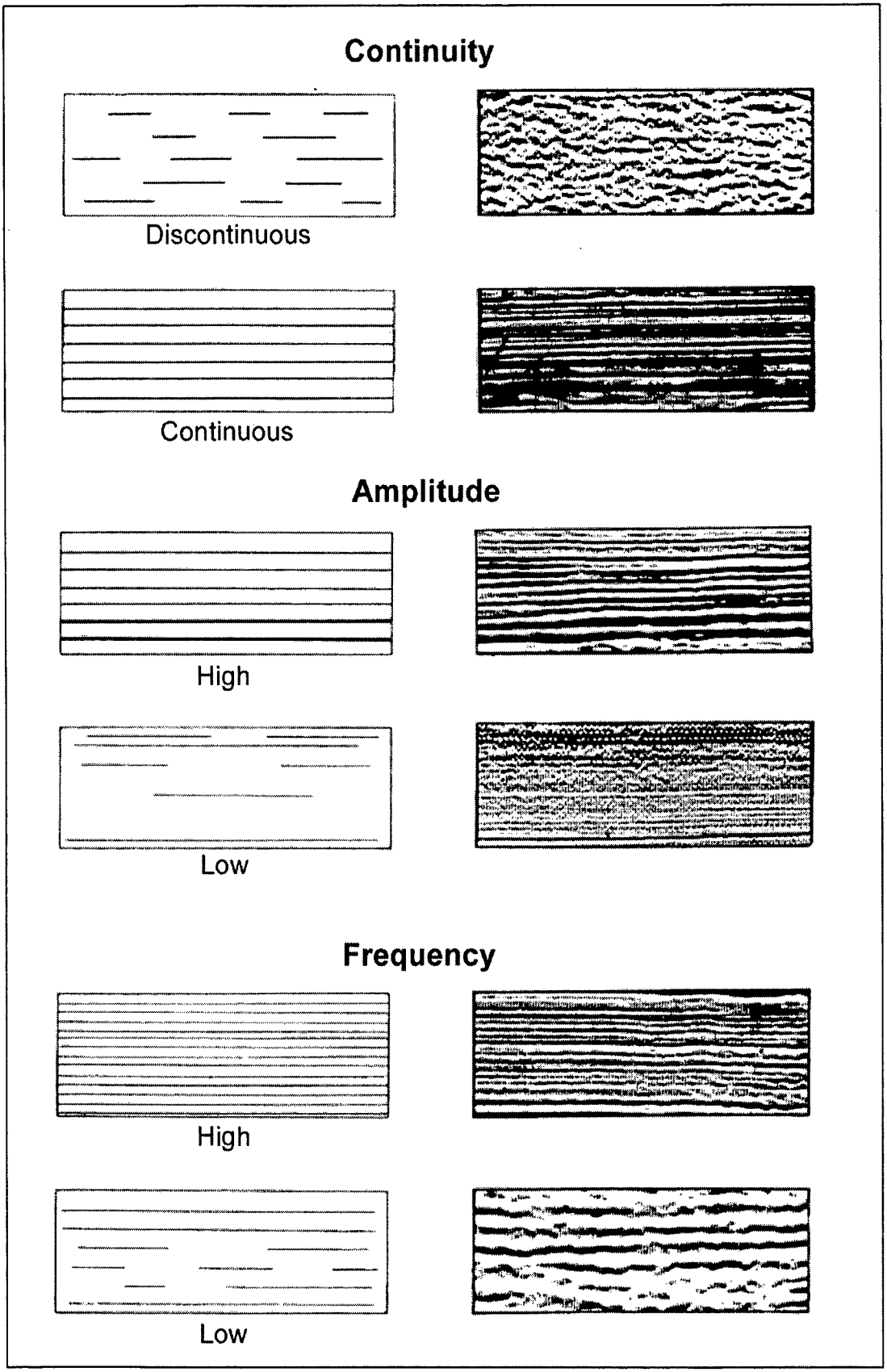


**Figure 4.1** Seismic reflection parameters (Sheriff 1980).

An understanding of the relation of seismic reflections to lithologic unit and geologic time is fundamental to interpreting stratigraphy from seismic data. The seismic reflections are generated by time surfaces which are chrono-stratigraphic rather than by boundary of litho-stratigraphic units. Sediment depositional sequences are more or less continuous in the marine sedimentary basins. These depositional sequences are represented as continuous seismic sequences in the seismic reflection profiles. Therefore, correlation of the interpreted seismic sequences with marine drill-well data or stratigraraphic chart containing litho- and chrono-stratigraphic information reveals lateral extension of stacked litho-stratigraphic units and their chrono-stratigraphic development. This helps to study depositional history in a sedimentary basin. A procedure for seismic stratigraphic analysis is given in Figure 4.2.

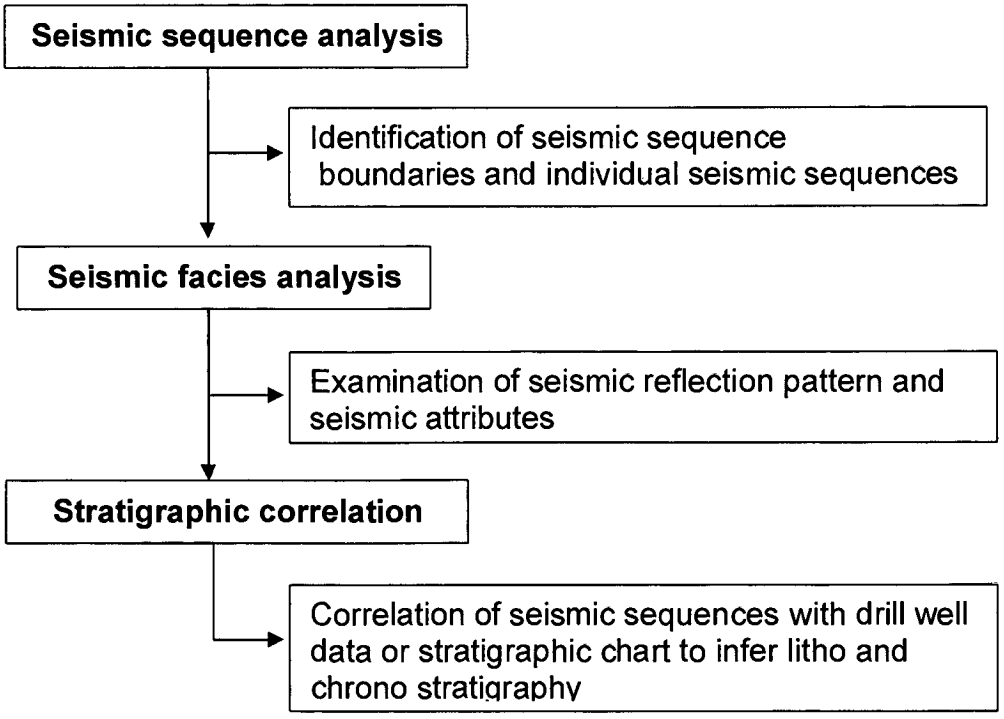


**Figure 4.2** Procedure for seismic stratigraphic analysis.

**Table 4.1** Types of seismic reflection patterns

| | | | | |
|---|---|---|---|---|
| **1** | **Simple seismic reflection patterns** | | | |
| 1.1 | Parallel / Even | | 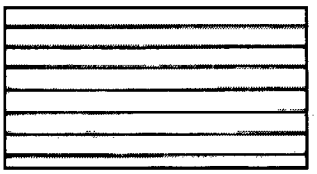 | Relatively parallel reflectors. Deposition in wide spread and uniform environment interbedded with periodic high and low energy deposition. |
| 1.2 | Sub parallel | | 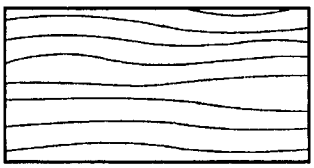 | Sub parallel reflectors. Deposition in wide spread but non-uniform environment with non-periodic high and low energy deposition. |
| 1.3 | Divergent | | 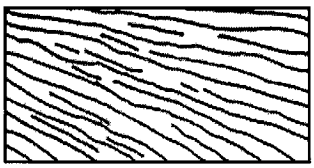 | Divergent reflectors gradually spread out in the down dip direction. Indicate differential subsidence of the basin during deposition. |
| **2** | **Seismic reflection patterns at sequence boundaries** | | | |
| 2.1 | Upper Boundary | Top lap | 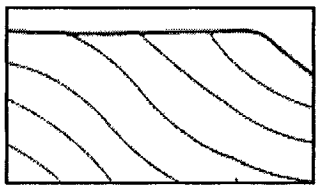 | Reflectors are convergent or tangential to the upper boundary of the seismic sequence. Deposition occurs near the wave base of appreciable energy. |
| 2.2 | Upper Boundary | Erosional truncation | 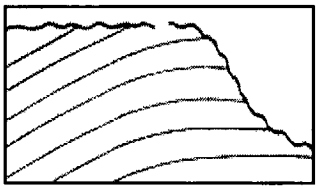 | Reflectors are truncated upward into an erosional surface. Indicate that the top of the sedimentary unit was removed off by high energy condition. |
| 2.3 | Lower Boundary (Base lap) | Onlap | 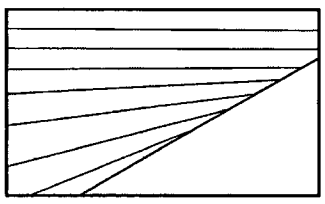 | Reflectors are flat to dipping upward and thin at its termination along a sloping unconformity surface. Onlap forms close to the coast as a result of sedimentation and marine transgression on to the land. |

| | | | |
|---|---|---|---|
| 2.4 | Downlap | 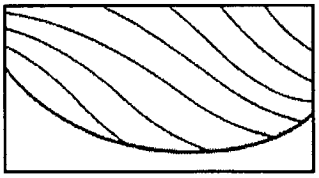 | Reflectors dipping downward and thins at its termination along a gently sloping unconformity surface. Downlap forms towards the seaward end of the depositional sequence. |
| 2.5 | Concordance | 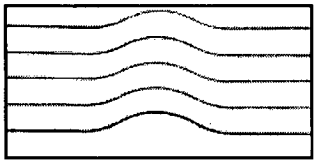 | Reflectors are conformable to the bounding surfaces of the seismic sequence. It is the result of slow and uniform deposition with low energy. |
| **3** | **Prograding clinoforms** | | |
| 3.1 | Sigmoid | 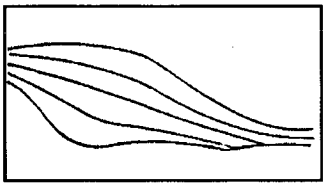 | 'S' shaped reflectors resulting from low depositional energy and rapid subsidence of the basin. Reflections downlap at the base and concordant with the top of the sequence. |
| 3.2 | Oblique | 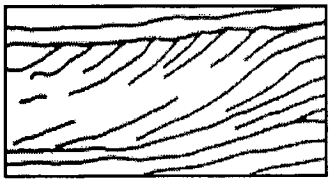 | Oblique reflectors resulting from high depositional energy with slow or no basin subsidence. Prograding simultaneous with erosion. Reflections downlap at the base and terminates by top lap at the top of the sequence. |
| 3.3 | Complex | 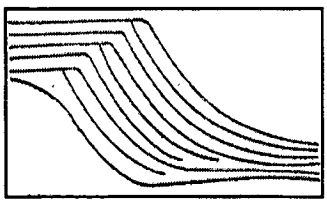 | Reflections downlap at the base of the sequence, but shows alternate series of toplap and concordant reflectors towards top of the sequence. It is formed by alternate high and low depositional energy. |
| 3.4 | Shingled | 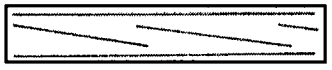 | Gently dipping reflectors with parallel oblique clinoforms. Indicate deposition prograding into bodies of shallow water. |

| | | | |
|---|---|---|---|
| | | | Individual clinoforms often show little or no overlap. |
| **4** | **Complex seismic reflection patterns** | | |
| 4.1 | Wavy | 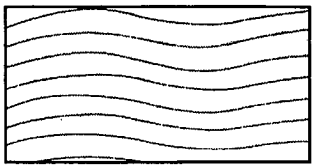 | Complex reflection patterns are the result of complex and disturbed energy condition during sediment deposition. Also indicates the complications produced by tectonic activities and obstructions caused by structural and diapiric features. |
| 4.2 | Lenticular | 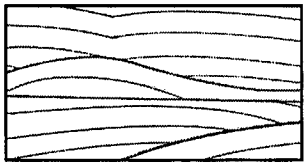 | |
| 4.3 | Disrupted | 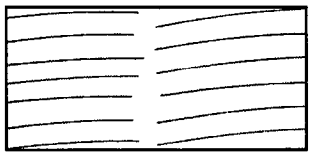 | |
| 4.4 | Chaotic | 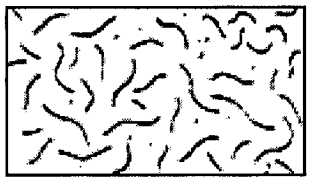 | |
| 4.5 | Contorted | 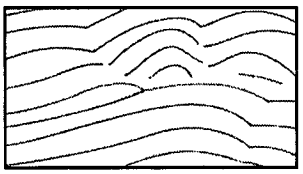 | |
| 4.6 | Hummocky | 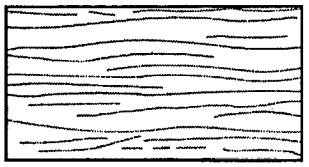 | |
| 4.7 | Reflection free |  | Reflection free patterns indicate deposition of unstratified and homogenous material. The reef buildings are normally seen as reflection free zones in seismic section. |

## 4.3 Analysis and interpretation of MCS reflection data

Processed MCS reflection profiles are analyzed to identify the seismic sequences, seismic reflection pattern and parameters, subsurface structural features and acoustic basement using seismic sequence analysis technique mentioned in section 4.2.

Prominent seismic reflectors have been identified based on their reflection characters such as amplitude, continuity and coherence. These reflectors are either seismic sequence boundaries or structural features. The reflection boundaries between seismic sequences were picked up in the sedimentary basins of the study area and continued on either side of the basins to establish the lateral continuity of the seismic sequences. Major seismic sequences are interpreted from the MCS reflection profiles across the SWCMI, within the study area. These seismic sequences are named following Chaubey et al. (2002b). Five major seismic sequences H1 (oldest) – H5 (youngest) are interpreted from the continental shelf-slope region and Laccadive Basin. Whereas, the seismic sequences interpreted from the deep sediment grabens of the Laccadive Ridge are named as L1 (oldest) – L5 (youngest). Four seismic sequences A1 (oldest) – A4 (youngest) are identified from the MCS reflection profile extended into the Arabian Basin. The seismic sequences H6 and L6 as interpreted by Chaubey et al. (2002b) are not discernable in most of the study area. Therefore, these sequences are interpreted along with the underlying seismic sequences H5 and L5.

The term basement used herein refers to the "Acoustic basement". The acoustic basement is the deepest correlatable seismic reflectors in the seismic profiles. The acoustic basement is interpreted at places as crystalline basement based on reflection pattern (characteristic of crystalline basement), and P-wave seismic velocity, wherever available.

The interpreted sequence boundaries and structural features are digitized with reference to shot points on X-axis and TWT (s) on Y-axis using Windig - a digitizing software. In order to obtain geographic location (latitudes and

longitudes) of shot points, basemap of shot point was digitized using Arc-GIS software. The seismic horizon database consists of shot point numbers, their position and depth to the interpreted horizons in TWT (s); at each shot points. The digitized data were used to plot interpreted line drawings of seismic sections in various scales using Generic Mapping Tools (GMT) software. The interpreted line drawing of seismic profiles is presented in terms of distance (km) as well as shot point numbers on X-axis. Whereas depth to seismic sequence boundaries and various subsurface features are presented in TWT (s) on Y-axis.

The seafloor topography, configuration of underlying basement and disposition of seismic sequences warrant the description of seismic profiles in terms of four geological domains of the study area. Therefore each seismic profile is divided into four domains such as i) continental shelf-slope, ii) Laccadive Basin, iii) Laccadive Ridge and iv) Arabian Basin and discussed accordingly. In the following sections the MCS reflection profiles are discussed individually for each geological domain of the study area, and seismic characteristics and inferred age of the interpreted seismic sequences are tabulated.

### 4.3.1 MCS reflection profile RE23

MCS reflection profile RE23 is the southernmost seismic profile used for seismic stratigraphic analysis of the study area. This 472 km long, ENE-WSW oriented profile runs from continental shelf across continental slope, Laccadive Basin and Laccadive Ridge into the Arabian Basin (Figure 3.1). As discussed above, the MCS profile is divided into four geological domains for the ease of analysis. The interpreted line drawing of the seismic profile is shown in Figure 4.3. Water depth along this profile varies from 75 m at its ENE end to 3450 m at its WSW end. Seismic reflection characteristics of identified seismic sequences from each geological domain, and their inferred ages are tabulated in Table 4.2.

#### *Continental shelf and slope*

Shelf break on this profile occurs at about 150 m water depth at shot point 8750. Maximum sediment thickness on the continental shelf-slope is observed as ~3.0 s

TWT between shot points 9400 and 8290 in the profile (Figure 4.3). From the shelf break, the continental slope dips to the shot point 8290 where slope morphology is modified by basin floor morphology of the Laccadive Basin. Five prominent seismic sequences H1-H5 are identified in the sediment column of the region. The base of the sequence H1 is imperceptible due to the presence of multiples and boundary between the seismic sequences H2 and H3 are undistinguishable. Upper boundary of the sequence H1 is dissected by a series of faults towards seaward end of the continental slope. Seismic sequences H1, H2 and H3 are uplifted by the crest of an underlying basement high between shot points 8500 and 7800. This indicates a post depositional upliftment and faulting of the sediment sequences after deposition of the sequence H3. A prograding sigmoid pattern of maximum thickness of 2.25 s TWT constituted by the seismic sequences H4 and H5 is identified between shot points 9080 and 8300 (Figure 4.4). This prograding sigmoid pattern suggests a huge sediment influx after deposition of the sequence H3. It is clearly evident from the seismic profile that the top of the prograding sigmoid pattern is disrupted by sediment slumps between shot points 8640 and 8290 (Figure 4.3). Two paleo shelf breaks are identified on the seismic sequence boundaries H1-top and H3-top at shot points 9005 and 9000 respectively. The paleo shelf break of H3-top is aggraded and receded for about 250 m from the paleo shelf break of H1-top (Figure 4.3 and Figure 4.4)

***Laccadive Basin***

Laccadive Basin is depicted in the MCS reflection profile between shot points 8750 (shelf break) and 4250 (Figure 4.3). The basin is about 225 km wide with water depth of 200 – 2650 m. A gently sloping westerly tilted and 15.5 km wide physiographic rise with a maximum relief of about 165m is identified between shot points 8025 and 7715. This physiographic rise is bounded by shallow penetrating faults and interpreted as sediment slump from continental rise towards the Laccadive Basin floor. Five major seismic sequences (H1-H5) identified in the continental shelf-slope are also identified in the Laccadive Basin. The lowest seismic sequence H1 is interrupted by numerous faults indicating a highly disrupted basement. Since the seismic sequence H2 which overlies sequence H1

is not affected by such faults, it is suggested that the deposition of the sequence H2 is not affected by major tectonic events that caused highly dissected sequence H1. The undisturbed seismic sequences H2-H5 appeared to be deposited during a tectonic quiescence.

The basin is divided into two by a basement high identified between shot points 6790 and 6520 (Figure 4.3 and Figure 4.5). The high has a maximum relief of about 600 m above the adjacent seafloor and interpreted as part of the Prathap Ridge (PR). The water depth immediately west of the basement high is about 150 m more than the water depth east of it. This indicates that the Prathap Ridge plays an important role in sediment distribution within the Laccadive Basin. All the seismic sequences identified in the basin are onlapping to the steep scarps of the Prathap Ridge suggesting its pre-sedimentational existence in the basin. Presence of another basement high (Figure 4.3 and Figure 4.5) is inferred between the shot points 6200 and 5780. The high is about 21 km wide at its base and is represented by a bathymetric rise, about 6 km wide, at a water depth of about 3225 m. It may be noted that the overlying seismic sequences H1-H5 are thinned and uplifted by its aperture. This suggests that the basement high is a result of recent tectonic or magmatic intrusive activity.

The boundary between H4 and H5 could not be traced to the western part of the basin from the shot point 5540 (Figure 4.3). A prominent, high amplitude and continuous reflector is identified between shot points 5720 and 4545 dividing the sequence H3 into two parts. The maximum sediment thickness of about 2.9 s TWT is estimated at shot point 7905 in the basin. Thickness of the sedimentary unit within the Laccadive Basin gradually thins towards the eastern flank of the Laccadive Ridge.

***Laccadive Ridge***

To the west of the Laccadive Basin the seismic profile crosses a broad (207 km wide) physiographic high of the Laccadive Ridge between the shot points 4250 and 120 (Figure 4.3). The water depth over the ridge varies between 1575 m and 2250 m. A sedimentary basin of about 6.5 km width, represented by a bathymetric low and bounded by two narrow physiographic highs of relief <135 m, is identified

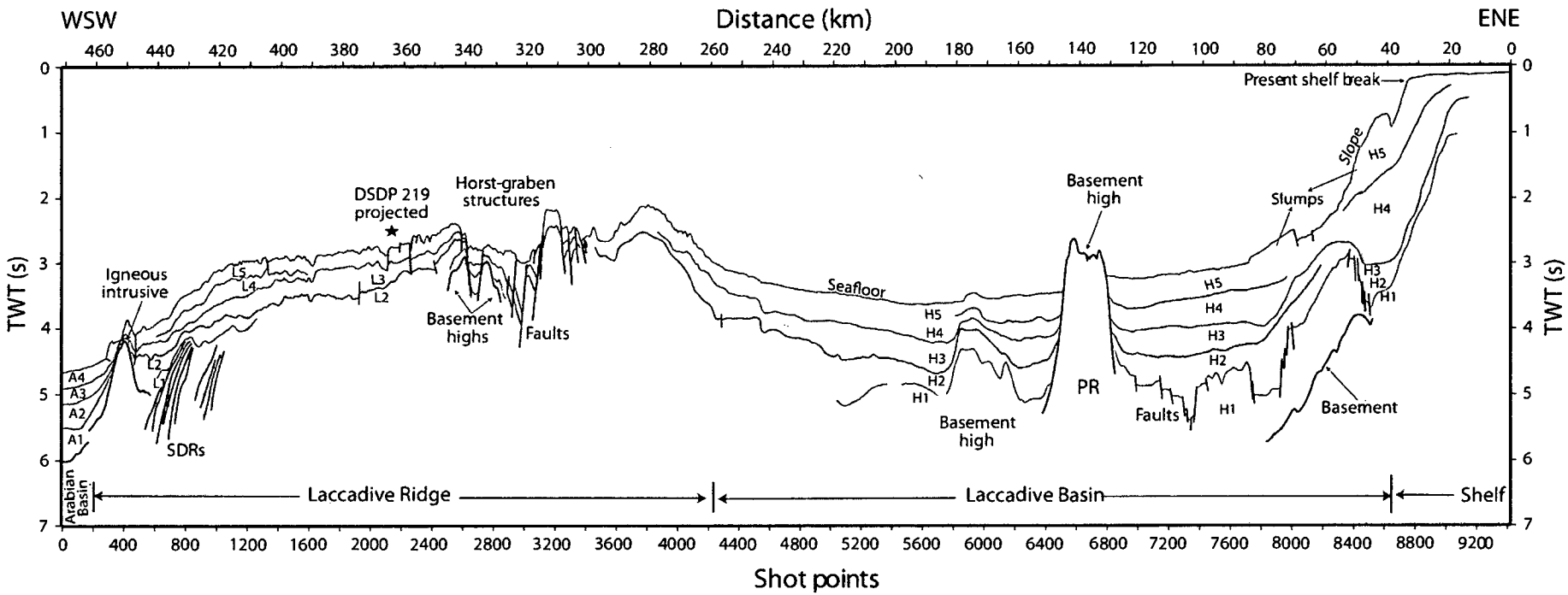


**Figure 4.3** Interpreted line drawing of MCS reflection profile RE23. PR: Prathap Ridge; SDRs: Seaward Dipping Reflectors. Location of the profile is shown in Figure 3.1.

between shot points 3600 and 3470. Five seismic sequences L1-L5 are identified in the sediment grabens of the Laccadive Ridge. The lower most sequence L1 is not discernable in most part of the ridge. Seismic boundary between L4 and L5 is distinguished well only between shot points 1600 and 620. Among the seismic sequences identified on the ridge, the sequence L3 shows maximum thickness of ~0.46 s TWT at shot point 1920. The crystalline basement of the ridge could not be identified due to the absence of parabolic, irregular and non-correlatable reflectors. However, the trend of gently westerly tilted basement can be deduced by the attitude of the lowest discernable seismic sequence L2. A zone (41 km wide) of horst-graben structures and tilted fault blocks bounded by numerous gravity and thrust faults are identified between the shot points 3410 and 2590 (Figure 4.3 and Figure 4.6). Two subsurface basement highs centered at the shot points 2750 and 2620 are also identified beneath the sediment column of this zone. All the seismic sequences overlying the aperture of these basement highs are thinned and elevated, developing a fault bounded sediment graben of width 14 km between the highs. This graben with a sediment thickness of not less than 0.8 s TWT is located between shot points 2730 and 2635 at a water depth of about 2063 m. A 6 km wide horst, bounded by a series of faults and tilted fault blocks on both sides, is identified between the shot points 3240 and 3120 (Figure 4.6). A set of westerly dipping seismic reflectors overlain by a sediment column of thickness not less than 0.9 s TWT are noticed on the western flank of the Laccadive Ridge between the shot points 1080 and 540 (Figure 4.3). They extend seaward for about 27 km below sequence L2. These seaward dipping and diverging seismic reflectors are interpreted as Seaward Dipping Reflectors (SDRs) and discussed in chapter- 6. A deep 13.5 km wide sediment graben with a sediment column of thickness ~1 s TWT, comprising all the seismic sequences L1-L5, is identified between the shot points 720 and 450. The lower seismic sequences L1 and L2 abut on to the eastern flank of a prominent basement high. This basement high, which is interpreted as an igneous intrusive body, is identified beneath the sediment column at foot of the western flank of the Laccadive Ridge in association with a physiographic rise centered at shot point 420. The seismic sequences are considerably thinned and uplifted by the aperture of the basement high and have under gone faulting along the eastern and western scarps of the high.

### *Arabian Basin*

The seismic profile runs into the eastern part of the Arabian Basin for about 9 km between the shot points 180 and 1 (Figure 4.3). The smooth seafloor of the basin gently dips to the west. Four distinct seismic sequences A1-A4 with increasing thickness to the west are identified in the Basin. All the seismic sequences appeared to be lying more or less conformably over each other following the trend of basement. The lower seismic sequences A1-A3 onlap to the western flank of the basement high located at the shot point 420. The seismic sequences A1 and A2 are significantly thicker than the other sequences (A3 and A4) suggesting huge influx of sediment into the eastern Arabian Basin during their deposition.

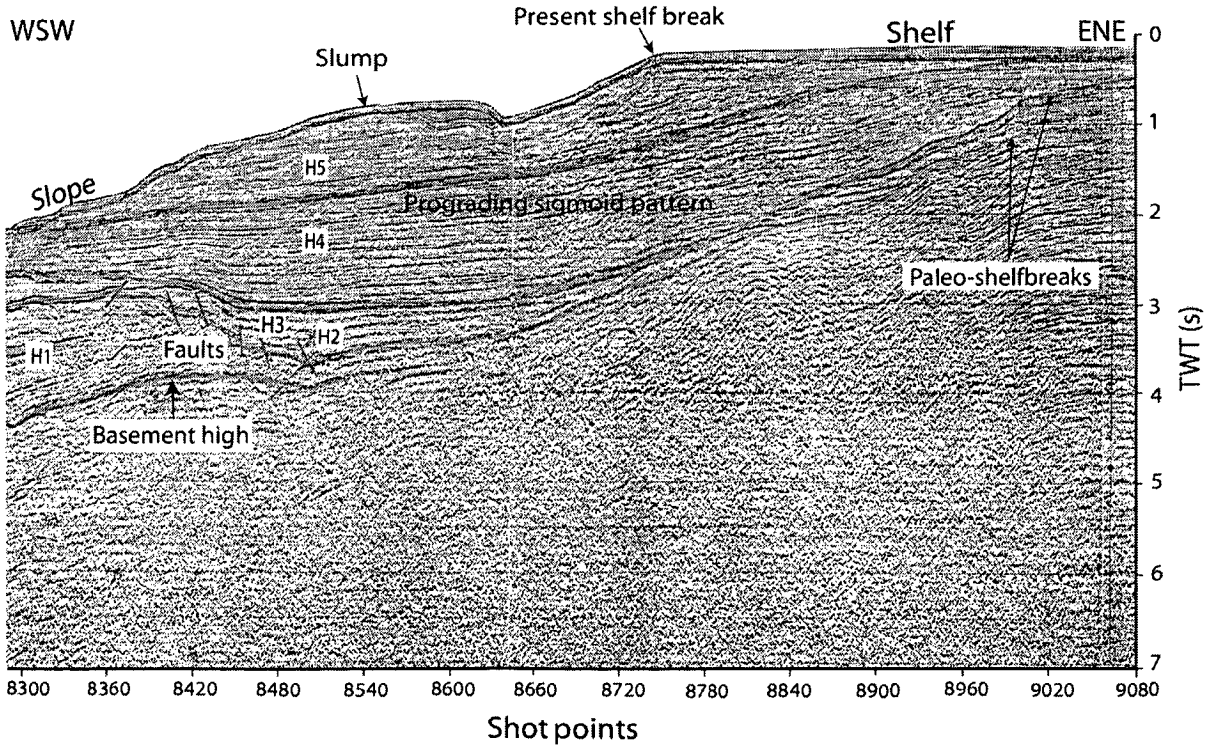


**Figure 4.4** Prograding sigmoid pattern, sediment slump and other sub-surface features of continental shelf-slope imaged in MCS profile RE23. Interpreted line drawing is shown in Figure 4.3.

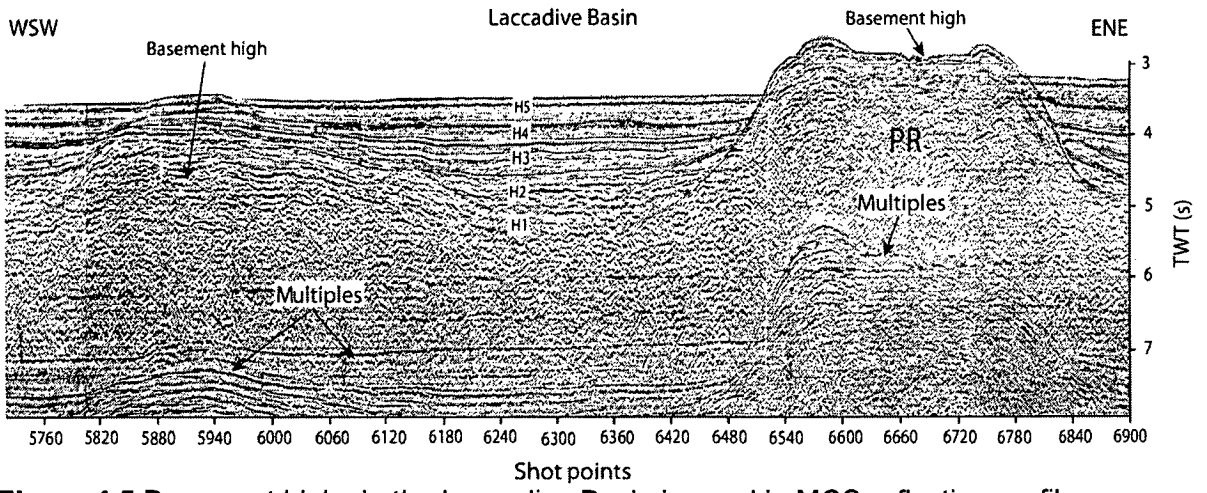


**Figure 4.5** Basement highs in the Laccadive Basin imaged in MCS reflection profile RE23. Interpreted line drawing is shown in Figure 4.3.

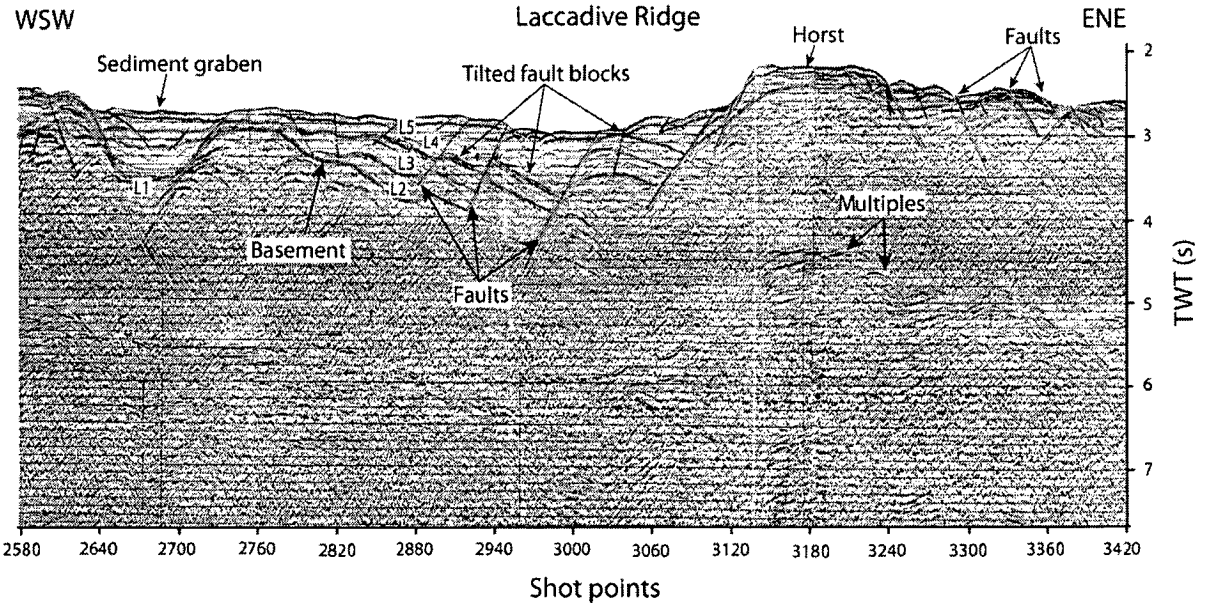


**Figure 4.6** Zone of horst-graben structures and tilted fault blocks identified on top of the Laccadive Ridge depicted in MCS profile RE23.

**Table 4.2** Summary of seismic characters of MCS reflection profile RE23.

| | Continental shelf and slope | | | | Laccadive Basin | |
|---|---|---|---|---|---|---|
| **Seismic sequences** | **Inferred age** | **Thickness TWT (s)** | | **Seismic character** | **Thickness TWT (s)** | **Seismic character** |
| **H5** | Upper L. Miocene-Recent | 0.12-1.05 | | Low to medium amplitude, high frequency, moderate reflection continuity, sub parallel to divergent reflectors with contorted reflectors at places | 0.15-0.76 | Low amplitude and frequency, poor to moderate reflection continuity, sub parallel reflectors |
| **H4** | Lower-Upper L. Miocene | 0.45-1.4 | | Medium to high amplitude, high frequency, fairly good reflection continuity, parallel to sub parallel and divergent reflectors | 0.15-0.62 | Low to high amplitude and frequency, moderate reflection continuity, parallel to sub parallel reflectors with hummocky reflectors at places |
| **H3** | E. Oligocene-L. Miocene | Boundary is not discernable | 0.2-0.65 | High amplitude, low frequency, good reflection continuity, parallel to sub parallel and hummocky reflectors | 0.05-0.55 | Medium to high amplitude, low frequency, moderate to good reflection continuity, parallel to sub parallel reflectors with hummocky reflectors at places |
| **H2** | L. Paleocene-E. Oligocene | | | | 0.05-1.0 | Medium to high amplitude, low frequency, moderate reflection continuity, parallel to sub parallel with hummocky reflectors at places |
| **H1** | L. Cretaceous-L. Paleocene | Lower boundary is not discernable in the major part | | Low to medium amplitude, high frequency, poor reflection continuity, poorly coherent reflectors | Lower boundary is not discernable in the major part of the basin | High amplitude and frequency, moderate reflection continuity, sub parallel and poorly coherent reflectors |

Table 4.2 continued...

| Laccadive Ridge | | | | Arabian Basin | | | |
|---|---|---|---|---|---|---|---|
| **Seismic sequences** | **Inferred age** | **Thickness TWT (s)** | **Seismic character** | **Seismic sequence** | **Inferred age** | **Thickness TWT (s)** | **Seismic character** |
| **L5** | E. Pliocene-Recent | 0.12 - 0.80 | Low to medium amplitude, low frequency, poor reflection continuity, sub parallel to divergent reflectors with hummocky to contorted reflectors at places | **A4** | L. Pliocene-Recent | 0.19-0.26 | Low amplitude and frequency, nearly reflection free |
| **L4** | M. Miocene-E. Pliocene | | | **A3** | E. Miocene-L. Pliocene | 0.2-0.24 | Low to medium amplitude, low frequency, poor reflection continuity, sub parallel to hummocky reflectors |
| **L3** | M. Eocene-M. Miocene | 0.07-0.45 | Low to medium amplitude, low frequency, poor reflection continuity, sub parallel to divergent and hummocky reflectors | **A2** | M. Eocene-E. Miocene | 0.32-0.37 | Low to medium amplitude, low frequency, poor reflection continuity with poorly coherent reflectors |
| **L2** | L. Paleocene-M. Eocene | 0.1-0.32 | Low to medium amplitude, low frequency, poor reflection continuity, sub parallel to hummocky reflectors | **A1** | Undated | 0.34-0.5 | Low to medium amplitude, high frequency, poor reflection continuity with poorly coherent reflectors |
| **L1** | L. Paleocene | Lower boundary is not discernable | Low to medium amplitude, low frequency, poor reflection continuity with poorly coherent reflectors | | | | |

### 4.3.2 MCS reflection profile RE21

The ENE-WSW oriented 410 km long MCS profile RE21 runs from continental shelf, across continental slope and Laccadive Basin, to the foot of western flank of the Laccadive Ridge (Figure 3.1). The profile is located about 136 km north of the profile RE23. Water depth along the profile varies from 113 m at its ENE end to 2926 m at its WSW end. The interpreted line drawing of this MCS reflection profile is given in Figure 4.7. Seismic reflection characteristics of the seismic sequences identified from each geological domain are tabulated in Table 4.3 with their inferred ages.

***Continental shelf and slope***

The gently dipping continental shelf joins the continental slope at shelf break located at shot point 465 in a water depth of about 263 m. The continental slope joins with abyssal plain of the Laccadive Basin at about 1838 m water depth. Even though the four prominent seismic sequences H1-H4 are demarcated, boundary between the sequences H4 and H5 could not be traced clearly from the seismic profile. A faulted acoustic basement is identified at an average depth of 3.75 s TWT between shot points 179 and 850. Paleo shelf breaks are identified on seismic sequence boundaries H2-top and H3-top at shot points 117 and 101 respectively (Figure 4.8). The paleo shelf break of seismic sequence H3 is identified about 18 km east of the present shelf break. The aggraded continental shelf of the sequence H3 is receded for about 800 m from the shelf break of the underlying sequence H2 between shot points 101 and 117. Boundary between the seismic sequences H1 and H2 is not discernable till the shot point 738 due to presence of large scale faults and the complex nature of the seismic reflectors. A deep, sediment graben, of 18 km wide, is identified between shot points 125 and 485. A faulted basement is identified between shot points 435 and 635. These faults penetrate upward into lower part of the overlying seismic sequence H3 by disrupting the sequences H1 and H2 and tilting the resultant fault blocks to the west. This suggests that the region experienced a major tectonic event some times during initial phase of deposition of the sequence H3. The seismic sequences H4 and H5 display a typical sigmoid pattern of maximum thickness ~1.85 s, near the shelf break indicating progradation of continental shelf.

***Laccadive Basin***

The Laccadive Basin is depicted between the shot points 465 and 3185 in this profile (Figure 4.7). The basin is about 136 km wide with a water depth varying between 262.5 m and 2250 m. The seismic sequences H1-H5 are identified also from this region. As in the case of continental shelf and slope, the boundary between the seismic sequences H4 and H5 is not perceptible. A zone of acoustic turbidity of about 50 km wide is identified in the upper seismic sequence H4+H5 between shot points 1105 and 2115. The seismic sequences H1, H2 and H3 are characterized by acoustic columns of complex, up-doming and up-thrusted seismic reflectors below the zone of acoustic turbidity at two locations between shot points 1569 and 1617, and 1955 and 2059 (Figure 4.9). The seismic sequence boundaries H1-top and H2-top are breached below these columnar acoustic disturbances. Over the zone of acoustic turbidity, the sea bed is characterized by a V-shaped depression associated with strong hyperbolic reflectors about the shot point 1960. This bathymetric depression is interpreted as a pockmark. The seismic sequences identified in the Laccadive Basin gradually thin towards eastern flank of the Laccadive Ridge.

***Laccadive Ridge***

Laccadive Ridge, depicted between the shot points 3185 and 3705, begins with a broad and subdued basement high of width about 26 km at its eastern end (Figure 4.7). Water depth varies from 863 m to 1463 m on the ridge. A highly undulating basement with numerous basement highs is distinguished below the sediment unit. Five major seismic sequences L1-L5 are identified in deep sediment grabens. Since the boundary between the seismic sequences L4 and L5 are imperceptible, they are considered as a single sequence. The lower most sequence L1 is not discernable along major part of the ridge. The boundary between the sequences L1 and L2 over the ridge is identified only between shot points 3640 and 4315. A basement high, of about 32 km wide with a depth of ~2.6 s TWT to its crest, is identified between the shot points 4325 and 4960. The seismic sequences L1, L2 and L3 abut on both sides. The sequence L4+L5 deposited over the crust of this basement high show a physiographic fall of more

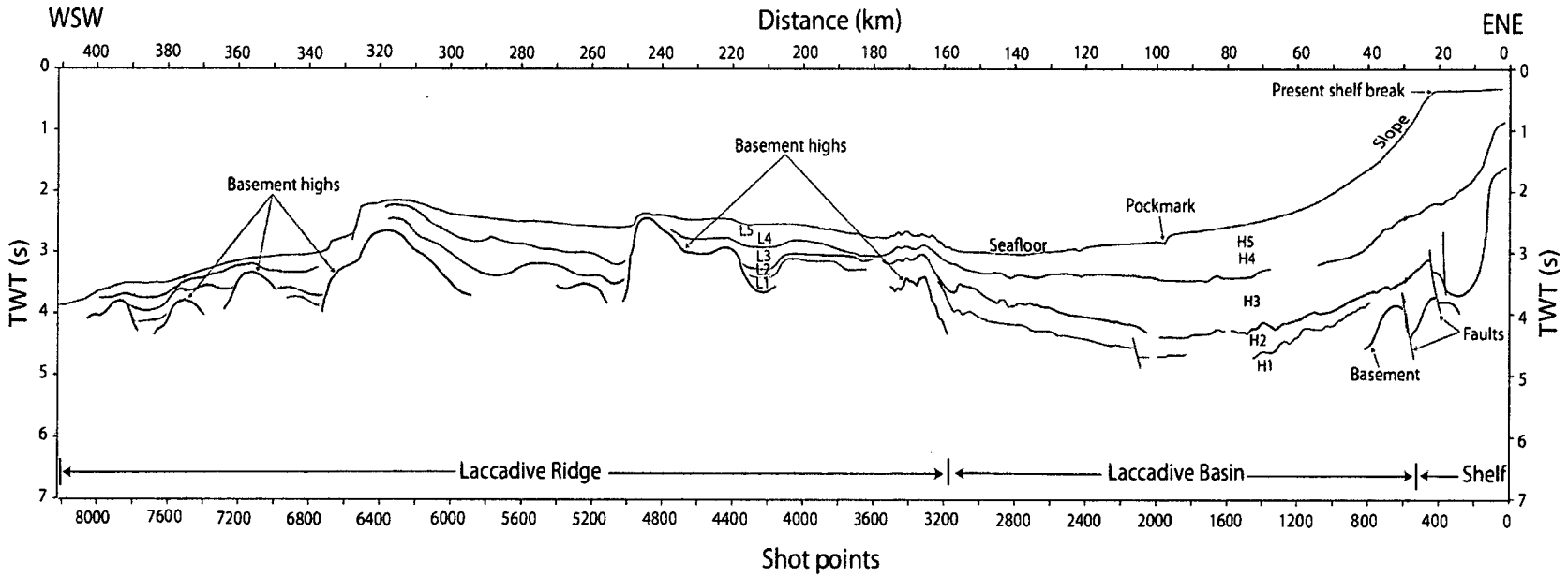


**Figure 4.7** Interpreted line drawing of MCS reflection profile RE21. Location of the profile is shown in Figure 3.1.

or less 150 m to the west about shot point 4950. A 55 km wide sediment graben of thickness ~1.2 s TWT is identified between shot points 5000 and 6100. This sediment graben is bounded to the west by a basement high centered at shot point 6325 with a crust at a depth of ~2.7 s TWT. The entire sediment sequences are thinned and uplifted by the crest of this basement peak. Further west, the seismic sequences L1 and L2 are interrupted by three subdued basement highs centered at shot points 7180, 7520 and 7872 respectively, and located towards the foot of western flank of the Laccadive Ridge.

Since the MCS profile RE21 traverses form continental shelf to the western flank of the Laccadive Ridge discussion on the Arabian Basin is hindered.

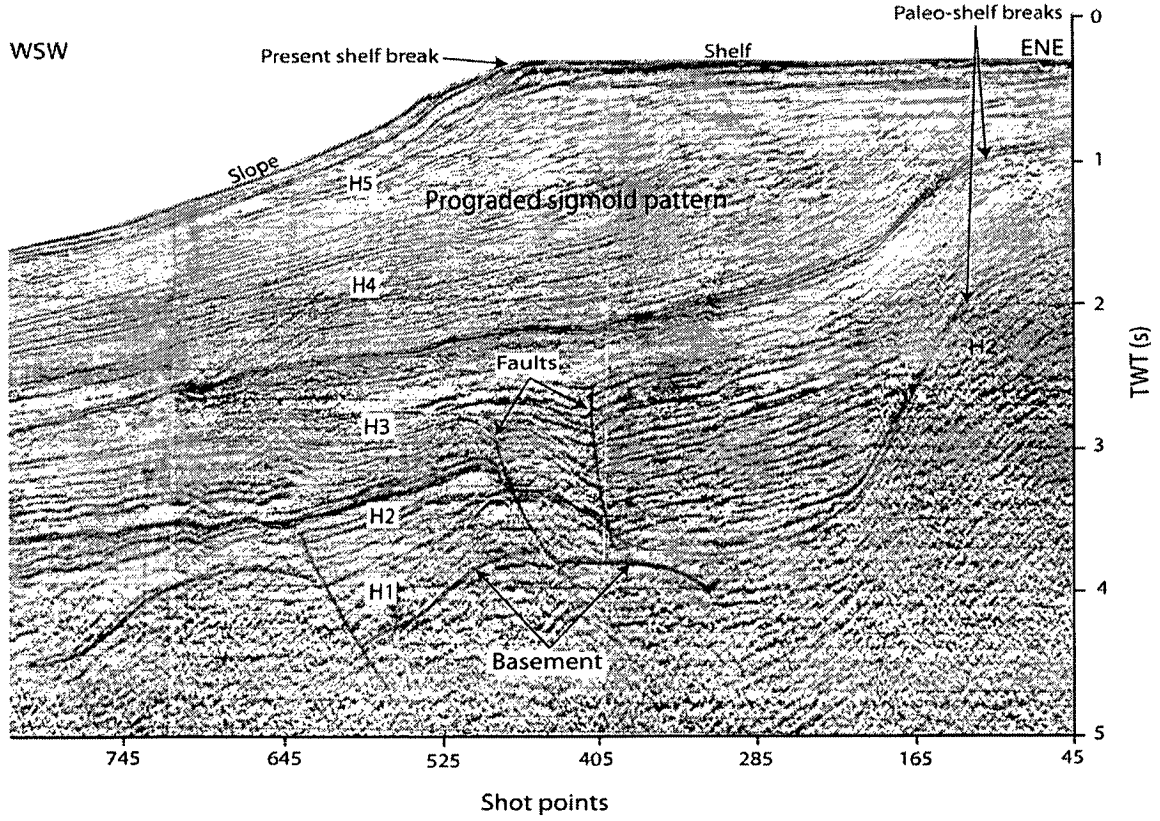


**Figure 4.8** Prograding sigmoid pattern and other sub-surface features of the continental shelf imaged in MCS profile RE21. Interpreted line drawing is shown in Figure 4.7.

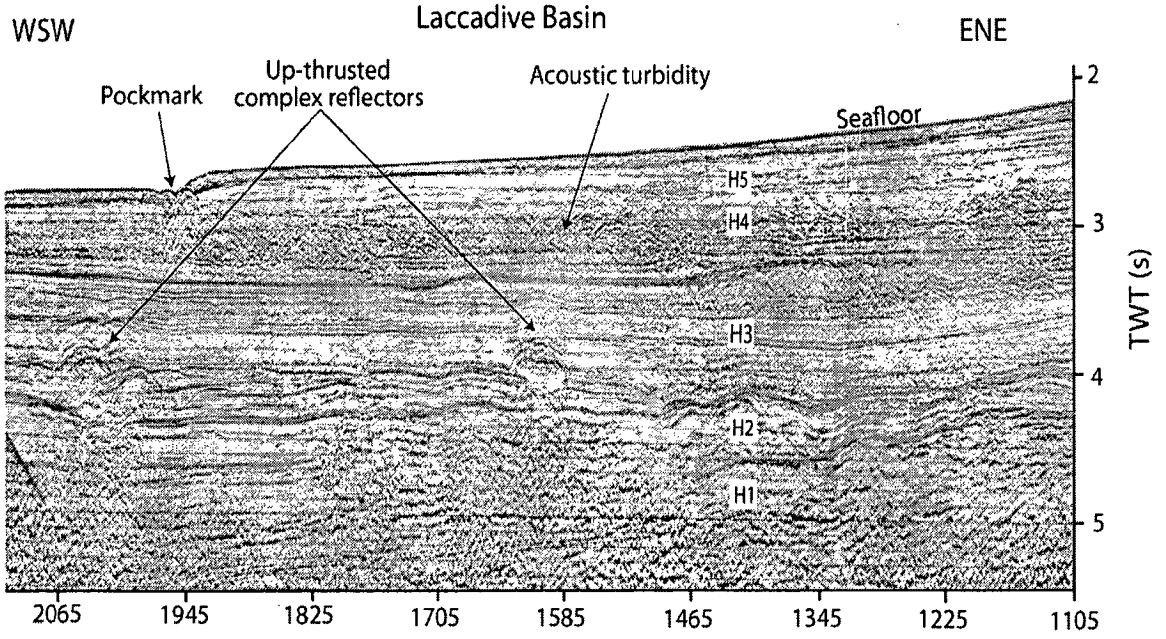


**Figure 4.9** Zone of acoustic turbidity and columnar zones of up-thrusted complex reflectors identified from the Laccadive Basin imaged in MCS profile RE21. Interpreted line drawing is shown in Figure 4.7.

**Table 4.3** Summary of seismic characters of MCS reflection profile RE21

| | Continental shelf and slope | | | Laccadive Basin | |
|---|---|---|---|---|---|
| **Seismic sequences** | **Inferred age** | **Thickness TWT (s)** | **Seismic character** | **Thickness TWT (s)** | **Seismic character** |
| **H5** | Upper L. Miocene-Recent | 0.67 – 1.98 | High amplitude and frequency, poor to fairly good reflection continuity, sub parallel to divergent and hummocky reflectors | 0.21 - 0.9 | Low to medium amplitude, low frequency, poor reflection continuity, non coherent reflectors. |
| **H4** | Lower-Upper L. Miocene | 0.68 – 1.55 | High amplitude and frequency, moderate to good reflection continuity, sub parallel and discordant reflectors with disrupted, contorted and hummocky reflection at places | 0.27 - 0.95 | High amplitude, low to high frequency, moderate to good reflection continuity, parallel to sub parallel reflectors with contorted and disrupted reflections at places |
| **H3** | E. Oligocene-L. Miocene | | | | |
| **H2** | L. Paleocene-E. Oligocene | 0.1– 0.4 | High amplitude, low frequency, poor to moderated reflection continuity, contorted to hummocky reflectors | 0.5 - 0.4 | Low to medium amplitude, low frequency, nearly reflection free with isolated and non coherent reflectors at places |
| **H1** | L. Cretaceous-L. Paleocene | 0.35 – 0.7 | Medium to high amplitude, low frequency, poor reflection continuity, non coherent reflectors | Lower boundary is not discernable | High amplitude and frequency, poor reflection continuity with non coherent reflectors |

Table 4.3 Continued...

| Laccadive Ridge | | | |
|---|---|---|---|
| **Seismic sequences** | **Inferred age** | **Thickness TWT (s)** | **Seismic character** |
| **L5** | E. Pliocene-Recent | 0.1 - 0.67 | Low to high amplitude, low frequency, nearly reflection free with isolated non coherent reflectors at places |
| **L4** | M. Miocene-E. Pliocene | | |
| **L3** | M. Eocene-M. Miocene | 0.05 - 0.6 | Low to high amplitude, low frequency, moderate reflection continuity, lenticular to hummocky reflectors at places |
| **L2** | L. Paleocene-M. Eocene | 0.08 - 0.15 | Low to high amplitude, low frequency, moderate reflection continuity, contorted to hummocky reflectors at places |
| **L1** | L. Paleocene | Lower boundary is not discernable | High amplitude and frequency, poor reflection continuity, non coherent reflectors |

### 4.3.3 MCS reflection profile RE19

The profile RE19 extends 400 km westward from the continental slope across the Laccadive Basin and Laccadive Ridge into the eastern part of the Arabian Basin (Figure 3.1), between the water depth 1162 and 3938 m. The profile is located about 103 km north of the seismic profile RE21. Interpreted line drawing of this seismic profile is shown in Figure 4.10. Seismic reflection characteristics of the identified seismic sequences and their inferred ages are tabulated in Table 4.4.

***Continental shelf and slope***

Since the seismic profile starts from the continental slope, the continental shelf is absent in the profile. The seismic sequences H2, H3, H4 and H5 are well developed and easily identified from the continental slope imaged in this profile (Figure 4.10 and Figure 4.11). The sequence H1 could not be identified due to non coherent reflectors. The seismic sequence H2 and the bottom set of reflectors of seismic sequence H3 are faulted between shot points 7910 and 7950, indicating that the faults were formed after the commencement of deposition of the sequence H3. High amplitude and lenticular seismic reflectors within the seismic sequence H3, between shot points 7940 and 7500, indicate paleo-slumping which occured during late stage deposition of sequence H3 (Figure 4.11). The sequence H4 with a maximum thickness of not less than 1.35 s TWT is characterized by converging seismic reflection pattern to the west and thins to the foot of continental slope to a thickness of ~0.4 s TWT. The seismic sequence H5, characterized by low amplitude and frequency, more or less follows the bathymetry.

***Laccadive Basin***

The water depth in the basin varies between 1988 and 2175 m along the profile. The seismic sequences H1-H5 are identified from the deep sediment graben located between shot points 5620 and 5170 (Figure 4.10 and Figure 4.12). Boundary between the seismic sequences H4 and H5 are discontinuous at places within the basin. Several subsurface basement highs characterized by high amplitude, discontinuous and correlatable seismic reflectors are identified

between the shot points 6670 and 5420. These basement highs are interpreted as part of the Prathap Ridge. The seismic sequences H1-H3 over the basement highs are intensely faulted. Parabolic and undulating reflections from the basement high between shot points 5550 and 5240 suggest presence of numerous closely spaced faults on the surface of basement highs. The horizontal and lateral continuity of the seismic sequences H4 and H5 suggest a more or less undisturbed and uniform depositional environment in major part of the basin. The sediment unit in the basin gradually thins to eastern flank of the Laccadive Ridge.

***Laccadive Ridge***

The Laccadive Ridge is depicted between shot points 4950 and 295 with water depth varying between 488 m and 3675 m (Figure 4.10). The seismic sequences L1-L5 are identified from the sediment grabens of the ridge. The basement could not be discernable except in some locations. Four prominent physiographic highs with average relief of 1388 m, 488 m, 713 m, and 435 m are identified on the ridge centered at shot points 4850, 4275, 3570 and 2600 respectively. Even though the basement beneath these physiographic highs could not be distinguished, the thinned and uplifted sediment sequences suggest that they are affected by upliftment of underlying basement highs. The physiographic highs centered at the shot points 4850, 4275 and 3570 are characterized by complex internal reflection pattern baffling the identification of sequence boundaries (Figure 4.13). This complex internal reflection pattern is attributed to growth of corals over the crests of the highs when they were in euphotic zone. Whereas, the physiographic high, located to the west of the ridge centered at shot point 2600, is broad and subdued with distinct seismic sequences (Figure 4.10). This physiographic high is immediately followed by a bathymetric low of width about 9.25 km to the west, between shot points 2515 and 2330. The bathymetric low, characterized by irregular and parabolic reflections on its sides and bottom, is interpreted as an erosional channel migrated more or less vertically from the upper boundary ofsequence L2 (L2 top). The irregular and parabolic reflections represent rugged erosional surfaces of the channel. The sequences L3 and L4, deposited in a sediment graben identified between shot points 3515 and 2980, are thicker than those deposited in adjacent sediment grabens suggesting high rate of subsidence

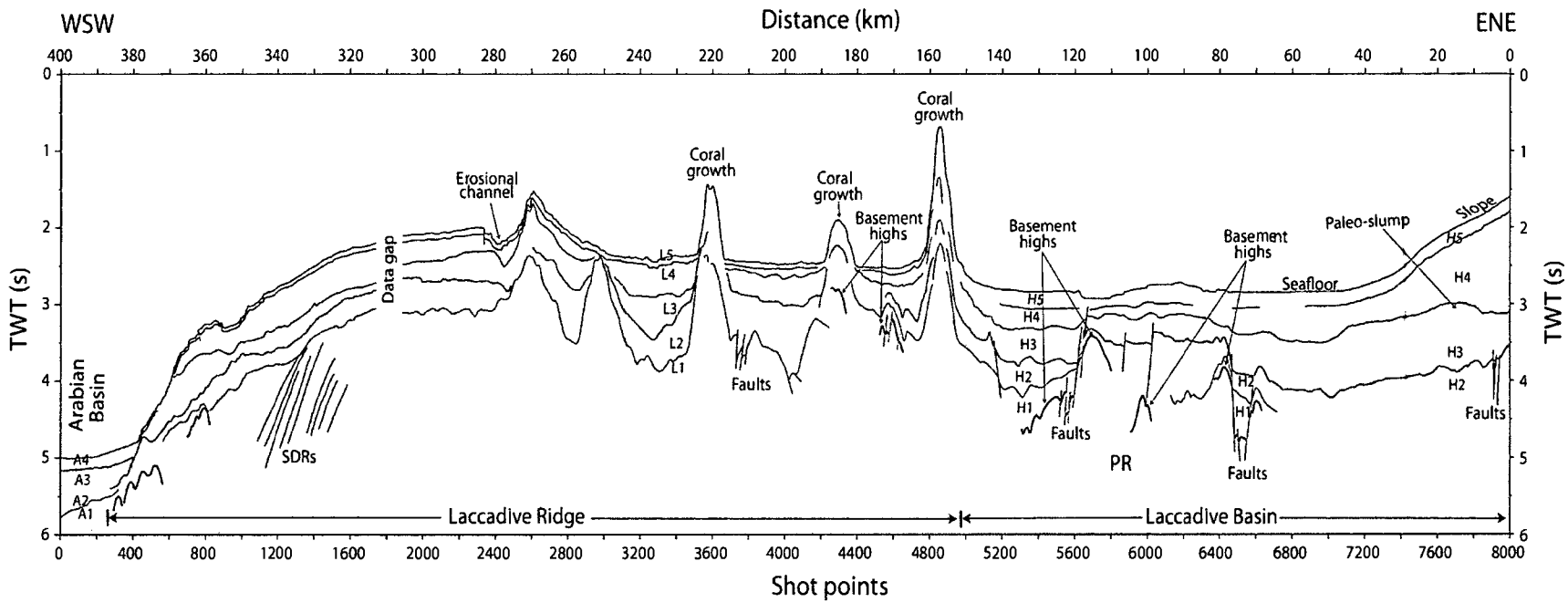


**Figure 4.10** Interpreted line drawing of MCS profile RE19. PR: Prathap Ridge; SDRs: Seaward Dipping Reflectors; Location of the profile is shown in Figure 3.1.

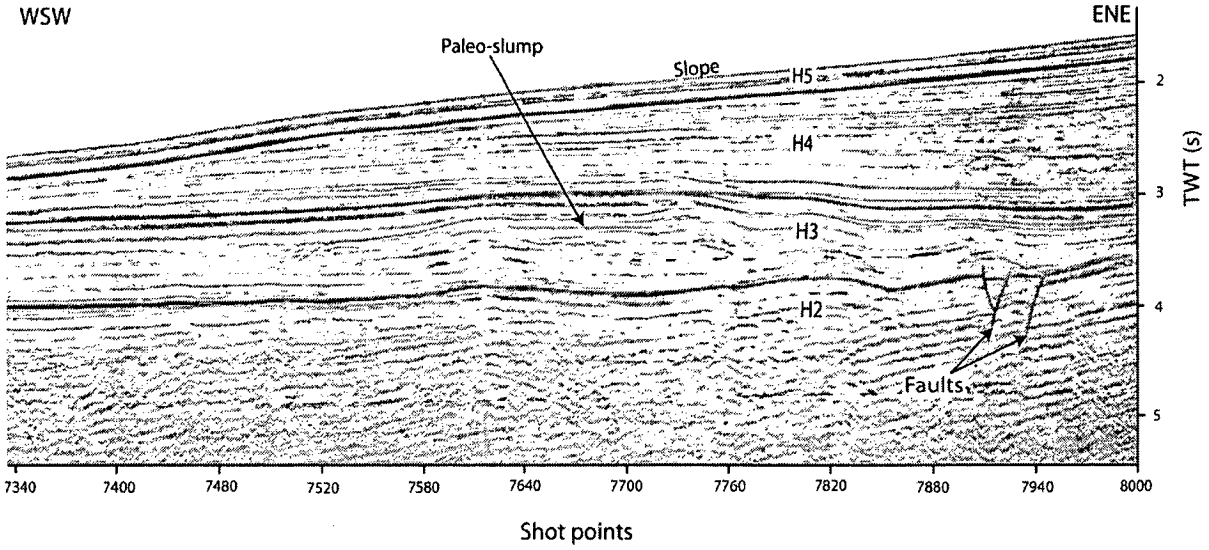


**Figure 4.11** Paleo slump identified below continental slope imaged in MCS profile RE19. Interpreted line drawing is shown in Figure 4.10.

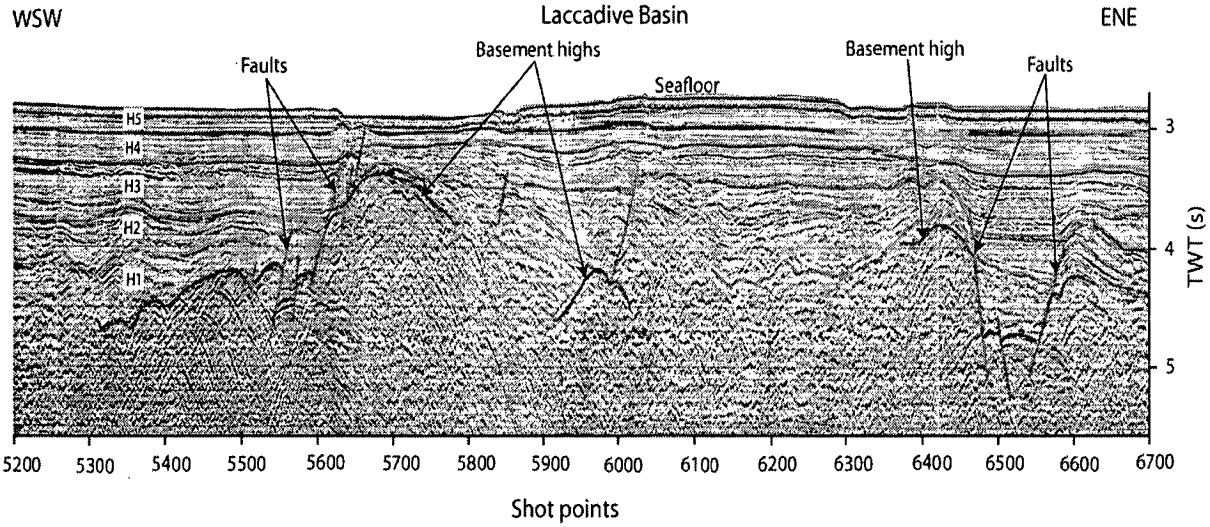


**Figure 4.12** Faulted basement highs, sediment strata and other structural features identified from the Laccadive Basin region depicted in MCS profile RE19. Interpreted line drawing is shown in Figure 4.10.

during deposition of the sequences L3 and L4. A set of westerly dipping seismic reflectors overlain by 1.2 s TWT thick sediment is identified along western flank of the Laccadive Ridge between shot points 1680 and 1140. These reflectors, which extend 27 km seaward, are interpreted as seaward dipping reflectors and discussed in chapter-6. Further west of the ridge, subdued basement highs are identified by high amplitude and coherent seismic reflectors beneath the sediment column.

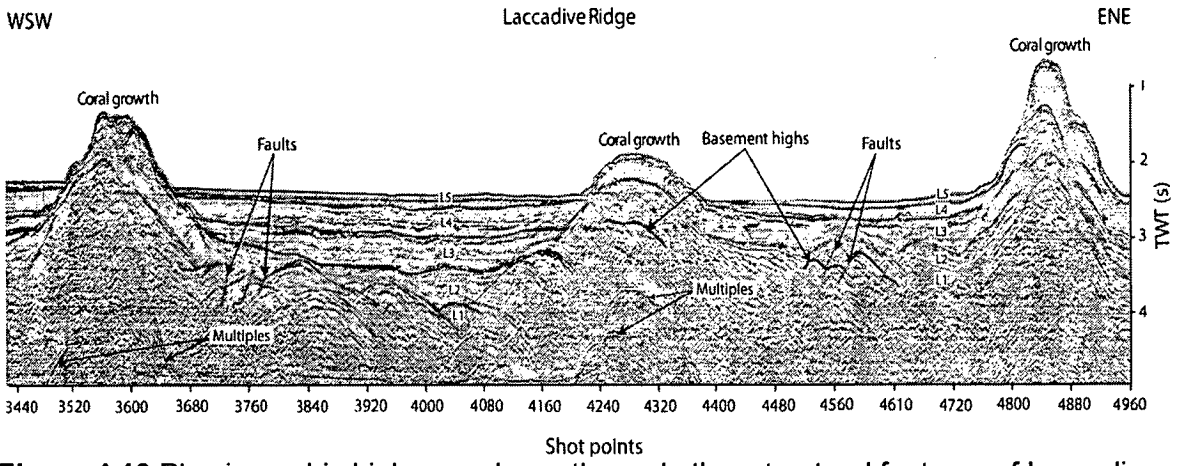


**Figure 4.13** Physiographic highs, coral growths and other structural features of Laccadive Ridge imaged in MCS profile RE19. Interpreted line drawing is shown in Figure 4.10.

### *Arabian Basin*

The seismic profile runs into the abyssal plain of the eastern Arabian Basin for about 15 km between shot points 300 and 1 (Figure 4.10). The seafloor is more or less smooth and gently dipping to the west. Four distinct seismic sequences A1-A4 are identified in the basin. Seismic sequences A3 and A4 abut on to the seismic sequence L2. The seismic sequence A3 is significantly thicker than the other sequences. All the identified seismic sequences in the basin appear to follow the basement trend.

**Table 4.4** Summary of seismic characters of MCS reflection profile RE19.

| | Continental shelf and slope | | | Laccadive Basin | |
|---|---|---|---|---|---|
| **Seismic sequences** | **Inferred age** | **Thickness TWT (s)** | **Seismic character** | **Thickness TWT (s)** | **Seismic character** |
| **H5** | Upper L. Miocene-Recent | 0.12-0.20 | Low amplitude and frequency, nearly reflection free | 0.15-0.29 | Low amplitude and frequency, nearly reflection free |
| **H4** | Lower-Upper L. Miocene | 0.04-1.35 | High amplitude and frequency, good reflection continuity with parallel to sub-parallel reflectors | 0.13-0.45 | Low to medium amplitude, low frequency, fairly good reflection continuity with parallel to sub parallel reflectors |
| **H3** | E. Oligocene-L. Miocene | 0.45-0.9 | High amplitude, low frequency, fairly good reflection continuity, sub parallel and contorted reflectors | 0.14-0.75 | High amplitude and frequency, moderate reflection continuity, parallel to sub parallel reflectors, disrupted to hummocky at places |
| **H2** | L. Paleocene-E. Oligocene | No lower boundary could be traced | High amplitude, low frequency, fairly good reflection continuity, sub parallel, disrupted and hummocky reflectors at places | 0.1-0.85 | High amplitude and frequency, moderate to fairly good reflection continuity, disrupted, hummocky and contorted at places |
| **H1** | L. Cretaceous-L. Paleocene | --- | Not discernable | 0.08-0.73 | High amplitude, high frequency, poor reflection continuity with discontinuous and contorted reflectors at places |

Table 4.4 Continued...

| | Laccadive Ridge | | | Arabian Basin | | | |
|---|---|---|---|---|---|---|---|
| Seismic sequences | Inferred age | Thickness TWT (s) | Seismic character | Seismic sequence | Inferred age | Thickness TWT (s) | Seismic character |
| L5 | E. Pliocene-Recent | 0.07-0.1 | Low amplitude and frequency, nearly reflection free | A4 | L. Pliocene-Recent | 0.16-0.21 | Low amplitude and frequency, moderate reflection continuity, parallel to sub parallel reflectors |
| L4 | M. Miocene-E. Pliocene | 0.05-0.5 | Low to medium amplitude, low frequency, nearly reflection free at places, moderate reflection continuity, parallel reflectors disrupted and contorted at places | A3 | E. Miocene-L. Pliocene | 0.1-0.35 | Medium to high amplitude, high frequency, fairly good reflection continuity, parallel to sub parallel reflectors disrupted at places |
| L3 | M. Eocene-M. Miocene | 0.12-0.6 | Low to high amplitude, high frequency, poor to fairly high reflection continuity, parallel to sub parallel, disrupted and hummocky reflectors | A2 | M. Eocene-E. Miocene | 0.1-0.27 | High amplitude and frequency, poor reflection continuity, hummocky reflectors |
| L2 | L. Paleocene-M. Eocene | 0.05-0.98 | Medium to high amplitude, high frequency, moderate reflection continuity, contorted to hummocky reflectors | A1 | Undated | 0.1-? | Medium to high amplitude, high frequency, discontinuous and semi coherent reflectors contorted at places |
| L1 | L. Paleocene | 0.05- ? | Medium to high amplitude, high frequency, discontinuous and semi coherent reflectors disrupted and contorted at places | | | | |

### 4.3.4 MCS reflection profile RE17

The ENE-WSW oriented 460 km long profile runs from continental shelf across continental slope and Laccadive Basin to the foot of the Laccadive Ridge (Figure 3.1). The profile is located about 125 km north of the profile RE19. Water depth along the profile varies from about 128 m on its eastern end to about 3750 m on its western end. The interpreted line drawing of the MCS profile is given in Figure 4.14. The seismic reflection characters of identified seismic sequences are tabulated in Table 4.5 with their inferred ages.

***Continental shelf and slope***

Continental shelf dips gently seaward up to the present shelf break which is identified at shot point 1125 (Figure 4.14 and Figure 4.15). The seismic sequences H1-H5 are distinguished from sediment column. A bathymetric low bounded by near vertical faults is identified between shot points 1190 and 1310. Two prominent paleo-shelf breaks are identified on H2-top and H3-top at shot points 807 and 870 respectively. The seismic sequences H4 and H5 constitute a prograded sigmoid pattern (maximum thickness ~1.9 s TWT) between shot points 860 and 1710. The continental slope is modified by a physiographic high identified between shot points 1715 and 1970 at a water depth of about 1148 m. The physiographic high identified at the foot of the continental slope is formed as a result of upliftment of the entire sediment column by a basement high which can be interpreted as a recently intruded igneous body. Even though the base of the seismic sequence H1 is imperceptible by complex and non-coherent reflectors, the upper boundary of the sequence H1 (H1 top) is exemplified by a series of faulting over the igneous intrusive body. The entire sediment sequences are considerably thinned by the igneous intrusive body before they enter into the Laccadive Basin from the continental slope.

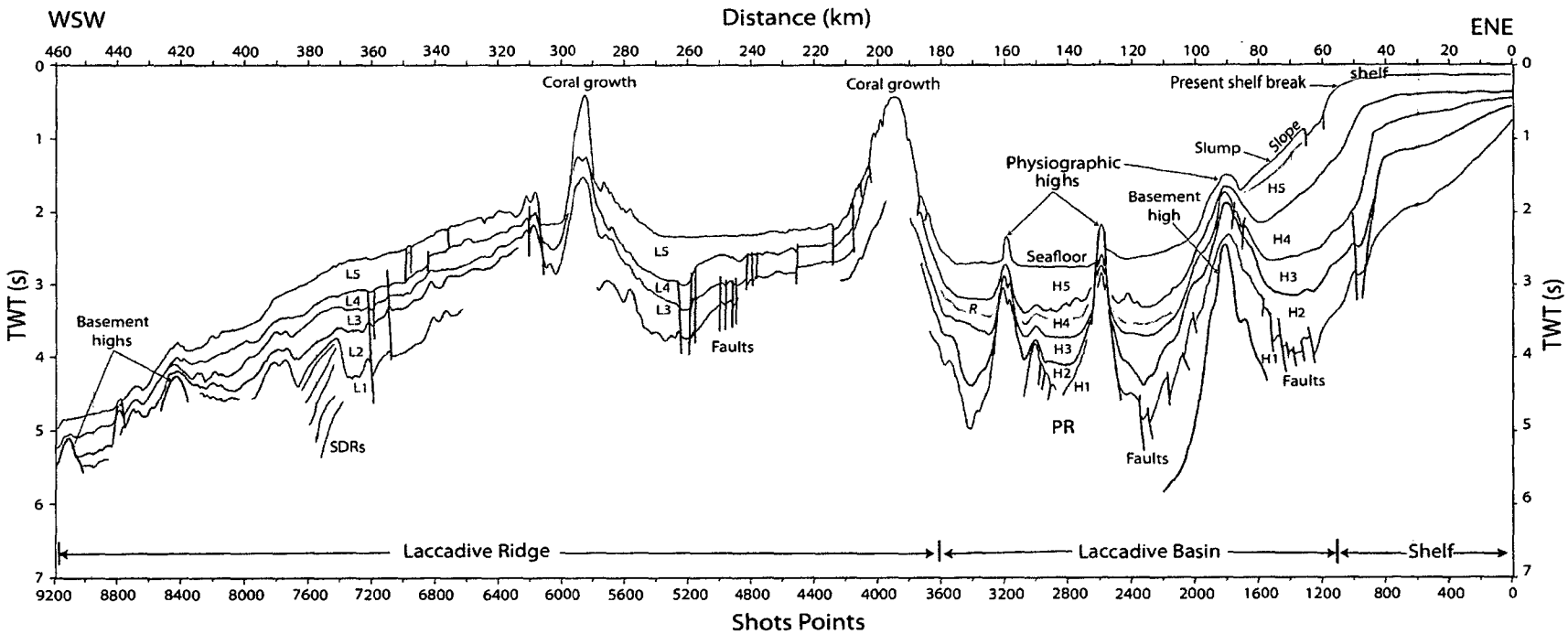


**Figure 4.14** Interpreted line drawing of MCS profile RE17. PR: Prathap Ridge; SDRs: Seaward Dipping Reflectors. Location of the profile is shown in Figure 3.1.

***Laccadive Basin***

The Laccadive Basin is depicted between shot points 1940 and 3600 with water depth varying between 1650 m and 2085 m (Figure 4.14). The seismic sequences H1-H5 are easily identified from the sediment column of the basin. Two physiographic highs are identified centered at the shot points 2585 and 3180. These physiographic highs are formed as a result of upliftment of the sedimentary sequences (H3-H5) by underlying basement highs of Prathap Ridge. The physiographic high centered at the shot point 2585 is bounded by deep faults along its flanks. Since the seismic sequences H1 and H2 terminate on the flanks of these basement highs, it can be suggested that, they are pre-depositional to the sequences H1 and H2. The uplifted sequences H3-H5 over crest of the basement highs were resulted from a recent upliftment of the basement highs. Thickness of sediment column is estimated as not less than 1.8 s TWT in deep sediment grabens. An additional seismic reflector R of remarkably good reflection continuity is identified between shot points 2120 and 3690 dividing the sequence H4 into two.

***Laccadive Ridge***

The Laccadive Ridge depicted in the profile begins with a physiographic high identified between shot points 3680 and 4120 with a relief of about 1538 m (Figure 4.14 and Figure 4.16). Another physiographic high of relief not less than 900 m is identified between the shot points 5800 and 5980, followed by ~8.5 km wide sediment graben to its west. Both these physiographic highs are characterized by complex reflection patterns at their crusts and perplex the identification of seismic sequence boundaries. This complex reflection pattern indicates coral growth on the crust of the basement highs towards euphotic zone. Five prominent seismic sequences L1-L5 are identified from deep sediment graben between shot points 6370 and 7360. The lower seismic sequences L1-L4 are affected by numerous faults compared to the upper sequence L5. A set of westerly dipping seismic reflectors overlain by a sediment column of thickness not less than 0.95 s TWT and extending seaward for about 15 km are identified between the shots 7400 and 7700 at a depth of ~3.8 s TWT. These seaward

dipping and diverging seismic reflectors are interpreted as Seaward Dipping Reflectors (SDRs) and discussed in chapter-6. Further west of the Laccadive Ridge, two subdued basement highs are identified beneath the sediment column.

The Arabian Basin cannot be discussed as the profile RE17 does not depict the basin.

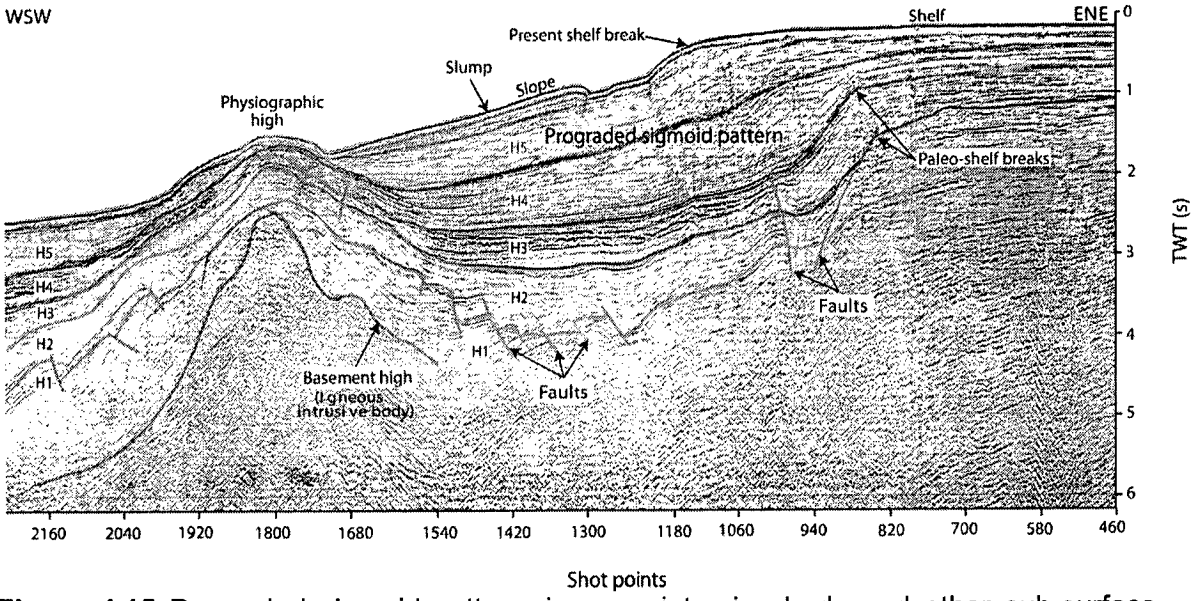


**Figure 4.15** Prograded sigmoid pattern, igneous intrusive body and other sub-surface features of continental shelf-slope imaged in the MCS profile RE17. Interpreted line drawing is shown in Figure 4.14.

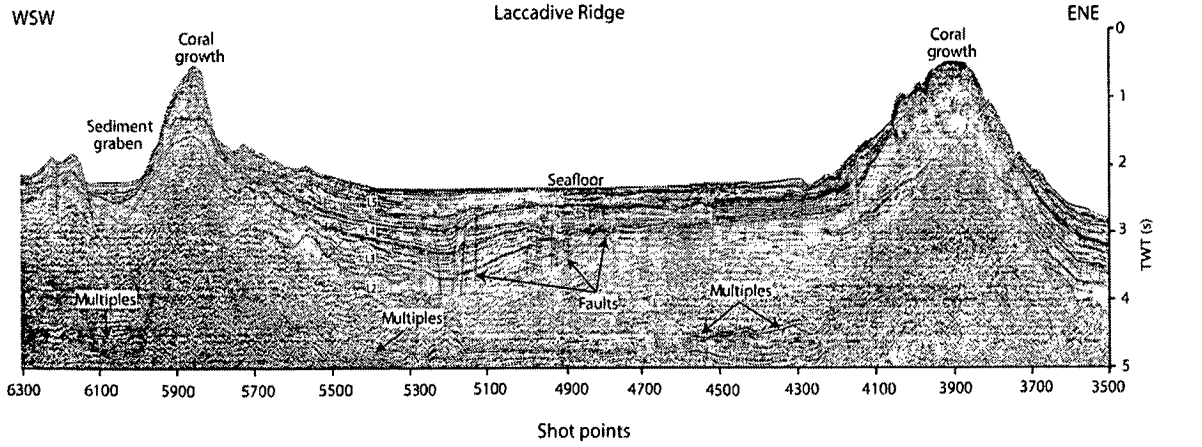


**Figure 4.16** Physiographic highs with coral growth and other sub-surface features of the Laccadive Ridge depicted in the seismic profile RE17. Interpreted line drawing is shown in Figure 4.14.

**Table 4.5** Summary of seismic characters of MCS reflection profile RE17

| | Continental shelf and slope | | | Laccadive Basin | |
|---|---|---|---|---|---|
| **Seismic sequences** | **Inferred age** | **Thickness TWT (s)** | **Seismic character** | **Thickness TWT (s)** | **Seismic character** |
| **H5** | Upper L. Miocene-Recent | 0.2-0.95 | Low to medium amplitude, high frequency, moderate reflection continuity, nearly reflection free in most of the parts | 0.09-0.75 | Low to high amplitude, high frequency, poor reflection continuity, nearly reflection free in most of the parts, disrupted and lenticular reflectors at the bottom |
| **H4** | Lower-Upper L. Miocene | 0.17-1.05 | Medium to high amplitude, high frequency, moderate reflection continuity | 0.03-0.42 | Medium to high amplitude, high frequency, near parallel reflectors, fairly good reflection continuity |
| **H3** | E. Oligocene-L. Miocene | 0.1-0.6 | Medium to high amplitude, high frequency, moderate reflection continuity, nearly concordant reflectors | 0.03-0.8 | Medium to high amplitude, high frequency, moderate reflection continuity, nearly concordant reflectors |
| **H2** | L. Paleocene-E. Oligocene | 0.25-0.9 | Medium to high amplitude, high frequency, moderate reflection continuity, nearly concordant reflectors | 0.1-0.63 | Medium amplitude, low frequency, poor reflection continuity |
| **H1** | L. Cretaceous-L. Paleocene | --- | High amplitude and frequency, poor reflection continuity and non coherent reflectors | --- | High amplitude and frequency, discontinuous and non coherent reflectors |

Table 4.5 Continued...

| Laccadive Ridge | | | |
|---|---|---|---|
| **Seismic sequence** | **Inferred age** | **Thickness TWT (s)** | **Seismic character** |
| **L5** | E. Pliocene-Recent | 0.15 – 0.67 | Medium to high amplitude, high frequency, moderate reflection continuity, hummocky reflectors at places. |
| **L4** | M. Miocene-E. Pliocene | 0.07 – 0.5 | Medium to high amplitude, high frequency, good reflection continuity, disrupted reflectors at places |
| **L3** | M. Eocene-M. Miocene | 0.05 – 0.65 | Medium to high amplitude, high frequency, fairly good reflection continuity, disrupted reflectors at places |
| **L2** | L. Paleocene-M. Eocene | 0.1 – 0.7 | Low to medium amplitude, high frequency, Poor reflection continuity, nearly lenticular reflectors at places |
| **L1** | L. Paleocene | --- | Medium amplitude, high frequency, discontinuous and non coherent reflectors |

### 4.3.5 MCS reflection profile RE15

The 852 km long profile RE15 runs from continental shelf across continental slope, Laccadive Basin and Laccadive Ridge into central Arabian Basin (Figure 3.1). The profile which begins from the continental shelf at a water depth of 188 m, terminates at a water depth of 4275 m in the Arabian Basin. The profile traverses about 176 km north of the MCS profile RE17. The interpreted line drawing of the profile is shown in Figure 4.17. Seismic reflection characters of identified seismic sequences and their inferred ages are tabulated in Table 4.6.

***Continental shelf and slope***

The continental shelf dips gently to the shelf break located at shot point 1160 (Figure 4.17 and Figure 4.18). Seismic sequences H1-H5 are identified along the continental shelf and slope. However, base of the seismic sequence H1 is not distinguished in this region. Boundary between the seismic sequences H4 and H5 is also not discernable between shot points 880 and 1280. Paleo-shelf breaks represented by the seismic sequence boundaries H1-top, H2-top and H3-top are identified at shot points 680, 770 and 760 respectively. The paleo shelf break of the sequence H3, identified about 20 km east of the present shelf break, is receded for about 500 m from that of the underlying shelf break of sequence H2. The seismic sequences H4 and H5 together constitute about 44 km wide prograded sigmoid pattern with a maximum thickness of not less than ~2.8 s TWT between the shot points 720 and 1600. A structural high is identified along the continental slope between the shot points 1680 and 1920. The high of 300 m height is characterized by a flat summit of width 12 km. Three seismic sequences H3-H5 are distinguished over the flat summit of the structural high. The concave nature of the seismic sequences between the shelf breaks and the structural high indicate gradual subsidence of the sediment layers after deposition.

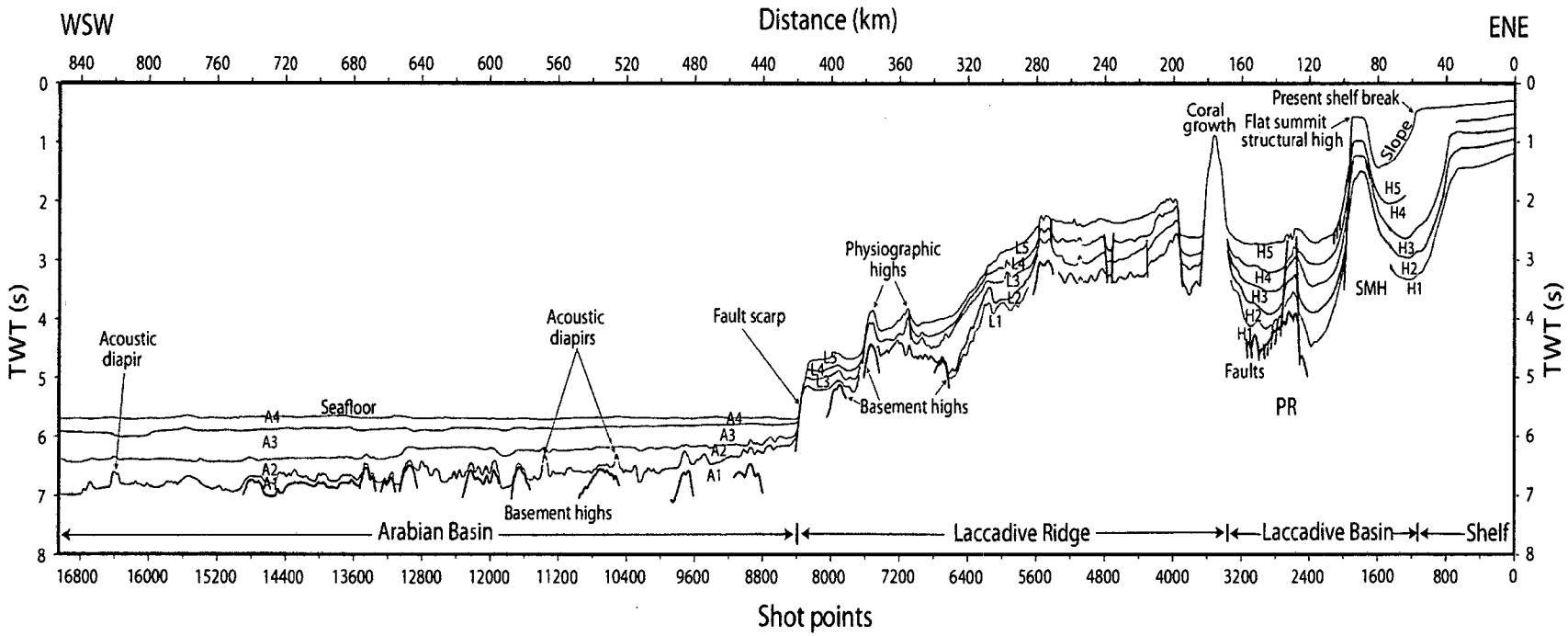


**Figure 4.17** Interpreted line drawing of MCS profile RE15. PR: Pratahp Ridge. Location of the profile is shown in Figure 3.1.

***Laccadive Basin***

The Laccadive Basin, which is bounded by flat summit structural high to the east, is extended up to the shot point 3360 (Figure 4.17). The 72 km wide Laccadive basin is characterized by a sediment column of maximum thickness of not less than 2.4 s TWT. Five major seismic sequences H1-H5 are identified from the basin. A subdued heavily faulted basement high of the Prathap Ridge, characterized by two major faults which penetrate through the overlying sediment column, is identified between the shot points 2535 and 2720. The upper seismic sequences H4 and H5 are folded and disrupted between these faults. The seismic sequences H1, H2 and H3 over the high appeared to be elevated not only due to upliftment by the basement high but also due to subsidence of the adjacent sedimentary basins. To the west of the basin the seismic sequences are thinning towards eastern flank of the Laccadive Ridge.

***Laccadive Ridge***

The Laccadive Ridge is depicted between shot points 3320 and 8360 (Figure 4.17). Water depth over the ridge varies between 638 and 3525 m. The ridge is characterized by a physiographic high with a relief of more than 1200 m at a water depth of about 600 m. The high is observed at the eastern end of the ridge between shot points 3320 and 3640. Complex reflection patterns hinder identification of the seismic sequences within the physiographic high. The physiographic high is followed by a sediment graben between the shot points 3640 and 3900 at a water depth of about 1950 m. The sequences L1-L5 are identified from the sediment grabens of the Ridge. Seismic sequence boundary between the sequences L1 and L2 are identified only between shot points 5700 and 6580. Columnar zones of complex, disrupted, up-doming and up-thrusting seismic reflectors are identified around the shot points 5120 and 5920 (Figure 4.19). Prominent basement highs, interpreted as igneous intrusive bodies, are identified to the west of the ridge between shot points 6620 and 8015. In this profile the Laccadive Ridge ends with a steep abrupt fault scarp to the west, around shot point 8360 (Figure 4.17).

***Arabian Basin***

The MCS profile extends into the Arabian Basin for about 432 km between shot points 8400 and 17045. The seafloor depicted in the profile is more or less smooth and horizontal with a water depth of about 4275 m. The seismic sequences A1-A4 are identified in the sediment column of the basin. The base of the seismic sequence A1 is not discernable in major part of the basin except between shot points 13550 and 14880. Several basement highs characterized by high amplitude and parabolic seismic reflections are identified. The boundary between the seismic sequences A1 and A2 (A1 top) is breached by local, complex and up-doming seismic reflectors at shot points 10510, 11360 and 16385. The sequences A1 and A2 are heavily interrupted and obtruded by these complex up-doming acoustic diapirs (Figure 4.17 and Figure 4.20).

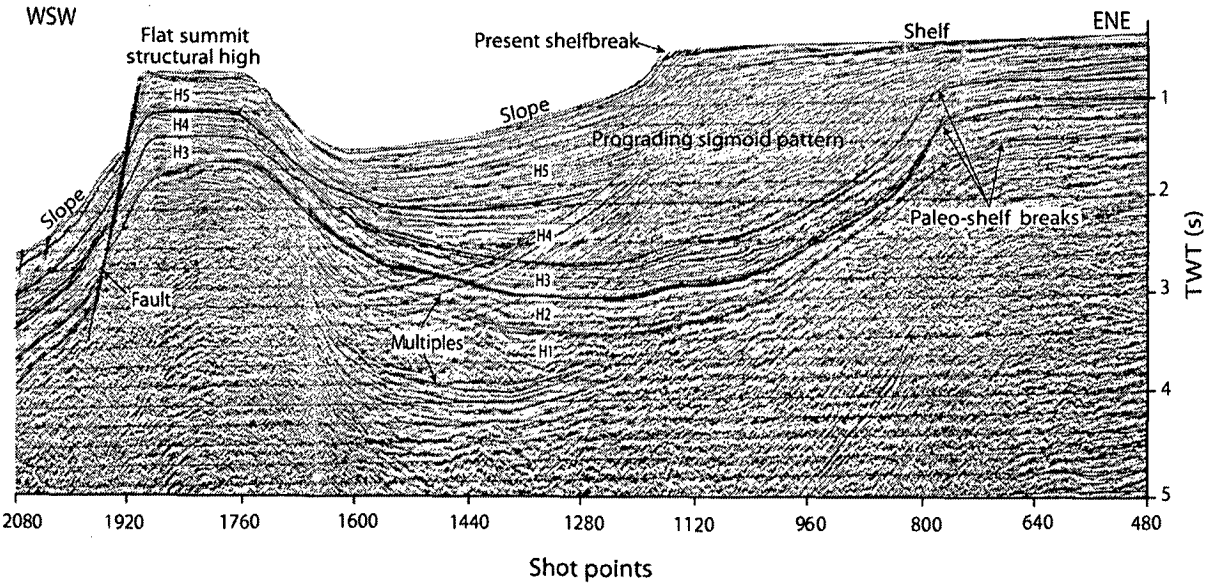


**Figure 4.18** Prograding sigmoid pattern and flat summit structural high identified along the continental shelf-slope imaged in the profile RE15. Interpreted line drawing is given in the Figure 4.17.

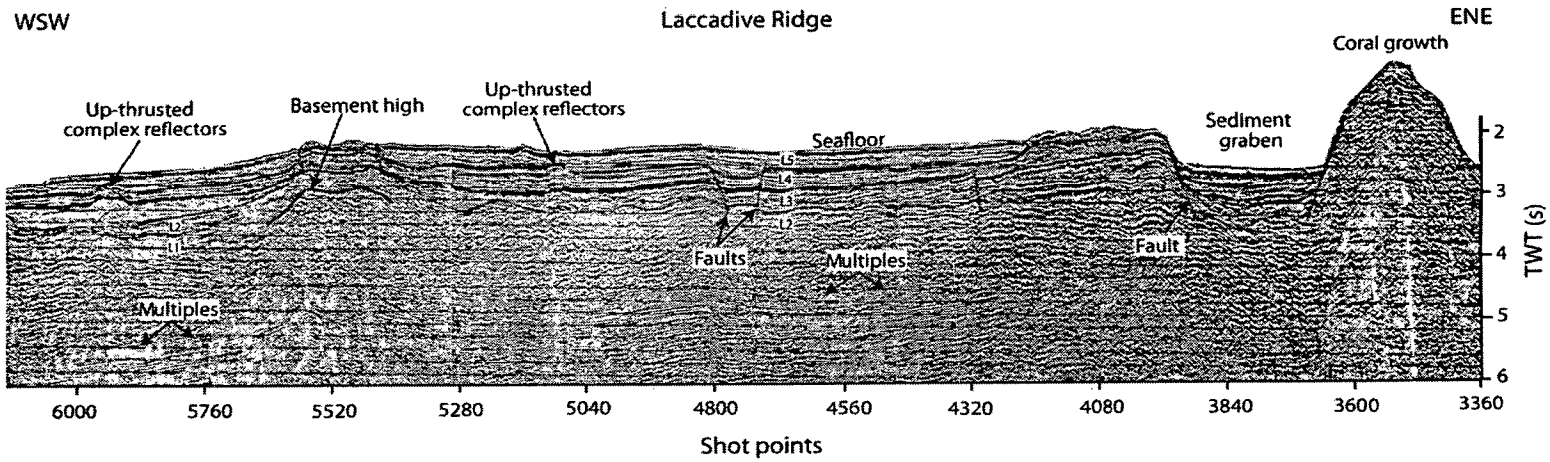


**Figure 4.19** Physiographic high with coral growth, up-thrusted complex reflectors and other surface and sub-surface features of the Laccadive Ridge depicted in the MCS profile RE15. Interpreted line drawing is given in the Figure 4.17.

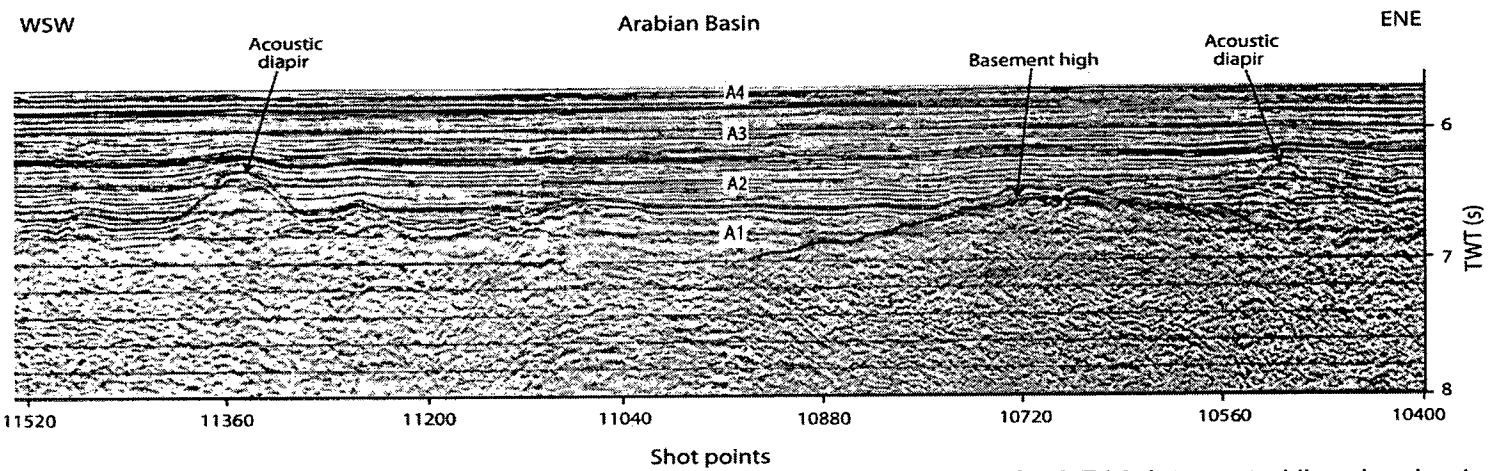


**Figure 4.20** Acoustic diapirs identified in the Arabian Basin imaged in the profile RE15. Interpreted line drawing is given in the Figure 4.17.

**Table 4.6** Summary of seismic characters of MCS reflection profile RE15.

| | Continental shelf and slope | | | Laccadive Basin | |
|---|---|---|---|---|---|
| Seismic sequenc | Inferred age | Thickness TWT (s) | Seismic character | Thickness TWT (s) | Seismic character |
| H5 | Upper L. Miocene-Recent | 0.24 - 0.9 | High frequency, medium to high amplitude, good reflection continuity, sub parallel to divergent reflectors | 0.11 - 0.43 | Low to medium amplitude, low to high frequency, fairly good reflection continuity, sub parallel reflectors |
| H4 | Lower-Upper L. Miocene | 0.12 - 0.76 | High amplitude and frequency, good reflection continuity, sub parallel to divergent reflectors | 0.1 - 0.5 | Medium to high amplitude, high frequency, good reflection continuity, sub parallel reflectors |
| H3 | E. Oligocene-L. Miocene | 0.16 - 0.44 | High amplitude and frequency, good reflection continuity, sub parallel to lenticular reflectors | 0.1 - 0.55 | Medium to high amplitude, low frequency, fairly good reflection continuity, sub parallel to lenticular reflectors |
| H2 | L. Paleocene-E. Oligocene | 0.2 - 0.52 | Medium amplitude, high frequency, fairly good reflection continuity, nearly concordant reflectors | 0.1 - 0.6 | Low to medium amplitude, low to high frequency, moderate reflection continuity, sub parallel to hummocky reflectors |
| H1 | L. Cretaceous-L. Paleocene | Lower boundary is not discernable | High amplitude and frequency, poor reflection continuity and non coherent | Lower boundary is not discernable | High amplitude and frequency, poor reflection continuity, sub parallel to lenticular reflectors |

Table 4.6 continued ...

| Laccadive Ridge | | | | Arabian Basin | | | |
|---|---|---|---|---|---|---|---|
| **Seismic sequenc** | **Inferred age** | **Thickness TWT (s)** | **Seismic character** | **Seismic sequenc** | **Inferred age** | **Thickness TWT (s)** | **Seismic character** |
| **L5** | E. Pliocene-Recent | 0.15 - 0.45 | Medium amplitude, low to high frequency, moderate reflection continuity, sub parallel reflectors | **A4** | L. Pliocene-Recent | 0.32 - 0.9 | Medium to high amplitude, high frequency, good reflection continuity, parallel to sub parallel reflectors |
| **L4** | M. Miocene-E. Pliocene | 0.08 - 0.4 | Medium to high amplitude, high frequency, good reflection continuity, sub parallel to concordant reflectors | **A3** | E. Miocene-L. Pliocene | 0.07 - 0.6 | High amplitude and frequency, good reflection continuity, parallel to wavy reflectors |
| **L3** | M. Eocene-M. Miocene | 0.125 - 0.7 | Medium to high amplitude, low to high frequency, moderate to good reflection continuity, lenticular, disrupted and contorted reflectors | **A2** | M. Eocene-E. Miocene | 0.09 - 0.3 | Medium to high amplitude, low to high frequency, moderate reflection continuity, sub parallel to lenticular reflectors |
| **L2** | L. Paleocene-M. Eocene | 0.05 - 0.3 | High amplitude and frequency, moderate reflection continuity, contorted to disrupted reflectors | **A1** | Undated | Lower boundary is not discernable | Medium to high amplitude, high frequency, poor reflection continuity. |
| **L1** | L. Paleocene | Lower boundary is not discernable | Medium to high amplitude, low to high frequency, discontinuous and non coherent reflectors | | | | |

### 4.3.6 MCS reflection profile RE13

The profile RE13 is the northern most among the MCS reflection profiles used for seismic stratigraphic analysis in the study. The ENE-WSW trending profile runs about 449 km from continental shelf across continental slope, Laccadive Basin and Laccadive Ridge into the eastern Arabian Basin (Figure 3.1). The profile is located about 126 km north of the seismic profile RE15. Water depth along the profile varies between 150 m and 4088 m. The interpreted line drawing of the seismic profile is given in Figure 4.21. Seismic reflection characters of the seismic sequences identified from each geological domain of the profile are tabulated in Table 4.7 with their inferred ages.

***Continental shelf and slope***

The continental shelf dips gently to the present shelf break identified at the shot point 1055 (Figure 4.21). The seismic sequences H1-H5 are identified from the continental slope. A maximum thickness of not less than 2.6 s TWT is estimated for the sediment column. The paleo shelf breaks, identified on H2-top and H3-top at shot points 825 and 805 respectively, indicate an aggraded continental shelf for the sequence H3. The shelf break of the sequence H3 is receded for about 1 km from the shelf break of underlying sequence H2. The present shelf break is prograded for about 11 km from the shelf break of sequence H3. The basement is distinguished between shot points 1050 and 1235. A prograded sigmoid pattern with a maximum thickness of ~1.8 s TWT and a width of about 34 km is identified between shot points 820 and 1500 (Figure 4.22). The sigmoid pattern, which is constituted by the sediment sequences H4 and H5, thins for about 0.48 s TWT to the foot of the continental slope.

***Laccadive Basin***

The Laccadive Basin is portrayed between shot points 1055 and 3250 in the seismic profile (Figure 4.21). The basin, of about 110 km wide, is characterized by an average water depth of 2063 m and a sediment thickness of not less than 2 s TWT.

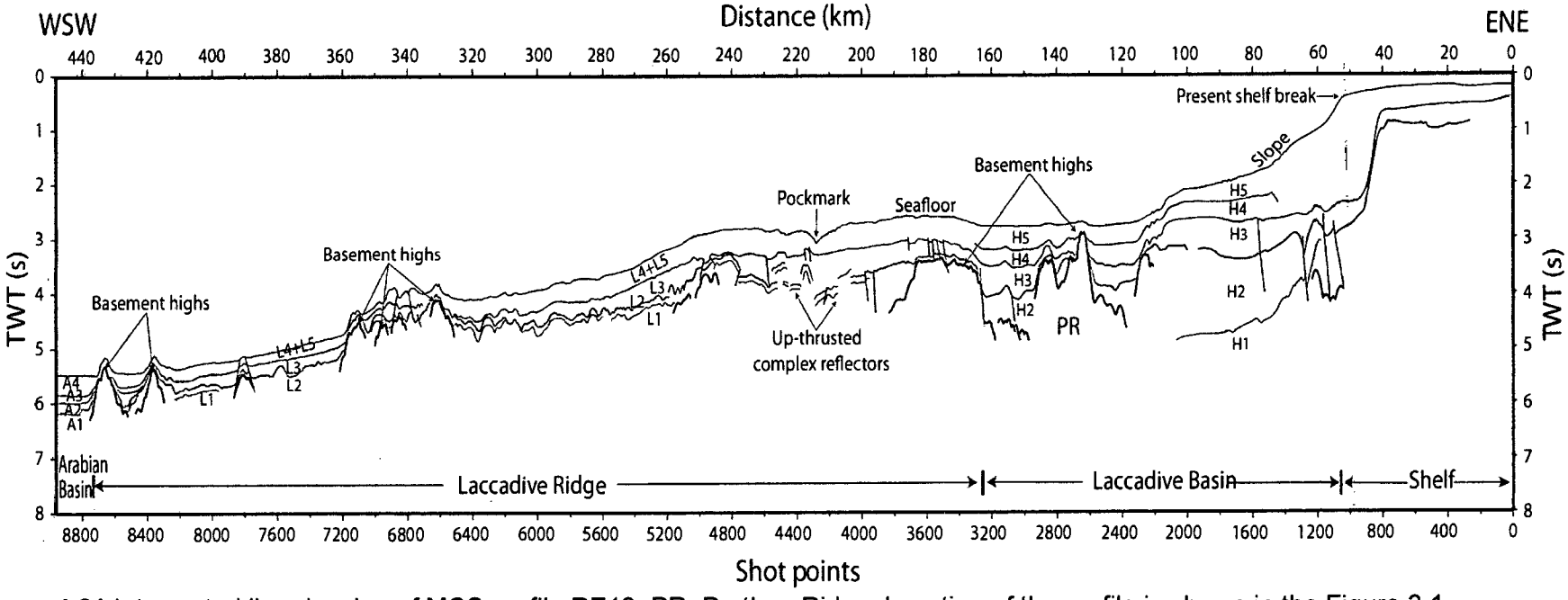


**Figure 4.21** Interpreted line drawing of MCS profile RE13. PR: Prathap Ridge. Location of the profile is shown in the Figure 3.1.

sequences concave to the east and abut to the western scarp of the igneous intrusive bodies located at the foot of the Laccadive Ridge. The seismic sequences are more or less horizontal and parallel to the west of the basin.

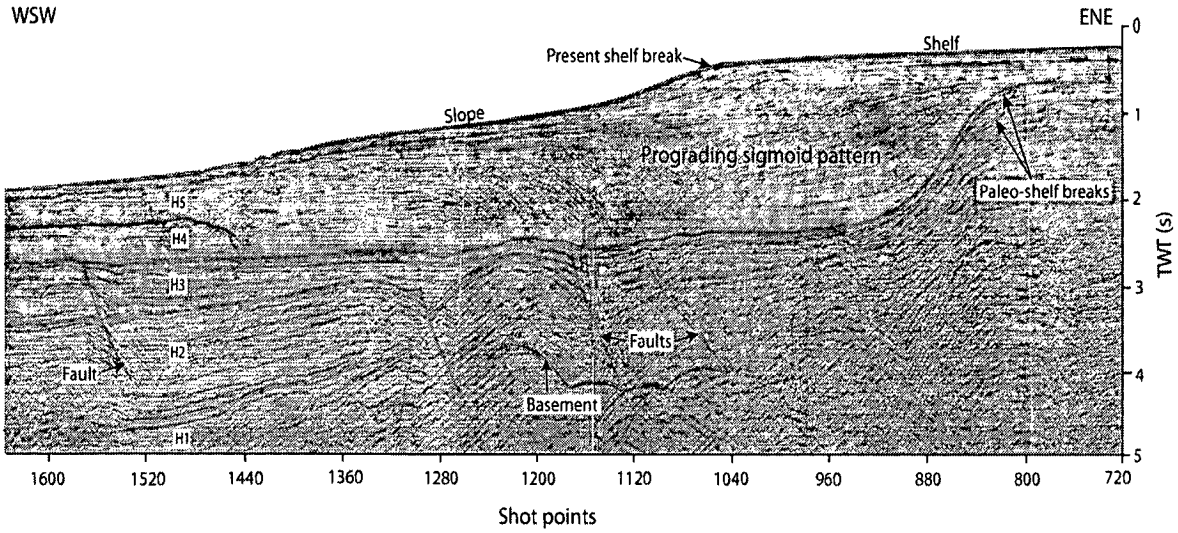


**Figure 4.22** Prograding sigmoid pattern and sub-surface features of the continental shelf-slope depicted in the seismic profile RE13. Interpreted line drawing is given in the Figure 4.21.

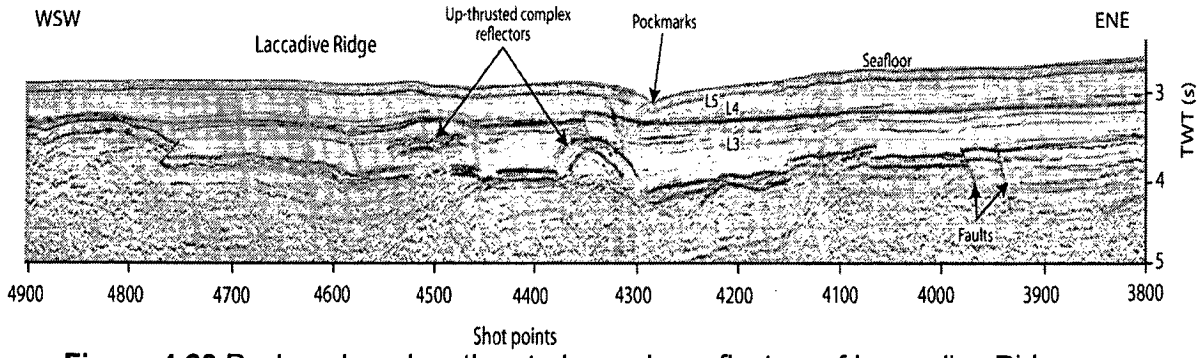


**Figure 4.23** Pockmark and up-thrusted complex reflectors of Laccadive Ridge imaged in seismic profile RE13. Interpreted line drawing is given in the Figure 4.21

**Table 4.7** Summary of seismic characters of MCS reflection profile RE13

| | Continental shelf and slope | | | Laccadive Basin | |
|---|---|---|---|---|---|
| **Seismic sequence** | **Inferred age** | **Thickness TWT(s)** | **Seismic character** | **Thickness TWT(s)** | **Seismic character** |
| **H5** | Upper L. Miocene-Recent | 0.22 - 0.97 | Medium to high amplitude, low frequency, moderate reflection continuity, sub parallel and contorted reflectors | 0.19 - 0.4 | Low amplitude and frequency, poor reflection continuity, nearly reflection free |
| **H4** | Lower-Upper L. Miocene | 0.3 - 0.45 | Low to medium amplitude, low frequency, moderate reflection continuity, nearly reflection free at lower part | 0.1 - 0.4 | Low to medium amplitude, low frequency, moderate reflection continuity, nearly reflection free at lower parts |
| **H3** | E. Oligocene-L. Miocene | 0.1 - 0.65 | High amplitude and frequency, good reflection continuity, sub parallel to disrupted reflectors | 0.1 - 0.55 | High amplitude and frequency, good reflection continuity, parallel to sub parallel and nearly concordant reflectors |
| **H2** | L. Paleocene-E. Oligocene | 0.6 – 1.7 | High amplitude and frequency, moderate to fairly good reflection continuity, sub parallel to divergent and hummocky reflectors | Lower boundary is not discernable | Medium to high amplitude, high frequency, moderate reflection continuity, sub parallel to lenticular reflectors |
| **H1** | L. Cretaceous-L. Paleocene | Lower boundary is not discernable | High amplitude and frequency, discontinuous and non coherent reflectors | Not discernable | |

Table 4.7 continued...

| Laccadive Ridge | | | | Arabian Basin | | | |
|---|---|---|---|---|---|---|---|
| **Seismic sequence** | **Inferred age** | **Thickness TWT(s)** | **Seismic character** | **Seismic sequence** | **Inferred age** | **Thickness TWT(s)** | **Seismic character** |
| **L5** | E. Pliocene-Recent | 0.28 - 0.95 | Low to high amplitude, low frequency, moderate reflection continuity, parallel to sub parallel reflectors | **A4** | L. Pliocene-Recent | 0.17 - 1.5 | Low to medium amplitude, low frequency, fairly good reflection continuity, parallel to sub parallel reflectors |
| **L4** | M. Miocene-E. Pliocene | | | **A3** | E. Miocene-L. Pliocene | 0.05 - 0.15 | Low to medium amplitude, low frequency, fairly good reflection continuity, parallel to sub parallel reflectors |
| **L3** | M. Eocene-M. Miocene | 0.04 - 0.5 | Low to high amplitude, low frequency, moderate reflection continuity, sub parallel to diverging reflectors | **A2** | M. Eocene-E. Miocene | 0.1 - 0.2 | Medium to high amplitude, low frequency, good reflection continuity, parallel to sub parallel reflectors |
| **L2** | L. Paleocene-M. Eocene | 0.05 - 0.2 | Low to high amplitude, low to high frequency, poor reflection continuity, sub parallel to hummocky reflectors | **A1** | Undated | Lower boundary is not discernable | High amplitude and frequency, moderate reflection continuity, sub parallel to hummocky reflectors |
| **L1** | L. Paleocene | Lower boundary is not discernable | Medium to high amplitude, low frequency, poor reflection continuity, non coherent reflectors | | | | |

## 4.4 Litho-Stratigraphic Correlation of Seismic Sequences

The litho- and chrono-stratigraphy of the SWCMI is known from few drill wells CH-1-1, K-1-1, KK-OS-VI-1, KG-1-1, KR-1-1, KK-OS-II/B-1, Well-D and DSDP site 219 located along the continental shelf and slope regions, and Laccadive Ridge. The interpreted seismic sequences are correlated with the major stratigraphic units of the study area (Figure 4.24 and 4.25). The chrono- stratigraphic information is obtained from the stratigraphic chart prepared by Mathur et al. (1993) and later modified by Rao et al. (2002). Even though most of the drill wells are distributed along the continental shelf and slope, the deep offshore extension of the litho-stratigraphic units are identified by offshore extension of correlated seismic sequences in the present study. General seismic characters of seismic sequences and their correlation with litho-stratigraphic units are discussed in the following sections with their inferred chrono-stratigraphic position and depositional conditions.

### 4.4.1 Continental shelf-slope and Laccadive Basin

Five seismic sequences H1-H5 are identified from the part of MCS profiles depicting the continental shelf-slope and Laccadive Basin. These seismic sequences are correlated with the major litho-stratigraphic units of Kerala-Konkan Basin (Figure 4.24).

Seismic sequence H1 is the lower most among the identified seismic sequences from this geological domain. Base of the sequence H1 is discernable only at those places where the basement reflectors are identified. The seismic sequence is generally characterized by high amplitude and frequency, poor reflection continuity, non-coherent to poorly coherent reflectors with sub parallel to lenticular reflection pattern at places. The seismic characters of this sequence indicate that it was deposited in a disturbed, complex and non uniform energy conditions produced by tectonic disturbances, and obstructions caused by intrusive structures. This seismic sequence is correlated with the Late Cretaceous to Late Paleocene sedimentary sequence of Cochin Formation which is mainly composed of shale, sandstone with clay and altered flow basalts (Table 4.8). The stratum of flow basalt associated with the Cochin Formation indicates a sub aerial environment of deposition.

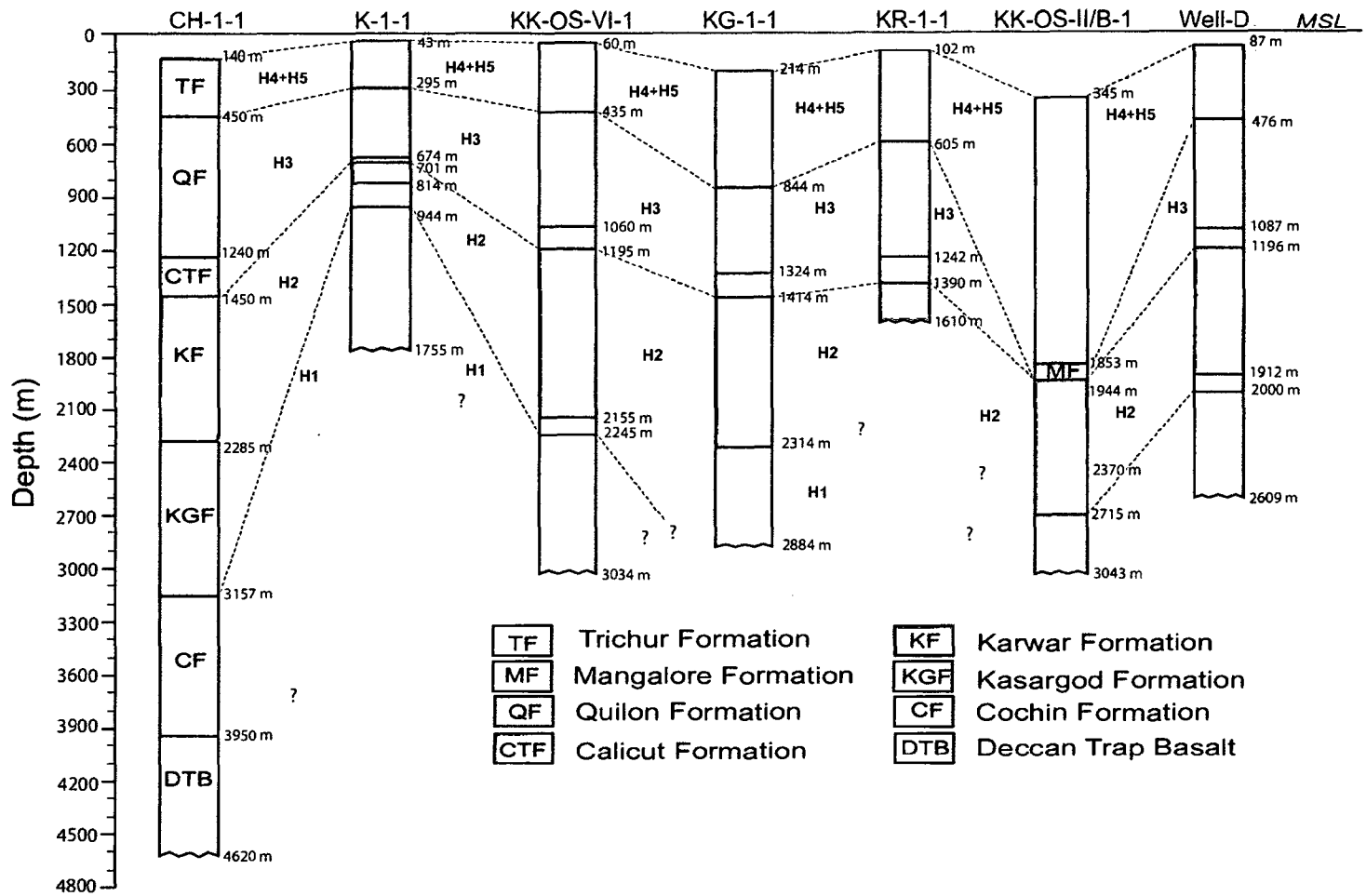


**Figure 4.24** Correlation of seismic sequences with the Litho-stratigraphic units delineated from the drill wells located in continental shelf-slope and Laccadive Basin.

The seismic sequence H1 is overlain by the sequence H2 of thickness 0.1-1.7 s TWT in the continental shelf-slope, and 0.05-0.85 s TWT in the Laccadive Basin. This seismic sequence is characterized by medium to high amplitude, high frequency, poor to fairly good reflection continuity with concordant, contorted and hummocky reflection patterns at places. The concordant reflections indicate slow and uniform deposition under alternate low and high energy condition, whereas, the hummocky reflection pattern suggests a complex and disturbed environment of deposition. The obstructions caused by various structural features and the sediment slumping from the elevated regions can cause the contorted reflection pattern within the seismic sequence. The near reflection free nature of the sequence in certain areas of the Laccadive Basin suggests an undisturbed and nearly homogenous sedimentation. The sequence H2 is correlated with the Late Paleocene to Early Oligocene sedimentary sequence of both the Kasargod and Karwar formations. This sequence is unconformably overly the Cochin Formation. The Kasargod Formation, deposited during Late Paleocene to Middle Eocene, is composed of shale, sandy clay, sandstone, siltstone and limestone occasionally inter bedded with lignite to the bottom of the formation (Rao et al., 2002). The Karwar Formation is deposited during Middle Eocene to Early Oligocene and is composed mainly of limestone with marl, silt and lignite bands. In the Laccaddive Basin the carbonates of the Karwar Formation become shaly and have been designated as Panaji Formation (Figure 3.2). It can be noted that the formation is bounded to the top by a major unconformity surface formed by Late Eocene depositional hiatus, particularly in the deep offshore region.

The seismic sequences H3, overlying the sequence H2, shows high amplitude and frequency, and moderate to good reflection continuity. Thickness of the sequence is calculated as 0.1-0.9 s TWT in the continental shelf-slope, and 0.03-0.8 s TWT in the Laccadive Basin. The sequence is characterized by parallel to sub parallel and nearly concordant reflectors with complex reflection patterns (disrupted, contorted, lenticular and hummocky) at places. The parallel to sub parallel and concordant reflectors indicate slow and uniform deposition with alternate low and high energy conditions, whereas the complex reflection patterns

suggest highly disturbed energy conditions during the deposition. This seismic sequence is correlated with two distinct lime rich sedimentary sequences named as Calicut and Quilon formations (Table 4.8). The Calicut Formation is formed by the deposition of limestone with occasional thin interbeds of grey shale during Early to Late Oligocene (Rao et al., 2002). The limestone is found to be dolomitised in several depositional intervals, and chalky at certain places. The Quilon Formation is essentially composed of grey to buff coloured limestones with associated carbonated sandstone, sandy clay, white corals and shell fragments, and is deposited during Late Oligocene to Late Miocene following the deposition of Calicut Formation. The Quilon Formation is more or less similar to the Calicut Formation with dolomitised and chalky limestones. The Calicut Formation and lower part of the Quilon Formation (Late Oligocene to Early Miocene) show lateral change into the clastic facies of the Mayyanad Formation below shallow continental shelf (Figure 3.2). Even though both the formations are correlated with single seismic sequence H3 due to their remarkable similarities in the lithology and composition, they appeared to be distinct in the MCS profile RE23 between shot points 5720 and 4545 dividing the sequence H3 into two (Figure 4.3).

Seismic sequence H4, lying over the sequence H3, is 0.04-1.4 s TWT thick in the continental shelf-slope, and 0.03 - 0.62 s TWT thick in the Laccadive Basin. The sequence H4 is characterized by low to high amplitude and frequency, moderate to good reflection continuity with sub parallel to divergent reflection pattern. The sub parallel and divergent reflectors suggest an alternate high and low energy depositional environment and subsidence of the basin. Some parts of this sequence are complex with near reflection free and hummocky reflection patterns. Near reflection free patterns suggests uniform and homogenous deposition of sediment, whereas, the hummocky reflection patterns indicate complex and disturbed environment of deposition. This seismic sequence H4 is correlated with remarkably terrigenous sedimentary sequences of Mangalore Formation deposited during Lower to Upper Late Miocene, and rests over a pronounced unconformity surface over the Quilon Formation (Figure 3.2).

**Table 4.8** Litho-stratigraphy of continental shelf, slope and offshore basins of SWCMI

| Inferred Age | Seismic sequences | Litho-stratigraphy | | Lithology |
|---|---|---|---|---|
| Upper Late Miocene to Recent | H5 | Trichur Foramation | | Sandy and silty clay, alluvial clay and lateritic clay |
| Lower to Upper Late Miocene | H4 | Mangalore Formation | | Clay, silt stone and Inter bedded shale |
| Late Oligocene to Late Miocene | H3 | Quilon Formation | | Carbonated sand stone and sandy clay bands, lime stone, white corals and shell fragments |
| Early Oligocene to Late Oligocene | | Calicut Formation | | Chalky, dolomitic lime stone, thin interbeds of grey shale |
| Early Eocene to Early Oligocene | H2 | a) Karwar Formation | b) Panaji Formation | a) Dolomitic lime stones with marl, silt and lignite bands b) Clay with interbedded shale |
| Late Paleocene to Early Eocene | | Kasargod Formation | | Sandy clay, shale, sand-stone, silt stone and lignite with lime stone towards bottom |
| Late Cretaceous to Late Paleocene | H1 | Cochin Formation | | Sand stone with clay, shale and altered and weathered flow basalt |
| Basement complex | | | | |

The upper seismic sequence H5 shows low to high amplitude and frequency, and poor to good reflection continuity. The seismic sequence is generally characterized by sub parallel to divergent reflection pattern. Complex reflection patterns (contorted, hummocky, lenticular, disrupted and near reflection free), identified locally, are produced by unstable and disturbed energy conditions during sediment deposition caused by waves, currents, sediment slumping and reactivation of the structural features by neotectonic activities. Thickness of the seismic sequence is calculated as 0.06-1.83 s TWT in the continental shelf-slope

region, and 0.03-0.8 s TWT in the Laccadive Basin. The seismic sequence H5 is correlated with terrigenous sediment sequence of Trichur Formation deposited during upper Late Miocene to Recent. The formation is mainly composed of alluvial, sandy, silty and lateritic clays, and unconformably lies over the Mangalore/Quilon formations. It differs from the underlying Mangalore formation in the absence of interbedded shale.

### 4.4.2 Laccadive Ridge

The seismic sequences interpreted from the part of the seismic profiles depicting Laccadive Ridge are correlated with the DSDP drill site 219 (Figure 4.25) located over the Ridge (Whitmarsh et al., 1974). The lower seismic sequence L1 is characterized by medium to high amplitude, high frequency and poor reflection continuity with semi coherent reflectors. This sequence is correlated with the Late Paleocene sediment sequence composed mainly of sandstone and siltstone with the deposition of glauconitic limestone to the top.

The seismic sequence L2, underlain by the seismic sequence L1, is characterized by low to high amplitude and frequency, poor to moderate reflection continuity. The sub parallel, disrupted, hummocky and contorted reflection patterns (Table 4.1) of this sequence suggest disturbed and unstable energy conditions during the deposition. The thickness of sequence L2 varies between 0.05 and 0.98 s TWT. This sequence is correlated with a sedimentary sequence deposited during Late Paleocene to Middle Eocene and composed of chalk, ooze and limestone with intermittent layers of Early to Middle Eocene chert stingers.

The sequences L3 is separated from the underlying sequence L2 by a depositional unconformity interpreted as L2 top. This seismic sequence of thickness 0.05-0.7 s TWT shows poor to good reflection continuity, and sub parallel to divergent, disrupted, hummocky and contorted reflection patterns. The sub parallel to divergent reflection configuration indicate non-uniform environment of deposition with differential subsidence. This seismic sequence is correlated with the sediment sequence of chalk and ooze, deposited during Middle Eocene to Middle Miocene.

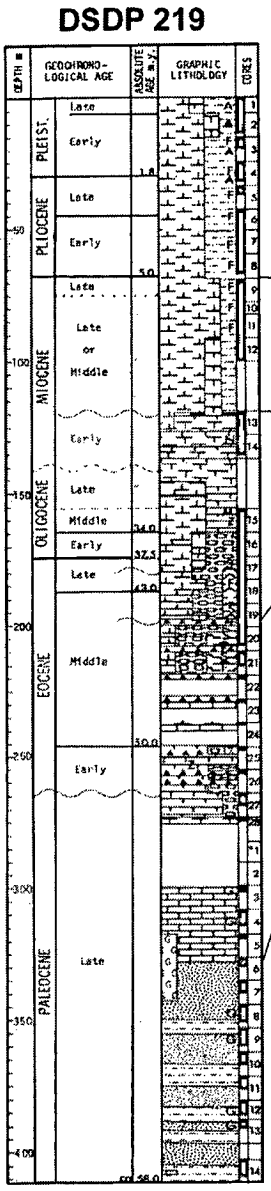


| Seismic sequences | Lithology | Inferred Age |
|---|---|---|
| L5 | Clay, silty clay, clayey silt and nanno ooze | Early Pliocene to Recent |
| L4 | Nanno ooze, Foraminiferal ooze and silty caly | Middle Miocene to Early Pliocene |
| L3 | Chalk and Ooze | Middle Eocene to Middle Miocene |
| L2 | Chalk, chert and lime-stones | Late Paleocene to Middle Eocene |
| L1 | sandstone, silt stone and glauconitic lime stone to the top | Late Paleocene |
| Unknown basement | | |

**Figure 4.25** Litho-stratigraphic correlation of seismic sequences identified from the Laccadive Ridge with the DSDP site 219.

The seismic sequences L4 of thickness 0.05-0.5 s TWT is characterized by low to high amplitude and frequency, moderate to good reflection continuity, and parallel to concordant reflectors with disrupted and contorted reflection patterns at places. This seismic sequence, which represents uniform environment of deposition in more or less low energy condition, is correlated with the sedimentary sequence deposited during Middle Miocene to Early Pliocene. This sedimentary sequence is composed mainly of nanno ooze and Foraminiferal ooze with clay and silty clay.

The uppermost seismic sequence L5 of thickness 0.15-0.75 s TWT is characterized by low to medium amplitude, low frequency, poor reflection continuity and near reflection free zones which represents more or less uniform and homogenous sedimentation. This sequence is correlated with the terrigenous sedimentary sequence deposited during Early Pliocene to Recent, and composed mainly of clay, silty clay, clayey silt and nanno ooze.

# Chapter-5

# STRUCTURAL FEATURES AND BASEMENT DEPTH ANOMALY

# Chapter-5

# STRUCTURAL FEATURES AND BASEMENT DEPTH ANOMALY

## 5.1 Introduction

Analysis of MCS reflection profiles carried out in this study revealed numerous structural and tectonic features associated with the sediment units and the underlying basement. These interpreted structural and tectonic features are correlated with satellite altimetry derived free-air gravity anomaly map of the WCMI to demarcate the boundaries of major features as well as trend of the magmatic intrusive bodies emplaced into the sediment column. In addition computation of basement depth anomalies in the Arabian Basin is presented. In light of this result, impact of Rèunion hotspot on the crust of the Arabian Basin as well as SWCMI is discussed.

## 5.2 Structural and Tectonic Features

Structural features characteristic of tectonic regime is termed as tectonic features. It may be mentioned here that, even though, the tectonic features are structural features, all the structural features may not be tectonic features. In this study numerous structural and tectonic features are identified and demarcated based on analyses of MCS profiles. The prominent structural features in the study area include i) submarine slumps along the continental slope, ii) present and paleo-shelf breaks, iii) submarine erosional channel, iv) acoustic columns of complex and up-thrusting seismic reflectors, v) faults and horst-graben structures, vi) shelf margin high, vii) Prathap Ridge, viii) Laccadive Ridge and ix) Seaward dipping reflectors.

### 5.2.1 Submarine slumps

Submarine slumps are defined as gravity driven slope failures characterized by minimal mass translation and breakage within the block of sediment (Vestal and Lowrie, 1982). The block of sediment slides down along a glide plane with a disorganized down slope motion during slumping. Submarine slumps are observed in the MCS reflection profiles RE23, RE19 and RE17 along the continental slopes (Table 5.1). The glide planes could not be distinguished except

in the profile RE17. In the profile RE23 the slump is identified between shot points 8640 and 8290 with an E-W extent of about 17.5 km in water depth ranging from 600 to 1575 m (Figure 4.3 and Figure 4.4). Another slump with an E-W extension of about 15.5 km, is also identified from the same profile between shot points 8025 and 7715 in water depth of 1875-2213m. A paleo slumping of the Middle Miocene time is identified at the foot of the continental slope, within the seismic sequence H3 of the seismic profile RE19 (Figure 4.10 and Figure 4.11). The paleo slump lies at a depth of about 3 s TWT with an E-W extent of about 22 km. Another slump is identified along the continental slope depicted in the profile RE17, between shot points 1300 and 1700, in water depth of 698 – 1275 m with an E-W extension of about 20 km (Figure 4.14 and Figure 4.15). The average E-W extent of the sediment slumps identified along the continental slope of SWCMI is 19 km.

The slumps can be caused by several factors such as re-activation of existing fault system, erosion by ocean currents, high sedimentation rate and subsidence, igneous activity, sea level changes, turbidity currents, gas hydrate destabilization, seismic triggers and tsunamies (Naini and Kolla, 1982; Vestal and Lowrie, 1982; Chauhan and Chaubey, 1992; Subrahmanyam et al., 1993b; Hanumantha Rao et al., 2002; Owen et al., 2007). Sediment slumps are not uniformly distributed all along the continental slope of SW India. The heavily faulted Cenozoic sediments and massive nature of the sediment slumps along the SWCMI suggest that the slumps were formed as a result of neo-tectonic activities caused by reactivation of existing structural trends. Part of the above results is published in a proceeding volume (Chaubey and Ajay, 2008).

**Table 5.1** Sediment slumps along the continental shelf-slope of SWCMI

| Slumps | MCS lines | Shot Points | E-W extent (km) |
|---|---|---|---|
| Recent slumps | RE17 | 1300-1700 | 20 |
| | RE23 | 8640-8290 | 17.5 |
| | | 8025-7715 | 15.5 |
| Paleo slump | RE19 | 7940-7500 | 22 |

### 5.2.2 Shelf breaks

Shelf breaks are the point of maximum curvature where the continental shelf and slope coincides. The continental shelf of the SWCMI, depicted in the MCS reflection profiles, exemplified by four distinct shelf breaks: i) Late Paleocene, ii) Early Oligocene, iii) Middle Miocene and iv) Present. These shelf breaks are interpreted along the seismic sequence boundaries H1-top, H2-top, H3-top and H5-top respectively. The present and Middle Miocene shelf breaks identified along SWCMI are presented in Figure 5.1. The relative positions of Middle Miocene (on H3-top) and Present shelf breaks (on H5 top) suggest that the Middle Miocene continental shelf is prograded seaward to the present shelf break for an average distance of 15 km with characteristic sigmoid pattern. This indicates a heavy influx of terrigenous sediments derived from the adjacent western Dharwar Craton into the Arabian Sea after the Middle Miocene. The drastic increase in clastic sediment supply into the Arabian Sea is related to the onset of intense Indian monsoon and establishment of well developed fluvial system, as a result of the collision between Indian and Eurasian plates and upliftment of the Himalayas during the Middle Miocene (Valdiya, 1999). The rise of Himalaya and establishment of Indian monsoon caused intense weathering, erosion and deposition of terrigenous clastics into continental shelf/slope and Laccadive Basin and drastic reduction in carbonate deposition (Rao and Srivastava, 1984; Nair et al., 1992; Singh and Lal, 1993; Whiting et al., 1994; Singh et al., 1999;). Due to rapid and heavy influx of terrigenous sediments, a thick pack of sediments was piled up in the continental slope region resulting in seaward progradation of the shelf edge forming a characteristic sigmoid depositional pattern.

The Middle Miocene shelf break of the seismic sequence H3 is aggraded from the shelf breaks of underlying seismic sequences H1 and H2. This aggraded phase of sedimentation, from Late Paleocene to Middle Miocene, can be linked to the development of thick pelagic carbonate sedimentary sequence deposited as a result of increased sea level and warmer climate (Rao and Srivastava, 1984; Nair et al., 1992; Singh and Lal, 1993; Whiting et al., 1994; Clift et al., 2001; Molnar, 2004). The Middle Miocene shelf break, imaged in the seismic profiles RE21, RE15 and RE13, is receded to the east (landward) from the Early Oligocene shelf

break (H2- top) with a lateral shift of about 0.8 km, 0.5 km and 1.0 km respectively (Figures 4.8, 4.18 and 4.22). These receded Middle Miocene shelf breaks may have formed due to high submarine erosional activities during the pelagic carbonate sedimentation. Whereas in the profile RE17, the aggraded Middle Miocene shelf break is also prograded seaward for a lateral distance of about 3.15 km from the Early Oligocene shelf break (Figure 4.15). The aggraded and prograded Middle Miocene shelf break in this location may indicate weak submarine erosional activities and continuous sediment influx.

### 5.2.3 Submarine erosional channel

Submarine erosional channels transport sediments from the shallow to deeper areas and function as a final pathway for the sediments to rush out of the areas of huge sediment influx. A well developed submarine erosional channel is identified on the Laccadive Ridge between shot points 2330 and 2515 of the profile RE19 (Figure 4.10). The channel is about 9 km wide and is seismically characterized by discontinuous, high amplitude, irregular and parabolic reflections to its bottom, and continuous, near parallel reflectors to the top. The high amplitude discontinuous reflectors to the bottom of the channel represent coarse sediments deposited as erosional laid down when the turbidity currents were relatively strong during low sea level. The irregular and parabolic reflections at the bottom of the channel suggest that the channel floor is an erosional unconformity surface formed as a result of strong turbidity currents within the channel during shallow marine conditions over the ridge. The upper layer of continuous and near parallel reflectors indicates channel fill, formed by hemipelagic sedimentation, subsequent to the cessation of turbidity current activities by sea level rise. The chrono stratigraphic correlation of seismic sequences identified within the channel indicates that the channel is migrated from the Middle Eocene (L2-top) with alternate erosional and depositional features. Migration of the channel in time and space is indicated by vertical shift of channel bed to the upper sequences.

### 5.2.4 Acoustic columns, acoustic turbidity and pockmarks

Acoustic columns are identified in two MCS reflection profiles RE21 and RE13, associated with pockmarks on the seafloor (Figure 4.9 and Figure 4.23). Acoustic

columns are the localized columnar zones of complex, up-doming and up-thrusting seismic reflectors within the seismic sequences. They are characterized by strong, breached and coherent reflectors obliterating all seismic reflections from below and creating acoustic blankets (Hovland and Judd, 1988; Taylor, 1992, Garcia-Gil et al., 2002). These acoustic columns are interpreted as vertical fluid migration zones through the sedimentary sequences. The migrating fluids can create an acoustic turbidity zone in the upper sediment sequences. About 50 km wide horizontal zone of acoustic turbidity is identified within the seismic sequence H4+H5 of the seismic profile RE21 between the shots 1105 and 2115 (Figure 4.9). The acoustic turbidity is formed by the variable degree of disturbance, produced by reflection and scattering of acoustic energy by gas bubbles present in the sediment, provoking a dark smear in the seismic records (Hovland and Judd, 1988; Garcia-Gil et al., 2002). V-shaped morphological depressions are identified on seafloor in the profiles RE21 and RE13. They are associated with strong hyperbolic reflectors indicating seismic characters of the pockmarks. Pockmarks are the morphological evidence of fluid seepage from seafloor. In most cases the seeping fluid is gas (Hovland and Judd, 1988). The term pockmark is proposed by King and MacLean in 1970 for the gas seeping morphologic depressions on the seafloor. However, when seepage occurs, pockmarks may or may not be formed. The hyperbolic reflections associated with V-shaped depressions are most probably artifacts produced by the interference of reflections from the pockmark walls (Hovland and Judd, 1988).

In the MCS profile RE15 the seismic sequences A1 and A2, interpreted from the Arabian Basin, are heavily interrupted and obtruded by local complex and up-doming seismic reflectors which are termed as acoustic diapirs (Figure 4.17 and Figure 4.20). Even though these complex acoustic diapirs are acoustically similar to the vertical fluid migration zones, they are not associated with the acoustic turbidity zone and/or pockmarks. Therefore, these local acoustic diapirs are interpreted as diapiric structures (salt or mud diapirs ?) within the lower sequences A1 and A2 of the Arabian Basin.

### 5.2.5 Faults and host-graben structures

The faults interpreted from the MCS reflection profiles indicate that the pre-Middle Miocene sedimentary sequences are more intensively affected by the faults than those of the post-Middle Miocene sediments. A number of normal and reverse faults are identified from the continental slope of the SWCMI, offsetting the lower seismic sequences H1, H2 and H3. Numerous deep penetrating faults are interpreted also from the Laccadive Ridge. Most of such faults are identified with the horst-graben structures. Several deep structural grabens filled with sediments of thickness not less than 0.5 s TWT are identified over the ridge. About 41 km wide zone of well developed horst-graben structures, associated with numerous faults and tilted crustal blocks, is identified from the southern part of the Laccadive Ridge imaged in the seismic profile RE23 (Figure 4.3 and Figure 4.6). The tilted crustal blocks are comprised mainly of the seismic sequences L1, L2 and L3 of pre-Middle Miocene age, and overlain by relatively less faulted post-Middle Miocene seismic sequences L4 and L5. The horst-graben structures extend for about 326 km with more or less NS trending axis, from the southernmost seismic profiles SK1203 to the profile RE19 (Figure 5. 1). The density of faults and horst-graben structures in the SWCMI indicate heavily faulted nature of crystalline basement beneath the sediment cover. Biswas (1987) has pointed out that the horst-graben structures and fault patterns of the western continental margin of India are formed due to rifting, and relative movements along the Precambrian structural trends indicating a weakened and extended crust. Since the pre-Middle Miocene sediments in the SWCMI are intensively affected by numerous faults and horst-graben structures, it can be suggested that the region has undergone a major tectonic event immediately after the deposition of Middle Miocene sediments. This tectonic event is correlated with hard collision between Indian and Eurasian plates, uplifting the Himalaya, during the Middle Miocene (Patriat and Achache, 1984; Valdiya, 1999) as a result of increase in rate of seafloor spreading along the Carlsberg Ridge between chrons 5c (14.04 Ma) and 6a (22.4 Ma) (Chaubey et al., 1993).

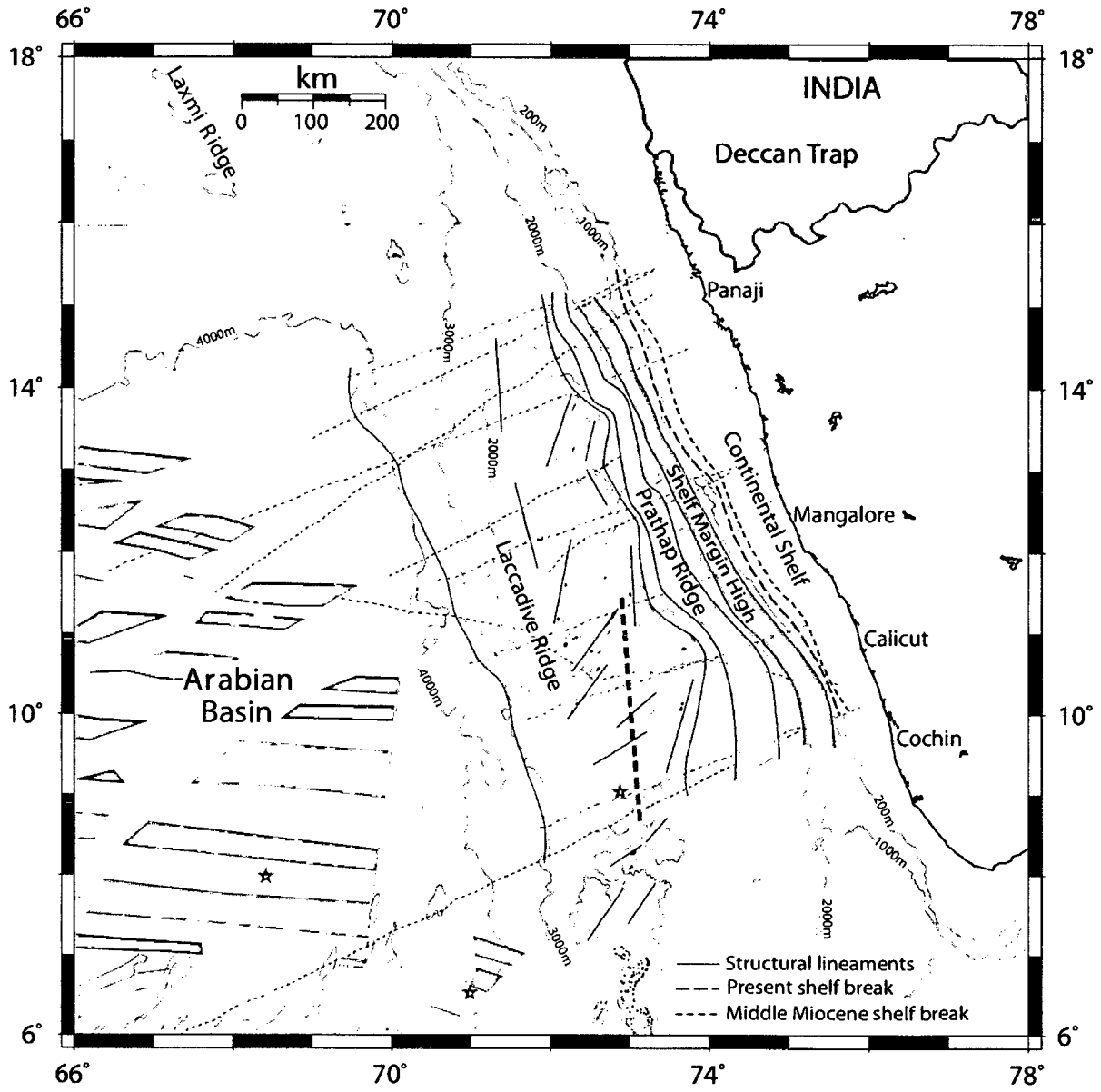


**Figure 5. 1** Map showing Middle Miocene and Present shelf break along SWCMI. The axis of horst-graben zone over the Laccadive Ridge is shown by thick dashed blue line. Structural lineaments and redefined boundaries of Laccadive Ridge, Prathap Ridge and Shelf margin high are adopted from Figure 5.2. The boundaries of Laccadive and Prathap ridges inferred from earlier studies are shown by yellow dashed lines.

### 5.2.6 Shelf margin high

In the present study, shelf margin high constituted by several flat summit structural highs are identified along continental slope of the SWCMI based on MCS reflection and shipborne as well as satellite altimetry derived free-air gravity anomaly data. Boundaries of these highs are demarcated between present shelf break and Prathap Ridge (Figure 5.2). The highs are located in a NNW-SSE

trending zone of width ranging between 17.4 and 43.5 km, more or less parallel to the west cost of India. Similar kind of flat-topped bathymetric highs (Chaubey et al., 2002b; Mukhopadhyay et al., 2008) are also reported from the continental slope region.

A structural high with flat summit and a width of about 12 km is presented as an illustrative example between shot points 1680 and 1920 of seismic profile RE15 (Figure 4.17 and Figure 4.18). The isolated structural high is characterized by high amplitude free-air gravity anomalies (Figure 5.2). The width of the shelf margin high in the study area varies between 17 and 44 km. Even though the high is covered by considerably thick sediment cover, the lower sequences H1 and H2 could not be identified from the sediment column over its crest. The flat summit and the absence of lower sedimentary sequences H1 and H2 over the high, suggest that it was under sub-aerial erosion during the deposition of those sequences. Sub-aerial exposure followed by weathering/erosion caused plaination of summit of the highs. The identification of the upper sequences H3, H4 and H5 over the structural high indicates submergence of the high to a sufficient depth during deposition of these sequences. The uplifted seismic sequences (H3-H5) over the high suggest upliftment of the high to its present depth during the deposition of sequence H5. The upliftment of structural highs since Pliocene is also reported (Mohan, 1985; Biswas, 1987; Whiting et al., 1994).

The chain of flat summit structural highs, identified along continental slope of the SWCMI, is continental slivers and horst structures which broke away from the continental margin during rifting (Gopala Rao et al., 2010).

### 5.2.7 Prathap Ridge

Prathap Ridge which is mostly buried under the sediment cover of the Laccadive Basin is identified in the MCS reflection profiles as basement highs intruded and/or extruded through the sediment apparently dividing the basin into two parts. In the profile RE23, identified seismic sequences are terminated on to the steep scarps of the basement high of Prathap Ridge indicating pre-sedimentational existence of the high within the Laccadive Basin (Figure 4.3 and Figure 4.5).

Intense faulting is evident on crests of the basement highs of Prathap Ridge identified from the profiles RE19 and RE15 (Figure 4.10, Figure 4.12 and Figure 4.17). The seismic sequences H1, H2 and H3, overlying the Prathap Ridge, are thinned, faulted and uplifted by the basement highs imaged in the MCS profiles RE19 and RE13 (Figure 4.10 and Figure 4.21). This indicates reactivation and upliftment of the ridge during Middle – Late Miocene. A recent reactivation of the ridge is also identified in the MCS profiles RE17 and RE15, by the presence of near vertical faults penetrating through the entire sediment column overlying the basement highs, and upliftment of the sedimentary sequences along these faults (Figure 4.14 and Figure 4.17).

The ridge is characterized by well-developed and high amplitude free-air gravity anomalies over the basement highs. The boundary of the Prathap Ridge is redefined by integrated analysis of ship-borne as well as satellite altimetry derived free-air gravity anomalies and the MCS reflection profiles in the study area (Figure 5.2). The Prathap Ridge trends in a NNW-SSE direction, dividing the Laccadive Basin into two, between shelf margin high in the east and Laccadive Ridge in the west (Figure 5.1 and Figure 5.2). In the study area the width of the ridge varies from 17 km in the north to 65 km in the south. It has been debated whether the genesis of Prathap Ridge is related to Rèunion hotspot volcanism (Krishna et al., 1992) or to a part of Precambrian fabric separated from the main land during the process of rifting between India and Madagascar (Subrahmanyam et al., 1995). Since the seismic responses of basement highs of the Prathap Ridge, imaged in the MCS reflection profiles, are characteristically related to the igneous intrusive/extrusive bodies rather than the rifted and block faulted continental blocks, it is suggested that the genesis of Prathap ridge is related with the Rèunion hotspot volcanism. The conical structural highs of Prathap Ridge to the west of flat topped structural highs of the shelf margin high, and their volcanic nature are reported also by Mukhopadhyay et al. (2008).

### 5.2.8 Laccadive Ridge

Analysis of MCS reflection profiles indicate a number of normal and reverse faults, horst graben structures associated with tilted fault blocks and igneous intrusive

bodies over the Laccadive Ridge. The sediment thickness over the ridge is highly variable. Several deep sediment grabens with sediment thickness of >0.5 s TWT are identified. Five sedimentary sequences L1-L5, of inferred age Late Paleocene to Recent, are interpreted from the seismic profiles. The basement reflectors are not discernable in most part of the ridge. However, the seismic sequences, which show highly variable thickness and complex faulting, suggest a raised and heavily faulted crystalline basement below the sediment. Seismically imaged physiography of the Laccadive Ridge shows relatively steep eastern flank compared to the gently dipping western flank indicating a westerly tilt for the basement of the ridge.

A zone of well developed horst graben structures is identified on the Laccadive Ridge with a more or less NS trending axis of length 326 km (Figure 5.1). The intensively faulted and tilted crustal blocks of pre-Middle Miocene age indicate the major tectonic event of hard collision between Indian and Eurasian plates, uplifting the Himalaya, during the Middle Miocene (Patriat and Achache, 1984; Valdiya, 1999). The western flank of the Laccadive Ridge, depicted in most of the MCS reflection profiles, is characterized by prominent igneous intrusive bodies. However, the ridge imaged in the MCS profile RE15 terminates abruptly into the Arabian Basin with a steep fault scarp (Figure 4.17), suggesting a deep faulted continental crustal block along the western flank of the ridge in this region.

The integrated analysis of ship-borne as well as satellite altimetry derived free-air gravity anomalies and the interpreted MCS reflection profiles over the ridge facilitate the redefining of the ridge boundaries (Figure 5.2). Width of the ridge varies between 238 and 304 km in the study area. The ridge is wider in the north compared to the south. High amplitude free-air gravity anomalies are observed over the igneous intrusive bodies interpreted from the MCS reflection profiles. The correlation of such high amplitude free-air gravity anomalies revealed a number of structural lineaments characterized by emplacement of magmatic intrusives/extrusives as revealed from the seismic profiles (Figure 5.1 and Figure 5.2). These structural lineaments are more or less parallel to the major Precambrian structural trends of the SWCMI. The Precambrian trends are the zones of deformed and weakened basement crust

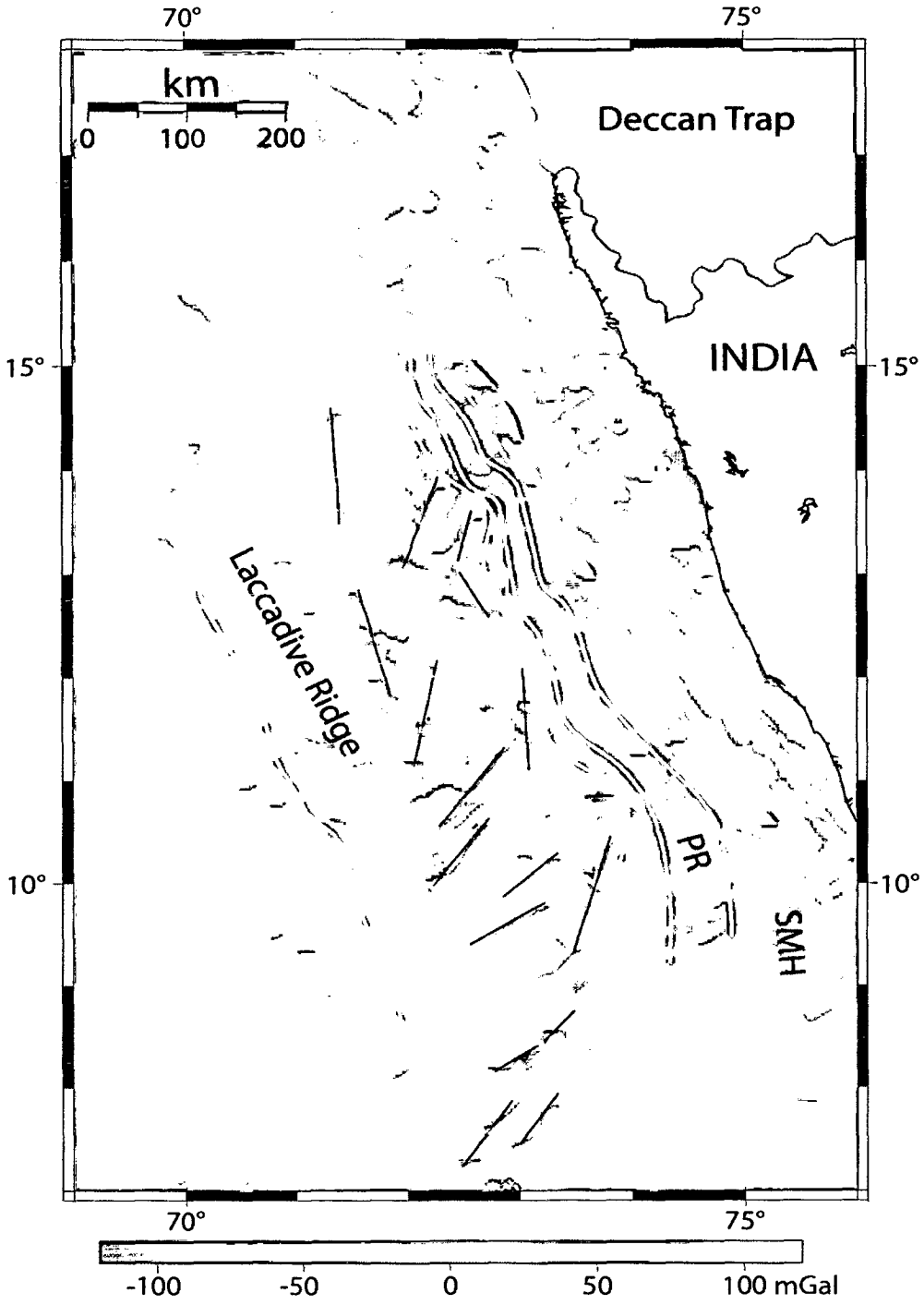


**Figure 5.2** Satellite gravity image of the study area and redefined boundaries of the Laccadive Ridge, Prathap Ridge and Shelf margin high. Structural lineaments associated with magmatic intrusives/extrusives are shown by blue lines. Dotted lines represent the MCS lines. PR: Prathap Ridge; SMH: Shelf Margin High.

formed as a result of Precambrian Orogenisis (Biswas 1982, 1987, 1988; Gombos et al., 1995). Therefore, the structural lineaments could be the fracture zones formed in the older continental crust by availing intrusive/extrusive magmatism during the continental rifting episode and the activities of Marion (~88 Ma) and Rèunion (~65 Ma) hotspots. However, it is difficult to segregate the magmatism caused by the Marion and Rèunion hotspots. Volcanic successions of seaward dipping reflectors are identified along the western flank of the ridge adjacent to the known oceanic crust of the Arabian Basin. The detailed discussion on this is presented in chapter-6. The highly faulted, fractured and intruded nature of the ridge crust suggests a stretched and thinned continental crust, and infers a continental fragment origin for the Laccadive Ridge.

### 5.2.9 Seaward Dipping Reflectors

Several westerly dipping seismic reflectors are identified from the western flank of the Laccadive Ridge depicted in the MCS reflection profiles RE23, RE19 and RE17 (Figure 4.3, Figure 4.10 and Figure 4.14). These reflectors are later interpreted as Seaward Dipping Reflectors (SDRs) based on their seismic velocity, seismic reflection characters and geographic locations, and are discussed in chapter-6.

## 5.3 Basement depth anomalies in the Arabian Basin

According to the theory of plate tectonics, new oceanic lithosphere accreted at spreading ridges cools, contracts and subsides uniformly as it moves away from the spreading ridges. The change in depth to seafloor from the spreading ridge crest to the ocean basin is a unique function of crustal age (Menard 1969), caused by cooling and thickening of oceanic lithosphere, and follows empirical age-depth relationships (Menard 1969, 1973; Sclater and Francheteau 1970; Davis and Lister 1974; Parsons and Sclater 1977; McKenzie et al. 1980; Hayes 1988; Stein and Abbott 1991; Stein and Stein 1992; Hillier and Watts 2004; Louden et al. 2004). However, some areas in the oceans do not follow this generally accepted age-depth relationship and therefore, are characterized by anomalous depth to the basement. The Arabian Basin is one such region in the Arabian Sea. In the

present study, the term 'basement depth anomaly' (Menard 1973) is used to define the difference between the present depth of oceanic basement of known age (corrected for sediment load) and the predicted depth of the oceanic basement of the same age. Further, the rise and subsidence of the present oceanic basement with respect to the predicted oceanic basement are termed as negative and positive basement depth anomalies respectively.

### 5.3.1 Computation of basement depth anomalies

The basement depth anomalies in the Arabian Basin are computed using published results (Figure 3.1 and Table 3.3) of seismic refraction (Naini and Talwani, 1983), DSDP sites 220 and 221 (Whitmarsh et al., 1974), and magnetic isochron (Chaubey et al., 2002a) in the following two major steps:

i) Calculation of predicted basement depth
ii) Calculation of present basement depth corrected for sediment load

The predicted basement depths have been calculated using the lithospheric thermal model for Global Depth and Heat-flow (GDH1) of Stein and Stein (1992), derived for the crust older than 20 Ma. The predicetd basement depth D(t) at a given ocean floor of age t Ma (t≥20 Ma) is given as:

$D(t) = 5651 - 2473 \exp(-0.0278t)$ .....(1)
Where basement age $t \geq 20$ Ma

The age of the oceanic basement was obtained using the regional magnetic isochron map of Chaubey et al. (2002a) and the geomagnetic reversal timescale (Cande and Kent 1995). The basement age in the Arabian Basin varies from ~62.5 Ma (anomaly 28ny) in the northern part to ~38.4 Ma (anomaly 18ny) in the southern part. The basement age at each refraction station is calculated by linear interpolation using the half spreading rate and the identified magnetic isochron pattern. The predicted basement depths in the Arabian Basin are then calculated from the estimated age using equation (1) and presented in Table 5.2.

In order to compute present basement depth corrected for sediment load, at first, the depth to oceanic basement and sediment thickness overlying the oceanic crust are computed at each refraction station. Oceanic basement in the study area is identified by considering 5.51 km/s as the representative interval velocity of oceanic crustal layer 2 underlying the sediments. Thickness of each sediment unit is calculated from the interval velocity and two way travel time. Total thickness of sediment units and the water depth together give depth to observed oceanic basement at each refraction station. Finally, the observed basement depths are corrected for the sediment load.

The corrections for the isostatic compensation of sediment load ($\Delta S$) overlying the basement at each seismic refraction station are computed using the following formula (Crough 1983):

$$\Delta S = d(\rho_a - \rho_s)/(\rho_a - \rho_w) \quad \ldots\ldots(2)$$

Where $\rho a$=3.3 gm/cm$^3$ and $\rho w$=1.03 gm/cm$^3$ are the densities of the upper mantle and seawater respectively, $\rho s$ and d are the density and thickness respectively of the sediment above the basement.

The depth to basement corrected for sediment load ($D_c$) was then calculated using the following formula (Hayes 1988):

$$D_c = d_w + \Delta S \quad \ldots\ldots(3)$$

Where $d_w$ is observed water depth.

The density of the sedimentary column is obtained from the Nafe–Drake velocity–density relationship curve (Nafe and Drake, 1963). The average seismic velocity ($V_a$) of a multi-layer sedimentary column was computed using the formula:

$$V_a = (e_1 + e_2 + \ldots + e_n / (e_1/v_1 + e_2/v_2 + \ldots + e_n/v_n) \quad \ldots\ldots(4)$$

Where $e_1$, $e_2$, ... $e_n$ and $v_1$, $v_2$, ... $v_n$ are the thicknesses and interval velocities of the sedimentary layers 1, 2, ...n respectively, as obtained from the seismic refraction data.

By subtracting basement depth predicted by the GDH1 model from sediment-corrected basement depth, the basement depth anomalies of the study area are computed, and presented in Table 5.2. The depth anomalies obtained after removal of the lithospheric cooling effect can be interpreted in terms of crustal and upper mantle sources and flexure of the lithosphere.

### 5.3.2 Results on basement depth anomalies

The computed basement depth anomalies (Table 5.2) in the Arabian Basin suggest that subsidence in this basin does not follow the age–depth relationship of normal oceanic crust. The anomalous depths to the oceanic basement of the basin indicate the presence of both positive and negative anomalies which vary from +501 to –905 m. These anomalies, observed over 63–42 Ma old oceanic crust of the basin, are not distributed randomly but rather show a distinct pattern – a zones of negative anomalies, followed by a zone of positive anomalies (Figure 5.3). The negative depth anomaly zone, mapped in the eastern part of the basin immediately west of the Laccadive Ridge, indicates a rise of oceanic basement i.e., basement depth shallower than predicted. The positive depth anomaly zone, mapped in the western part of the basin, indicates excess subsidence of oceanic basement i.e., deeper basement depth than predicted.

Large (>300 m) positive depth anomalies (deeper basement than predicted) are observed at locations of seismic refraction stations 64V, 66V, 67C and 68C in the positive depth anomaly zone. These locations show excess subsidence and coincide with the major sediment depocentre of the Arabian Basin. The depocentre region, which is located between about 64 and 67°E and 14 and 17°N, approximately corresponds to the centre of the Indus Cone where over 3 km of sediment has accumulated (Naini 1980).

In the negative depth anomaly zone (shallower basement than predicted), the negative anomalies increase from west to east towards the Laccadive Ridge, even though the basement age increases in the same direction. This indicates that the

corrected basement depth becomes shallower towards the Laccadive Ridge, and does not follow the depth predicted by the thermal cooling and thickening of normal oceanic lithosphere in this part of the Arabian Basin. The shoaling of the basement is related to the Reunion hotspot which was active during the early Tertiary, when it interacted with the northward moving Indian plate to build the Laccadive Ridge on the rifted continental crust of India.

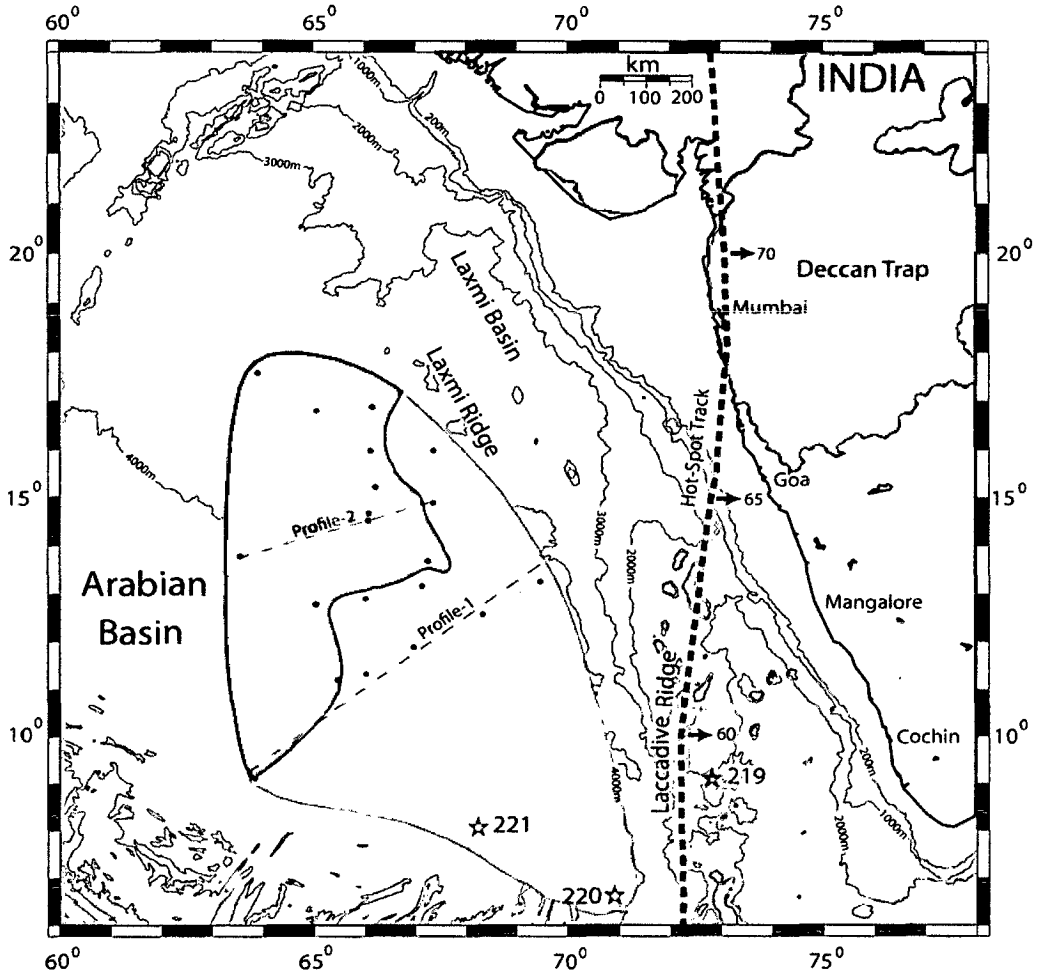


**Figure 5. 3** Map showing distribution of basement depth anomalies in the Arabian Basin. The anomalies display two distinct patterns a zone of negative anomalies (shaded by purple) followed by a zone of positive anomalies (shaded by blue). Depth anomaly curves shown in Figure 5.4 have been prepared along profiles 1 and 2. Locations refraction stations and computer modeled Rèunion hotspot track are shown as solid dots and thick dash lines respectively. Numbers along hotspot track are predicted ages in My.

Two profile, which show observed basement depths, basement depths obtained after sediment load correction, and basement depths predicted by the lithospheric thermal model GDH1 of Stein and Stein (1992), are presented across the Arabian Basin (Figure 5.3 and Figure 5.4). These profiles pass from southwest to

northeast, and traverse from positive to negative depth anomaly zones. It may be noted that even though the age of the oceanic crust along the profile progressively increases towards the northeast, basement depths (corrected for sediment load) do not follow the predicted basement trend. Profile 1 shows low-amplitude positive depth anomalies (deeper basement than predicted), followed by an increase in negative depth anomalies (shallower basement than predicted) towards the northeast. Profile 2, by contrast, shows a general increase in positive depth anomalies, implying deeper basement than predicted by the lithospheric thermal cooling model. This deepening of the basement attains its maximum value in the sediment depocentre region and gradually become less pronounced towards the Laccadive Ridge. These results are published as a scientific paper (Ajay and Chaubey, 2008).

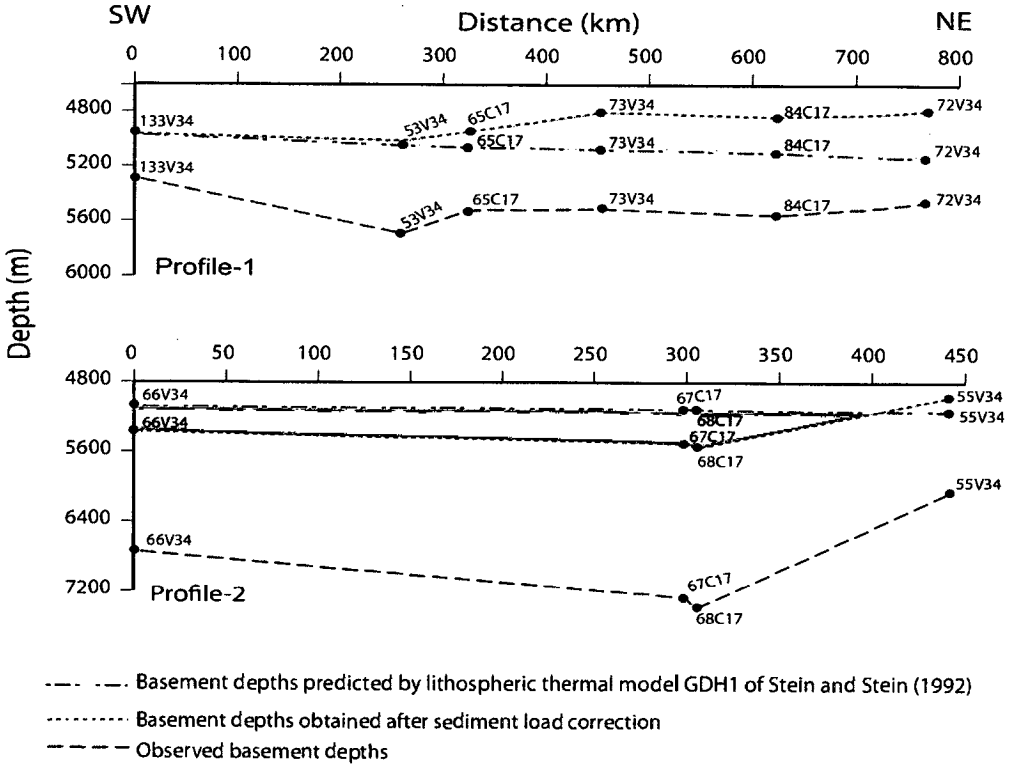


**Figure 5.4** Two northeast–southwest profiles (cf Figure 5.3) across the Arabian Basin, showing observed basement depths, basement depths obtained after sediment load correction and predicted basement depths. Location of refraction stations (solid dots) are shown in Figure 3.1.

**Table 5.2** Basement depth anomalies computed at refraction stations in the Arabian Basin

| Refraction stations | Age (Ma) | Water depth (m) | Sediment thickness (m) | Present basement depth (m) | Predicted basement depth (m) | Average seismic velocity (km/sec) | Sediment density (gm/cc) | Sediment load correction (m) | Sediment corrected basement depth (m) | Basement depth anomaly (m) |
|---|---|---|---|---|---|---|---|---|---|---|
| 61V | 60.303 | 3505 | 3640 | 7145 | 5188 | 2.72 | 2.15 | 1838 | 5343 | 155 |
| 70 C | 61.436 | 3580 | 3770 | 7350 | 5203 | 2.71 | 2.15 | 1910 | 5490 | 287 |
| 50 V | 59.570 | 3538 | 3580 | 7118 | 5179 | 2.68 | 2.14 | 1829 | 5367 | 188 |
| 80 C | 61.410 | 3720 | 970 | 4690 | 5202 | 2.06 | 1.95 | 577 | 4297 | -905 |
| 69 C | 59.223 | 3730 | 3070 | 6800 | 5174 | 2.60 | 2.14 | 1574 | 5304 | 130 |
| 64 V | 55.885 | 3703 | 3380 | 7083 | 5128 | 2.64 | 2.14 | 1726 | 5429 | 301 |
| 55 V | 56.439 | 3769 | 2290 | 6059 | 5136 | 2.38 | 2.07 | 1237 | 5006 | -130 |
| 68 C | 54.916 | 3840 | 3550 | 7390 | 5114 | 2.73 | 2.17 | 1775. | 5615 | 501 |
| 67 C | 54.639 | 3780 | 3490 | 7270 | 5110 | 2.62 | 2.14 | 1785 | 5565 | 455 |
| 66 V | 52.903 | 3992 | 2750 | 6742 | 5083 | 2.60 | 2.12 | 1425 | 5417 | 334 |
| 70 V | 54.270 | 3814 | 2660 | 6474 | 5104 | 2.56 | 2.11 | 1393 | 5207 | 103 |
| 54 V | 53.347 | 3983 | 1860 | 5843 | 5090 | 2.41 | 2.07 | 1006 | 4989 | -101 |
| 66 C | 52.663 | 4030 | 1950 | 5980 | 5079 | 2.56 | 2.11 | 1021 | 5051 | -28 |
| 52 V | 52.290 | 3996 | 2050 | 6046 | 5073 | 2.36 | 2.06 | 1123 | 5119 | 46 |
| 72 V | 56.255 | 4017 | 1440 | 5457 | 5133 | 2.29 | 2.05 | 794 | 4811 | -322 |
| 84 C | 53.855 | 4120 | 1430 | 5550 | 5098 | 2.54 | 2.11 | 752 | 4873 | -225 |
| 73 V | 52.197 | 4128 | 1380 | 5508 | 5072 | 2.73 | 2.16 | 696 | 4824 | -248 |
| 65 C | 51.380 | 4220 | 1300 | 5520 | 5058 | 2.18 | 2.00 | 744 | 4964 | -94 |
| 53 V | 50.780 | 4198 | 1490 | 5688 | 5048 | 2.15 | 1.99 | 863 | 5061 | 13 |
| 133 V | 46.260 | 4361 | 925 | 5286 | 4968 | 1.75 | 1.82 | 603 | 4964 | -4 |
| DSDP221 | 48.440 | 4650 | 261 | 4911 | 5008 | 1.65 | 1.75 | 178 | 4828 | -180 |
| DSDP220 | 52.198 | 4036 | 330 | 4366 | 5072 | 1.60 | 1.70 | 232 | 4268 | -804 |

# Chapter-6

# SEAWARD DIPPING REFLECTORS AND CRUSTAL STRUCTURE

# Chapter-6

# SEAWARD DIPPING REFLECTORS AND CRUSTAL STRUCTURE

## 6.1 Introduction

The western continental margin of India is considered as a typical passive rifted margin (Biswas, 1982, 1987; Chandrasekharam, 1985; Mahadevan, 1994) evolved during three distinct rifting episodes as discussed in chapter-2. The southern part of the WCMI is generally considered as a non volcanic passive margin produced during the break-up between southern India and eastern Madagascar. Whereas, the northern part of the WCMI is a volcanic passive margin, developed during breakup of India-Laxmi Ridge-Seychelles continental block contemporaneous with predominant Deccan volcanic episode of excess volcanism. Despite the fact that the India-Madagascar break-up produced an extensive volcanic province along eastern Madagascar and basaltic flows and intrusives on the SWCMI as well as southwest Indian shield, the nature of this margin is not yet investigated enough to classify it as a volcanic margin.

In this chapter, the seaward dipping seismic reflectors identified from three MCS reflection profiles RE23, RE19 and RE17 along the western flank of the Laccadive Ridge, are analyzed under constraints of seismic refraction derived P-wave velocities. As discussed later in this chapter, these reflectors are interpreted as Seaward Dipping Reflectors (SDRs) – one of the diagnostic tectono-magmatic features of the volcanic continental margin.

Further, 2D gravity modeling is carried out along five transects (RE23, RE21, RE19, RE17 and RE15) of the southwest continental margin of India to achieve consistent geological models, which can account for interpreted feature of the present study and provide improved picture on crustal models reported earlier. Improved crustal structure of the SWCMI is important in constraining the geometry and structural parameters of the continental margins as well as continent-ocean transition.

## 6.2 Seaward dipping reflectors

Volcanic passive margins differ from non volcanic passive margins mainly due to presence of diagnostic tectono-magmatic features. These characteristic features are the huge volume of magma emplaced during initial stage of seafloor spreading typically as seaward dipping reflector sequences, numerous intrusive/extrusive bodies emplaced into the sedimentary basin (Berndt et al., 2001), and a lower crustal body with high P-wave velocity of more than 7.1 km/s (Planke et al., 1991; Eldholm et al., 1995). The studies carried out so far on passive continental margins worldwide suggest that Seaward Dipping Reflectors (SDRs) – one of the most distinctive features of a volcanic passive margin - represent flood basalts rapidly extruded during either rifting or initial stage of seafloor spreading. These Seaward Dipping Reflectors mark the offshore limit of the continent crust, thereby used to define Continent-Ocean Transition (COT) – a transitional boundary between continental and oceanic crust.

SDRs are a stack of laterally continuous, divergent and offlapping reflectors capable of yielding important evidence of evolution of continental margins. During continental break-up extensive extrusive constructions are emplaced along divergent volcanic margins. These constructions commonly include formations which appear as SDR sequences in the seismic record (Figure 6.1). Therefore, the SDRs are interpreted as voluminous basaltic flows emplaced sub aerially and/or in a shallow sub-aqueous environment during the latest period of rifting and earliest phase of sea floor spreading (Hinz, 1981; Austin and Uchupi, 1982; Mutter et al., 1982; Mutter, 1985; Planke and Eldholm, 1994; Gladczenko et al., 1998). These flows may be interbedded with sediments similar to those drilled on the Hatton Bank (Roberts et al., 1984). According to Hinz (1981) and Mutter et al. (1982) the regions of SDRs generally mark areas of rifted continent and their dips arose from the subsidence due to isostatic compensation of enormous volumes of basaltic lava flows emplaced during initial continental split-up.

The seaward dipping reflectors show diagnostic appearance in the seismic reflection profiles. Mutter (1985) noticed following consistent features of the SDR

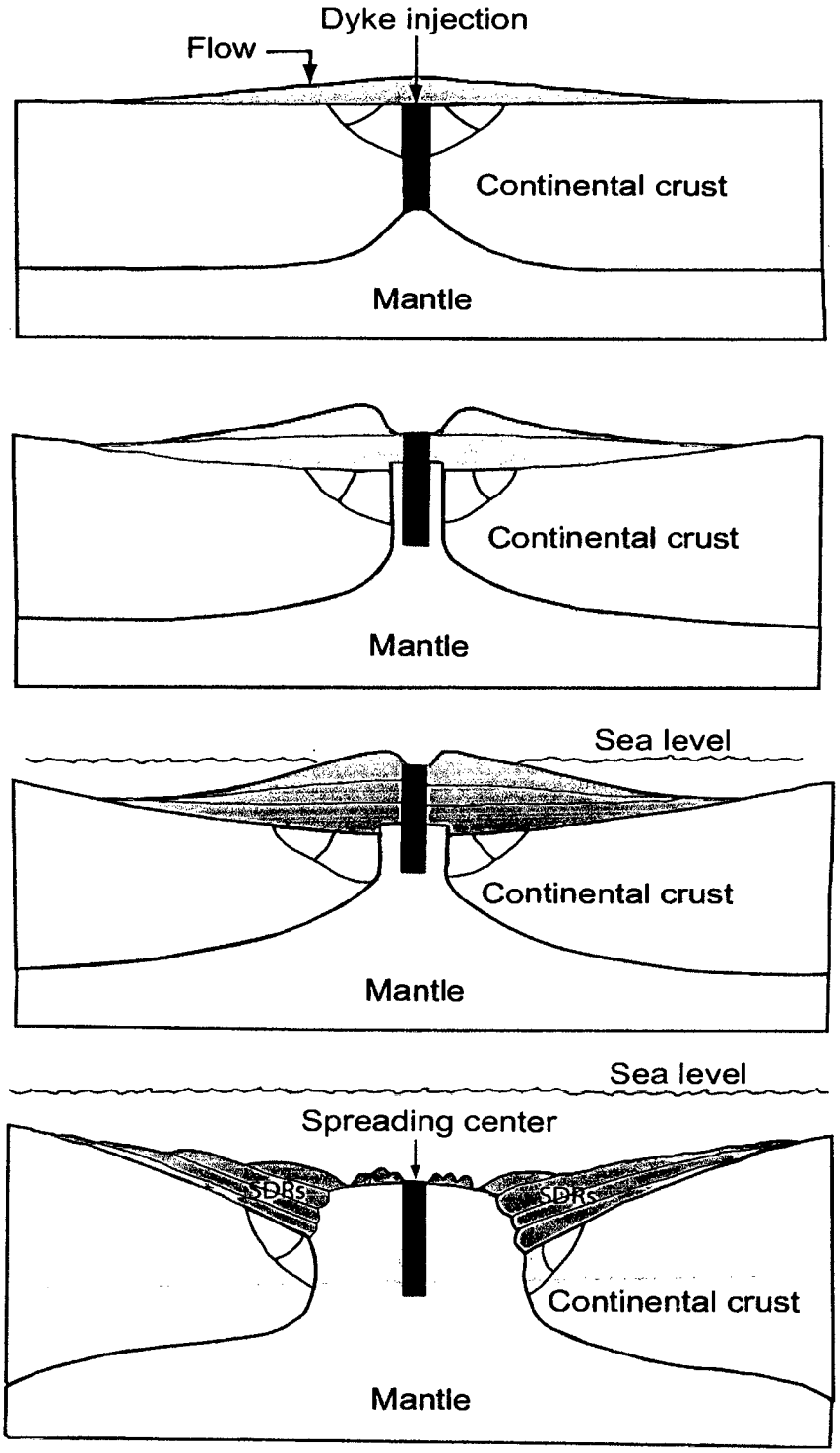


**Figure 6.1** Schematic diagrams showing genesis of SDRs along a linear zone of dyke injection in attenuated continental crust (Hinz, 1981).

sequences based on observations made from the multi-channel seismic reflection profiles acquired along the Norwegian continental margin.

i) The reflector sequences dip ubiquitously seaward. At the landward limit of the sequences they often assume a horizontal to near-horizontal attitude.
ii) The reflectors usually exhibit arcuate shapes indicating upward convexity.
iii) The reflectors diverge seaward and show an overall seaward offlap.
iv) The reflectors are distributed in the form of a sea-ward dipping wedge or fan shaped configuration. The seaward limit of the wedges is seldom well defined and shows no distinct basal reflector.

It has been observed that the SDRs occur immediately landward of the oldest mapped seafloor spreading type magnetic lineation, where the magnetic lineations could jointly define with the SDR sequences on a continental margin. In some cases they are associated directly with the oldest part of the anomaly sequence (Mutter et al., 1982). Seaward transition of SDRs to presumed oceanic crust could be marked by a topographic high. The SDR sequences are generally characterized by broad feather edge to the seaward and thin progressively landward to its interpreted apex. Feather edge of the SDRs have been used to demarcate seaward extent of the continental crust of the Voring Plateau of Norwegian margin, Argentina margin and east coast of US (White et al., 1987).

### 6.2.1 Seismic characters and identification of SDRs

In the present study, a set of westerly dipping seismic reflectors are observed below sedimentary column at three locations (Figure 6.2) along the western flank of the Laccadive Ridge imaged in the MCS reflection profiles RE23, RE19 and RE17. The dipping reflectors are a stack of laterally discontinuous to continuous, high amplitude, divergent and offlapping, westerly dipping reflectors (Figures 6.3, 6.4 and 6.5).

The MCS reflection profile RE23 depicts two sets of westerly dipping reflector sequences (u1 and u2) separated by ~5 km (Figure 6.3). These reflector sequences, occur at a depth of ~4.2 s TWT, are overlain by ~0.9 s TWT thick sediments and extend seaward for about 27 km. Another well developed dipping

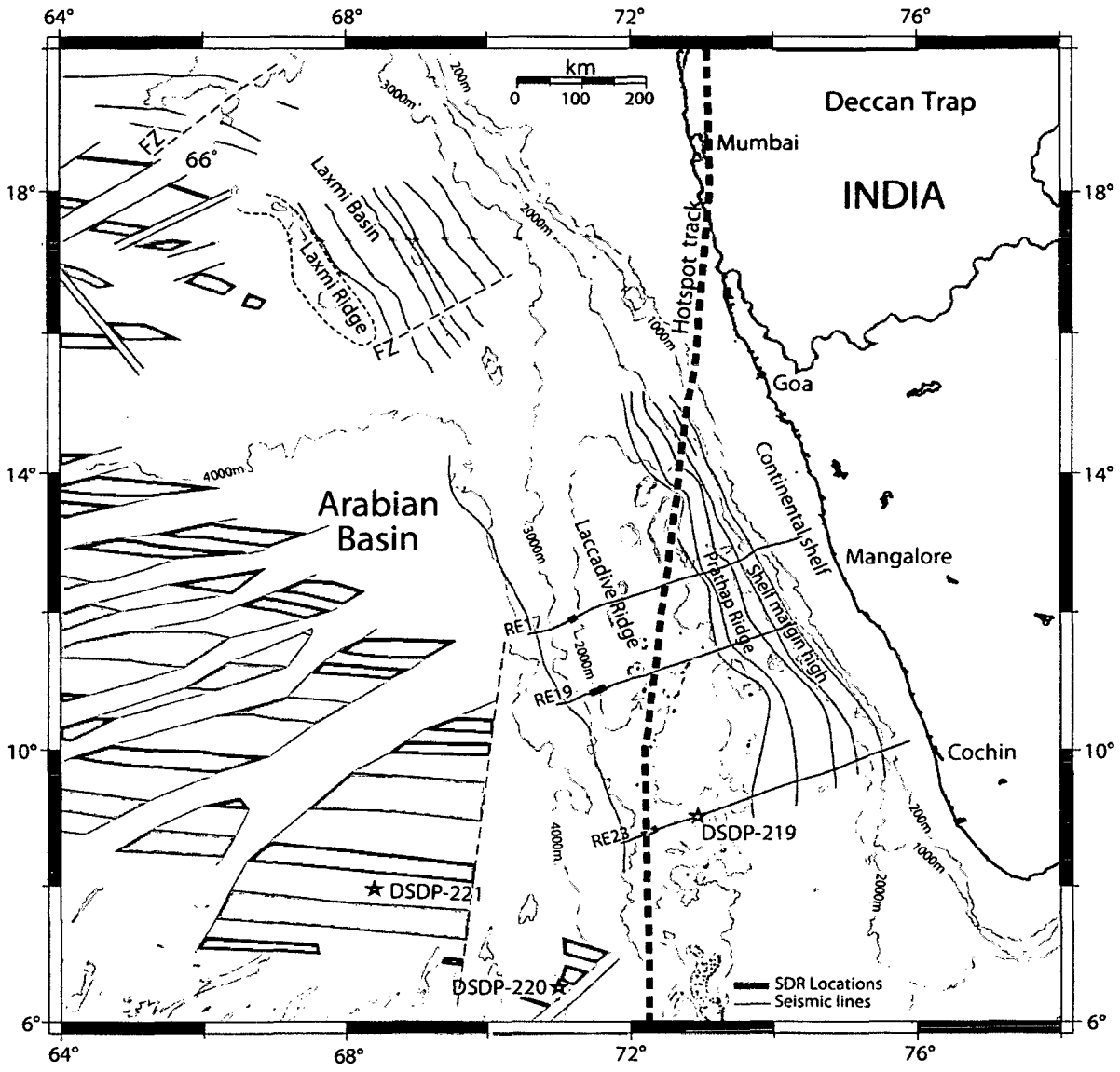


**Figure 6.2** Locations of SDRs identified along western flank of the Laccadive Ridge depicted in the seismic lines. Location of refraction station L08V (11.9067°N, 71.1750°E) is not shown in the map as it nearly falls on the SDR location of RE17. Other details are given in the Figure 5.1.

reflectors which extends seaward for about 27 km and overlain by ~1.2 s TWT thick sediments is identified along the profile RE19 (Figure 6.4). The top of the dipping reflectors lies at a depth of ~3.6 s TWT. Along the profile RE17 (Figure 6.5), the westerly dipping reflectors are overlain by ~0.95 s TWT thick sediments. Individual reflectors can be traced for about 15 km down dip and the depth to the highest distinguishable point of the reflectors is ~3.8 s TWT.

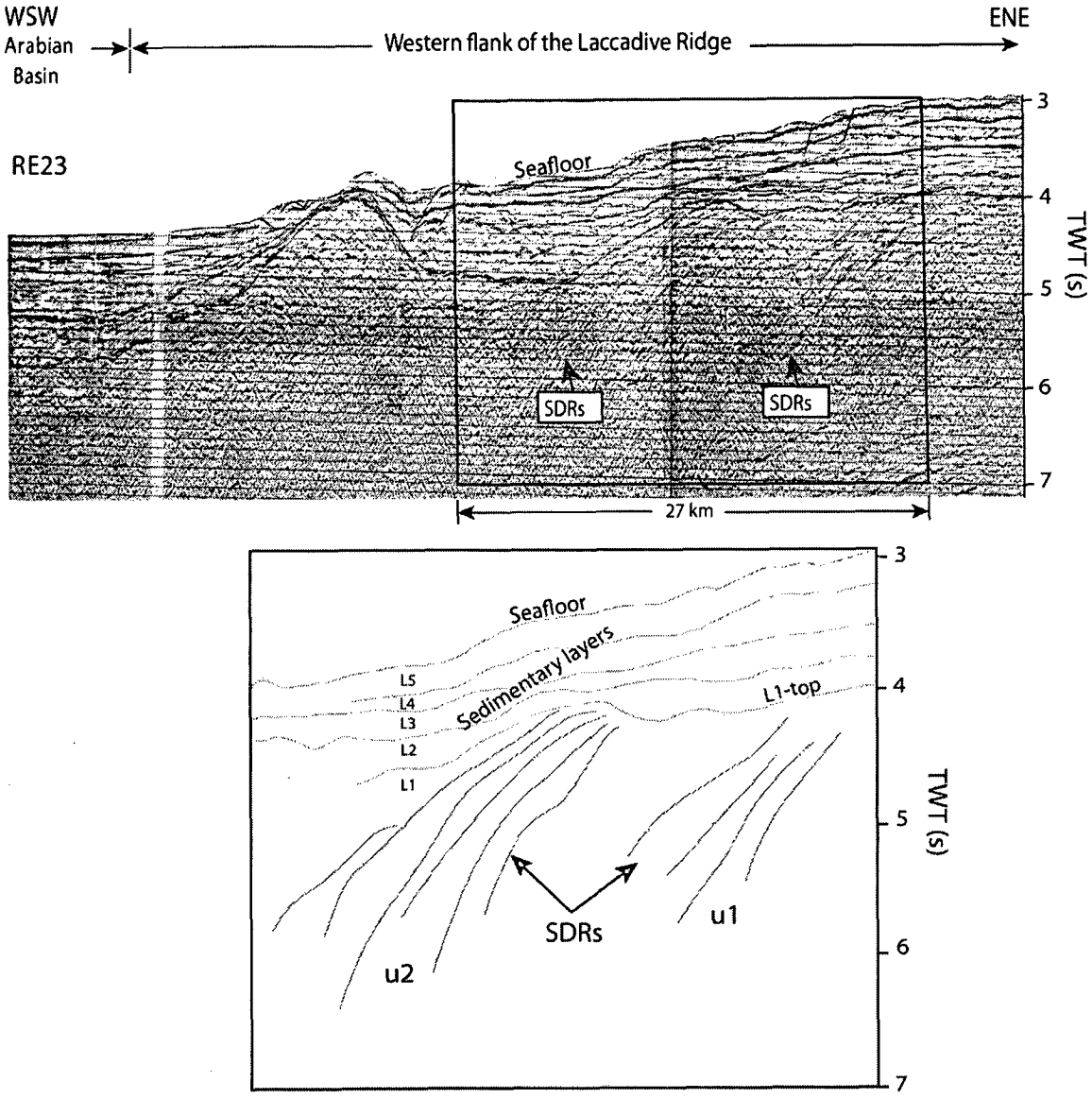


**Figure 6.3** SDRs interpreted along part of the seismic profile RE23 depicting western flank of the Laccadive Ridge. u1, u2 and reflector L1-top are explained in the text.

In order to investigate the nature of the dipping seismic reflectors, published results of DSDP Site 219 (Whitmarsh et al., 1974) and refraction study at site L08V (Naini and Talwani, 1983) located on the crest and western flank of the Laccadive Ridge respectively are used. The velocity structure at site L08V (Table 6.1) which is close to the dipping seismic reflectors observed at seismic line RE17 shows the interval velocities of 1.65-2.12 km/s, 4.4 km/s, 5.6 km/s, 6.3 km/s and 7.2 km/s. The presence of chert layer of P-wave velocity 4.0 km/s of Early and Middle Eocene age overlain by about 1 km thick sediment over the Laccadive Ridge was inferred at DSDP Site 219. The chert layer appears as a strong diffuse reflector often with irregular surface and sawtooth appearance

(Whitmarsh et al., 1974). Chaubey et al. (2002b) observed that reflection character of chert layer is of high-amplitude, and discontinuously associated with numerous diffraction hyperbolae.

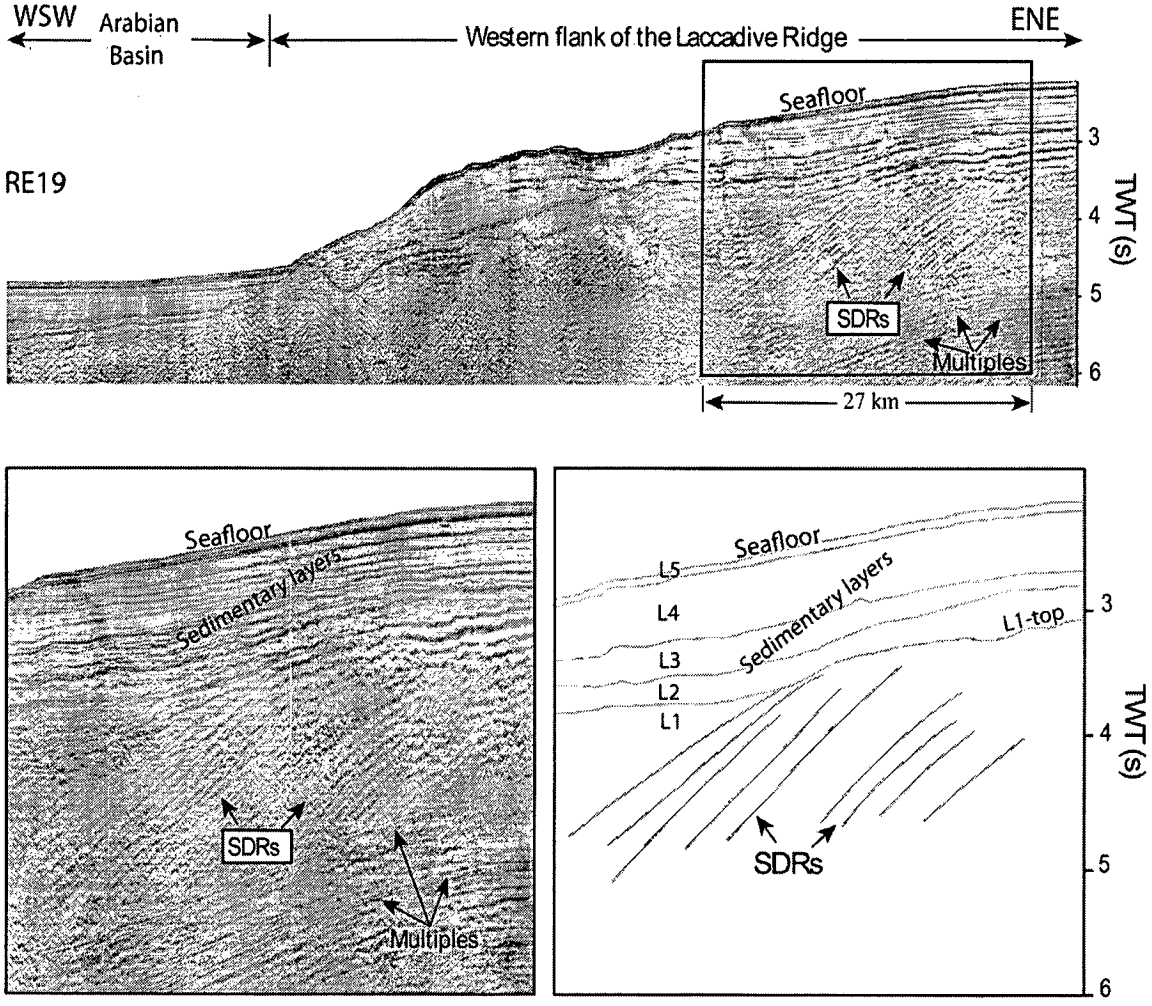


**Figure 6.4** SDRs interpreted along western flank of the Laccadive Ridge imaged in the seismic profile RE19.

Such reflection character at bottom of the sedimentary strata (Figures 6.3, 6.4 and 6.5) is not observed in the study area. Instead, it displays high amplitude and continuous reflector of the seismic sequence boundary L1-top. Below the reflector L1-top discontinuous to continuous, high amplitude, divergent, westerly dipping and offlaping reflectors are observed in the profiles RE23, RE19 and RE17.

The velocities in the range of 5.8-6.4 km/s are generally considered as characteristic of granitic layer in continental crust (Tucholke et al., 1981). From a compilation of global crustal model Mooney et al. (1998) suggested 6.1-6.3 km/s

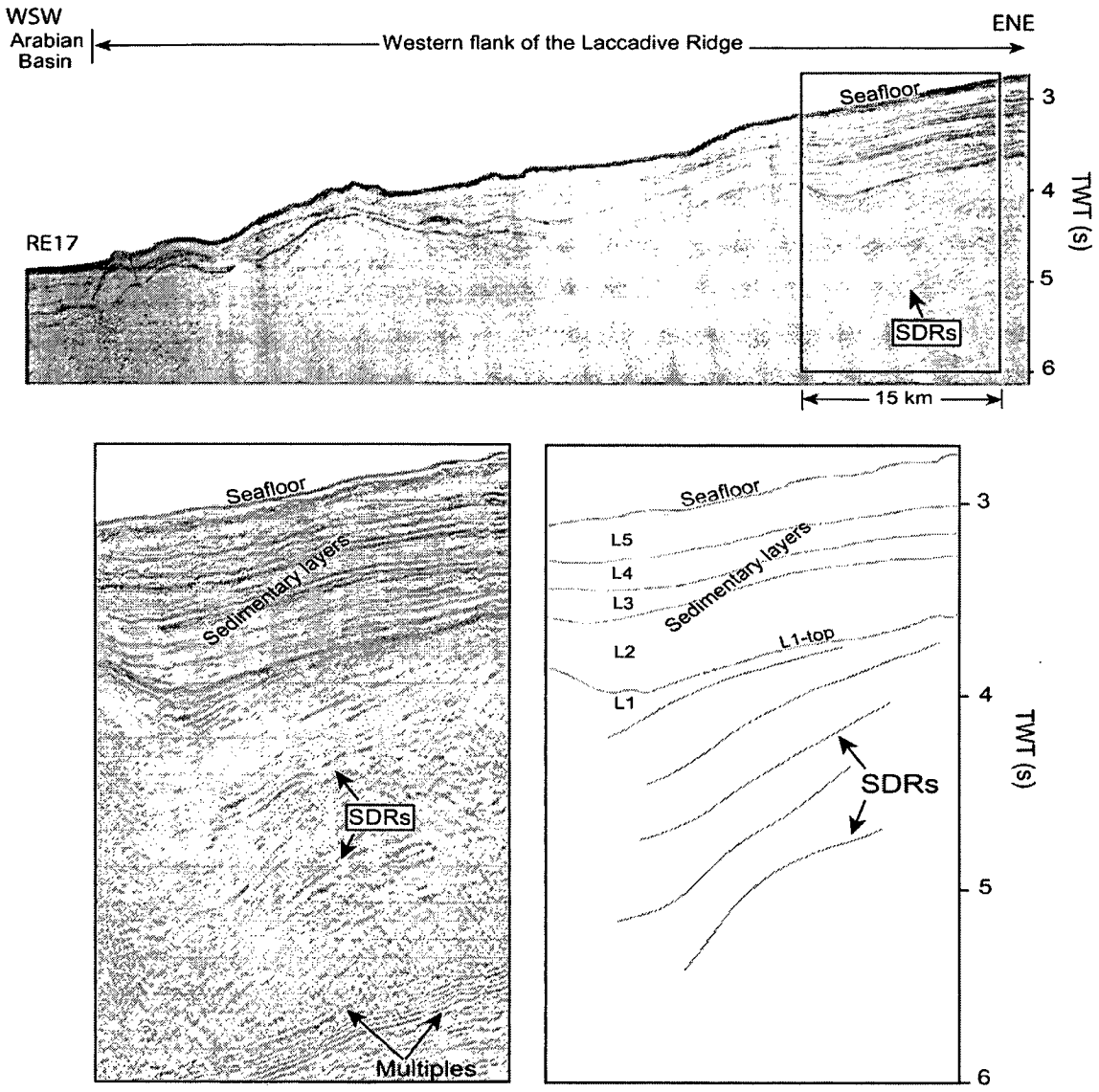


**Figure 6.5** SDRs interpreted from part of the seismic profile RE17 depicting western flank of the Laccadive Ridge.

velocity to upper–middle crustal layer of extended continental crust. Deep seismic sounding investigations of the western Indian shield suggested that seismic velocity of Deccan flow basalt, lying below thick sediment column, varies between 4.7 to 5.1 km/s (Kaila et al., 1979, 1981; Reddy, 2005). From the study of dipping reflector sequence on Hatton Bank, White et al. (1987) suggested that the seismic velocities increase through the SDRs from typically 3.5 km/s at the top to about 6 km/s at the base. Therefore, seismic velocity of ≥4.4 km/s is assigned (below sediment column of velocity 1.65-2.12 km/s) for the dipping seismic reflectors considering the velocity structure of refraction station L08V (Table 6.1) located close to the dipping seismic reflectors on RE17. These seismic reflectors are therefore interpreted as volcanic reflectors. Considering the geographic location

and seismic characters, these dipping volcanic reflectors are interpreted as Seaward Dipping Reflectors (SDRs).

The dipping volcanic reflectors, interpreted as SDRs, do not represent dipping normal faults because the seismic reflectors are not associated with half-graben structures which are formed during initial stage of continental rifting. Further, in the locations where the SDRs are interpreted, the sub-surface is clearly devoid of normal fault characteristics. In view of this, the dipping volcanic reflectors identified on the western flank of the Laccadive Ridge are well developed SDRs. Considering the genesis of SDRs, it is suggested that the dip of the SDRs arose by subsidence of basaltic lava flows subsequent to their emplacement during initial continental split-up.

Since the SDRs are interpreted as voluminous basaltic flows emplaced during the latest period of rifting, the identified SDRs along the western flank of the Laccadive Ridge are interpreted as indicative of rifted continental margin and the volcanism prior to the onset of seafloor spreading. The seaward feather edge of the SDR sequences indicates location of continent-ocean transition along western margin of the Laccadive Ridge. These results are published as a scientific research paper (Ajay et al., 2010).

**Table 6.1** Seismic velocity of crustal layers at refraction station L08V.

| Layer velocity(km/s) | 1.50 | 1.65 | 2.12 | 4.40 | 5.60 | 6.30 | 7.20 |
|---|---|---|---|---|---|---|---|
| Layer thickness(km) | 2.12 | 0.41 | 0.42 | 0.66 | 1.49 | 4.69 | 8.40 |
| Layer thickness{(TWT (s)} | 2.83 | 0.50 | 0.40 | 0.30 | 0.53 | 1.49 | 2.33 |
| Cumulative layer thickness{(TWT (s)} | 2.83 | 3.33 | 3.73 | 4.03 | 4.56 | 6.05 | 8.38 |

## 6.3 Crustal structure of SWCMI

Crustal structure of the southwest continental margin of India is obtained by 2D forward modeling of the free-air gravity anomalies along five traverses of the margin. Ship-borne as well as satellite altimetry derived free-air gravity anomalies are considered for the gravity modeling. Although crustal structure derived from gravity modeling is non-unique, modeling under constraints of seismic reflection

and refraction data provide better constrained results and thereby improve the interpretational reliability of the crustal structure.

### 6.3.1 Seismic velocity and density of crustal layers

2D gravity model studies are carried out under the constraints of seismic reflection and refraction results. For this purpose, the interpreted seismic reflection profiles of the present study, and refraction velocities (Francis and Shor, 1966; Rao, 1970; Naini and Talwani, 1983) from the stations 54V, 55V, 70V, 73V, 74V, 64V, 65C, 66C, 67C, 68C, 69C, 84C and ST2-3 in the Arabian Basin, L13V, L08V and L12V along the Laccadive Ridge, 85C, 88C, 87C and S4 along the continental shelf (Table 3.3) are used. Published results of Deep Seismic Sounding (DSS) on western Indian shield (Kaila et al., 1979, 1981; Krishna et al., 1991 and Reddy, 2005) are used to estimate the Moho depth on the continental shelf region.

The DSS investigations along Kavali-Udipi profile in the south, and Koyna-I and Koyna-II profiles in the north of the peninsular India shield revealed that the P-wave velocities vary between i) 4.7 and 5.1 km/s in Deccan Traps; ii) 5.5 and 5.8 km/s in Cuddapah sediments and Dharwar schists, and iii) 5.8 and 6.2 km/s in granites and granitic gneisses (Kaila et al., 1979; 1981, Reddy, 2005). The refraction velocity data, compiled from SWCMI, comprise of 1.65-3.5 km/s, 4.1-4.6 km/s, 5.4-5.7 km/s, 6.1-6.4 km/s and 7.2-7.4 km/s (Table 6.2). The seismic velocities 1.65-3.5 km/s represent sedimentary column, whereas 4.1-4.6 km/s represent basaltic flows/Chert. The rocks with velocities of 5.4-5.7 km/s and 6.1-6.4 km/s below sedimentary strata are similar to the velocities observed in Dharwar schists/Cuddapah sediments and granitic gneisses respectively. Therefore the seismic velocities 5.4-5.7 km/s may be considered as metasediments. The velocities 7.2-7.4 km/s may represent lower continental crust and heavily intruded lower crustal body. It may be noted that the granitic crustal velocities 6.1-6.4 km/s are slightly higher compared to those of DSS results. The high velocity may indicate altered granitic layer due to intrusive volcanism during rift related extensional tectonics and/or hotspot magmatism. The Arabian Basin characterized by the refraction velocities 2.15-3.74 km/s, 5.3-5.75 km/s and 6.36-6.65 km/s represents sedimentary layer, layer 2 and layer 3 of the oceanic crust respectively.

The seismic refraction velocities, discussed above, have been used to infer the density configuration for the continental as well as the oceanic crust. Densities for various crustal layers were obtained from velocity-density conversion table of Barton (1986) and presented in Table 6.2. The crustal velocities of the continental shelf, Laccadive Basin and Laccadive Ridge suggest four layers of densities 2.1, 2.65, 2.8 and 2.9 g/cm$^3$. The density of 2.1 represents a sedimentary layer. The density 2.65 g/cm$^3$ may represent a thick metasedimentary layer. The densities 2.8 and 2.9 g/cm$^3$ represent upper and lower stretched continental crust respectively. In the model, a high density 3.0 g/cm$^3$ is assumed for heavily intruded lower crust of the Laccadive Ridge. In addition a density of 2.4 g/cm$^3$

**Table 6.2** Crustal seismic velocities and inferred densities (after Barton, 1986)

| | | Thickness (km) | Velocity (km/s) | Average Velocity (km/s) | Density (gm/cm$^3$) |
|---|---|---|---|---|---|
| Arabian Basin | Sediment | 0.48-3.55 | 2.15-3.74 | 2.65 | 2.1 |
| | Oceanic Layer-2 | 1.28-2.43 | 5.3-5.75 | 5.5 | 2.7 |
| | Oceanic Layer-3 | 2.41-3.1 | 6.36-6.65 | 6.6 | 2.95 |
| | Moho | - | 8.1-8.3 | 8.2 | 3.3 |
| Laccadive Ridge, Basin and Shelf | Sediment | 0.43-2.8 | 1.65-3.5 | 2.58 | 2.1 |
| | Chert/Trap | 0.66-2.0 | 4.1-4.6 | 4.35 | 2.4 |
| | Metasediment | 1.49-1.93 | 5.4-5.7 | 5.55 | 2.65 |
| | Upper crust | 1.84-4.69 | 6.1-6.4 | 6.25 | 2.8 |
| | Lower crust | 7.99-8.4 | 7.2-7.4 | 7.3 | 2.9 |
| | Lower Crustal Body (LCB) | - | - | - | 3.0 |
| | Moho | - | >8.0 | - | 3.3 |

is used for basaltic-flow/chert, and 2.65 g/cm$^3$ density for SDRs in this study. In the Arabian Basin the crustal velocities suggest three layers of densities 2.1, 2.7 and 2.95 g/cm$^3$ representing sediment, layer 2 and layer 3 of the oceanic crust respectively. A uniform value of 3.3 g/cm$^3$ is assumed for the upper mantle.

### 6.3.2 Gravity modeling

Five uniformly spaced transects of the SWCMI are selected along the lines RE23, RE21, RE19, RE17 and RE15 to carry out gravity modeling under the constraints of seismic reflection and refraction results. The four seismic lines RE23, RE21, RE19 and RE17 were extended into deep Arabian Basin till 68°E for the purpose of crustal modeling from known oceanic crust of the Arabian Basin to continental shelf. Satellite altimetry derived gridded free-air gravity anomaly database of Sandwell and Smith (1997) are used to reconstruct the gravity profile where the ship-borne free-air gravity anomaly data are either partly available or absent along the seismic lines. The resolution of the satellite data was first evaluated by comparing profiles extracted from the gridded satellite gravity data with coinciding ship-borne gravity profile. The very good match between the gravity profiles from two different data sources (Figure 6.6) gave confidence that the resolution of the satellite-derived gravity data was adequate for crustal structure modeling.

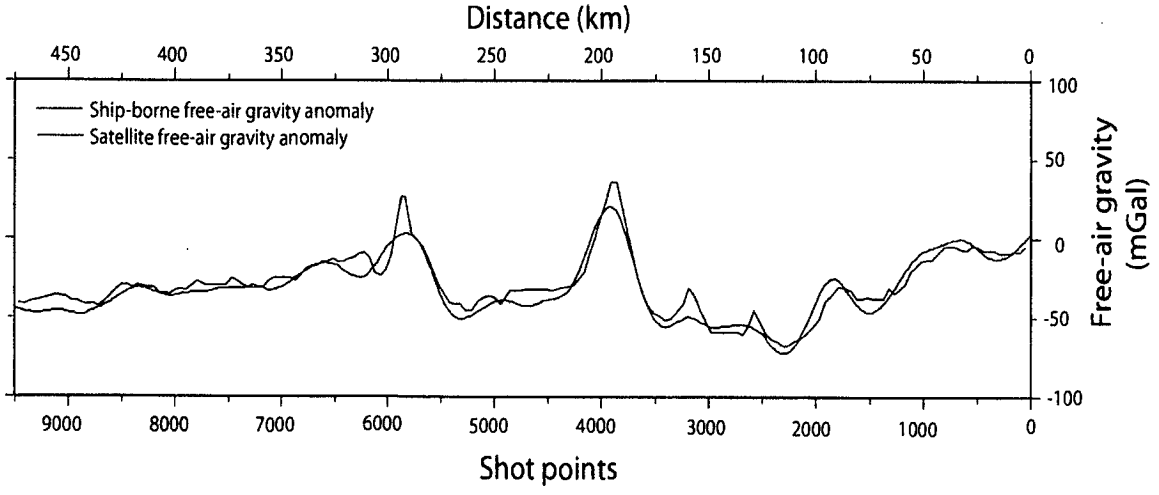


**Figure 6.6** Match between ship-borne as well as satellite altimetry derived gridded free-air gravity anomaly data along the seismic line RE17.

For gravity modeling, main crustal layers and its thicknesses are identified based on seismic reflection results of the present study, and refraction results (Francis and Shor, 1966; Rao, 1970 and Naini and Talwani, 1983) reported for the study area. 2D gravity modeling was carried out using the GM-SYS software. Modeling was performed by applying small adjustments to the geometries of crustal layers in order to obtain a crustal model which satisfies both the geometrical constraints and an acceptable fit between observed and calculated free-air gravity anomalies. In order to obtain an acceptable fit between the observed and calculated gravity anomalies over the Laccadive Ridge, a high density (3.0 g/cm$^3$) Lower Crustal Body (LCB) is introduced below the Ridge. A reasonable fit between the computed and observed gravity anomalies is obtained with an RMS error <5 mGal. In the models, igneous intrusive bodies are expressed only in sediments and water column as there is no appreciable lateral density contrast with other adjoining crustal layers.

### 6.3.3 Results on crustal structure

Crustal structure obtained from 2D gravity modeling along five representative transects of the southwest continental margin of India are presented in Figures 6.7, 6.8, 6.9, 6.10 and 6.11. The crustal models suggest two major crustal domains: continental and oceanic. The stretched continental crust; comprised of continental shelf-slope, Laccadive Basin, and Laccadive Ridge and characterized by a number of magmatic intrusive/extrusive bodies; gradually thin towards west and juxtaposed with the oceanic crust of the Arabian Basin. The models show average crustal thicknesses of 22.5,19 and 6.5 km for the outer shelf, Laccadive Ridge and Arabian Basin respectively. The COT is demarcated immediately west of the Laccadive Ridge, seaward of the SDRs, where the free-air gravity anomaly shows a prominent low and the Moho is characterized by significant shoaling to an average depth of 10.5 km to the Arabian Basin. Despite having a number of common structural characteristics, each of the transect exhibits considerable variation in crustal thickness and several unique structural features, therefore they are described individually in the following sections.

### 6.3.3.1 *Transect RE23*

Transect RE23 extends 923 km to west from continental shelf to the oceanic domain of the Arabian Basin (Figure 6.7). The 2D gravity model along the transect shows very good fit between the long wavelength components of the observed and calculated anomalies. However, the short wavelength components show minor misfits which may be largely attributed to the presence of tilted faulted blocks, grabens, igneous intrusive bodies and SDRs along the transect. Maximum crustal thicknesses of 22, 19.5 and 6.3 km are estimated for the continental shelf, Laccadive Ridge and Arabian Basin respectively from the crustal model.

Moho depth is highly varying between 5 and 22 km along this transect. The Maximum Moho depth estimated below outer continental shelf, Laccadive Ridge and Arabian Basin are 22, 21 and 10 km respectively. The Moho is shallow (13.5 km) and more or less flat below major part of the Laccadive Basin. The Moho below the Arabian Basin shows gradual rise from 10 km near west of Laccadive

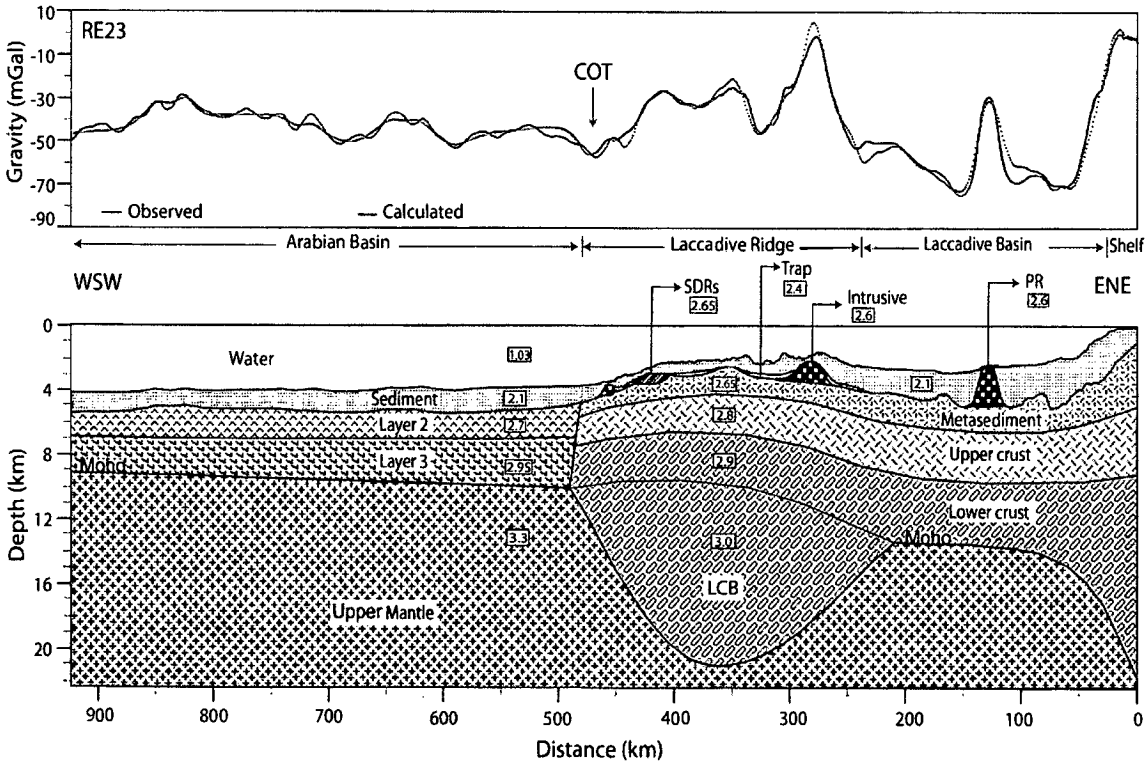


**Figure 6.7** 2D crustal model based on free-air gravity anomaly across the southwest continental margin of India along the seismic line RE23. PR: Prathap Ridge, SDRs: Seaward Dipping Reflectors, LCB: Lower Crustal Body, COT: Continent-Ocean Transition.

Ridge to 9.3 km at the WSW end of transect. A lower crustal body of maximum thickness 11.4 km is interpreted below the Laccadive Ridge indicating heavily intruded lower continental crust of the Laccadive Ridge. The ridge is associated with several magmatic structures such as igneous intrusives, basaltic flows/Trap and SDRs. COT is demarcated immediately west of the Laccadive Ridge, seaward of the identified SDRs, where the Moho shows a sharp rise to a depth of 10 km with a prominent drop in free-air gravity anomaly. The Prathap Ridge, associated with a significant free-air gravity anomaly high, is interpreted as uncompensated feature as it does not show flexure in the Moho.

### 6.3.3.2 *Transect RE21*

The transect RE21 extends from the continental shelf for 840 km to the oceanic domain of the Arabian Basin (Figure 6.8). Maximum crustal thicknesses estimated below the continental shelf, Laccadive Ridge and Arabian Basin are 19, 17.3 and 6.8 km respectively. The Moho depth varies between 9.8 and 19 km along this transect. A maximum Moho depth of 19 km is estimated below outer shelf and Laccadive Ridge. Below the Arabian Basin the maximum depth to Moho is 10 km. The Moho shoals from 19 km below the outer shelf to 13.3 km beneath the

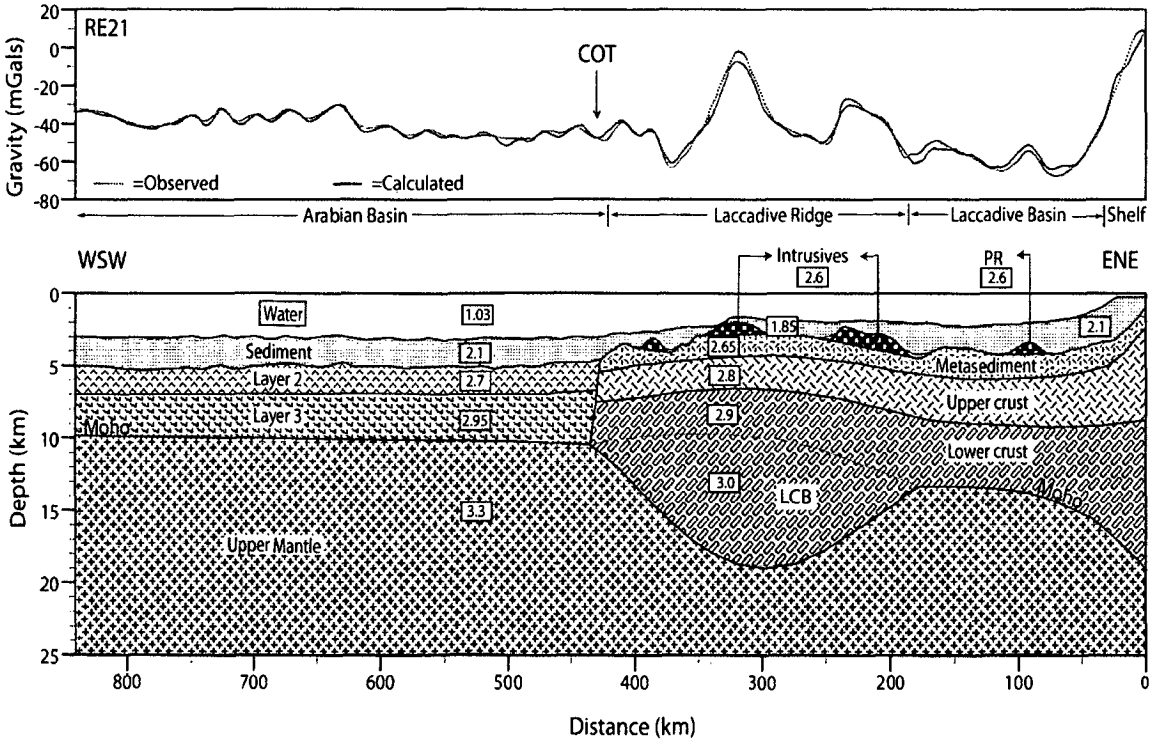


**Figure 6.8** 2D crustal model based on free-air gravity anomaly across the southwest continental margin of India along the seismic line RE21.

Laccadive Basin. The Moho is more or less flat beneath the basin. The Moho shows gradual decreases in depth from 10 to 9.8 km, below the Arabian basin to the WSW end of the transect. The LCB interpreted below the Laccadive Ridge has a maximum thickness of 9 km. COT is demarcated immediately west of the Laccadive Ridge where the Moho is characterized by a sharp shoaling to a depth of about 10 km associated with free-air gravity anomaly low. The Prathap Ridge is associated with relatively subdued gravity high. The uncompensated ridge is overlain by significantly thick sediment in the Laccadive Basin.

#### 6.3.3.3 *Transect RE19*

Transect RE19 extends from the continental shelf to the Arabian Basin for about 780 km (Figure 6.9). The continental shelf, Laccadive Ridge and Arabian Basin, shown in the model, are characterized by maximum crustal thicknesses of 23, 19.5 and 8 respectively. The Moho depth is highly varying between 10.2 to 23 km along this transect. Maximum Moho depths of 23, 20.8 and 11 km are estimated below the outer shelf, Laccadive Ridge and Arabian Basin respectively. The Moho

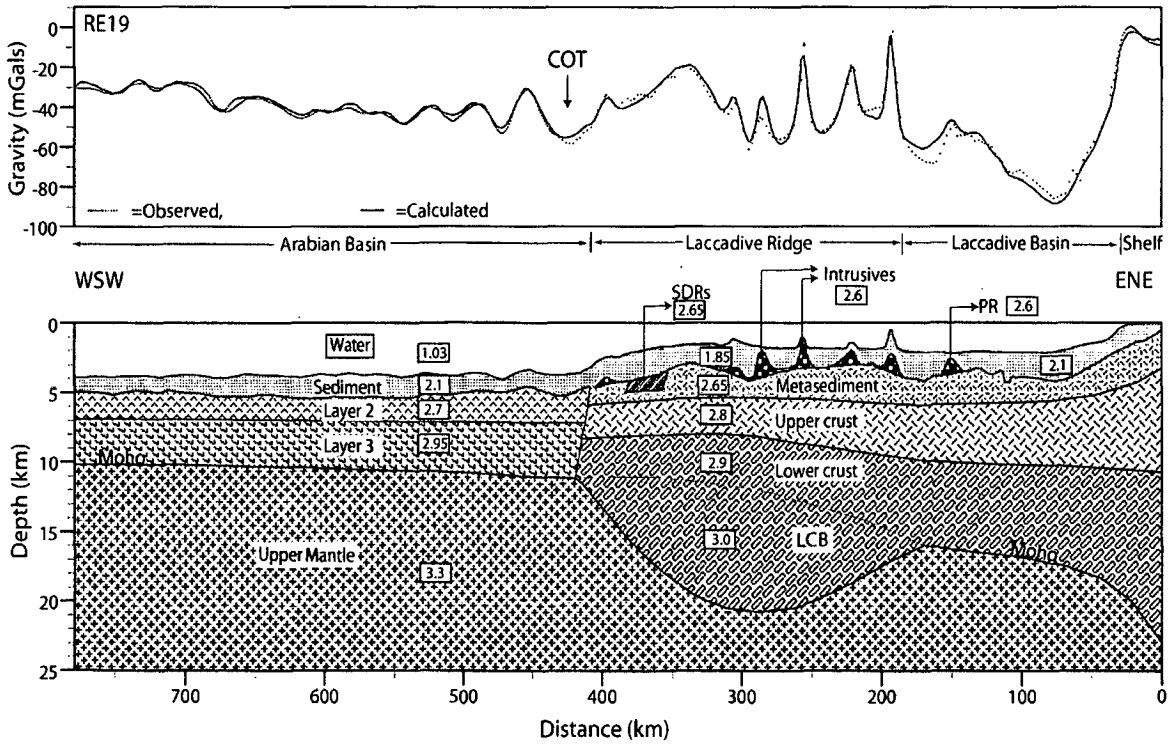


**Figure 6.9** 2D crustal model across the southwest continental margin of India along the seismic line RE19.

risees below Laccadive Basin to a depth of 16 km. The Arabian Basin is characterized by gradual decrease in Moho depth from 11 km near west of the Laccadive Ridge to 10.2 km to the WSW end of the transect. The Laccadive Ridge is associated with several intrusive bodies showing prominent gravity anomaly high. The interpreted LCB has a maximum thickness of 8.7 km. The COT is demarcated to the west of the Laccadive Ridge, seaward of the SDRs, where the Moho depth decreases sharply to a depth of 11 km associated with a prominent free-air gravity anomaly low.

#### 6.3.3.4 *Transect RE17*

Gravity model along the 754 km long transect RE17 extends from the continental shelf to the Arabian Basin (Figure 6.10). The model suggests maximum crustal thicknesses of 25, 18.9 and 7 km for continental shelf, Laccadive Ridge and Arabian Basin. The Moho depth varies from 10 to 25 km along the transect. The maximum Moho depths estimated below the continental shelf, Laccadive Ridge and Arabian Basin are 25, 19.3 and 10.5 km respectively. Below the Laccadive

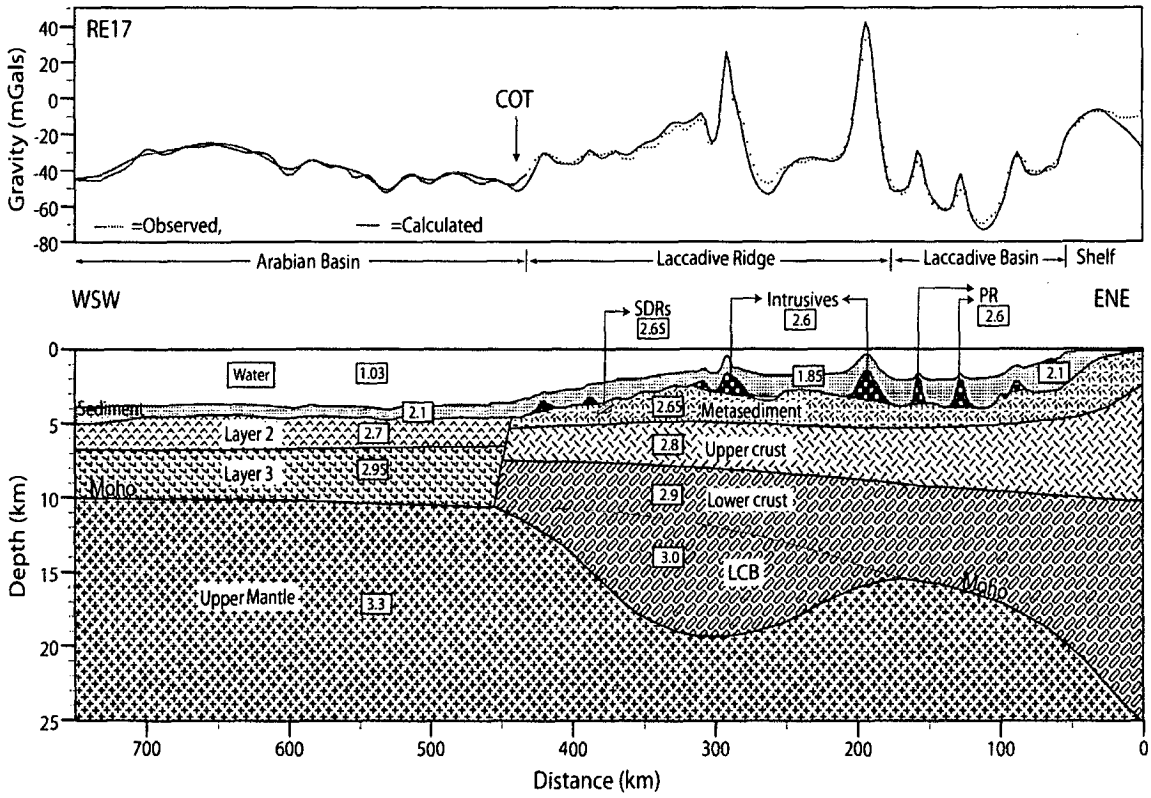


**Figure 6.10** 2D crustal model across the southwest continental margin of India along the seismic line RE17.

Basin the Moho rises gradually to a depth of 15.4 km. The Moho depth below the Arabian Basin gradually decreases to the SW end of the transect from 10.5 to 10 km. The LCB interpreted below the Laccadive Ridge has a maximum thickness of 7.6 km. The COT is demarcated to the west of Laccadive Ridge, seaward of the identified SDRs, where the Moho shows sharp shoaling to a depth of 10.5 km associated with a low in free-air gravity anomaly. The uncompensated Prathap Ridge is associated with prominent free-air gravity anomaly highs in the Laccadive Basin.

### 6.3.3.5 *Transect RE15*

Transect RE15 extends for about 832 km from the continental shelf to the Arabian Basin (Figure 6.11). The continental shelf, Laccadive Ridge and Arabian Basin show maximum crustal thickness of 23.6, 20.2 and 6.9 km respectively. The Moho depth, along the transect, is varying between 10.5 and 23.6 km. The maximum depth to Moho estimated below the continental shelf, Laccadive Ridge and Arabian Basin are 23.6, 22 and 11 km respectively. The Moho depth below the

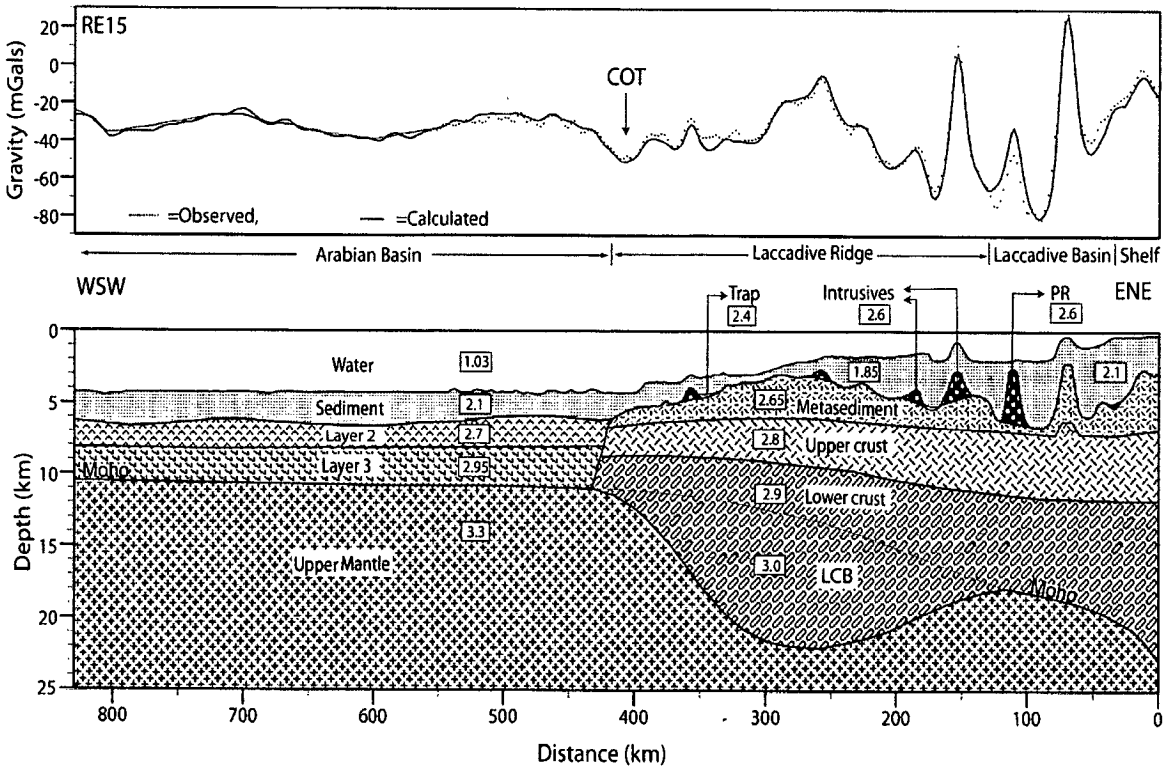


**Figure 6.11** 2D crustal model across the southwest continental margin of India along the seismic line RE15.

Laccadive Basin decreases to 18 km. Below the Arabian Basin the Moho is characterized by gradual rise from 11 to 10.5 km to the end of the profile. The interpreted LCB shows a maximum thickness of 9 km. COT is demarcated west of the Laccadive Ridge where the Moho shows a sharp rise to a depth of 11 km associated with a free-air gravity anomaly low. The Prathap Ridge as well as the uplifted flat summit structural high, covered by the sediment, shows prominent free-air gravity anomaly highs in the Laccadive Basin.

# Chapter-7

# SEDIMENTATION HISTORY AND TECTONICS OF THE SOUTHWEST CONTINENTAL MARGIN OF INDIA

# Chapter 7

# SEDIMENTATION HISTORY AND TECTONICS OF THE SOUTHWEST CONTINENTAL MARGIN OF INDIA

## 7.1 Introduction

As discussed in the chapter-2, the sedimentary basins of the SWCMI are formed as a result of continental rifting between India and Madagascar during the Late Cretaceous and later modified by Rèunion hotspot during the Early Tertiary. Initially the basins received thick volcanics and volcanogenic sediments, derived from Marion and Rèunion hotspot volcanism. In the process of development of the basins, sediments of pelagic, hemipelagic and clastic origin are deposited during the Cenozoic time. The 2-6 km thick pelagic carbonate sedimentation of Middle Eocene to Middle Miocene took place during increased sea level and warmer climatic condition prevailed over Indian plate when the plate was in warm latitude belt with very low terrigenous influx (Clift et al., 2001; Molnar, 2004). Post Middle Miocene clastic sedimentation in the basins is associated with accelerated weathering and erosion of the Indian landmass as a result of emergence of the Himalaya during the Middle Miocene and onset of Indian Monsoon (Valdiya, 1999). The shelf and slope sedimentation patterns reveal aggraded sedimentation from the Late Paleocene to Middle Miocene and prograded sedimentation since the Middle Miocene. Based on the litho/chrono stratigraphic correlation of the seismic sequences identified from the MCS reflection profiles, the sedimentation history of the SWCMI is discussed in this chapter. Further the chapter discusses improved understandings, emerged out of the present study, on volcanic nature of the SWCMI, impact of Rèunion hotspot, continent to oceanic transition and neotectonic activities along the SWCMI.

## 7.2 Sedimentation history

Sediment depositional history of the SWCMI is delineated by the correlation of the seismic sequences with litho- and chrono- stratigraphic information of the continental shelf-slope, Laccadive Basin and Laccadive Ridge. Sedimentation along the SWCMI has begun as a result of formation of numerous local and

regional structural grabens along the stretched continental crust of SWCMI due to extensional tectonics during the rifting between India and Madagascar in the Late Cretaceous. These structural grabens became depocentres for the syn-rift and post-rift sediments. Based on seismic sequence analysis and drill well information the sedimentation history of the study area is discussed under two geological domains: i) continental shelf – Laccadive Basin, and ii) Laccadive Ridge.

**Continental shelf – Laccadive Basin**

The Kerala-Konkan Basin (KKB) and Laccadive Basin constitute major depocentres in the continental shelf – Laccadive Basin domain. Sedimentary units deposited in the KKB are highly varying in thickness since they are deposited in coast parallel grabens separated by numerous local basement highs. Late Cretaceous sediments ranging in age from Santonian to Maestrichian are drilled from deep, narrow sedimentary grabens located in the southern part of the KKB (Rao et al., 2002). Sediment thickness in the Laccadive Basin generally shows gradual decrease from north to south. However, the sediment thickness changes drastically over buried Prathap Ridge and Shelf Margin High. Eight major litho-stratigraphic units deposited since Late Cretaceous have been correlated with the seismic sequences interpreted from the continental shelf – Laccadive Basin depicted in the MCS reflection profiles (Table 4.8).

The lowest seismic sequence H1 is correlated with the Cochin sedimentary formation. The reflection patterns of this sequence indicate that it was deposited in a disturbed, complex and non uniform energy conditions produced by tectonic agitations. The Cochin Formation, which is deposited during Late Cretaceous to Late Paleocene, is interbedded with altered flow basalts to its bottom deposited under a sub-aerial condition. This suggests that towards close of the Late Cretaceous there was an episode of marine regression due to decrease in depth of basin to near sea level. This episode of upliftment of basins and marine regression is associated with the onset of rifting between Seychelles and India. Based on paleo-bathymetry studies, Raju et al. (1999) suggested shallow depths of less than 100 m for sedimentation within KKB during the Late Cretaceous. This event of upliftment was followed by a period of non-deposition and formed Middle Paleocene depositional hiatus (Singh and Lal, 1993).

The sedimentation in the basin resumed during Late Paleocene as a result of marine transgression probably in response to passive subsidence initiated after the rifting at the start of the Late Paleocene (Campanile et al., 2008). As a result, another major sedimentary sequence (correlated with the seismic sequence H2) was deposited. The sequence H2 is seismically characterized by concordant, contorted and hummocky reflection patterns. This suggests the deposition of the sequence from a nearly undisturbed homogenous to a complex high energy condition. This sedimentary sequence, deposited during Late Paleocene to Early Oligocene, comprises Kasargod and Karwar formations (Table 4.8). The Kasargod Formation was deposited during the Late Paleocene to Early Eocene. The formation is separated from the underlying Cochin Formation by an unconformity surface which is identified as H1-top in the seismic profiles. To the end of Early Eocene the Kasargod Formation composed of clay, shale, sandstone, siltstone and lignite-seams shows gradual development of interbedded limestone. A lime rich sedimentation in KKB became conspicuous since Middle Eocene under a shallow marine environment. This lime rich sedimentation above Carbon Compensation Depth (CCD) formed the Karwar Formation. But the sedimentation in the Laccadive Basin was taking place in a deeper marine environment below CCD. Therefore, the carbonates of the Karwar Formation became shaly in the Laccadive Basin to form a carbonate poor shaly formation, termed as Panaji Formation (Figure 3.2). Both the Karwar and Panaji Formations are bounded to the top by a major unconformity surface, particularly in the deep offshore region, formed during the Late Eocene depositional hiatus. This unconformity surface is identified as H2-top in the seismic profile. The carbonaceous nature of the Karwar Formation in the KKB and the presence of an erosional unconformity on top of the formation indicate that the environment of deposition changed from deeper continental shelf to lagoonal. This suggests that the basin has witnessed a major tectonic upliftment at the end of Eocene.

Further subsidence of the basins to a shallow water condition in the Early Oligocene initiated another episode of marine transgression and the deposition of a prominent carbonate sedimentary sequence. This limestone rich sedimentary sequence of Calicut and Quilon formations is correlated with the seismic sequence H3 (Table 4.8) deposited during Early Oligocene to Late Miocene over

the Late Eocene unconformity surface H2-top. The reflection patterns of the seismic sequence suggest that it was deposited in a slow and uniform to highly disturbed energy condition. This sedimentary sequence extends from the onland coastal region to the deep Laccadive Basin (Figure 3.2), and represents a major transgressive period in the sedimentary basins of SWCMI. The Quilon Formation deposited through Late Oligocene to Late Miocene exhibits a period of regional westward tilting of the sedimentary basins that caused an inland marine transgression from the end of Early Miocene to Late Miocene, and development of carbonate banks in elevated areas (Raju et al., 1981; Rao et al., 2002). The development of thick carbonate sequences of Karwar, Calicut and Quilon formations throughout the basins of SWCMI is linked not only to the increased sea level but also a warmer climatic condition from Early Eocene to Late Miocene, when Indian subcontinent was in the warmer latitude belt of the equator. The entire source of sediments during this period consists of abundant pelagic fossil tests, suggesting that much of the peninsula was submerged and characterized by pelagic sedimentation (Raju et al., 1981).

The SWCMI experienced a heavy influx of terrigenous sediments derived from the Western Dharwar Craton during the Late Miocene (Singh et al., 1999). This phase of high sedimentation is associated with the formation of numerous fractures and faults, reactivation of existing fault trends and collapse of the parts of continental shelf in response to the tectonic imbalance following the collision of India with Eurasia and upliftment of Himalaya during Middle Miocene (Biswas, 1987; Ghosh and Zutshi, 1989; Subrahmanyam et al., 1995; Clift et al., 2001). As a result, the cessation of carbonate buildup and accumulation of markedly thicker terrigenous sediment deposits in the sedimentary basins were initiated during the Late Miocene. In the MCS reflection profiles the heavy influx of the post Miocene terrigenous sediments into the SWCMI is represented by the significant progradation of the continental shelf. The present shelf break is prograded into the sea for an average distance of about 15 km from the Middle Miocene shelf break. This sequence of terrigenous sediments is correlated with the seismic sequences H4 and H5 which are distinguished as Mangalore and Trichur formations respectively (Figure 3.2 and table 4.8). The general sub parallel to divergent reflection pattern shown by the seismic sequences indicate alternate high and low

energy of deposition associated with the subsidence of the basin. The complex reflection patterns identified locally indicate unstable and disturbed energy conditions during sediment deposition caused by waves, currents, sediment slumping and reactivation of the structural features by neotectonic activities. The sedimentary sequence of the Mangalore Formation, composed mainly of clay and siltstone, was deposited during lower to upper Late Miocene over the unconformity surface H3-top overlying the Quilon Formation. The Mangalore Formation constitutes lower part of the heavy terrigenous sediment sequence deposited along the SWCMI following the major orogenic event of the upliftment of Himalaya in the Middle Miocene. The upper most clastic sedimentary sequence of the Trichur Formation composed of sandy, silty, alluvial and lateritic clay is being depositing since Early Pliocene. It may be mentioned here that the lithological similarity of Mangalore and Trichur formations complicate the proper identification of the seismic boundary between the sequences H4 and H5.

**Laccadive Ridge**

The lowest seismic sequence L1 identified from the Laccadive Ridge is correlated with the sedimentary sequence deposited during the Late Paleocene (Figure 4.25). This Late Paleocene detrital sedimentary sequence is composed mainly of sandstone and siltstone with glauconitic limestone to the top. This sequence has been deposited on a subsiding seabed within a near shore shallow water environment of less than 100 m water depth (Whitmarsh et at., 1974 and Weser, 1974). The detrital component in the sediment decreased towards the end of the Late Paleocene and started deposition of glauconitic limestone.

In the Early Eocene the seabed began to sink in response to the tectonic events caused by the initial contact between India and Eurasia. As a result, a deep water depositional environment was produced and pelagic sedimentary sequences, mainly composed of chalk, ooze, biogenic silica and limestone, were deposited. These pelagic sedimentary sequences were deposited at a slower and uniform rate during Late Paleocene to Middle Miocene. The biogenic silica, later, began to accumulate as chert within the pelagic sedimentary sequence. This sedimentary sequence is correlated with the seismic sequence L2 deposited during Late

Paleocene to Middle Eocene. The seismic reflection patterns of the sequence suggest disturbed and unstable energy conditions during its deposition. These disturbed and unstable depositional conditions probably indicate the tectonic agitations caused by the initial contact between India and Eurasia.

The supply of biogenic silica became scarce in the sediments by Early Oligocene and carbonate rich chert free pelagic sedimentary sequence was deposited. This sedimentary sequence is correlated with the seismic sequence L3 deposited during Middle Eocene to Middle Miocene. The sub parallel to divergent reflection patterns of the seismic sequence indicate non-uniform environment of deposition due to differential subsidence of the sedimentary basins due to compressional stress developed by the active spreading ridges in the Arabian Basin and the collision of India with Eurasia.

By the advent of Middle Miocene the region began to receive terrigenous sediments derived from the land as a result of tectonic upliftment of Himalaya and development of its fluvial system in the Middle to Late Miocene. This post Middle Miocene terrigenous sedimentation is correlated with two seismic sequences L4 and L5. The Middle Miocene to Early Pliocene sedimentary sequence, correlated with the seismic sequence L4, is characterized by detrital clay and silt with the pelagic sedimentation of nanno and foraminiferal ooze.

The detrital sediment component increases in the upper sedimentary sequence deposited since Early Pliocene. This sedimentary sequence is correlated with the seismic sequence L5 characterized by parallel to concordant reflection patterns. The seismic reflection patterns shown by both the seismic sequences L4 and L5 suggest more or less uniform environment of deposition since Middle Miocene. The strong upwelling and bottom currents which appear to have begun in the Middle Miocene may have carried the terrigenous materials in suspension to the depositional sites of the Laccadive Ridge and continues to the present day (Whitmarsh et al., 1974).

## 7.3 Seaward dipping reflectors – evidence for volcanic passive margin

Seismically imaged Seaward Dipping Reflector (SDR) sequences discussed in chapter-6 are one of the most important results of the present study since they are reported for the first time from the SWCMI. SDRs are identified along western flank of the Laccadive Ridge at three locations below sedimentary strata (Figure 6.2). Seaward of their occurrences, the Laccadive Ridge gradually thins and juxtaposed with the Early Tertiary normal oceanic crust of the Arabian Basin. The oldest sediment recovered from the DSDP drill well 219 located (9.02917°N, 72.87783°E) at the crest of the Laccadive Ridge has a dated age of ~58 My. Weser (1974) suggested that Site 219 was much closer to shoreline of India than it is today based on the typical shelf type nearshore shallow water sedimentation (limestone, sandstone and silt). Though, the identified SDRs are away from site 219, it may be interpreted that (i) the SDRs are older than 58 m.y. as they are found below the sedimentary column, and (ii) the SDRs are emplaced under sub-aerial condition. In paleo-geographic reconstructions, it is presumed that the southwest India rifted from the eastern margin of Madagascar during the Late Cretaceous (White and McKenzie, 1989; Storey et al., 1995, 1997; Torsvik et al., 1998; Raval and Veeraswamy, 2003). The rifting was associated with the Marion hotspot volcanism which occurred at Volcan del'Androy, southeast Madagascar and caused widespread eruption of basalts and rhyolites in Madagascar and Fe-Ti-enriched tholeiites in southwest India. Therefore, the occurrence of SDRs along the SWCMI strongly suggest extrusive volcanic episodes under sub-aerial condition during rifting between the eastern Madagascar and Laccadive Ridge which was a part of Indian mainland. It may be noted that volcanic rifted margin segment may be predominantly volcanic without SDRs being imaged in seismic records. Therefore, SDRs can be considered as sufficient condition for volcanic margin classification (Eldholm et al., 1995). SDRs of the present study, indeed, suggest that SWCMI is a volcanic passive margin developed during breakup between Madagascar and Laccadive-India in the Late Cretaceous with COT to the west of the inferred feather edge of the SDR sequences identified along the western flank of the Laccadive Ridge.

## 7.4 Basement depth anomalies – evidence for thermal uplift

Computation of previously unreported basement depth anomalies in the Arabian Basin (discussed in chapter-5) is another prominent finding of the present study. The depth anomalies in the basin vary from +501 to −905 m (Table 5.2). The anomalous depths to the basement of the basin suggest that subsidence in the basin does not follow the age-depth relationship of normal oceanic crust. The magnitude and regional distribution of basement depth anomalies documented over 63–42 My old oceanic crust of the Arabian Basin are comparable with those obtained from different parts of the world ocean. Depth anomalies have been reported from the Atlantic Ocean (Hayes, 1988; Louden et al., 2004) and the Southeast Indian Ocean (Hayes, 1988). One of the world's largest depth anomalies which is named as 'superswell' by McNutt and Fischer 1987 is reported in the South Pacific Ocean.

Several hypotheses have been forwarded to explain the origin of the basement depth anomalies in the oceans. According to Sleep (1990), the regional domal uplift is a characteristic feature of the presence of mantle plumes. The change from vertical upwelling to horizontal flow along base of the lithosphere induces an upward force on the plate (Menard, 1973), causing a dome-shaped uplift around the centre of upwelling. Compilation of depth anomalies and hotspot locations of the world oceans indicates a strong correlation between depth anomalies and occurrence of hotspots (Crough, 1979). Mostly negative depth anomalies correlate with hotspots such as Iceland, the Azores, Cape Verde and Bermuda in the North Atlantic Ocean. Another possible contributor to oceanic depth anomalies is compositional buoyancy due to basalt extraction (Jordan, 1979; Robinson, 1988). Melting depletes fertile mantle in garnet, and raises the MgO/FeO ratio of the residuum. As a consequence, it becomes less dense (O'Hara, 1975; Boyd and McCallister, 1976; Oxburgh and Parmentier, 1977), and therefore causes upliftment. The thinning hypothesis (Detrick and Crough, 1978) postulates that there is a high mantle heat flux associated with each hotspot. Since the lithosphere is a thermal boundary layer, additional heat in the base of the lithosphere causes the lithospheric thickness to decrease. Since the lithosphere is

colder and, therefore, denser than the asthenosphere, this thinning generates isostatic uplift and the formation of a topographic swell.

The negative basement depth anomalies (shallower than predicted depth) documented in the present study from the eastern part of the Arabian Basin is due to its proximity to the high thermal regime of the former Rèunion hotspot. It is suggested that vertical upwelling due to convection, followed by a lateral across-axis flow driven by excess near-field pressure by the hotspot, may have induced an upward force resulting regional swell. Thereafter, the oceanic lithosphere started subsiding, and is presently relatively shallow compared to the depth of the normal oceanic crust predicted by lithospheric thermal model of Stein and Stein (1992), even if the cause of the uplift have ceased to operate in the region. It may be mentioned here that the Arabian Basin was evolved due to a complex pattern of spreading-ridge propagation between magnetic chrons 28n (~63 Ma) and 20n (~43 Ma; Dyment, 1998; Chaubey et al., 1998, 2002a). As a result, asymmetric crustal accretion was occurred in the basin over this whole period. Although the origin and change in direction of propagation of the palaeo-propagators in the basin are not well understood, a linkage between the former Reunion hotspot and the spreading-ridge propagation has been postulated in earlier studies (Dyment, 1998; Chaubey et al., 1998). Royer et al. (2002) argued that the former Reunion hotspot may have generated a regional swell which was large enough to affect the bathymetry of the region, which would explain the spreading-ridge propagation 'downhill' along the bathymetry or gravity gradient (Morgan and Sandwell 1994). These views support the postulate (Dyment, 1998; Chaubey et al., 1998) that the nearby former Reunion hotspot influenced the evolution of the oceanic crust of the basins. Therefore, the zone of negative depth anomalies in the study area is caused by vertical upwelling due to convection, followed by a lateral across-axis flow facilitated by the Reunion hotspot. This is further supported by the spatial as well as temporal proximity of the Reunion hotspot to the Early Tertiary seafloor-spreading regime in the eastern part of the Arabian Basin (Whitmarsh, 1974; Morgan, 1981; Shipboard Scientific Party, 1988).

The zone of positive depth anomalies located in the western part of the Arabian Basin indicates excess subsidence of the oceanic crust relative to that predicted

by lithospheric thermal model and thickening of normal oceanic lithosphere. The excess subsidence of the western part of the Arabian Basin could have caused by the combination of isostatic adjustment due to sediment loading and relatively cold mantle compared to the nearby eastern part of the basin affected by the intense thermal field of the former Reunion hotspot. Lin et al. (2002) proposed that dynamic interaction between relatively cold mantle beneath spreading ridges and the ambient flow renders a transient nature to the subsidence of the seafloor.

## 7.5 Continent-Ocean Transition

Continent-Ocean Transition (COT), a zone of transition from continental to oceanic crust, is associated with a narrow zone of crustal thinning and significant volume of breakup related magmatic intrusives and extrusives. Whereas Continent-Ocean Boundary (COB) is defined as the line of maximum extent of continental crust material (Maillard et al., 2006) representing change from crystalline continental basement to oceanic basement. In the present study COT is inferred based on crustal structure, igneous intrusive bodies limiting the western extent of the Laccadive Ridge, feather edge of the identified SDRs and characteristic free air gravity anomalies.

Igneous intrusive bodies with steep scarps are observed along the western flank of the Laccadive Ridge limiting the seaward extent of the ridge. These intrusives are associated with high amplitude free air gravity anomalies. Similar features are reported for basement ridges of many passive margins, e.g. the Gabon-Congo region of west Africa (Belmonte et al., 1965) and Norwegian margins (Talwani and Eldholm, 1972). Talwani and Eldholm (1973) opined that major changes in the basement elevation normally occur at the boundary between oceanic and continental crust. Chaubey et al. (2002b) suggested that the volcanic features at the western edge of the Laccadive Ridge mark boundary of the rifted crust and early rift-emplaced volcanics.

The SDRs are generally used to identify volcanic passive continental margins (Hinz, 1981; Mutter et al., 1982, Eldholm et al., 1995) and to demarcate seaward extent of the rifted continental crust (White et al., 1987). In the present study, the presence of SDRs and its feather edge along the western flank of the Laccadive

Ridge lead to the identification of the edge of the rifted continent, and thereby to demarcate COT along western margin of the ridge. The crustal structure derived from the best-fit 2D gravity models along the five traverses (RE23, RE21, RE19, RE17 and RE15) the SWCMI reveal considerable variation in crustal thickness, and basement elevation across the margin (Figures 6.7, 6.8, 6.9, 6.10 and 6.11). The crustal structure models suggest that continental Laccadive Ridge gradually thins towards offshore and juxtaposed with the oceanic crust of the Arabian Basin, outlining the COT.

The COT along the SWCMI (Figure 7.1) is delineated based on combined interpretation of 2D multi channel seismic and free air gravity anomaly data, as well as crustal structure derived from the gravity modeling. The identification of igneous intrusive bodies along the western flank of the Laccadive Ridge, sharp gradient in the free air gravity anomalies to the west of the ridge, SDRs along the western flank of the ridge with their feather edges towards the Arabian Basin, and oceanic crust of the Arabian Basin provide good indication of the location of COT along western margin of the Laccadive Ridge. The COT is demarcated between the inferred feather edge of the SDR sequences identified along the western flank of the Laccadive Ridge, and the oceanic crust of the Arabian Basin where the Moho is characterized by significant shoaling to an average depth of 10.5 km associated with a prominent free-air gravity low. The COB, is not clearly defined along SWCMI, however, it can be placed within the COT which is confined to a narrow zone of width 30-55 km.

## 7.6 Lower crustal body and rift related magmatism

The Lower Crustal Body (LCB) is a localized zone of anomalous high P-wave velocities (7.2-7.8 km/s) located within the rifted continental margins. The LCB is formed as a result of rift related magmatism within the lower continental crust. Anomalous high velocity (7.2-7.4 km/s) lower crustal bodies have been identified in different geological domains of the western continental margin of India, which were interpreted as underplated lower crust (Pandey et al., 1996; Radha Krishna et al., 2002; Minshul et al., 2008; Collier et al., 2009). The lower crusts with anomalous high P-wave velocities (7.2 to 7.8 km/s) are one of the characteristic

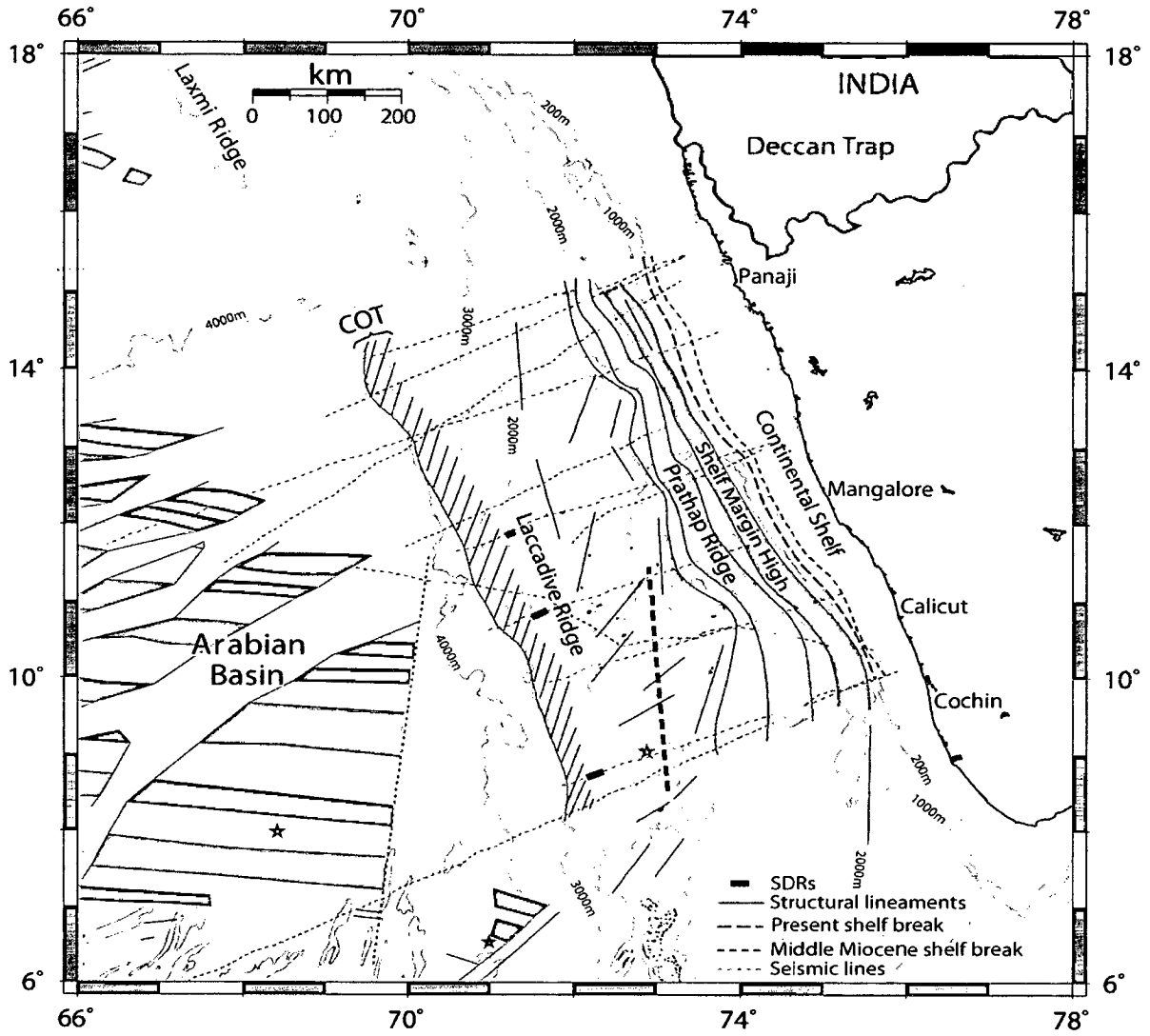


**Figure 7.1** Continent-Ocean Transition (COT) demarcated between the feather edge of the SDR sequences identified along the western flank of the Laccadive Ridge, and the oceanic crust of the Arabian Basin. Other details are given in the Figure 5.1.

features of the volcanic continental margins. The geophysical expression of the anomalous high velocity/density lower crustal body is complex. Such lower crustal bodies are interpreted as either a magmatic structure or a stretched continental crust loaded with dykes and sills injected during early stage of volcanic margin development.

2D crustal models across SWCMI suggest occurrence of LCB characterized by high density material beneath the Laccadive Ridge. The thick high-density (3.0 g/cm$^3$) lower crustal body below the ridge might have formed due to magmatic intrusions by the Marion hotspot during initial stage of rifting between Madagascar and Laccadive-India, and later by the Reunion hotspot when the Indian Plate

moved over the hotspot during its northward motion. However, Dev et al. (2007) have opined that the Marion hotspot might have played a limited role in the development of SWCMI. Nevertheless, the results of the present study (SDRs, LCB, crustal structure) suggest that the SWCMI could be described as a volcanic rifted margin whose early development have been affected by Marion hotspot magmatism in the south, unlike wide spread magmatism by the Reunion hotspot in the north.

## 7.7 Neotectonic activities

Differential displacements of the interpreted seismic sequences are identified in the MCS reflection profiles. These displacements are depicted as slumping of the sedimentary blocks along the continental shelf/slope, and faulting of the sedimentary layers. The slumping of upper most sedimentary sequence H5 is identified along the continental slope depicted in the seismic reflection profiles RE23 and RE17 (Figure 4.4 and Figure 4.15) suggesting recent tectonic activity.

Near vertical faults, penetrating through the entire sedimentary column overlying the Prathap Ridge are interpreted in the MCS profiles RE17 and RE15 (Figure 4.14 and Figure 4.17). The upper sediment layers are heavily folded and disrupted between the faults. The result suggests recent reactivation of the existing basement highs of the Prathap Ridge resulting into the intense faulting.

Interpretation of seismic sequences on the flat topped shelf margin high and adjacent region (Figure 4.17 and Figure 4.18) suggests upliftment due to re-activation of the high after the deposition of the upper most sedimentary sequence H5. The basement highs and/or igneous bodies associated with thinned and uplifted sedimentary column over its crust are identified in the Laccadive Basin and at the foot of the continental slope (Figures 4.3, 4.5, 4.14, 4.15 and 4.21). The upliftment and thinning of the sediment column suggests recently intruded or uplifted igneous bodies and/or basement highs. The reactivation of the horst-graben structures over the Laccadive Ridge are indicated by the fault bounded up-thrown and down-thrown tilted sedimentary blocks (Figure 4.3 and Figure 4.6). The faulted, folded, tilted and slumped blocks of the post Middle Miocene

sedimentary sequences and recently intruded or uplifted igneous intrusive bodies suggest neotectonic activities along the SWCMI.

The reactivation of Precambrian structural trends in the Indian subcontinent is attributed to: i) tectonic imbalance produced by the collision of India with Eurasia and upliftment of Himalaya during Middle Miocene (Ghosh and Zutshi, 1989; Biswas, 1987; Subrahmanyam et al., 1995, Clift et al., 2001), and ii) the compressional stress development due to spreading ridge push in the Indian Ocean and resistive forces at the Himalayan collision zone (Gowd et al., 1992 and Gowd et al., 1996). The reactivations of Precambrian fault trends caused the neotectonic activities and slumping along the western continental margin of India (Raha et al., 1983; Chandrasekharam, 1985; Nair and Subramanyan, 1989; Ramasamy, 1989; Chauhan and Almeida, 1993; Subrahmanyam et al., 1993b; Subrahmanya, 1998; Widdowson and Mitchell, 1999; Hanumantha Rao et al., 2002; Rao et al., 2002). The ENE-WSW trending transform faults of the Carlsberg Ridge and the structural lineaments of the Indian Ocean floor are known to be tectonically active. Nair and Subramanyan (1989) suggested that the ENE-WSW lineaments identified in the SWCMI constitute the youngest set since it abuts all other lineaments and are known to be responsible for neotectonism observed in the region. Earth tremor loci in the adjacent continental region of SWCMI reported from the recent past are aligned in ENE-WSW direction (Sharma and Varghese, 1979). Therefore, it could be surmised that the tectonic imbalance formed along the WCMI due to continued collision between India and Eurasia, upliftment of Himalaya, and the stress build up in the tectonically active zones of the Carlsberg Ridge and its transform faults are responsible for the reactivation of the Precambrian lineaments that caused neotectonic activities in the SWCMI.

# Chapter-8

# SUMMARY AND CONCLUSIONS

# Chapter-8

# SUMMARY AND CONCLUSIONS

## 8.1 Summary

The present study carried out on the Southwest Continental Margin of India (SWCMI) addresses: i) stratigraphy and sedimentation history, ii) new results on continental margin tectonics, iii) impacts of Rèunion hotspot along the margin and adjacent oceanic region, and iv) crustal structure of the margin. 2D Multi-Channel Seismic (MCS) reflection profiles, used as primary data set, have been analyzed and interpreted to delineate major sedimentary sequences, and structural and tectonic features of the study area. The ship-borne as well as satellite altimetry derived free-air gravity anomaly data, seismic refraction results and magnetic isochrons of the Arabian Basin are used for 2D crustal modeling across the margin, and to compute the basement depth anomalies in the Arabian Basin.

The MCS reflection profiles revealed five major seismic sequences H1 (oldest) – H5 (youngest) of the continental shelf and Laccadive Basin. The sequences are correlated with the sedimentary formations deposited from the Late Cretaceous to Recent. The seismic sequences L1 (oldest) – L5 (youngest) of the Laccadive Ridge are correlated with the sedimentary sequences deposited from Late Paleocene to Recent. Four seismic sequences A1 (oldest) - A4 (youngest) are interpreted from the eastern part of the Arabian Basin. Distinct shelf breaks of i) Late Paleocene (H1-top), ii) Early Oligocene (H2-top), iii) Middle Miocene (H3-top) and iv) Present (H5- top) are interpreted from the continental shelf of the SWCMI. The present continental shelf is prograded for about 15 km with characteristic sigmoid pattern from the Middle Miocene shelf break to present shelf break. The progradation of present shelf break indicate heavy influx of terrigenous sediments into the Arabian Sea as a result of onset of intense Indian monsoon and establishment of well developed fluvial system following the collision between Indian and Eurasian plates and upliftment of the Himalayas during the Middle Miocene. An aggraded continental shelf identified from Late Paleocene to Middle Miocene shelf breaks. The aggradation of continental shelf

indicate development of thick pelagic carbonate sedimentary sequence deposited as a result of increased sea level and warmer climatic condition in Indian subcontinent. Acoustic columns and a zone of ~50 km wide acoustic turbidity, which represent vertical fluid migration and gas accumulation zones respectively, are interpreted from the sedimentary columns of the Laccadive Basin and Laccadive Ridge. These zones are associated with the gas seeping morphologic depressions, known as pockmarks, on the seafloor. A submarine erosional channel of width ~9 km, identified over the Laccadive Ridge, indicates a channel migrated from the Middle Eocene with alternate erosional and depositional history.

Numerous faults and horst-graben structures are interpreted along the SWCMI. A zone (~41 km wide) of well developed horst-graben structures, associated with numerous faults and tilted crustal blocks, is identified from the southern part of the Laccadive Ridge. A chain of structural highs with flat summit are identified and demarcated along continental slope of the SWCMI. The highs are observed in a NNW-SSE trending zone of width ranging between 17.4 and 43.5 km. The boundary of the Prathap and Laccadive ridges are redefined based on integrated interpretation of the seismic profiles, gravity anomalies and crustal structure models of the study area. The width of the Prathap Ridge varies from 17 km in the north to 65 km in the south, whereas, the width of the northward widening Laccadive Ridge varies between 238 and 304 km in the study area.

The Seaward Dipping Reflectors (SDRs) identified along western flank of the Laccadive Ridge indicates extrusive volcanic episodes under sub-aerial condition during rifting between the eastern Madagascar and India under the influence of the Marion hotspot. Seaward of their occurrences, the Laccadive Ridge gradually thins and juxtaposed with the Early Tertiary normal oceanic crust of the Arabian Basin. Even though the volcanic rifted margins may be predominantly volcanic without SDRs, the occurrence of SDRs along the rifted margins can be considered sufficient condition to classify them under volcanic rifted margins (Eldholm et al., 1995). Therefore, the SDRs along the SWCMI indeed suggest that the margin is a volcanic rifted margin developed during breakup between Madagascar and India in the Late Cretaceous.

Identification of basement depth anomalies in the Arabian Basin suggests that subsidence in the basin does not follow the age-depth relationship of normal oceanic crust. The anomalous depths to oceanic basement of the basin indicate presence of both positive and negative anomalies which vary from +501 to −905 m. The negative basement depth anomalies (shallower than predicted depth) documented from the eastern part of the Arabian Basin is related to its proximity to the high thermal regime of the former Rèunion hotspot. The hotspot might have caused a regional swell by vertical upwelling due to convection, followed by a lateral across-axis flow. Thereafter, the oceanic lithosphere started subsiding, and is presently relatively shallow compared to the predicted depth of the normal oceanic crust even if the cause of the uplift ceased to operate in the region. The zone of positive depth anomalies documented from the western part of the Arabian Basin indicates excess subsidence of the oceanic crust relative to the predicted crust. The excess subsidence of could have caused by the combination of isostatic adjustment due to sediment loading and the relatively cold and condensed mantle compared to the eastern part of the basin which was affected by the intense thermal field of the former Reunion hotspot.

2D gravity modeling along five transects of the SWCMI spanning from continental shelf to the Arabian Basin suggests average crustal thicknesses of 22.5, 19 and 6.5 km for the outer shelf, Laccadive Ridge and Arabian Basin respectively. Three crustal layers of densities 2.1, 2.7 and 2.95 g/cm$^3$ representing the sedimentary layer, layer 2 and layer 3 of the oceanic crust respectively, are interpreted for the Arabian Basin. The crustal models suggest a stretched continental crust characterized by a number of magmatic intrusive/extrusive bodies below the Laccadive Basin and Laccadive Ridge. Four crustal layers of densities 2.1, 2.65, 2.8 and 2.9 g/cm$^3$ representing sediments, metasediments, upper and lower crusts respectively are inferred across the SWCMI. Densities ranging from 2.4-2.65 g/cm$^3$ are inferred for igneous intrusive bodies, chert/basaltic flow and SDRs. The metasediments underlie the sedimentary layer and/or chert/basaltic flow. A lower crustal body of a high density (3.0 g/cm$^3$) is inferred below the Laccadive Ridge. Moho is shallow below the Laccadive and Arabian basins with average depths of 15 and 10 km respectively. Deeper Moho depths of about 20 and 22.5 km are estimated beneath the Laccadive Ridge and continental shelf respectively.

The combined interpretation of the crustal structure models, seismic reflection and free-air gravity anomaly profiles suggest the location of Continent-Ocean Transition (COT) along the western margin of Laccadive Ridge between the SDR sequences and the oceanic crust of the Arabian Basin where the Moho is characterized by significant shoaling to an average depth of 10.5 km.

## 8.2 Conclusions

Important conclusions drawn from the present study are:

1. The analysis and interpretation of MCS reflection profiles traversing the SWCMI revealed five major seismic sequences H1 (oldest), H2, H3, H4 and H5 (youngest) from the sediment column of the continental shelf and Laccadive Basin. Five major seismic sequences L1(oldest), L2, L3, L4 and L5 (youngest) are interpreted from the Laccadive Ridge. Four major seismic sequences A1(oldest), A2, A3 and A4 (youngest) are identified from the eastern part of the Arabian Basin.

2. The seismic sequences identified from the continental shelf-Laccadive Basin and Laccadive Ridge are correlated with the sedimentary formations deposited during Late Cretaceous to Recent, Late Paleocene to Recent respectively.

3. Four distinct shelf breaks: i) Late Paleocene, ii) Early Oligocene, iii) Middle Miocene and iv) Present are interpreted from the seismic reflection profiles.

4. The present continental shelf is prograded for an average distance of 15 km with characteristic sigmoid pattern from the Middle Miocene shelf break to present shelf break. An aggraded continental shelf is identified from the Late Paleocene to Middle Miocene shelf breaks.

5. Submarine slumps along the present and paleo continental slopes formed as a result of tectonic activities caused by reactivation of Precambrian structural trends.

6. A submarine erosional channel, migrated from the Middle Eocene to the present is identified on the Laccadive Ridge. The channel is characterized by alternate erosional and depositional features formed due to strong turbidity currents followed by hemipelagic sedimentation.

7. Acoustic columns interpreted as vertical fluid migration through the sedimentary sequences, associated with pockmarks on the seafloor, are identified from the Laccadive Basin and Laccadive Ridge. About 50 km wide zone of acoustic turbidity formed by migrating fluids is identified from the Laccadive Basin.

8. A zone of horst-graben structures, extended for about 326 km with a N-S trending axis and associated with numerous faults and tilted crustal blocks, is identified from the southern part of the Laccadive Ridge.

9. Shelf margin high constituted by several flat summit structural highs and associated with gravity anomaly high is demarcated between present shelf break and Prathap Ridge.

10. The boundaries of the Prathap and Laccadive ridges are redefined based on integrated interpretation of seismic and gravity data.

11. The basement depth anomalies are identified for the first time in the Arabian Basin. The anomalies, vary from +501 to −905 m, suggest that subsidence in the basin does not follow the age-depth relationship of normal oceanic crust.

12. The negative depth anomalies (shallower than predicted depth), located east of the Laccadive Ridge, is related to the high thermal regime of the former Rèunion hotspot.

13. The crustal models across the SWCMI suggest a stretched and thinned continental crust below the continental shelf, Laccadive Basin and Laccadive Ridge with four major crustal layers. From the crustal models a Lower Crustal Body (LCB) of a high density (3.0 g/cm$^3$) is infered below the Laccadive Ridge representing heavily intruded lower crust of the Laccadive Ridge.

14. Seaward Dipping Reflectors (SDRs) are identified, for the first time, along western flank of the Laccadive Ridge. The SDRs indicate extrusive volcanic episodes under sub-aerial condition during rifting between the eastern Madagascar and India under the influence of the Marion hotspot, and suggest that the southwest continental margin of India is a volcanic rifted margin developed during breakup.

15. The Continent-Ocean Transition (COT) along the SWCMI is inferred between the SDR sequences identified along the western flank of the Laccadive Ridge, and the oceanic crust of the Arabian Basin.

# References

# References


Acharyya, S.K., 2000. Break up of Australia–India–Madagascar block, opening of the Indian Ocean and continental accretion in southeast Asia with special reference to the characteristics of the peri-Indian collision zones. Gond. Res., 3:425–443.

Ajay, K.K. and Chaubey, A.K., 2008. Depth anomalies in the Arabian Basin, NW Indian Ocean. Geo-Mar. Lett., 28:15-22.

Ajay, K.K., Chaubey, A.K., Krishna, K.S., Rao, D.G. and Sar, D., 2010. Seaward dipping reflectors along the SW continental margin of India: Evidence for volcanic passive margin. J. Earth Syst. Sci., 119:803-813.

Anil Kumar, Pande, K., Venkatesan, T.R. and Bhaskar Rao, Y.J., 2001. The Karnataka Late Cretaceous dykes as products of the Marion hotspot at the Madagascar-India breakup event: evidence from $^{40}Ar/^{39}Ar$ geochronology and geochemistry. Geophys. Res. Lett., 28:2715-2718.

Austin, J.A. and Uchupi, E., 1982. Continental-oceanic crustal transition off southwest Africa. Am. Assoc. Petrol. Geol. Bull., 66(9):1328-1347.

Aubert, O. and Droxler, A.W., 1996. Seismic stratigraphy and depositional signatures of the Maldive carbonate system (Indian Ocean). Mar. Petrol. Geol., 13:503-536.

Avraham, Z.B. and Bunce, E.T., 1977. Geophysical study of the Chagos-Laccadive Ridge, Indian Ocean. J. Geophys. Res., 82:1295 -1305.

Babenko, K.M., Panaev, V.A., Svistunov, Yu.I. and Shlezinger, A.E., 1981. Tectonics of the eastern margin of the Arabian Sea according to seismic data. Bull. ONGC., 18:37-62.

Baksi, A.K. and Farrar, E., 1991. $^{40}Ar/^{39}Ar$ dating of the Siberian Traps, USSR: evaluation of the ages of the two major extinction events relative to episodes of flood-basalt volcanism in the USSR and Deccan Traps, India. Geology., 19:461-464.

Balakrishnan,T.S., 1997. Major Tectonics Elements Of The Indian Sub Continent And Contiguous Area: A Geophysical View. Geol. Soc. India, Mem., 38,155p.

Balakrishna, T.S. and Sharma, D.S., 1981. Tectonics of west coast of India. Bull. ONGC., 18:25-26.

Barton, P.J., 1986. The relationship between velocity and density in the continental crust- a useful constraint ?. Geophys. J .R. Astron. Soc. 87., 195-208.

Basu, A.R., Renne, P.R., Dasgupta, D.K., Teichmann, F. and Poreda, R.J., 1993. Early and late alkali igneous pulses and high-$^{3}$He plume origin for the Deccan flood besalts. Science., 261:902-906.

Belmonte, Y., Hirtz, P. and Wenger, R., 1965. The salt basin of the Gabon and Congo (Brazzaville), In: W.Q. Kennedy (Ed.), Salt basins around Africa. London Inst. Petroleum., pp 55-74.

Berndt, C., Planke, S., Alvestad, E., Tsikalas, F. and Rasmussen, T., 2001. J. Geol. Soc. London., 158:413-426.

Bertram, G.T. and Milton, N.J., 1996. Seismic stratigraphy, In: D. Emery and K.J. Myers (Eds), Sequence stratigraphy. BP Exploration, Stockley Park Uxbridge, London, 45-60.

Besse, J. and Courtillot, V., 1988. Paleogeographic maps of the continents bordering the Indian Ocean since the Early Jurassic. J. Geophys. Res., 93:11791-11808.

Bhattacharji, S., Chatterjee, N., Wampler, J.M., Nayak, P.N. and Deshmukh, S.S., 1996. Indian Intraplate and continental margin rifting, lithospheric extension, and mantle upwelling in Deccan flood basalt volcanism near the K/T boundary: Evidence from mafic dike swarms. Geology., 104:379-398.

Bhattacharya, G.C., Murty, G.P.S., Srinivas, K., Chaubey, A.K., Sudhakar, T. and Nair, R.R., 1994b. Swath bathymetric investigation of the seamounts located in the Laxmi Basin, eastern Arabian Sea. Mar. Geodesy., 17:169-182.

Bhattacharya, G.C. and Chaubey, A.K., 2001. Western Indian ocean – A glimpse of the Tectonic Scenario, In: R. Sen Gupta and E. Desa (Eds), The Indian Ocean - A perspective. Oxford & IBH Publishing Co. pvt. Ltd., New Delhi, pp 691-729.

Bhattacharya, G.C and Subrahmanyam, V., 1991. Geophysical study of a seamount located on the continental margin of India. Geo-Mar. Lett., 11:71-78.

Bhattacharya, G.C. and Subrahmanyam, V., 1986. Extension of the Narmada-Son Lineament on the continental margin off Saurashtra, Western India as obtained from magnetic measurements. Mar. Geophys. Res., 8:329-344.

Bhattacharya, G.C., Chaubey, A.K., Murty, G.P.S., Gopala Rao, D., Scherbakov, V.S., Lygin, V.A., Philipenko, A.I. and Bogomyagkov, A.P., 1992. Marine magnetic anomalies in the northeastern Arabian Sea. In: B.N. Desai (Ed.), Oceanography of the Indian Ocean. Oxford-IBH, New Delhi., pp 503-509.

Bhattacharya, G.C., Chaubey, A.K., Murty, G.P.S., Srinivas, K., Sarma, K.V.L.N.S., Subrahmanyam, V. and Krishna, K.S., 1994a. Evidence for seafloor spreading in the Laxmi Basin, northeastern Arabian Sea. Earth Planet. Sci. Lett., 125:211-220.

Biswas, S.K., 1982. Rift basins in western margin of India and their hydrocarbon prospects with special reference to Kutch Basin. Bull. Am. Assoc. Pet. Geol., 66:1497-1513.

Biswas, S.K., 1987. Regional tectonic framework, structure and evolution of the western marginal basins of India. Tectonophysics., 135:307-327.

Biswas, S.K., 1988. Structure of the western continental margin of India and related igneous activity. Mem. Geol. Soc. Ind., 10:371-390.

Biswas, S.K. and Singh, N.K., 1988. Western continental margin of India and hydrocarbon potential of deep-sea basins. Proc. 7th offshore south east Asia conference, Singapore., pp 170-181.

Biswas, S.K., 1989. Hydrocarbon exploration in western offshore basins of India. Geol. Surv. Ind. Spl. Pub., 24:185-194.

Boyd, F.R. and McCallister, R.H., 1976. Densities of sterile and fertile garnet peridotites. Geophys. Res. Lett., 3:509–512.

Campanile, D., Nambiar, C.G., Bishop, P., Widdowson, M. and Brown, R., 2008. Sedimentation record in the Konkan-Keral Basin: implications for the evolution of the Western Ghats and the Western Indian passive margin. Basin Research., 20:3-22.

Cande, S.C. and Kent, D.V., 1995. Revised calibration of the geomagnetic polarity timescale for the Late Cretaceous and Cenozoic. J. Geophys. Res., 100:6093-6095.

Chakraborty, B., Mukhopadhyay, R., Jauhari, P., Mahale, V.P., Shashikumar, K., Rajesh, M., 2006. Fine scale analysis of shelf slope physiography across the western continental margin of India. Geo. Mar. Lett., 26(2):114-119.

Chandrasekharam, D., 1985. Structure and evolution of the western continental margin of India deduced from gravity, seismic, geomagnetic and geochronological studies. Phys. Earth Planet. Inter., 41:186-198.

Chaubey, A.K., Bhattacharya, G.C., Murty, G.P.S. and Desa, M., 1993. Spreading history of the Arabian Sea: Some new constraints. Mar. Geol., 112:343-352.

Chaubey, A.K., Bhattacharya, G.C. and Rao, D.G., 1995. Seafloor spreading magnetic anomalies in the southeastern Arabian Sea. Mar. Geol., 128:105-114.

Chaubey, A.K., 1998. Marine geophysical investigations over a part of the Eastern Arabian Sea, Northwestern Indian Ocean. Ph.D. Thesis, Goa University, Goa, 217p.

Chaubey, A.K., Bhattacharya, G.C., Murty, G.P.S., Srinivas, K., Ramprasad, T. and Gopala Rao, D., 1998. Early Tertiary seafloor spreading magnetic anomalies and paleo-propagators in the northern Arabian Sea. Earth Planet. Sci. Lett., 154:41-52.

Chaubey, A.K., Dyment, J., Bhattacharya, G.C., Royer, J.-Y., Srinivas, K. and Yatheesh, V., 2002a. Paleogene magnetic isochrons and paleo-propagators in the Arabian and Eastern Somali basins, Northwest Indian Ocean. In: The Tectonic and Climatic Evolution of the Arabian Sea Region, P.D. Clift, D. Kroon, C. Gaedicke and J. Craig (Eds). Geological Society, London, Special Publications., 195:71-85.

Chaubey, A.K., Gopala Rao, D., Srinivas, K., Ramprasad, T., Ramana, M.V. and Subrahmanyam, V., 2002b. Analyses of multichannel seismic reflection, gravity and magnetic data along a regional profile across the central-western continental margin of India. Mar. Geol., 182:303-323.

Chaubey, A.K and Ajay, K.K., 2008. Structure and tectonics of Western Continental Margin of India: Implication for Geological Hazards. In: Workshop on Natural hazards and coastal processes of Indian coast, proceedings volume, NIO Regional Centre, Visakhapatnam, pp 25-33.

Chaubey, A.K., Srinivas, K., Ashalatha, B. and Gopala Rao, D., 2008. Isostatic response of the Laccadive Ridge from admittance analysis of gravity and bathymetry data. J. Geody., 46:10-20.

Chauhan, O.S. and Chaubey, A.K., 1992. Submarine physiography off the Lakshadweep Islands, Arabian Sea. In: B.N. Desai (Ed.), Oceanography of the Indian Ocean. Oxford-IBH, New Delhi., pp 487-491.

Chauhan, O.S. and Almeida, F., 1993. Influences of Holocene sea level, regional tectonics, and fluvial gravity and slope currents induced sedimentation on the regional geomorphology of the continental slope off northwestern India. Mar. Geol., 112:313-328.

Clift, P.D., Shimizu, N., Layne, G.D., Blusztajn, J.S., Gaedicke, C., Schluter, H.U., Clark, M.K. and Amjad, S., 2001. Development of the Indus fan and its significance for the erosional history of the Western Himalaya and Karakoram. Geol. Soc. Am. Bull., 113:1039-1051.

Coffin, M.F. and Eldholm, O., 1992. Volcanism and continental breakup: a global compilation of large igneous provinces. Geol. Soc. London Spec. Pub., 68:21-34.

Collier, J.S., Minshull, T.A., Hammond, J.O.S., Whitmarsh, R.B., Kendall. J.M., Sansom, V., Lane, C.I. and Rumpker, G., 2009. Factors influencing magmatism during continental break up: New insights from a wide-angle seismic experiment across the conjugate Seychelles–Indian margins. J. Geophys. Res., 114:B03101, doi: 10.1029/2008JB005898.

Courtillot, V., Besse, J., Vandamme, D., Montigny, R., Jaeger, J.J. and Cappetta, H., 1986. Deccan flood basalts at the Cretaceous/Tertiary boundary?. Earth Planet. Sci. Lett., 80:361-374.

Courtillot, V., Feraud, G., Maluski, H., Vandamme, D., Moreau, M.G. and Besse, J., 1988. Deccan flood basalts and the Cretaceous/Tertiary boundary. Nature., 333:843-846.

Courtillot, V., Jaupart, C., Manighetti, I., Tapponneir, P., Besse, J., 1999. On casual links between flood basalts and continental breakup. Earth Planet. Sci. Lett., 166:177-195.

Courtillot, V.E. and Renne, P.R., 2003. On the ages of flood basalt events. C. R. Geosci., 335(1):113-140.

Crough, S.T., 1979. Hotspot epeirogeny, In: T.R. McGetchni, R.B. Merrill (Eds), Plateau uplift: mode and mechanism. Tectonophysics., 61:321–333.

Crough, S.T., 1983. The correction for sediment loading on the sea floor. J Geophys Res., 88:6449-6454.

Curray, J.R., 1980. The IPOD programme on passive continental margins. Phil. Trans. R. SOC. London., A-294, pp 17-33.

Das, S.R. and Ray, A.K., 1976. Fracture pattern, hot springs and lineaments of the west coast. J. Geol. Surv. Ind., 125 Year News Lett., 1-6.

Davis, E.E., Lister, C.R.B., 1974. Fundamentals of ridge crest topography. Earth Planet. Sci. Lett., 21:405–413.

Detrick, R.S., Crough, S.T., 1978. Island subsidence, hotspots and lithospheric thinning, J. Geophys. Res., 83:1236–1244.

Dev, S.V., Radhakrishna, M. and Subrahmanyam, C., 2007. Estimates of elastic thickness along the southwest continental margin of India using coherence analysis of gravity and bathymetry data – geodynamic implications. J. Geol. Soc. India., 70:475–487.

Devey, C.W., Stephens, W.E., 1991. Tholeiitic dykes in the Seychelles and the original spatial extent of the Deccan. Journal of the Geological Society., 148:979-983.

Duncan, R.A., 1990. The volcanic record of the Reunion hotspot. In: R.A. Duncan, J. Backman, L.C. Peterson et al. (Eds), Proc. ODP, Sci. Results., 115:College Station, TX (Ocean Drilling Program), 3-10.

Dyment, J., 1998. Evolution of the Carlsberg Ridge between 60 and 45 Ma : Ridge propagation, spreading asymmetry, and the Deccan-Reunion hotspot. J. Geophys. Res., 103:24067-24084.

Eldholm, O., Skogseid, J., Planke, S. and Gladczenko, T.P., 1995. Volcanic margin concepts, In: E. Banda, M. Torné and M. Talwani (Eds), Rifted Ocean-Continent Boundaries. Kluwer Acad. Publ, London., pp 1-16.

Eremenko, N.A. and Datta, A.K., 1968. Regional geological framework and evaluation of the petroleum prospects of the Laccadive archipelago and the adjoining offshore territory, southwest India. Bull. ONGC., 5:29-40.

Francis, T.J.G. and Shor, G.G., 1966. Seismic refraction measurements in the northwest Indian Ocean. J. Geophys. Res., 71:427–449.

Garcia-Gil, S., Vilas, F. and Garcia-Garcia, A., 2002. Shallow gas features in incised valley fills (Ría de Vigo, NW Spain): a case study. Cont. Shelf Res., 2303-2315.

Ghosh, B.N. and Zutshi, P.L., 1989. Indian West Coast shelf break tectonic features. Geol. Surv. India Spec. Publ., 24:309-318.

Ghosh, J.G., de Wit, M.J. and Zartman, R.E., 2004. Age and tectonic evolution of Neoproterozoic ductile shear zones in the Southern Granulite Terrain of India, with implications for Gondwana studies. Tectonics., 23:doi:10.1029/2002TC001444.

Gilchrist, A.R. and Summerfield, M.A., 1990. Differential denudation and flexural isostasy in formation of rifted margin upwarps. Nature., 346:739-742.

Gladczenko, T.D., Skogsied, J. and Eldhom, O., 1998. Namibia volcanic margin. Mar. Geophys. Res., 20:313-34.

Gombos, A.M., Powell, W.G. and Norton, I.O., 1995. The tectonic evolution of Western India and its impact on hydrocarbon occurrences – an overview. Sediment. Geol., 96:119-129.

Gopala Rao, D. and Bhattacharya, G.C., 1977. Marine magnetic anomalies off the southwest coast of India and their analysis. J. Geol. Soc. India., 18:504-508.

Gopala Rao, D., 1984. Marine magnetic anomalies off Ratnagiri, Western continental shelf of India. Mar. Geol., 61:103-110.

Gopala Rao, D., Bhattacharaya, G.C., Subba Raju, L.V., Ramana, M.V., Subrahmanyam, V., Raju, K.A.K., Ram Prasad, T. and Chaubey, A.K., 1987. Regional marine geophysical studies of the south western continental margin of India. Contribution in Marine Sciences, felicitation volume., pp 427-437.

Gopala Rao, D., Paropkari, A.L., Krishna, K.S., Chaubey, A.K., Ajay, K.K. and Kodagali, V.N., 2010. Bathymetric highs in the mid-slope region of the western continental margin of India - Structure and mode of origin. Mar. Geol., 276(1-4):58-70.

Gowd, T.N., Srirama Rao, S.V. and Gaur, V.K., 1992. Tectonic stress-field in the Indian Subcontinent. J. Geophys. Res., 97:11879-11888.

Gowd T N, Srirama Rao S V and Chary K B 1996. Stress field and seismicity in the Indian shield: Effect of collision between India and Eurasia. Pure and Appl. Geophys., 146:503–531.

Gunnel, Y., 2001. Fluvial routing systems and the signatures of onshore denudation in the offshore sedimentary record of Western India. Geol. Soc. India, Mem., 47:279-292.

Hanumantha Rao, Y., Subrahmanyam, C., Rastogi, A. and Deka, B., 2002. Slope failures along the western continental margin of India: a consequence of gas-hydrate association, rapid sedimentation rate, and seismic activity. Geo-Mar. Lett., 22:162-169, doi:10.1007/s00367-002-0107-9.

Haq, B.U., Hardenbol, J. and Vail, P.R., 1987. Chronology of fluuctuating sea levels since the Triassic. Science., 235:1156-1167.

Harbison, R.N. and Bassinger, B.G., 1973. Marine geophysical study off western India. J. Geophys. Res., 78:432-440.

Hayes, D.E., 1988. Age-depth relationships and depth anomalies in the Southeast Indian Ocean and South Atlantic Ocean. J Geophys Res., 93:2,937-2,954.

Hillier, J.K. and Watts, A.B., 2004. "Plate-like" subsidence of the East Pacific Rise-South Pacific super swell system. J Geophys Res., 109:B10102.

Hinz, K., 1981. A hypothesis on terrestrial catastrophes: Wedges of very thick ocean warddipping layers beneath passive ciontinental margins—Their origin and paleoenvironmental significance. Geol. Jahrb. Ser., E 22:3-28

Hooper, P.R., 1990. The timing of crustal extension and the eruption of continental flood basalts. Nature., 345:246-249.

Hovland, M. and Judd, A.G., 1988. Seabed Pockmarks and Seepages. Impact on Geology, Biology and the Marine Environment. Graham and Trotman, London., 294p.

Jordan, T.H., 1979. Mineralogies, densities and seismic velocities of garnet lherzolites and their geophysical implications, In: F.R. Boyd, H.O.A. Meyer (Eds), The mantle sample: inclusions in kimberlites and other volcanic. American Geophysical Union, Washington D C., pp 1–14.

Joseph, S. and Nambiar, C. G., 1996. Alkaline nature and taphrogenetic affinity of felsic volcanic rocks of St. Mary's Islands, off Mangalore coast. Curr. Sci., 70:858-860.

Kahle, H. G. and Talwani, M., 1973. Gravimetric Indian Ocean geoid. Z. Geophys., 39:167-187.

Kaila, K.L., Chaudury, K.R., Reddy, P. R., Krishna, V.G., Harinarain, Subbotin, S.I., Sollogub,V.B., Chekunov, A.V., Kharetchko, G. E., Lazarenko, M.A. and Ilchenko, T. V., 1979. Crustal structure along Kavali-Udipi profile in the Indian Peninsular shield from deep seismic sounding. J. Geol. Soc. India., 20:307-333.

Kaila, K.L., Reddy, P. R., and Dixit, M. M., 1981. Deep crustal structure at Koyna, Maharashtra, indicated by deep seismic soundings,.J. Geol. Soc. India., 22:1-16.

Kennet, J.P., 1982. Marine Geology. Englewood cliffs, New Jersey.

Kessarkar, P. M., Rao, V. P., Ahmad, S. M. and Babu, G. A., 2003. Clay minerals and Sr-Nd isotopes of the sediments along the western margin of India and their implication for sediment provenance. Mar. Geol., 202:55-69.

King, L.H. and McLean, B., 1970. Pockmarks on the Scotian Shelf. Bulletin of the Geological Society of America., 81:3141–4148.

Kolla, V., Kostecki, J.A., Robinson, F. and Biscaye, E.E., 1981. Distributions and origins of clay minerals and quartz in surface sediments of the Arabian Sea. J. Sed. Petrol., 51:563-569.

Kolla, V. and Coumes, F., 1990. Extension of structural and tectonic trends from the Indian subcontinent into the Eastern Arabian Sea. Mar. Pet. Geol., 7:188-196.

Kothari,V., Waraich, R.S., Dirghangi, R.S., Baruah, R.M., Lal, N.K., Zutshi, P.L., 2001. A reassessment of the hydrocarbon prospectivity of Kerala–Konkan deep water basin, western offshore, India. In: A.K. Bhatnagar (Ed.), Hydrocarbon Exploration. Proc. Fifth Int. Pet. Conf. and Exbn, Petrotech-2001.

Krishna, K.S., Murty, G.P.S., Srinivas, K. and Gopala Rao, D., 1992. Magnetic studies over the northern extension of the Prathap Ridge complex, eastern Arabian Sea. Geo-Mar. Lett., 12:7-13.

Krishna, K.S., Murty, G.P.S. and Rao, D.G., 1994. Identification and origin of a subsurface ridge on the continental margin of western India. Mar. Geol., 118(3-4):283-290.

Krishna, K.S., Gopala Rao, D. and Sar, D., 2006. Nature of the crust in the Laxmi Basin (14° - 20°N), western continental margin of India; Tectonics TC1006.

Krishna, K.S., Chaubey, A.K., Rao, D.G., Reddy, P.R., 2010. Seismic structure and tectonics of the continental margins of India, In: P.R. Reddy (Ed.),

Seismic imaging of the Indian continental and oceanic crust. Professional Books, Hyderabad, India, pp 324-432.

Krishna, V.G., Kaila, K.L., and Reddy, P. R., 1991. Low velocity layers in the sub crustal lithosphere beneath Deccan Trap regions of western India. Physics of the Earth and planetary interior., 67:288-302.

Krishnan, M.S., 1968. Geology of India and Burma. Higgin-Bothams, Madras., 536p.

Lin, S.C., Chiao, L.Y. and Kuo, B.Y., 2002. Dynamic interaction of cold anomalies with the mid-ocean ridge flow field and its implications for the Australian-Antarctic Discordance, Earth Planet. Sci. Lett., 203:925–935.

Louden, K.E., Tucholke, B.E., Oakey, G.N., 2004. Regional anomalies of sediment thickness, basement depth and isostatic crustal thickness in the North Atlantic Ocean, Earth Planet. Sci. Lett., 224:193–211.

Mahadevan, T.M., 1994. Deep Continental Structure of India: A Review. Mem. Geol. Soc. Ind., 28, 569p.

Maillard, A., Malod, J.A., Tiébot, E., Sahabi, M., Klingelhöfer, F. and Réhault, J.P., 2006. Imaging a lithospheric detachment at the continent-ocean crustal transition off Morocco. Earth Planet. Sci. Lett., 241:686-698.

Malod, J.A., Droz, L., Kemal, B.M. and Patriat, P., 1997. Early spreading and continental to oceanic basement transition beneath the Indus deep-sea fan: northeastern Arabian Sea. Mar. Geol., 141:221-235.

Mascle, J., and Blarez, E., 1987. Evidence for transform margin evolution from the Ivory Coast: Ghana continental margin. Nature., 326:378-381.

Mascle, J., Guiraud, M., Benkhelil, J., Ch. Basile, Bouillin, J.P., Mascle, G., Cousin, M., Durand, M., Dejax, J. and Moullade, M., 1998. A geological field trip to the Côte d'Ivoire-Ghana Transfrom Margin. Oceanologica Acta., 21(1):1-20.

Mathur, R.B., Sreekantswamy, H.N., Ananthakrishna, K., Srivastava, U.C., Biswas, S. K., Krishna Ajay, Bhosale, J.S.,Rao, K.V.N., Satyanarayana, Y., Rathod, G.D., Bose, P.K. and Karwal Sangeeta., 1993. Lithostratigraphy of Indian Petroliferous basins –Kerala-Konkan basin: ONGC,Dehradun.

McKenzie, D. and Sclater, J.G., 1971. The evolution of the Indian Ocean since the Late Cretaceous. Geophys. J. R. Astron. Soc., 25:437-528.

McKenzie, D., Watts, A., Parson, B., Roufosse, M., 1980. Planform of mantle convection beneath the Pacific Ocean, Nature, 288:442–446.

McNutt, M.K. and Fischer, K.M., 1987. The south Pacific superswell. In: Keating, B.H., Fryer, P., Batiza, R. and Boehlert, G.W. (Eds), Seamounts, islands and atolls. American Geophysical Union, Washington DC. Geophys. Monogr. Ser., 43:25–34.

Menard, H.W., 1969. Elevation and subsidence of oceanic crust. Earth Planet. Sci. Lett., 6:275-284.

Menard, H.W., 1973. Depth anomalies and bobbing motion of drifting islands. J. Geophys. Res., 78:5128–5137.

Mercuriev, S., Patriat, P. and Sochevanova, N., 1996. Evolution de la dorsale de Carlsberg: evidence pour une phase d'expansion tres lente entre 40 et 25 Ma (A18 a A7). Oceanol. Acta., 19(1):1-13.

Miles, P.R., Munschy, M. and Segoufin, J., 1998. Structure and early evolution of the Arabian Sea and East Somali Basin. Geophys. J. Int., 134:876-888.

Miles, P.R. and Roest, W.R., 1993. Earliest sea-floor spreading magnetic anomalies in the north Arabian Sea and the ocean-continent transition. Geophys. J. Int., 115:1025-1031.

Minshull, T.A., Lane, C.I., Collier, J.S. and Whitmarsh, R.B., 2008. The relationship between rifting and magmatism in the northeastern Arabian Sea. Nature Geosci., 1:463-467.

Mishra, D.C., Arora, K. and Tiwari, V.M., 2004. Gravity anomalies and associated tectonic features over the Indian Peninsular Shield and adjoining ocean basins. Tectonophys., 379, 61-76.

Mitchum, Jr, R.M. and Vail, P.R., 1977. Seismic stratigraphy and global changes of sea level, Part 6: Stratigraphic interpretation of seismic reflection patterns in depositional sequences, In: C.E. Payton (Ed.), Seismic stratigraphy – applications to hydrocarbon exploration. AAPG Mem., 26:117-133.

Mitchum, Jr., R.M., Vail, P.R. and Sangree, J.B., 1977. Seismic stratigraphy and global changes of sea level, Part 6: Stratigraphic interpretation of seismic reflection patterns in depositional sequences, In: C.E. Payton (Ed.), Seismic stratigraphy – applications to hydrocarbon exploration, AAPG Mem. 26:117-133.

Mohan, M. and Narayanan, V., 1980. Paleogene unconformities and their significance in hydrocarbon accumulation in Bombay Offshore region. Proc. 3rd Indonesian Geological Congress., 125-149.

Mohan, M., 1985. Geohistory analysis of Bomaby High region. Mar. Petrol. Geol., 2:350-360.

Molnar, P., 2004. Late cenozoic increase in accumulation rates of terrestrial sediment: how might climate change have affected erosion rates?. Annu. Rev. Earth Planet. Sci. Lett., 32:67-89.

Mooney, W.D., Laske, G. and Masters, T.G., 1998. CRUST 5.1: A global crustal model at 5° x 5°. J. Geophys. Res., 103:727-747.

Morgan, J.P. and Sandwell, D.T., 1994. Systematics of ridge propagation south of 30°S. Earth Planet. Sci. Lett., 121:245–258.

Morgan, W.J., 1972. Plate motions and deep mantle convection. Geol. Soc. America Mem., 132:7-22.

Morgan, W.J., 1981. Hotspot tracks and the opening of the Atlantic and Indian Oceans. In: C. Emiliani (Ed.), The Sea, Vol. 7, Wiley Interscience, New York., pp 443-487.

Mukhopadhyay, R., Rajesh, M., De, Sutirtha; Chakraborty, B. and Jauhari, P., 2008 Structural highs on the western continental slope of India: Implications for regional tectonics. Geomorphology., 96(1-2):48-61.

Muller, R.D., Royer, J.-Y. and Lawver, L.A., 1993. Revised plate motions relative to the hotspots from combined Atlantic and Indian Ocean hotspot tracks. Geology, 21:275-278.

Murty, A.V.S., Arasu, R.T., Dhanawat, B.S., Subrahmanyam, V.S.R., 1999. Some aspects of deepwater exploration in the light of new evidences in the western Indian o!shore. In: Bhatnagar, A.K. (Ed.), Hydrocarbon Exploration. Papers of the Third International Petroleum Conference and Exhibition, Petrotech-99, Thompson, Faridabad, India, pp 457-463.

Mutter, J. C., 1985. Seaward dipping reflectors and the continent-ocean boundary at passive continental margins. Tectonophysics, 114:117-131.

Mutter, J.C., Talwani, M. and Stoffa, P.L., 1982. Origin of seaward-dipping reflectors in oceanic crust off the Norwegian margin by 'subaerial sea-floor spreading', Geology, 10:353–357.

Nafe, J.E. and Drake, C.L., 1963. Physical properties of marine sediments. In: Hill MN (Ed.) The Sea 3, Ideas and observations on progress in the study of the Sea. Wiley Interscience Publications, New York, pp 794-815.

Naini, B.R., 1980. A geological and geophysical study of the continental margin of western India, and the adjoining Arabian Sea including the Indus Cone. Unpublished Ph.D. thesis, Columbia University, New York, pp 167.

Naini, B.R. and Kolla, V., 1982. Acoustic character and thickness of sediments of the Indus Fan and the continental margin of western India. Marine Geology., 47:181-105.

Naini, B.R. and Talwani, M., 1983. Structural framework and the evolutionary history of the continental margin of western India. In: J.S. Watkins and C.L.

Drake (Eds), Studies in Continental Margin Geology, Am. Assoc. Pet. Geol. Mem., 34:167-191.

Nair, K.M., Rao, M.R., 1980. Stratigraphic analysis of Kerala Basin. Geol. Surv. India Spl. pub., 5:1-8.

Nair, K.M., Singh, N.K., Jokhan Ram, Gavarshetty, C.P. and Muraleekrishanan, B., 1992. Stratigraphy and sedimentation of Bombay offshore basin. J. Geol. Soc. India, 40:415-442.

Nair, M.M. and Subramanyan, K.S., 1989. Transform faults of the Carlsberg Ridge – their implication in neotectonic activity along the Kerala coast. Geol. Surv. India. Spl. Pub., 24:327-332.

Nair, P.R. and Qasim, S.Z., 1978. Occurrence of bank with living corrals off southwest coast of India. Indian J. Mar. Sci., 7:55-58.

Narain, H., Kaila, K.L., Verma, R.K., 1968. Continental margins of India. Can. J. Earth Sci., 5:1051–1065.

National Geophysical Data Centre. (1998) GEODAS CD-ROM, Worldwide Marine Geophysical Data. Washington, DC, National Oceanic and Atmospheric Administration, US Department of Commerce.

National research Council, 1979. Continental Margins, Geological and Geophysical Research Needs and Problems. Washington, DC.

Norton, I.O. and Sclater, J.G., 1979. A model for the evolution of the Indian Ocean and the breakup of the Gondwanaland. J. Geophys. Res., 84:6803-6830.

O'Hara, M.J., 1975. Is there an Icelandic mantle plume?, Nature., 253:708–710.

Ollier, C.D., 1985. Morphotectonics of passive continental margins: introduction, Zeitschr. Geomorphol. Suppl. –band., 54:1-9.

Ollier, C.D., Powar, K.B., 1985. The Western Ghats and the morphotectonics of peninsular India. Zeit. Geomorph., 54:57–69.

Owen, M., Day, S. and Maslin, M., 2007. Late Pleistocene submarine mass movements: occurrence and causes. Quaternary Sci. Rev., 26:958-978.

Oxburgh, E.R. and Parmentier, E.M., 1977. Compositional and density stratification in oceanic lithosphere – causes and consequences. J. Geol. Soc. London., 133:343–355.

Pande, K., Sheth, H.C. and Bhutani, R., 2001. $^{40}Ar$-$^{30}Ar$ age of the St. Mary's Island volcanics, Southern India: record of India-Madagascar breakup on the Indian sub continent. Earth Planet. Sci. Lett., 193:39-46.

Pandey, J., 1986. Some recent paleontological studies and their implications on the Cenozoic stratigraphy of Indian subcontinent. Bull. ONGC., 23:1-44.

Pandey, O.P., Agarwal, P.K. and Negi, J.G., 1996. Evidence for low density sub-crustal underplating beneath western continental region of India and Adjacent Arabian Sea: geodynamical considerations. J. Geodyn., 21:365-377.

Pandey, J. and Dave, A., 1998. Stratigraphy of Indian petroliferous basins. XVI Indian colloquium on micropaleontology and stratigraphy. National Institute of Oceanography, Goa., pp 248.

Parsons, B., Sclater, J.G., 1977. An analysis of the variation of ocean floor bathymetry and heat flow with age. J. Geophys. Res., 82:803–827.

Patriat, P. and Achache, J., 1984. India-Eurasia collision chronology has implications for crustal shortening and driving mechanism of plates. Nature, 311:615-621.

Patriat, P. and Segoufin, J., 1988. Reconstruction of the Central Indian Ocean. Tectonophysics., 155:211-234.

Planke, S. and Eldholm, O., 1994. Seismic response and construction of seaward dipping wedges of flood basalts: VØring volcanic margin. J. Geophys. Res., 99(B5):9263-9278.

Planke, S., Skogseid, J. and Eldholm, O., 1991. Crustal structure off Norway 62° to 70°N. Tectonophysics., 189:91-107.

Radhakrishna, M., Verma, R.K. and Purushotham, A.K., 2002. Lithospheric structure below the eastern Arabian Sea and adjoining west coast of India based on integrated analysis of gravity and seismic data. Mar. Geophys. Res., 23:25-42.

Radhakrishna, T., Dallmeyer, R.D. and Joseph, M., 1994. Paleomagnetism and $^{36}Ar/^{40}Ar$ vs. $^{39}Ar/^{40}Ar$ isotope correlation ages of dyke swarms in central Kerala, India: Tectonic implications. Earth Planet. Sci. Lett., 121:213-226.

Raha, P.K., Roy, S.S. and Rajendran, C.P., 1983. A new approach to the lithostratigraphy of the Cenozoic sequence of Kerala. J. Geol. Soc. India., 24:325-342.

Rai, S.S., Priestley K., Suryaprakasam K., Srinagesh D., Gaur V.K., and Du Z., 2003. Crustal shear velocity structure of the south Indian shield, Jour. Geophys. Res., 108:1029/2002JB001776.

Raju, D.S.N., Bhandari, A. and Ramesh, P., 1999. Relative sealevel fluctuations during Cretaceous and Cenozoic in India. Bull. ONGC., 36:185-202.

Raju, A.T.R., Sinha, R.N., Ramakrishna, M., Bisht, H.S. and Nashipudi, V.M., 1981. Structure, tectonics and hydrocarbon prospects of Kerala-Laccadive Basin, In: Rao, R.P. (Ed.). Workshop on geological interpretation of geophysical data., pp 123-127.

Ramakrishnan, M., Viswanantha, M.N., Swami Nath, J., 1976. Basement-cover relationship of peninsular gneiss with high grade schist and greenstone belts of southern Karnataka. J. Geol. Soc. India., 17:97-111.

Ramana, M.V., 1986. Regional tectonic trends on the inner continental shelf off Konkan and central west coast of India. Geo-Mar. Lett., 6:1-5.

Ramaswamy, G. and Rao, K.L.N., 1980. Geology of the continental shelf of the west coast of India. Can. Soc. Pet. Geol. Mem., 6:801-821.

Ramasamy, S.M., 1989. Morpho-tectonic evolution of east and west coasts of Indian peninsula.Geol. Surv. India. Spl. Pub., 24:333-339.

Rao, T.C.S., 1970. Seismic and magnetic surveys over the continental shelf off Konkan Coast. Symp. on Upper Mantle Project, National Geophysical Research Institute, Hyderabad, India., pp 59-71.

Rao, T.C.S., Bhattacharya, G.C., 1975. Seismic profiler and magnetic studies off Quilon, South-west India. Indian J. Mar. Sci., 4:110-114.

Rao, R.P. and Talukdar, S.N., 1980. Petroleum geology of Bombay high field, India. In: M.T. Halbouty (Ed.), Giant oil fields of the decade, 1968-1978. Am. Assoc. Pet. Geol. Mem., 30:487-506.

Rao, R.P. and Srivastava, D.C., 1981. Structure, tectonics and hydrocarbon prospects of Kerala-Laccadive Basin, In: Rao, R.P. (Ed.), Workshop on geological interpretation of geophysical data., pp 49-57.

Rao, R.P. and Srivastava, D.C., 1984. Regional seismic facies analysis of western offshore, India. Bull. Oil Nat. Gas Comm., 21:83-96.

Rao, P.S., Kodagali, V.N., Ramprasad, T. and Nair, R.R., 1993. Morphology of coral bank, western continental shelf of India: a mutibeam study. J. Geol. Soc. India., 41:33-37.

Rao, V.K., 1994. Paleogene sedimentation rates in Bomaby – Ratnagiri Offshore of western Indian Shelf and their implications in drift history events of Indian plate. Bull. ONGC Spec. Issue., 31:99-120.

Rao, V.P. and Rao, B.R., 1995. Provenance and distribution of clay minerals in the sediments of the western continental shelf and slope of India. Continent. Shelf Res., 15:1757-1771.

Rao, V.P. and Wagle, B.G., 1997. Geomorphology and surficial geology of the western continental shelf and slope of India: a review. Curr. Sci., 73:330-350.

Rao, S.V., Dasgupta, D.K., Bhushan, K.S., Sriivas, M.S. and Ghosh, D.R., 2002. Sedimentary processes and structural frame work of Konkan Basin-western offshore, India. Geol. Surv. India. Spec. Publ., 74:43-52.

Raval, U. and Veeraswamy, K., 2003. India-Madagascar seperation: breakup along a pre-existing mobile belt and chipping of the craton. Gondwana Res., 6:467-485.

Reddy, S.I., Roychowdhury, K., Drolia, R.K., Ashalata, B., Mittal, G.S., Subrahmanyam, C. and Singh, R.N., 1988. On the structure of the western continental margin off Mangalore coast, India. J. Assoc. Expl. Geophys., 9:181-189.

Reddy, P.R., 2005. Crustal velocity structure of western India and its use in understanding intraplate seismicity.Curr. Sci., Vol. 88, pp1652-1657.

Reeves, C. and de Wit, M., 2000. Making ends meet in Gondwana: retracing the transforms of the Indian Ocean and reconnecting continental shear zones. Terra Nova., 12:272-280.

Reeves, C. and Leven, J., 2001. The evolution of the west coast of India from a perspective of global tectonics. J. Geophys., 22(1):17-23.

Richards, M.A., Duncan, R.A. and Courtillot, V.E., 1989. Flood basalts and hotspot tracks: plume heads and tails. Science., 246:103–107.

Roberts, D.G., Schnitker, D. et al., 1984. Proceedings of the Ocean Drilling Program, Initial reports 81: Ocean Drilling Program. College Station, Tex., 923p.

Robinson, E.M., 1988. The topographic and gravitational expression of density anomalies due to melt extraction in the uppermost oceanic mantle. Earth Planet. Sci. Lett., 90:221–228.

Roychaudhury, S.C. and Deshpande, S.V., 1982. Regional distribution of carbonate facies, Bombay offshore region, India. Bull. Am. Assoc. Pet. Geol., 66(10):1483-1496.

Royer, J-Y., Sclater, J.G. and Sandwell, D.T., 1989. A preliminary tectonic fabric chart of the Indian Ocean. Earth Planet. Sci. Lett., 98:7–24.

Royer, J.-Y., Chaubey, A.K., Dyment, J., Bhattacharya, G.C., Srinivas, K., Yatheesh, V. and Ramprasad, T., 2002. Paleogene plate tectonic evolution of the Arabian and Eastern Somali basins. In: The Tectonic and Climatic Evolution of the Arabian Sea Region, P.D. Clift, D. Kroon, C. Gaedicke and J. Craig (Eds). Geological Society, London, Special Publications., 195:7-23.

Sandwell, D.T. and Smith, W.H.F., 1997. Marine gravity anomaly from Geosat and ERS 1satellite altimetry. J. Geophy. Res., 102:10039–10054.

Sarkar, D., Chandrakala, K., Padmavathi Devi, P., Sridhar, A.R., Sain, K. and Reddy, P.R., 2001. Crustal velocity structure of western Dharwar Craton, South India. J. Geody., 31:227-241.

Schlich, R., 1982. The Indian Ocean: aseismic Ridges, spreading centres and basins. In: A.E.M. Nairn, and Stehli, F.G. (Eds) The Ocean basins and margins. Plenum Press., 6:51-147.

Sclater, J.G. and Francheteau, J., 1970. The implications of terrestrial heat flow observations on current tectonic and geochemical models of the crust and upper mantle of the earth. Geophys. J. R. Astron. Soc., 20:509–542.

Scotese, C.R., Gahagan, L.M. and Larson, R.L., 1988. Plate tectonic reconstructions of the Cretaceous and Cenozoic ocean basins. In: C.R. Scotese and W.W. Sager (Ed.), Mesozoic and Cenozoic plate reconstructions. Tectonophysics., 155:27-48.

Şengör, A.M.C., 1979. Mid-Mesozoic closure of Permo-Triassic Tethys and its implications. Nature., 279:590–593.

Sharma, H.S.S. and Varghese, T.G., 1979. The role of seismic arrays in continuous monitoring of seismicity. Mausam., 30:237-245.

Sheriff, R.E., 1980. Seismic Stratigraphy. International Human Resource Development Corporation, Boston., 223p.

Shipboard Scientific Party, 1988. Site 715. In: Backman J., Duncan R.A. and 24 others (Eds) Proceedings Ocean Drilling Program, College Station, TX., pp 917–946.

Singh, N.K. and Lal, N.K., 1993. Geology and petroleum prospects of Konkan-Keral Basin, In: S.K. Biswas et al. (Eds), Proc. Second Seminar on Petroliferous Basins of India, Indian Petroleum Publishers, Dehra Dun, India., 2:461-469.

Singh, R.P., Rawat, S. and Chandra, K., 1999. Hydrocarbon potential in Indian deep waters. Explorat.Geophys., 30:83-95.

Singh, N.K. and Lal, N.K., 2001. Fluvial routing systems and the signatures of onshore denudation in the offshore sedimentary record of Western India. Geol. Soc. India, Mem., 47:279-292.

Singh, A.P., 2002. Impact of Deccan volcanism on deep crustal structure along western part of Indian mainland and adjoining Arabian Sea. Current Science., 82:316-325.

Sleep, N.H., 1990. Hotspots and mantle plumes: some phenomenology. J. Geophys. Res., 95:6715–6736.

Sreejith, K.M., Krishna, K.S. and Bansal, A.R., 2008. Structure and isostatic compensation of the Comorin Ridge, north central Indian Ocean. Geophys. J. Int., 175:729-741.

Stein, C.A., Abbott, D.H., 1991. Heatflow constraints on the south Pacific superswell. J. Geophys. Res., 96:16083–16099.

Stein, C.A. and Stein, S.,1992. A model for the global variation in oceanic depth and heat flow with lithospheric age. Nature., 359:123-129.

Storey, B.C.,1995. The role of mantle plumes in continental breakup: case histories from Gondwanaland. Nature., 377:301-308.

Storey, M., Mahoney, J.J., Saunders, A.D., Duncan, R.A., Kelley, S.P. and Coffin, M.F., 1995. Timing of hotspot related volcanism and the breakup of Madagascar and India. Science., 267:852-855.

Storey, M., Mahoney, J.J. and Saunders, A.D., 1997. Cretaceous basalts in Madagascar and the transition between plume and continental lithosphere mantle sources, In: J.J. Mahoney and M. Coffin (Eds), Large Igneous provinces: Continental, Oceanic, and Planetary Flood Volcanism. Am. Geophys. Union Monogr., Washington DC., pp 95–122.

Subrahmanyam, V., 1987. Offshore extension of the structural element of Udipi, confirmation from marine magneties. J. Geol. Soc. India., 29:256-263.

Subrahmanyam, V., Ramana, M.V. and Subba Raju, L.V., 1989. Marine geophysical studies off Karwar, west coast of India. J. Geol. Soc. India., 34:121-132.

Subrahmanyam, V., Rao, D.G., Ramprasad, T., KameshRaju, K.A., Rao, M.G., 1991. Gravity anomalies and crustal structure of the western continental margin off Goa and Mulki, India. Mar. Geol., 99:247-256.

Subrahmanyam, V., 1992. Structure and tectonics of part of western continental margin of India between Marmagao and Kasaragod from geophysical investigations. Ph.D. Thesis, Andhra University, Visakhapatnam., 270p.

Subrahmanyam, V., Gangadhara Rao, M. and Subba Raju, L.V., 1993a. Subsurface Precambrian ridge on the continental shelf of western India between Coondapoor and Kasargod. Mar. Geology., 112:329-341.

Subrahmanyam, V., Ramana, M. V., Gopala Rao, D., 1993b. Reactivation of Precambrian faults on the southwestern continental margin of India: evidence from gravity anomalies. Tectonophysics., 219:327-339.

Subrahmanyam, V.,Gopala Rao, D., Ramana, M. V., Krishna, K.S., Murty, G. P.S., and Gangadhara Rao, M., 1995. Structure and tectonics of the southwestern continental margin of India. Tectonophysics., 249:267-282

Subrahmanya, K.R., 1998. Tectono magmatic evolution of the west cost of India. Gond. Res.. 3/4:319-327.

Swaminath, J., Ramakrishnan, M., Viswanatha, M.N., 1976. Dharwar stratigraphic model and Karnataka craton evolution. Rec. Geol. Surv. Ind., 107(2):149-175.

Symonds, P.A., Eldhom, O., Mascle, J., Moore, G.F. 2000. Charecterisics of continental margins. Continental shelf limits: the scientific and legal interface. Cook, P.J., Carleton, C.M.(Eds.), Oxford University Press., pp 25-63.

Talwani, M. and Eldholm, O., 1972. Continental margin off Norway: a geophysical study. Geol. Soc. Am. Bull., 83:3575-3606.

Talwani, M. and Eldholm, O., 1973. Boundary between continental and oceanic crust at the margin of rifted continents. Nature., 241:325-330.

Talwani M and H.G. Kahle, 1975.In: Geological-geophysical atlas of the Indian Ocean. USSR Academy of sciences, Moscow, G.B. Udinstev (Ed.), sheet 2., 87p.

Talwani, M. and Reif, C., 1998. Laxmi Ridge – A continental sliver in the Arabian Sea. Mar. Geophy. Res., 20:259-271.

Taylor, D.I., 1992. Nearshore shallow gas around the UK coast. Continental Shelf Research., 12:1135–1144.

Thakur, S.S., Arasu, R.T., Subrahmanyam, V.S.R., Srivastava, A.K., Murthy, A.V.S., 1999. Basin configyration in Konkan deep waters: western indian offshore. J. Geol. Soc. India., 53:79-88.

Todal, A. and Eldholm, O., 1998. Continental margin off western India and Deccan Large Igneous Province. Mar. Geophy. Res., 20:273-291.

Torsvik, T.H., Tucker, R. D., Ashwal, L. D., Eide, E. A., Rakotosolofo, N. A. and de Wit, M. J., 1998. Late cretaceous magmatism in Madagascar: palaeomagnetic evidence for a stationary Marion hotspot. Earth Planet. Sci. Lett., 164:221-232.

Torsvik, T.H., Tucker, R.F., Ashwal, L.D., Carter, L.M., Jamtveit, B., Vidyadharan, K.T., Venkataramana, P., 2000. Late Cretaceous India-Madagascar fit and timing of break-up related magmatism. Terra Nova., 12:220-224.

Tucholke, B.E., Houtz, R.E. and Berrett, D.M., 1981. Continental crust beneath the Agulhas Plateau, southwest Indian Ocean. J. Geophys. Res., 86:3791-3806.

Valdiya. K.S., 1999. Rising Himalaya: advent and intensification of monsoon. Curr. Sci., 76:514-524.

Vallier, T.L., 1974. Volcanogenic sediments and their relation to landmass volcanism and sea floor-continent movements, Western Indian Ocean. In: E.S.W. Simpson, R. Schlich, (Eds), Initial Reports of the Deep Sea Drilling Project, Vol. 25, U.S. Govt. Printing Office, Washington D.C., pp 515-542.

Valsangkar, A.B., Radhakrishnamurthy, C., Subbarao, K.V. and Beckinsale, R.D., 1981. Paleomagnetism and potassium-argon age studies of acid igneous rocks from St. Mary islands. Geol. Soc. Ind. Mem., 3:265-276.

Vandamme, D., Courtillot, V., Besse, J. and Montigny, R. 1991. Paleomagnetism and age determination of the Deccan Traps (India): Results of a Nagpur-Bombay traverse and review of earlier work. Rev. Geophys., 29:159-190.

Venkatesan, T.R., Pande, K. and Gopalan, K., 1993. Did Deccan volcanism pre-date the Cretaceous/Tertiary transition?. Earth Planet. Sci. Lett., 119:181-189.

Verma, R.K., 1991. Geodynamics of the Indian Peninsula and the Indian plate margin. Oxford and IBH publishing Co., New Delhi., 357p.

Verzhbitsky, E.V., 2003. Geothermal regime and genesis of the Ninety-East and Chagos-Laccadive Ridges. J. Geodynam., 35:289-302.

Vestal, W. and Lowrie A., 1982. Large-scale slumps off southern India and Sri Lanka. Geo-Mar. Lett., 2:171-177.

Wellman, P. and McElhinny, M.W., 1970. K-Ar age of the Deccan Traps, India. Nature., 227:595-596.

Weser, O.E., 1974. Sedimentological aspects of strata encountered on Leg 23 in the northern Arabian Sea. In: R.B. Whitmarsh, O.E. Weser, D.A. Ross and others (Eds), Initial Reports of the Deep Sea Drilling Project, U.S. Goverment Printing Office, Washington D.C., 23:503-519.

White, R.S., Westbrook, G.K. et al., 1987. Hatton Bank (northwest UK) continental margin structure. Geophy, J. R. Astron. Soc., 89:265-267

White, R.S. and McKenzie, D.P., 1989. Magmatism at rift zones: The generation of volcanic continental margins and flood basalts. J. Geophys. Res., 94:7685-7729.

Whiting, B.M., Karner, G.D. and Driscoll, N.W., 1994. Flexural and stratigraphic development of the west Indian continental margin. J. Geophys. Res., 99:13791-13811.

Whiting, B.M., Karner, G.D. and Driscoll, N.W., 2001. Flexural and stratigraphic development of the western continental margin of India. In: Gunnel, Y and

Radhakrishna, B.P (Eds) Sahyadri, The great escarpment of the Indian subcontinent. Mem. Geol. Soc. India., 47:419-444.

Whitmarsh, R.B., 1974. Some aspects of plate tectonics in the Arabian Sea. In: R.B. Whitmarsh, O.E. Weser, D.A. Ross, et al. (Eds), Initial Reports of the Deep Sea Drilling Project, Washington (U.S. Goverment. Printing Office) 23:527-535.

Whitmarsh, R.B., Weser, O.E., Ross, D.A. et al., 1974. Initial Reports of the Deep Sea In: R.B. Whitmarsh, O.E. Weser, D.A. Ross, et al. (Eds),Drilling Project. Washington (U.S. Government. Printing Office)., 23:35-210.

Widdowson, M., 1997. Tertiary palaeosurfaces of the SW Deccan, Western India: implications for passive margin uplift. In: Widdowson, M (Ed.) Palaeosurfaces: Recognition, Reconstruction and Palaeoenvironmental Interpretation. Geol. Soc. Lond. Spec. Pub., 120:221-248.

Widdowson, M. and Gunnell, Y., 1999. Lateritization, geomorphology and geodynamis of a passive continental margin: the Konkan and Kanara coastal lowlands of Western Peninsular India. Spec. Publ. Int. Assoc. Sedimentologists., 27:245-274.

Widdowson, M. and Mitchell, C., 1999. Large-Scale stratigraphy, structural and geomorphological constraints for earthquakes in the Southern Deccan Traps, India: the case for denudationally-driven seismicity. Mem. Geol. Soc. India., 43:425-452.

Windley, B.F., 1996. The Evolving Continents (3 ed.). John Wiley & Sons., pp xvi, 526, ISBN 0471917397

Yatheesh, V., Bhattacharya, G.C. and Mahender, K., 2006. The terrace like feature in the mid-continental slope region off Trivandrum and a plausible model for India–Madagascar juxtaposition in immediate pre-drift scenario. Gond. Res., 10:179-185.

# Publications

# List of publications

## Published research papers:

1. **Ajay, K.K.** and Chaubey, A.K., 2008. Depth anomalies in the Arabian Basin, NW Indian Ocean. **Geo-Marine Letters,** 28:15-22.

2. Chaubey, A.K. and **Ajay, K.K.**, 2008. Structure and tectonics of western continental margin of India: implication for geological hazards. In: Workshop on natural hazards and coastal processes of Indian coast, proceedings volume, NIO Regional Centre, Visakhapatnam, pp 25-33.

3. **Ajay, K.K.,** Chaubey, A.K., Krishna, K.S., Gopala Rao, D and Sar, D., 2010. Seaward dipping reflectors along the SW continental margin of India: evidence for volcanic passive margin. **Journal of Earth System Science,** 119(6):803-813.

4. Gopala Rao, D., Paropkari, A.L., Krishna, K.S., Chaubey, A.K., **Ajay, K.K.** and Kodagali, V.N., 2010. Bathymetric highs in the mid-slope region of the western continental margin of India – Structure and mode of origin. **Marine Geology**, 276(1-4):58-70.

## Published abstracts:

1. Chaubey A.K., **Ajay, K.K.**, Krishna, K.S., Rao, D.G. and Sar, D., 2008. Structure and evolution of the southwestern continental margin of India. **EOS Trans. AGU, 89 (53)**, Fall meet. Suppl., Abstract T53G-07.

2. **Ajay, K.K.**, Chaubey, A.K., Rao, D.G., Krishna K.S. and Sar, D., 2008. Seaward dipping reflectors along the southwestern continental margin of India: Seismic evidence for ocean continent transition. **The 45$^{th}$ annual convention of the Indian Geophysical Union** and meeting on "Seismic hazard and crustal earthquakes: Indian scenario", held at Banaras Hindu University, Varanasi (UP), 122p.